PB-240 565

AIR POLLUTION: PROCEEDINGS OF THE SECOND MEETING OF THE EXPERT PANEL ON AIR POLLUTION MODELING, HELD IN PARIS, FRANCE, JULY 26-27, 1971

NATO Committee on the Challenges of Modern Society

Prepared for:

Environmental Protection Agency

July 1971

DISTRIBUTED BY:

NTIS
National Technical Information Service
U. S. DEPARTMENT OF COMMERCE

BIBLIOGRAPHIC DATA SHEET	1. Report No.	2.	PB 240 565

4. Title and Subtitle Air Pollution, Proceedings of the Second Meeting of the Expert Panel on Air Pollution Modeling,	5. Report Date July 26-27, 1971
	6.
7. Author(s)	8. Performing Organization Rept. No. 5
9. Performing Organization Name and Address NATO Committee on the Challenges of Modern Society, 1110 Bruxelles, Brussels, Belgium	10. Project/Task/Work Unit No.
	11. Contract/Grant No.
12. Sponsoring Organization Name and Address Office of Air and Waste Management, Environmental Protection Agency, Washington, D. C. 20460	13. Type of Report & Period Covered
	14.

15. Supplementary Notes

16. Abstracts

17. Key Words and Document Analysis. 17a. Descriptors

air pollution
air pollution modeling

17b. Identifiers/Open-Ended Terms

Reproduced by
NATIONAL TECHNICAL
INFORMATION SERVICE
US Department of Commerce
Springfield, VA. 22151

PRICES SUBJECT TO CHANGE,

17c. COSATI Field/Group

18. Availability Statement Available from NTIS	19. Security Class (This Report) UNCLASSIFIED	21. No. of Pages 389
I	20. Security Class (This Page UNCLASSIFIED	22. Price 10.25 / MF 2.25

FORM NTIS-35 (REV. 10-73) ENDORSED BY ANSI AND UNESCO. THIS FORM MAY BE REPRODUCED USCOMM-DC 8265-P74

PROCEEDINGS OF THE SECOND
MEETING OF THE EXPERT PANEL
ON AIR POLLUTION MODELING

NATO Committee on the Challenges
of Modern Society

Paris, France
July 26-27, 1971

II

OTHER NATO/CCMS AIR POLLUTION PUBLICATIONS

"Technical Report of the Conference on Low Pollution Power Systems Development, N.4"

"Guidelines to Assessment of Air Quality, N.6" **

"Air Quality Criteria for Sulfur Oxides, N.7" **

"Air Quality Criteria for Particulate Matter, N.8" **

"Air Quality Criteria for Carbon Monoxide, N.10" **

** Also available in French

Preface

The fifteen papers collected in these proceedings were all specifically prepared in connection with the NATO/CCMS air pollution study. They have been presented and discussed at the two meetings of the Panel on Modeling held to date (9 October 1970, Frankfurt, Germany; 26-28 July 1971, Paris, France) and relate to various aspects of the mathematical and physical modeling of urban air quality. The three primary topics are (a) the current air quality modeling efforts for Ankara, Turkey, and Frankfurt, Germany; (b) the possible applications of physical modeling using hydraulic and aerodynamic techniques in air pollution studies; and (c) the problems of physical and chemical transformations, particularly of photochemical reactions, in air pollution modeling. The Environmental Protection Agency, as part of its contribution to the pilot study, has compiled and published this document. In view of the current widespread interest in the modeling of environmental problems it is hoped that the publication between one set of covers of these recent contributions in the air pollution field will make the results more readily available to the technical community.

R. A. McCormick

R. A. McCormick, Chairman
NATO/CCMS Panel on Urban
Air Pollution Modeling

Director
Division of Meteorology
Environmental Protection Agency

PROCEEDINGS OF THE SECOND MEETING OF THE EXPERT PANEL ON AIR POLLUTION MODELING

TABLE OF CONTENTS

Contents:

CHAPTER | PAGE

I A CLIMATOLOGICAL MODEL FOR MULTIPLE-SOURCE URBAN AIR POLLUTION, I - 1
Kenneth L. Calder, United States of America

II A PROPOSED APPROACH ON MODELING TECHNIQUES FOR ECOLOGICAL PURPOSES USING DYNAMIC CRITERIA II - 1
A. Cardinale, A. Marzocchi, and E. Nardelli, Italy

III ESTIMATION METHODS OF DISPERSION OF GASEOUS POLLUTANTS DOWNWIND OF INDUSTRIAL STACKS III - 1
R. Deniau and P. Mery, France

IV PRACTICAL APPROACHES FOR SOLUTION OF SOME PROBLEMS IN CONNECTION WITH THE ESTIMATION OF AIR POLLUTION BY STACK EFFLUENTS, IV - 1
R. Deniau and P. Mery, France

V MATHEMATICAL-METEOROLOGICAL MODELING OF AIR QUALITY IN THE UNTERMAIN REGION (FRANKFURT) V - 1
Heinz Fortak, Federal Republic of Germany

VI DEPENDENCE OF POLLUTANT CONCENTRATION ON THE SPATIAL VARIATION OF A CROSSWIND LINE SOURCE, VI - 1
Suha Selamoglu, Turkey

VII MODIFICATIONS TO THE CLIMATOLOGICAL AIR POLLUTION MODEL FOR ANKARA, VII - 1
Suha Selamoglu, Turkey

VIII PHYSICAL AND CHEMICAL TRANSFORMATIONS IN AIR POLLUTION MODELING VIII -1
Suha Selamoglu, Turkey

IX REPRESENTATION OF GROUND SURFACE EFFECT BY SURFACE SOURCE DISTRIBUTION IN ATMOSPHERIC DIFFUSION OF POLLUTANTS, IX - 1
Suha Selamoglu, Turkey

Cont

CHAPTER		PAGE
X	SIMILARITY CRITERIA FOR THE APPLICATION OF PHYSICAL MODELS FOR THE STUDY OF AIR POLLUTION METEOROLOGY *William H. Snyder, United States of America*	X - 1
XI	ATMOSPHERIC PHYSICAL AND CHEMICAL TRANSFORMATION OF POLLUTANTS AS AFFECTING URBAN POLLUTION MODELING *Carel Andre Velds, The Netherlands*	XI - 1
XII	REMOVAL OF SULFUR DIOXIDE FROM THE ATMOSPHERE *Erich Weber, Federal Republic of Germany*	XII - 1
XIII	REPORT ON MATHEMATICAL MODELING OF PHOTOCHEMICAL SMOG *Frank L. Worley, United States of America*	XIII - 1
XIV	SULFUR DIOXIDE REACTIONS IN THE ATMOSPHERE *Frank L. Worley, United States of America*	XIV - 1
XV	SOME PRELIMINARY RESULTS OF MODELING FROM THE AIR POLUTION STUDY IN ANKARA, TURKEY *John R. Zimmerman, United States of America*	XV - 1

Chapter I-1

A CLIMATOLOGICAL MODEL FOR MULTIPLE SOURCE URBAN AIR POLLUTION

By

K. L. Calder*

Division of Meteorology
Bureau of Air Pollution Sciences
Office of Research and Monitoring
Environmental Protection Agency

Paper presented at the First Meeting of the NATO/CCMS Panel on Modeling: October 9, 1970, Frankfurt, Germany.

---

*On assignment from National Oceanic and Atmospheric Administration, Department of Commerce.

Acknowledgements

The Fortran computer program required for application of the model described in this paper was developed by Messrs. John R. Zimmerman and Adrian D. Busse, both of the Division of Meteorology, Environmental Protection Agency. Thanks are also due these gentlemen for the rather extensive numerical calculations that are described; especially to Mr. Zimmerman for helpful discussions of many other details.

Abstract

The paper describes a revised form of an urban air pollution model, originally proposed in 1968 by D.O. Martin and J.A. Tikvart, for estimating long-term average concentration of gaseous pollutant in terms of appropriate point- and area-source emission inventories for the urban area, together with climatological frequency data relating to wind speed, wind direction, atmospheric stability, and mixing depth. The model is also applied to the estimation of three-month average SO_2 concentrations in St. Louis, Missouri, during the winter of 1964-65. Some shortcomings of the present model are identified and discussed.

A CLIMATOLOGICAL MODEL FOR MULTIPLE SOURCE URBAN AIR POLLUTION

(A Revised Form of a Model First Proposed
by D. O. Martin and J. A. Tikvart)

by K. L. Calder

I. INTRODUCTION

A paper by Martin and Tikvart was presented at the annual meeting of the Air Pollution Control Association in June 1968. The paper described a computerized climatological model for urban air pollution from multiple sources. This source-oriented atmospheric diffusion model permits calculation of the long-period seasonal or annual-average pollutant concentration patterns resulting from multiple point or area-distributed stationary sources. The model input comprises a detailed specification of the magnitude and distribution of pollutant emissions and of the frequency of occurrence of various meteorological conditions during the time-period of concern. The output provides a quantitative estimate of the spatial distribution of urban air quality averaged over the time period considered.

The fundamental physical basis for the model is the assumption that the steady-state spatial concentration distribution from an elevated, continuously emitting point source is given by the Gaussian plume formula. However, following Meade and Pasquill (1958), this formula was first modified to give the long-term average concentration produced by a given source at any receptor for specified frequencies of occurrence of the various possible wind directions. Martin and Tikvart utilized this result in conjunction with a specified joint frequency function for the occurence of various possible combinations of wind direction, wind speed, and atmospheric stability to obtain the long-term average concentration for all the possible combinations of the meteorological conditions for a multiple source distribution.

The model clearly represents a natural development in the hierarchy of urban air pollution models that stem directly from the Gaussian plume hypothesis. The present paper provides a detailed account of the model which has not been previously available. Revisions have been incorporated to clarify some features of the original analysis. A major revision relates to the mathematical method for computing the concentration contributions from area-source distributions.

II. THE GAUSSIAN PLUME

A recent discussion of the structure and assumptions that underlie urban air pollution models based on the Gaussian plume has been given elsewhere (Calder, 1969). The common starting point is the assumption that meteorological conditions over short periods of time of the order of an hour can be regarded as steady-state. It is also assumed that these conditions may be adequately approximated with a unique horizontal mean wind direction for the entire urban area together with a constant and spatially uniform wind speed.

Let the origin of a rectangular coordinate system be taken at ground level, with the x-axis in the direction of the mean wind, y-axis crosswind and the z-axis vertical. Then for a constant, continuously emitting, elevated point-source of strength G located at x=0, y=0, z=h, the Gaussian plume formula gives the concentration $\chi(x, y, z)$ of material at position (x, y, z) as

$$\chi(x, y, z) = G\left(\frac{\exp\{-\frac{y^2}{2\sigma_y^2(x)}\}}{\sigma_y(x)\sqrt{2\pi}}\right) S(x, z) \qquad (1)$$

where

$$S(x, z) = \frac{1}{U\sigma_z(x)\sqrt{2\pi}}\left[\exp\{-\frac{(z-h)^2}{2\sigma_z^2(x)}\} + \exp\{-\frac{(z+h)^2}{2\sigma_z^2(x)}\}\right] \qquad (2)$$

and $\sigma_y(x)$, $\sigma_z(x)$ are horizontal and vertical diffusion functions that give respectively, the horizontal and vertical standard deviations of the Gaussian concentration distribution at downwind distance x. The above formula relates to the atmospheric transport and diffusion of a chemically stable gas or a cloud of particles sufficiently small that gravitational settling can be neglected. It is also assumed that no material is lost from the cloud to the ground surface. The method of images is invoked to satisfy this condition and the function S(x, z) is the sum of two terms representing (in the absence of the ground surface) the concentration contribution from the real source at z = h and that from its image in the plane z = 0, i.e., at z = -h. It is readily verified that equation (1) satisfies the equation for the conservation of matter, namely

$$\int_{-\infty}^{\infty}\int_{0}^{\infty} U\chi\ (x, y, z)\ dydz = G \qquad (3)$$

Equation (1) is assumed to be valid irrespective of the horizontal location of the source and of the horizontal mean wind direction that defines the orientation of the coordinate system.

The standard deviation functions $\sigma_y(x)$ and $\sigma_z(x)$ are dependent on meteorological conditions and are assumed to be parameterized in terms of an atmospheric stability category P first introduced in discussions of atmospheric diffusion by Pasquill (1961). Actually, a completely objective scheme for determing the appropriate stability category in terms of meteorological observations that are routinely taken at airports was suggested by Turner (1964) and used in the application of the model. This scheme admits five different Pasquill-type stability categories P_m(m = 1, 2, 3, ..5) for an urban environment, P_1 being a very unstable category and P_5 a slightly stable one. For given stability category P_m the standard deviation functions $\sigma_y(x; P_m)$ and $\sigma_z(x; P_m)$ are obtained as functions of the downwind distance x from some graphical plots of Gifford (1961). The latter are simple transforms of some rather crude empirically established dispersion curves first given by Pasquill (1961, 1962). For the final computerized model, it is convenient to represent the Gifford plots by simple formulae of the type

$$\sigma_z(x;\ P_m) = ax^b + c$$

where for each stability category a, b, c, are constants within given ranges of x.

The above values of $\sigma_z(x;\ P_m)$ refer to conditions where there are no restrictions to diffusion in the vertical direction so that $\sigma_z(x;\ P_m)$ increases continually with x. However, when a stable atmospheric layer exists above an unstable near-surface layer, the vertical diffusion will be limited to a mixing layer of finite depth L, within which pollutants will be trapped. If this occurs, a uniform vertical distribution of concentration would be expected throughout the depth of the mixing layer for sufficiently large values of x and some modification of the Gaussian formula will be necessary. Providing that the emission height h is small compared with L, a crude but simple method of allowing for this effect has been suggested by Pasquill (1962) and Turner (1969). By assigning h = 0 in the equation (2), it is readily verified that, when $z = 2.15\ \sigma_z$, the concentration is one-tenth its value at the ground surface. When this value is occurring at the level of the top of the mixing layer, it is assumed that the "lid" begins to influence appreciably the vertical distribution of concentration. Turner suggests the following rough method to allow for the situation. Use equations (1) and (2) for downwind distances such that $\sigma_z(x) \leq L/2.15$ or $\sigma_z(x) \leq 0.47\ L$ corresponding to downwind distances, say x_L. Assume that for $x \geq 2x_L$ the concentration has become uniform through the depth of the mixing layer, so that S(x, z) of equation (2) is replaced by

$$S(x,\ z) = \frac{1}{UL} \quad (x \geq 2x_L) \tag{4}$$

For $x_L \leq x \leq 2x_L$, Turner suggests linear interpolation between the concentration values for these two distances. This procedure was adopted in the Martin-Tikvart air pollution model.

A more refined method of correcting for the finite depth of the mixing layer is to utilize the "method of images" in the same manner that this technique is used to allow for the "reflecting" ground surface in establishing the function S of equation (2). For a point source situated between two parallel "reflecting" surfaces at distance L apart, i.e., the ground and the lid of the mixing layer, it is evident that an infinite series of image sources arises and the concentration distribution is thus expressed as an infinite series [Bierly and Hewson (1962), Fortak (1969)]. In this case it is readily shown

$$\chi(x, y, z) = \frac{G}{2LU} \left(\frac{\exp\{-\frac{y^2}{2\sigma_y^2}\}}{\sigma_y(x)\sqrt{2\pi}} \right) \left[\Lambda\{ \frac{z-h}{2L} ; \frac{\sigma_z^2}{2L^2} \} + \Lambda\{ \frac{z+h}{2L} ; \frac{\sigma_z^2}{2L^2} \} \right] \tag{5}$$

where the function Λ is defined by

$$\Lambda(v;w) \equiv \frac{1}{\sqrt{\pi w}} \sum_{n=-\infty}^{+\infty} \exp\{ -\frac{(v+n)^2}{w} \} \tag{6}$$

When $L \rightarrow \infty$, only the term corresponding to $n = 0$ remains in each of the two infinite series that are involved, and in this case (5) reduces to (1) with S given by (2). In the general case the infinite series converge rapidly, and it is only necessary to consider a few terms.

Before leaving this discussion of the Gaussian plume, it should be noted that the emission height h for large point sources can rarely be taken as the actual physical height of a pollutant emitting stack since there is normally considerable plume rise associated with the upward momentum of discharge and thermal buoyancy effects. Frequently a crude attempt to allow for these effects is made by simply adding an estimate of the plume rise to the stack height and using this sum as the quantity h in the diffusion formulae. Consideration of plume rise is a complicated and somewhat controversial topic, although it is generally regarded as an important element in realistic urban air pollution models. A comprehensive and hopefully definitive critical review of the subject has been recently prepared by Briggs (1969).

III. AVERAGE CONCENTRATION WITH VARIABLE WIND DIRECTION FROM A SINGLE SOURCE

For fixed locations of both source and receptor, the maximum concentration will occur at the receptor when the wind blows directly from the source towards the receptor. The concentration varies with wind direction. Therefore, the average value when the wind direction is a random variable governed by a probability or frequency distribution is considered first.

Relative to a rectangular coordinate system with x-axis along the wind direction, the point source concentration distribution will be given by equation (1), where

$$GS(x, z) = \int_{-\infty}^{\infty} \chi(x, y, z)\, dy \qquad (7)$$

In the diagram below, let the source be at the origin of a polar coordinate system, with (ρ,β) the polar coordinates of the receptor, and θ the angular direction measured clockwise from north from which the wind blows.

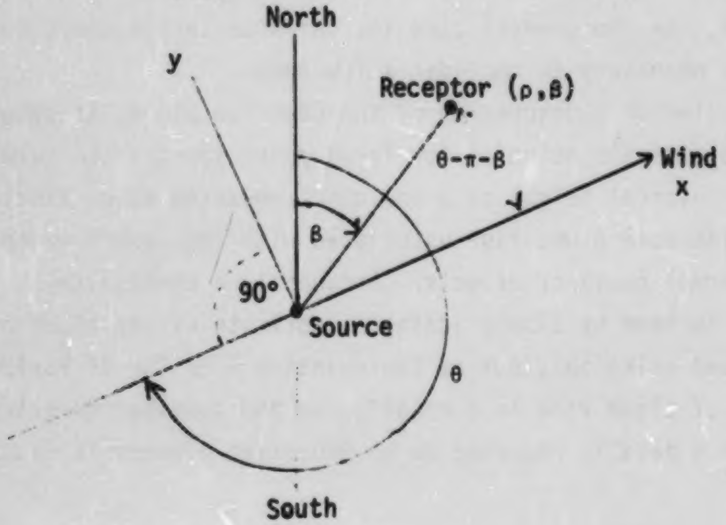

Then if $f(\theta)d\theta$ is the probability that the wind direction is in the angular range θ, $\theta + d\theta$, the average concentration at the receptor corresponding to all possible wind directions will be approximated by

$$\overline{\chi} = \int_{\pi+\beta-\Delta}^{\pi-\beta+\Delta} \chi(\rho\cos\overline{\theta-\beta-\pi},\ \rho\sin\overline{\theta-\beta-\pi},\ z)\ f\ (\theta)d\theta \qquad (8)$$

where, since the plume from a point source is normally narrow, Δ is a small angle. If the total range of integration were made larger than 2Δ, this would have negligible effect on the value of the integral. With $\psi = \theta - \beta - \pi$, equation (8) becomes

$$\overline{\chi} = \int_{-\Delta}^{\Delta} \chi(\rho\cos\psi,\ \rho\sin\psi,\ z)\ f\ (\psi + \beta + \pi)d\psi$$

or since ψ is small and hence $\cos\psi \underset{-}{\sim} 1$, we have, using equation (1),

$$\overline{\chi} = \frac{GS(\rho,\ z)}{\sigma_y(\rho)\sqrt{2\pi}} \int_{-\Delta}^{\Delta} e^{\frac{-\rho^2\sin^2\psi}{2\sigma_y^2(\rho)}}\ f(\psi + \beta + \pi)d\psi \qquad (9)$$

The integral in (9) could be evaluated numerically if the frequency function were specified. However, with small ψ, we have approximately

$$\overline{\chi} = \frac{GS(\rho,\ z)}{\sigma_y(\rho)\sqrt{2\pi}} \int_{-\Delta}^{\Delta} e^{\frac{-\rho^2\psi^2}{2\sigma_y^2(\rho)}}\ f(\psi + \beta + \pi)d\psi \qquad (10)$$

We now assume that, because of the smallness of the angular range $-\Delta \leq \psi \leq \Delta$, the variations of the wind direction frequency function in the integral of (10) can be disregarded and the function replaced by its central value $f(\beta + \pi)$

so that

$$\bar{\chi} = \frac{GS(\rho,\, z)}{\sigma_y(\rho)\sqrt{2\pi}}\, f(\beta + \pi) \int_{-\Delta}^{\Delta} e^{\frac{-\rho^2\chi^2}{2\sigma_y^2(\rho)}}\, d\phi = \frac{GS(\rho,\, z)}{\rho}\, f(\beta + \pi) \int_{\frac{-\rho\Delta}{\sigma_y}}^{\frac{\rho\Delta}{\sigma_y}} \frac{1}{\sqrt{2\pi}}\, e^{\frac{-w^2}{2}}\, dw \qquad (11)$$

The integral is recognized as that of the Gaussian probability function whose value tends to unity when both limits of the integration tend to infinity. However, the value of $\bar{\chi}$ is not affected by increasing the value of Δ as it appears in the limits of integration, which can only be so if the integral differs inapreciably from its asymptopic value of unity. With this approximation, we have

$$\bar{\chi} = \frac{GS(\rho,\, z)}{\rho}\, f(\beta + \pi) \qquad (12)$$

It may be noted that:

1) although both equations (9) and (10) for $\bar{\chi}$ involve the crosswind standard deviation function $\sigma_y(\rho)$, this is not so for the final approximate relation (12) which is independent of $\sigma_y(\rho)$.

2) equation (12) expresses $\bar{\chi}$ as the product of an "isotropic" meteorological-diffusion function $GS(\rho,\, z)/\rho$ and the directionally dependent wind frequency function.

3) although $\bar{\chi}$ is the average concentration at the receptor corresponding to all possible wind directions, the narrow plume assumption renders it possible to relate this average value to the frequency function for a particular wind direction, viz. the source-receptor direction.

With a 16-point compass if all wind directions within any given 22 1/2° sector are equally probable, then if the source-receptor direction [here defined by the angle $(\beta + \pi)$] is in the k-th sector $(k = 1, 2, \ldots 16)$ and

F(k) is the total frequency of wind directionsin the k-th sector, we have

$$f(\beta + \pi) \times \frac{2\pi}{16} = F(k)$$

so that from (12)

$$\overline{\chi} = \frac{16}{2\pi} F(k) \frac{GS(\rho, z)}{\rho} \tag{13}$$

With an 8-point compass the corresponding formula would be identical with one used by Meade and Pasquill (1958) in examining the average distribution of sulfur pollution around a power station in the U.K.

In the analysis leading to equation (13), only wind direction is considered to be a random variable. However, it is straightforward to generalize where several meteorological variables are regarded as random with values specified through a joint frequency function. Thus assume that the wind direction (defined by sectors $k = 1, 2, . . 16$), the urban wind speed* U_ℓ ($\ell = 1, 2, . . . 6$), and the Pasquill-type stability category P_m($m = 1, 2, . . . 5$) are such random variables having a joint frequency function $\phi(k, \ell, m)$ that expresses the relative frequency with which the wind is in the k-th sector with representative speed U_ℓ and stability category P_m. Such a three-variable joint frequency function was first used in the context of the present problem by Leavitt (1960) and subsequently by Szepsi (1964, 1967). Evidently in equation (13) the diffusion function $S(\rho, z) \equiv S(\rho, z; U_1, P_m)$ where, from equation (2), S involves P_m through the standard deviation function $\sigma_z(\rho) \equiv \sigma_z(\rho; P_m)$. It immediately follows from equation (13) that the average concentration $\overline{\chi}$ corresponding to all possible combinations of wind direction, wind speed, and stability will be given by

$$\overline{\chi} = \frac{16}{2\pi} \sum_{\ell} \sum_{m} \frac{\phi(k, \ell, m) GS(\rho, z; U_\ell P_m)}{\rho} \tag{14}$$

---

*Here wind speed is assumed to be specified in terms of one of the standard Weather Bureau classes (i.e., with wind estimated to an integral number of knots in the classes 0-3, 4-6, 7-10, 11-16, 17-21, and > 21 knots) and each class is represented by its central wind speed (i.e., 0.67, 2.46, 4.47, 6.93, 9.61, 12.52 meters per sec).

where as before the source-receptor direction is assumed to lie in the k-th wind section (N.B. the summation in equation (14) does not involve k). A virtually identical solution was first proposed by Szepsi (1964). In principle the Martin-Tikvart model simply sums equation (14) for a given receptor location over the multiplicity of contributing sources.

It is important to note that the summand in equation (14) cannot legitimately be used, as is attempted by Szepsi (1967), as a basis for analysis of the frequency occurrence of various levels of concentration. This is because it was obtained through averaging over all possible wind directions. It is this averaging process that eliminates the crosswind variance function $\sigma_y(\rho)$ that appears in the original point-source concentration distribution function of equation (1).

IV. THE MULTIPLE SOURCE POLLUTION MODEL

It is customary in estimating community air pollution emissions from fixed sources [e.g. Ozolins and Smith(1966)] and in modeling urban air pollution to distinguish between two main categories of pollutant sources. Very large sources with emissions in excess of 100 tons per year are readilyidentified and located individually as single (elevated) point-sources. However, when there are a large number of small sources too numerous to identify individually such as domestic heating units, then it is normal to combine these sources in any small area and to specify them through the total pollutant emission associated with the area. The size and number of the sub-areas are chosen in relation to the spatial uniformity of the source distribution. Thus a complete urban pollution emissions inventory for stationary sources will normally comprise the strenths and locations of all major point sources together with area-source strengths corresponding to a large number of area elements into which the total urban area has been sub-divided. In most emission inventories, it is difficult or impossible to specify with accuracy much detail concerning the temporal variations of the emissions, although an estimate of variation from season to season is frequently attempted. In the theoretical analysis of the previous section, it was assumed that the source strength G was constant. When the source is variable, it will only be legitimate to use the same formulae providing that the source strength and each of the meteorological variables are completely uncorrelated, and, in this case, G is given its arithmetic average value corresponding to the total time period considered (i.e., season or year). This assumption, however, may be questionable in some circumstances. For example, in winter very cold conditions with increased air pollution due to increased fuel consumption may occur most frequently with certain wind directions. If the source strength and meteorological conditions are not uncorrelated, a more sophisticated development is required that is outside the scope of the present analysis. Although this may be straightforward mathematically, the serious practical questions of specifying short-term temporal variations of source strength have yet to be resolved.

Considering equation (14) it is evident that if $k_n (k_n = 1, 2, \ldots 16)$ is the wind sector appropriate to the n-th point source (of strength G_n and distance ρ_n from receptor) and there are N point sources, then the average total concentration at the receptor, $\overline{C}_p$, due to all the point sources will be given by

$$\overline{C}_p = \frac{16}{2\pi} \sum_{n=1}^{N} \sum_{\ell} \sum_{m} \frac{\phi(k_n, \ell, m) G_n S(\rho_n, z; U_\ell, P_m)}{\rho_n} \qquad (15)$$

Obviously the contribution to the total from just those sources located in the k-th sector will be obtained by restricting the summation to these sources (i.e., those for which $k_n = k$).

To obtain the concentration contribution, say $\overline{C}_A$, at the receptor due to the area-soruce distribution we use a polar coordinate system with origin at the receptor and with angle θ measured clockwise from north as in specifying the wind direction.

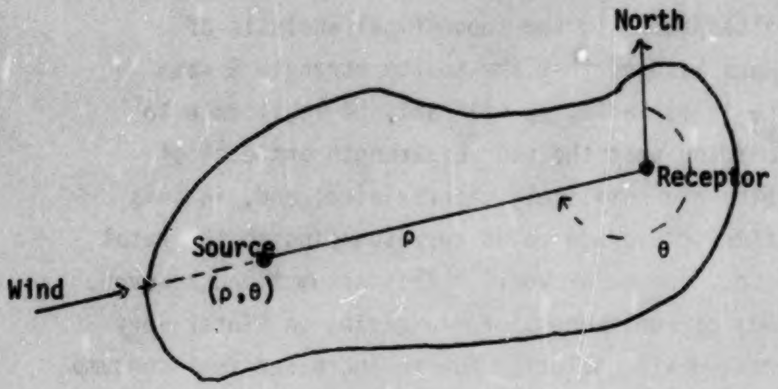

An element of area surrounding the point (ρ,θ) will have magnitude ρdθdρ. Let Q(ρ,θ) denote the magnitude (emission rate per unit area and unit time) of the area source strength at (ρ,θ), so that Q(ρ,θ) ρdθdρ is the total emission rate from the element of area surrounding (ρ,θ). Then by considering the area source contributions from the different 22 1/2° wind sectors, it immediately follows from (15) that the total average concentration due to the area-source distribution will be*

$$\bar{C}_A = \frac{16}{2\pi}\sum_{k=1}^{16}\sum_{\ell}\sum_{m}\phi(k, \ell, m)\int_0^\infty \frac{S(\rho, z; U_\ell, P_m)}{\rho}\left\{\int_{k\ \mathrm{sector}} Q(\rho,\theta)\rho d\theta\right\} d\rho \qquad (16)$$

Here the upper limit of integration for ρ can be taken as infinite since Q(ρ,θ) becomes zero outside the domain of the area-source distribution. Equation (16) can be rewritten as

---

*In equation (16), it is assumed that the effective height of the area source distribution can be regarded as a constant for the entire area. This is an assumption made in the original Martin-Tikvart Model. If the height is variable, then the function S becomes a function of θ and cannot be taken outside the sector integral sign in equation (16). This, of course, raises no fundamental problem but complicates the numerical integration.

$$\bar{C}_A = \frac{16}{2\pi} \int_0^\infty \left\{ \sum_{k=1}^{16} q_k(\rho) \sum_\ell \sum_m \phi(k, \ell, m)\, S(\rho, z; U_\ell, P_m) \right\} d\rho \tag{17}$$

where

$$q_k(\rho) \equiv \int_{k\ \text{sector}} Q(\rho,\theta)\,d\theta$$

so that $\frac{16}{2\pi} q_k(\rho)$ is the average value of Q in the k-th sector at a radial distance ρ. Evidently, if the integral in (17) is replaced by just a single term of its sum we obtain the average concentration from area sources lying within the corresponding wind sector.

The total average concentration $\bar{C}$ at the receptor due to both point and area sources is given by $\bar{C} = \bar{C}_A + \bar{C}_P$.

In applying equation (17), we have to determine for each receptor location the source functions Q (ρ,θ) and $q_k(\rho)$. The air pollution emission inventory for a stationary area source distribution is, of course, specified once and for all for areas of fixed locations on a map of the urban area. A typical inventory as used in the St. Louis Study referred to in a later section may divide the entire urban area into 5000 ft. squares with a seasonal emission rate assigned for each square. However, from such an inventory, it is simple to determine, for any given values of the polar coordinates relative to a selected receptor location, the appropriate numerical values of the source function $Q(\rho,\theta)$. The sector function $q_k(\rho)$ may then be determined by numerical integration of the values of Q (ρ,θ) along the appropriate circular arc. For this purpose the trapezoid rule of numerical integration was applied on each arc to Q -values spaced 2 1/4° apart, i.e., the 22 1/2" arc was subdivided into ten intervals. The second integration with respect to the radial distance ρ as required in equation (17) was also performed numerically by the trapezoid rule with an interval length in ρ of 100 meters.

V. MODEL INPUT DATA AND PARAMETERS

A basic feature of the present model is the assumption that for short time periods (of the order of one hour) meteorological conditions can be regarded as steady and uniform over the entire urban area and may be specified through some single representative value for wind direction, wind speed, stability category, and mixing depth. Since detailed urban meteorological observations are not normally available, it may be necessary in practice to utilize information collected at some nearby airport weather station with the assumption that this is roughly representative of the urban area. Thus, in using the Martin-Tikvart model to estimate seasonal or annual urban air quality, the standard hourly Weather Bureau data from the local airport station is normally used. The climatological joint frequency function $\phi(k, \ell, m)$ of the model can be readily obtained from the hourly airport observations using a computer program specially developed for this purpose by J. Tikvart.

The objective method proposed by Turner (1961, 1964) is used to estimate the hourly atmospheric stability category P_m at the airport. This method requires no vertical sounding data but is based on ground-level meteorological observations only (surface wind speed, cloud amount and height) supplemented by solar elevation data (latitude, time of day, and time of year).

The values of the standard deviation function $\sigma_z(x; P_m)$ used in the application of the model are those of Pasquill (1961) and Gifford (1961) and represented for the computation in the form

$$\sigma_z(x; P_m) = ax^b + c$$

where a, b, c are constants for each stability category, as shown in the following table..

	Stability Category					Distance
	1	2	3	4	5	x(Meters)
a	.001	.048	.119	2.610	52.600	>1000
	.001	.048	.119	.187	.135	100-1000
	.174	.143	.23	.080	.060	<100

Stability Category

	1	2	3	4	5	Distance x(Meters)
b	1.890	1.110	.915	.450	.150	>1000
	1.890	1.110	.915	.755	.745	100-1000
	.936	.922	.905	.881	.845	<100
c	9.600	2.000	.000	-25.500	-126.000	>1000
	9.600	2.000	.000	-1.400	-1.100	100-1000
	.000	.000	.000	.000	.000	<100

The values of $\sigma_z(x; P_m)$ described above were originally established from diffusion experiments conducted over flat and relatively smooth rural terrain. To make some crude allowance for the thermal and mechanical influences of the urban area, two types of correction have been suggested and are used with the model. The first is intended to reflect the fact that the lowest part of the typical urban atmosphere is less stable than its rural counterpart. To take this into account during the daytime a stability category one step more unstable than for the "rural" airport situation is used, i.e., m is decreased by unity except for the case m = 1, for all the area source calculations. When the rural stability category is P_5, corresponding to a nighttime surface inversion, the neutral stability category P_4 is assumed to apply for both the area and point source calculations in the urban situation (so that for urban applications the values of the constants a, b, c above are not needed for P_5).

The second modification of the values of $\sigma_z(x; P_m)$ attempts to incorporate an experimental finding of Pooler (1966) that for low level releases of tracer material in an urban area the data are best represented by assigning an initial value σ_0 at x = 0. [Note in the above table of σ-values $\sigma \rightarrow 0$ as $x \rightarrow 0$.] This initial value is added to the Pasquill-Gifford values obtained from the table above. In the urban air pollution model, an initial value of 30 meters is assumed for low level sources (an effective source height of 20 meters or less). Arbitrarily this initial value is decreased linearly to zero as the effective source height increases to 50 meters and is then taken as zero when the source height exceeds 50 meters. In all cases it is convenient to incorporate the effect of the initial σ_o by use of the virtual source concept, i.e., by regarding the σ_o-values as the result of diffusion from an imaginary source located upwind of the real source and then adding the virtual source distance to the actual physical distance.

The mixing depth L that occurs in the formulation of the model varies greatly diurnally, seasonally, and annually. Since it is impractical to account for all these variations, a procedure reflecting only major changes is used. The procedure determines an effective mixing depth by modifying the average maximum (afternoon) mixing depths, as tabulated by Holzworth (1964), depending on the stability category being considered. Stability categories P_1, P_2, P_3, are afternoon conditions, with P_1 corresponding to very unstable conditions. With P_1, the value of L is assumed to be 50% greater than the climatological value tabulated by Holzworth; with P_2 or P_3 the climatological value is adopted. According to the objective criteria of Turner, the stability category P_5 can only occur at night under conditions when ground-based inversions would occur over open level country. Since a shallow layer of neutral or weak lapse conditions has been found to occur over urban areas, even with strong nocturnal surface inversions in the surrounding rural areas, a mixing depth $L = 100$ meters is adopted for stability category P_5, when the latter is indicated by the objective criteria. The 100-meter value is suggested by some observations of Clarke (1969). Stability category P_4 is a neutral stability condition that may occur either during the day or at night. In the present version of the model, it was divided into day and night sub-classes. The Holzworth climatological mean value was associated with a daytime case, and the arithmetic average of the daytime value and the 100-meter value above associated with a nighttime case.

To apply the Martin-Tikvart model, it is necessary to estimate the effective heights of pollutant emission for both the area and point sources. For the low level area sources (predominately residential and commercial heating), an average height emission may be estimated roughly from consideration of building heights. It is not usual to apply any correction for plume rise to these small sources. In the application to St. Louis, Missouri, considered in the next section, a constant effective height of 20 meters was assumed for all the area sources. As previously indicated, if this height is not considered constant for the entire urban area, it is necessary to modify the procedure for numerical evaluation of the area source concentration integral of equation (17). For the large point sources considered through equation (15), the effective source height h is determined from the physical stack height h* and the estimated plume rise Δh, i.e., $h = h^* + \Delta h$. The plume rise equation used in the original Martin-Tikvart model (and in the calculations of the next section) is from Holland (1953) and is given by

$$\Delta h = \frac{V_s d}{U}\left[1.5 + 2.68 \times 10^{-3} P\left(\frac{T_s - T_a}{T_s}\right)d\right]$$

where V_s = stack gas exit velocity (meters/sec)
d = stack exit diameter (meters)
U = mean wind speed (meters/sec)
P = atmospheric pressure (mb)
T_s = stack gas exit temperature (°K)
T_a = ambient air temperature (°K)

Since this equation is appropriate for the neutral stability condition, it must be modified for application over a range of stability conditions. The following modification has been used to allow for a range from 1.3 Δh for very unstable conditions to $0.9\Delta h$ for the most stable.

$$h = h^* + \Delta h(1.4 - 0.1\, m) \qquad (m = 1, 2, 3, 4, 5)$$

and is a crude attempt to account for the increase of plume rise with decreasing stability. However, it is recommended that for future applications the old plume rise formula of Holland should be replaced with the more recent ones suggested by Briggs (1969).

Finally, note that for some point sources (e.g. power plants with tall stacks), the effective emission height ($h^* + \Delta h$) may be greater than the mixing depth when the latter is small. On the assumption that the plume will not diffuse downward through the stable layer, these cases are identified and eliminated from consideration in the Martin-Tikvart model.

VI. AN APPLICATION WITH DISCUSSION

The model was originally applied in 1968 to the calculation of average sulfur dioxide concentrations during the winter months (1 Dec. 1964 to 28 Feb. 1965) for St. Louis, Missouri, since comprehensive data was available from a special air pollution study (Farmer and Williams, 1966). However, the data on emissions inventory, air quality, and meteorological conditions that are used in the present calculations were specially compiled by Turner and Edmisten (1968). The area-source emissions inventory was provided for 1200 squares (30 x 40); each square was 5000 ft. on a side. This area completely surrounded a central region of 17 x 19 squares within which an air quality network of 40 sampling stations with 24-hour SO_2 bubblers was located for the 3-month period. In addition, 62 major point sources were considered individually in the emissions inventory. The meteorological joint frequency distribution required for use with the model was determined from hourly observations covering the 3-month period at the Lambert Field Weather Bureau. As the topography is relatively flat and umcomplicated, the observations are assumed to be representative of the entire St. Louis area. In effect, the joint frequency function pre-digests the meteorological data into a discrete number of possible cases. Since wind speed is classified into 6 categories, wind direction into 16 categories, and stability into 6 categories (here with differentiation between nighttime and daytime category 4), the distribution covers 6 x 16 x 6 = 576 cases. Finally, the average climatological mixing depth was estimated from rawinsonde observations made at neighboring Columbia, Missouri, and Peoria, Illinois. The mean depth for the three winter months in question was 800 meters.

Calculations of average air quality were made using an IBM 360-50 computer, and the running time was 1.6 minutes per receptor location. An IBM 1130 was then used to calculate regression lines of observed versus calculated concentrations, and, by coupling with a CALCOMP plotter*, also to generate the isopleths of average pollution concentrations that follow. The results of several different calculations are given in Figures 2 through 7.

Figure 1 is a computer generated map of the isopleths of 3-month average observed SO_2 concentrations (in $\mu g/m^3$) for the central area of 17 x 19 squares in which the air quality network was located. Figure 2 is the isopleth map for the average concentrations as calculated by straightforward application of the model, and Figure 3 is a corresponding regression of the observed versus calculated values for the 40 sampling stations of the network. If y and x denote observed and calculated values, respectively, then

$$y = 0.26x + 19.98$$

with a correlation coefficient $r = 0.775$. Therefore, in this case, the model overcalculates the average concentrations by an appreciable factor. In an attempt to improve agreement with observations, calculations were also made employing some simple modifications of the basic model. The latter only uses a single representative wind speed for a given time and thus disregards the known increase of wind speed with height above the ground. However, a wind speed more prepresentative of the transport and diffusion of pollutant from large, elevated point sources would probably be that estimated to occur at the appropriate effective height for each point source. A crude estimate of this speed may be made by extrapolating the surface speed (actually the 10-meter airport wind) using a simple power law of the form

$$\frac{u(z)}{u(z_1)} = \left(\frac{z}{z_1} \right)^p$$

where, following DeMarrais (1959), the exponent p is taken to be a function of the stability category. For the present calculations, the following values were assumed

---

*CALCOMP is the manufacturer's name for an X-Y plotter that is used to generate the isopleths. The program for this operation is an IBM routine entitled "Numerical Surface Techniques and Contour Map Plotting" (113-CX-11X).

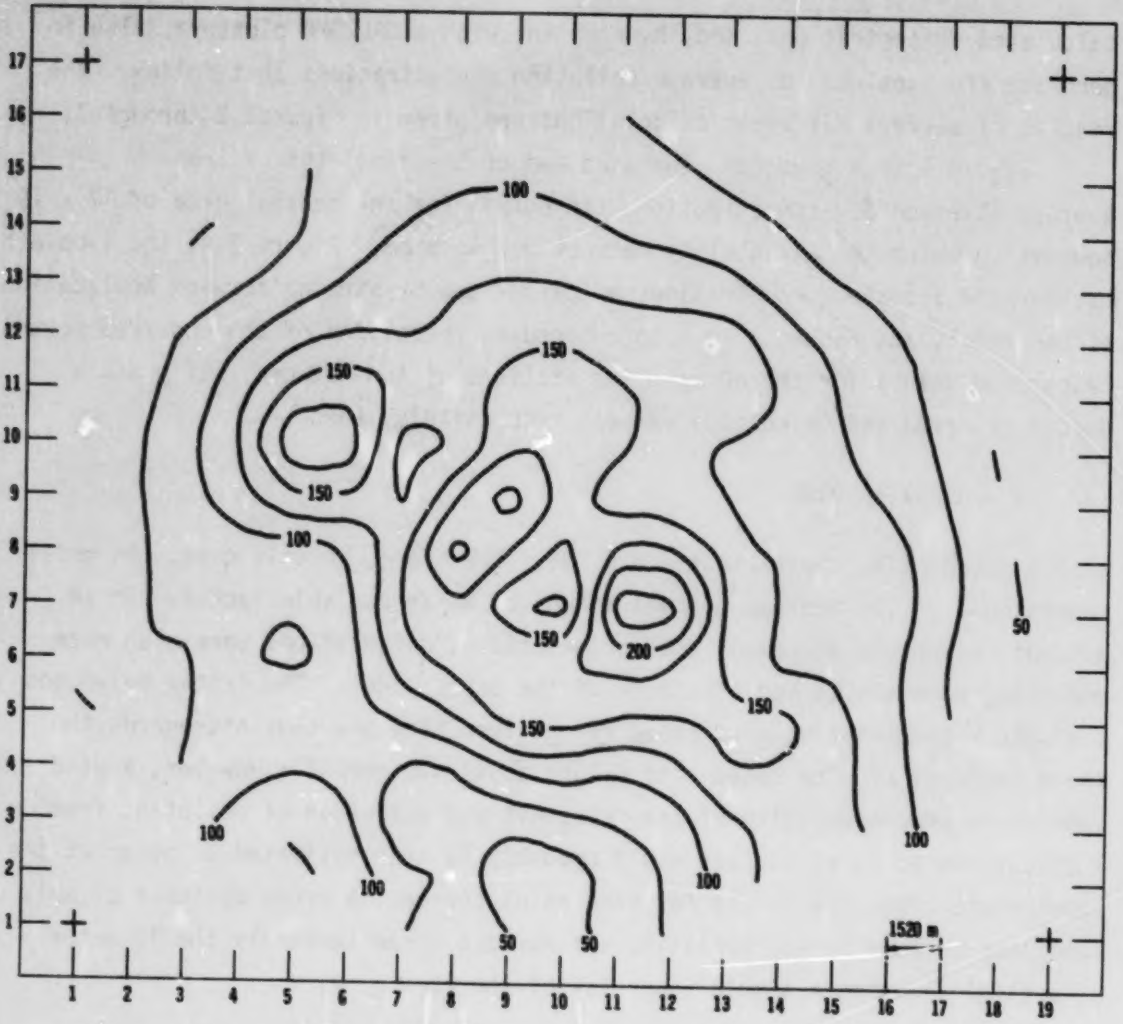
100
150
150
150
100
150
150
200
150
150
100
100
100
100
100
50
50
50
1520 m
1
2
3
4
5
6
7
8
9
10
11
12
13
14
15
16
17
18
19

Figure 1. Isopleths of observed average SO_2 concentration ($\mu g/m^3$) for period December 1, 1964, through February 28, 1965.

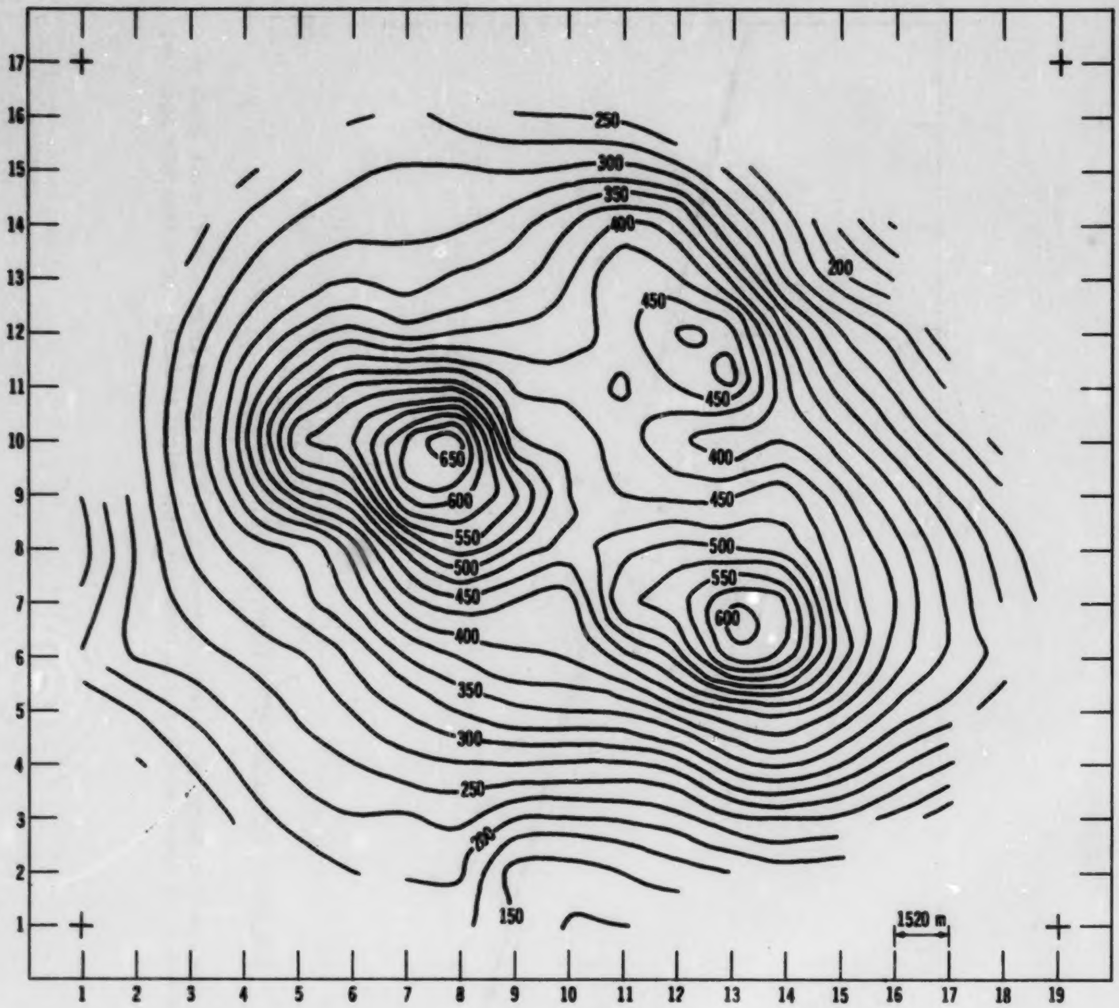
17
16
15
14
13
12
11
10
9
8
7
6
5
4
3
2
1
1
2
3
4
5
6
7
8
9
10
11
12
13
14
15
16
17
18
19
250
300
350
400
450
450
400
450
500
550
600
650
600
550
500
450
400
350
300
250
200
150
200
1520 m

Figure 2. Isopleths of computed average SO_2 concentration ($\mu g/m^3$) for the period December 1, 1964, through February 28, 1965. For this calculation, wind speed was assumed constant with height and SO_2 decay rate was assumed to be zero.

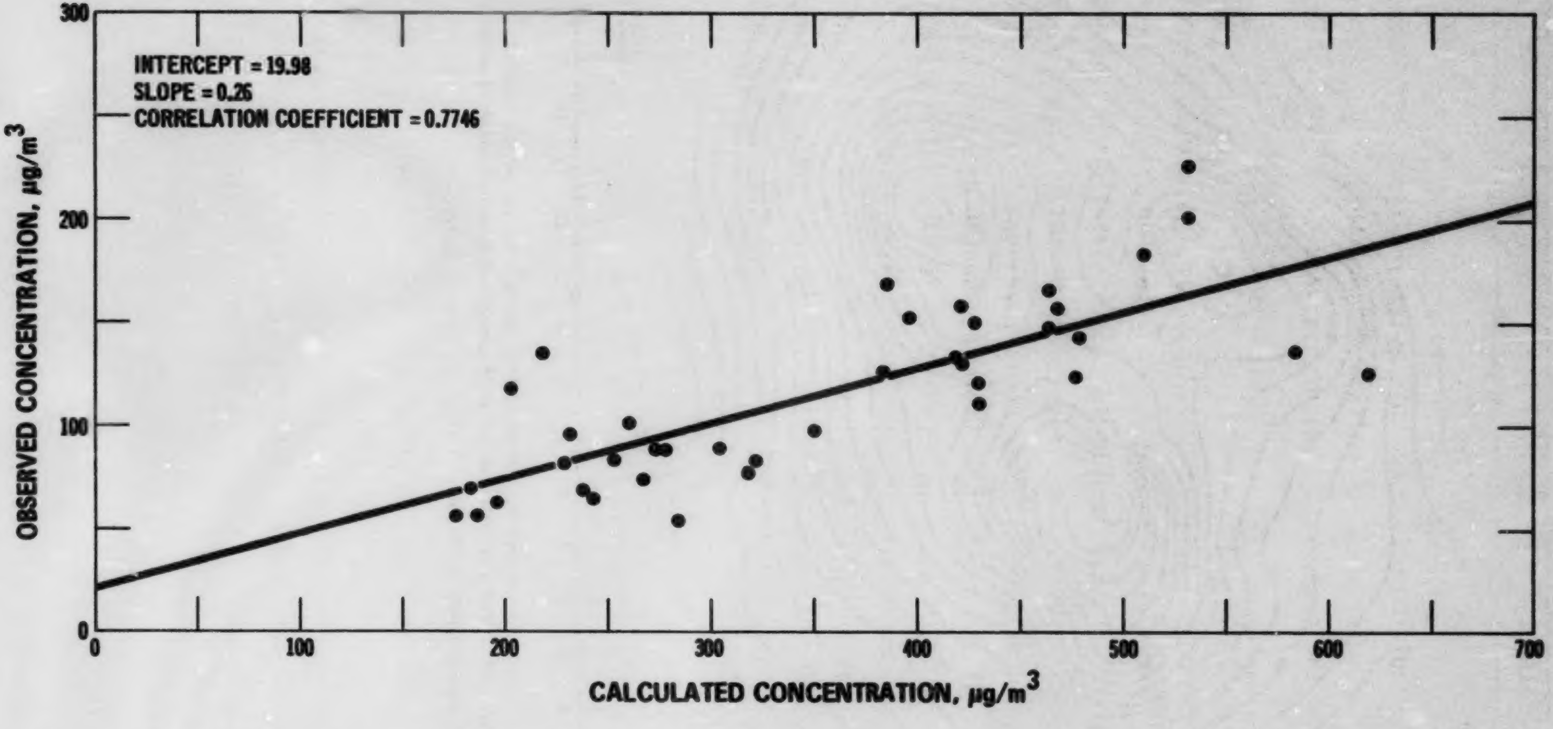

Figure 3. Regression line of observed versus calculated average SO_2 concentration ($\mu g/m^3$) for period December 1, 1964, through February 28, 1965. For this calculation, wind speed was assumed constant with height and SO_2 decay rate was assumed to be zero.

Stability category	1	2	3	4	5
P	0.1	0.15	0.2	0.25	0.3

The results of calculations made on this basis are shown in Figure 4 and 5. Figure 4 shows the calculated concentration isopleths, while Figure 5 shows the regression of the observed on calculated values. In this case,

$$y = 0.32x + 20.26$$

with a correlation coefficient $r = 0.772$. Again, the model overcalculates although to a slightly smaller degree. The final set of calculations, represented in Figures 6 and 7, were made to provide some indication of the effect of assuming that SO_2 pollutant is subject to some removal process in the atmosphere which might considerably reduce the ground-level concentrations. A recent paper (Weber, 1970) indicates that, depending on the meteorological conditions, a loss of almost 50% may occur in a period of 20 minutes to 1 hour. Calculations were, therefore, made assuming an exponential decay of SO_2 with travel time using a half-life value $T_{1/2} = 30$ minutes (also a single representative wind speed was assumed for these calculations). Figure 6 shows the isopleths based on the calculated values, and Figure 7 shows the regression line of observed on calculated values. In this case

$$y = 0.39x + 52.05$$

with a correlation coefficient $r = 0.786$. Thus, in spite of the high decay rate, the model still systematically overcalculates the average concentration values.

Unambiguous reasons for this feature are not clear, although a number of possibilities are under study at the present time. Some of the probable shortcomings of the model are identified in the discussion that follows. Although the model is conceptually quite simple, the superposition of the effects produced by a complex distribution of pollution emissions and under a complex sequence of meteorological conditions quickly obscure the simpler quantitative properties of the model in the massive details of particular

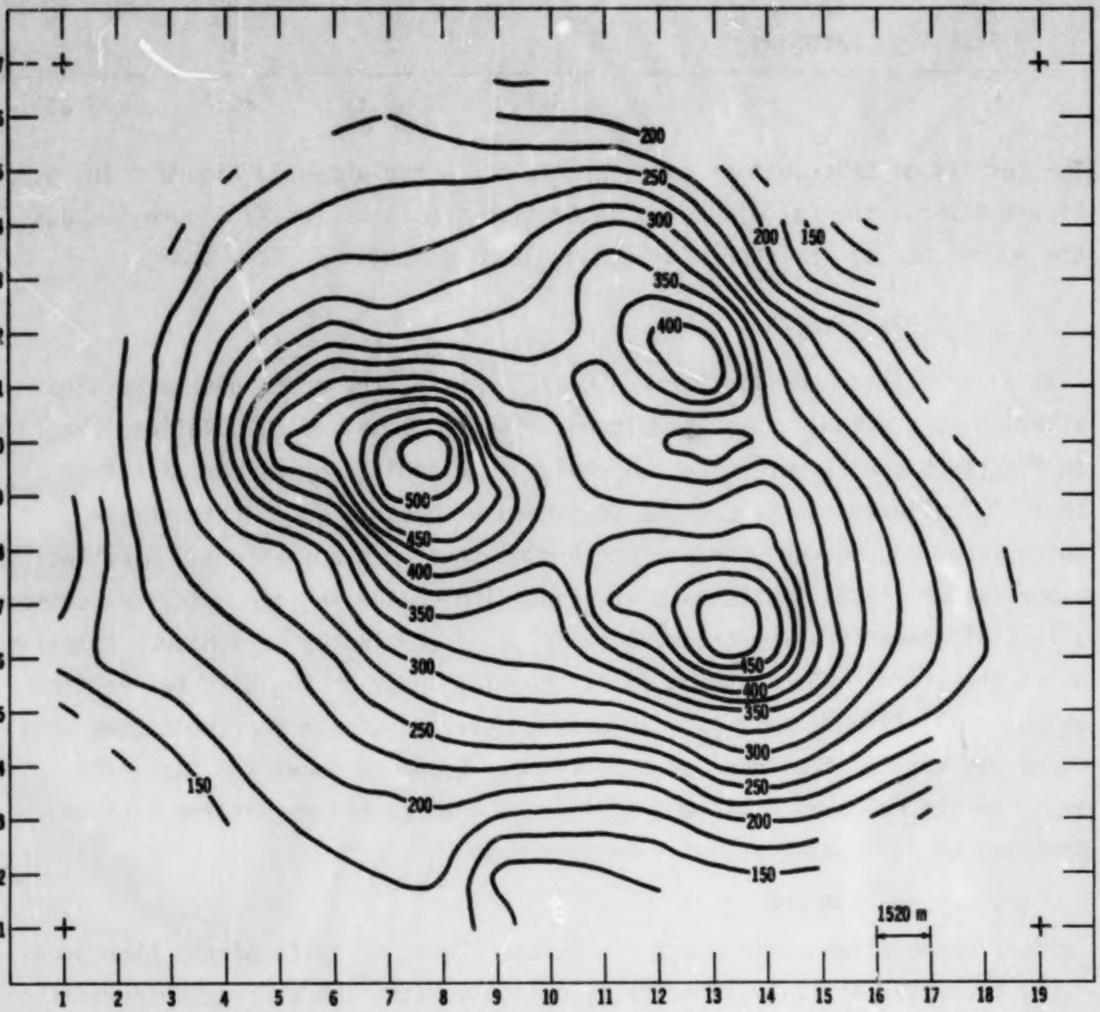
17
16
15
14
13
12
11
10
9
8
7
6
5
4
3
2
1
1
2
3
4
5
6
7
8
9
10
11
12
13
14
15
16
17
18
19
200
250
300
350
400
200
150
500
450
400
350
300
250
200
150
450
400
350
300
250
200
150
1520 m

Figure 4. Isopleth of computed average SO_2 concentration ($\mu g/m^3$) period December 1, 1964, through February 28, 1965. For this calculation, a power-law wind profile was introduced and SO_2 decay rate was assumed to be zero.

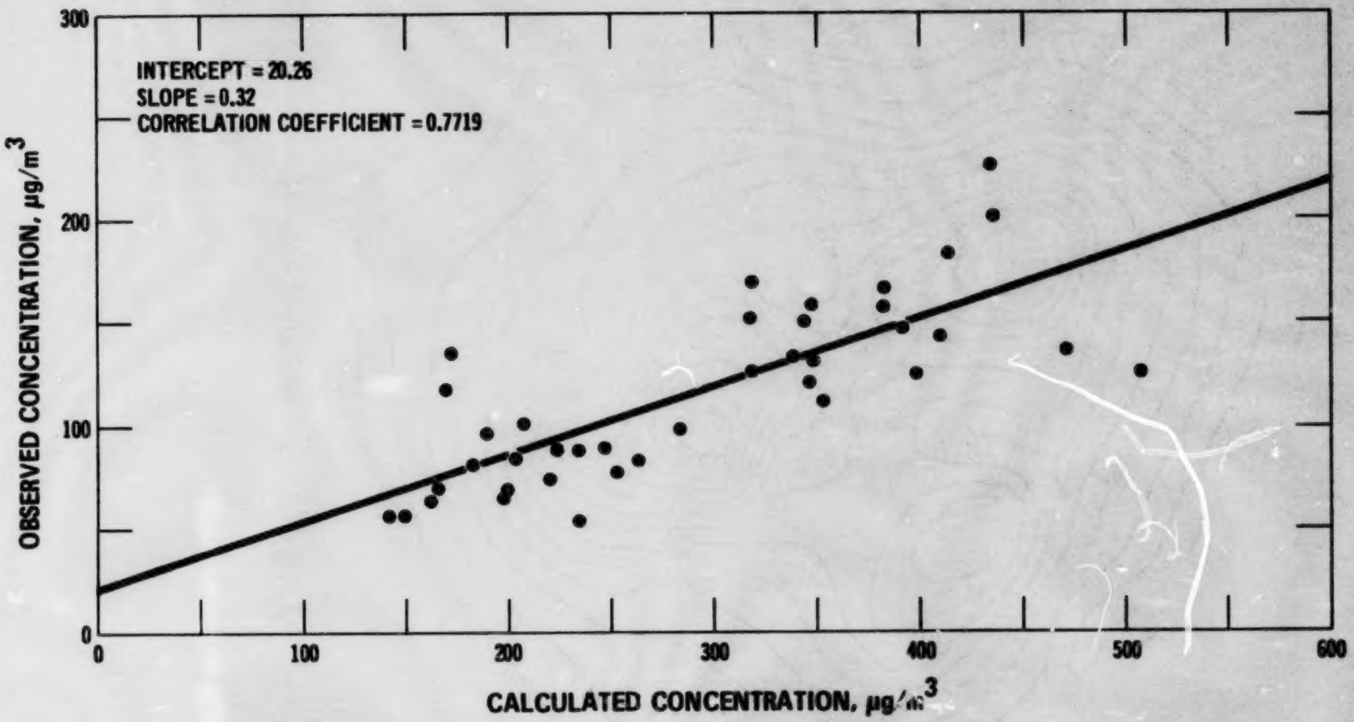

Figure 5. Regression line of observed versus calculated average SO_2 concentration ($\mu g/m^3$) for period December 1, 1964, through February 28, 1965. For this calculation, a power-law wind profile was introduced and SO_2 decay rate was assumed to be zero.

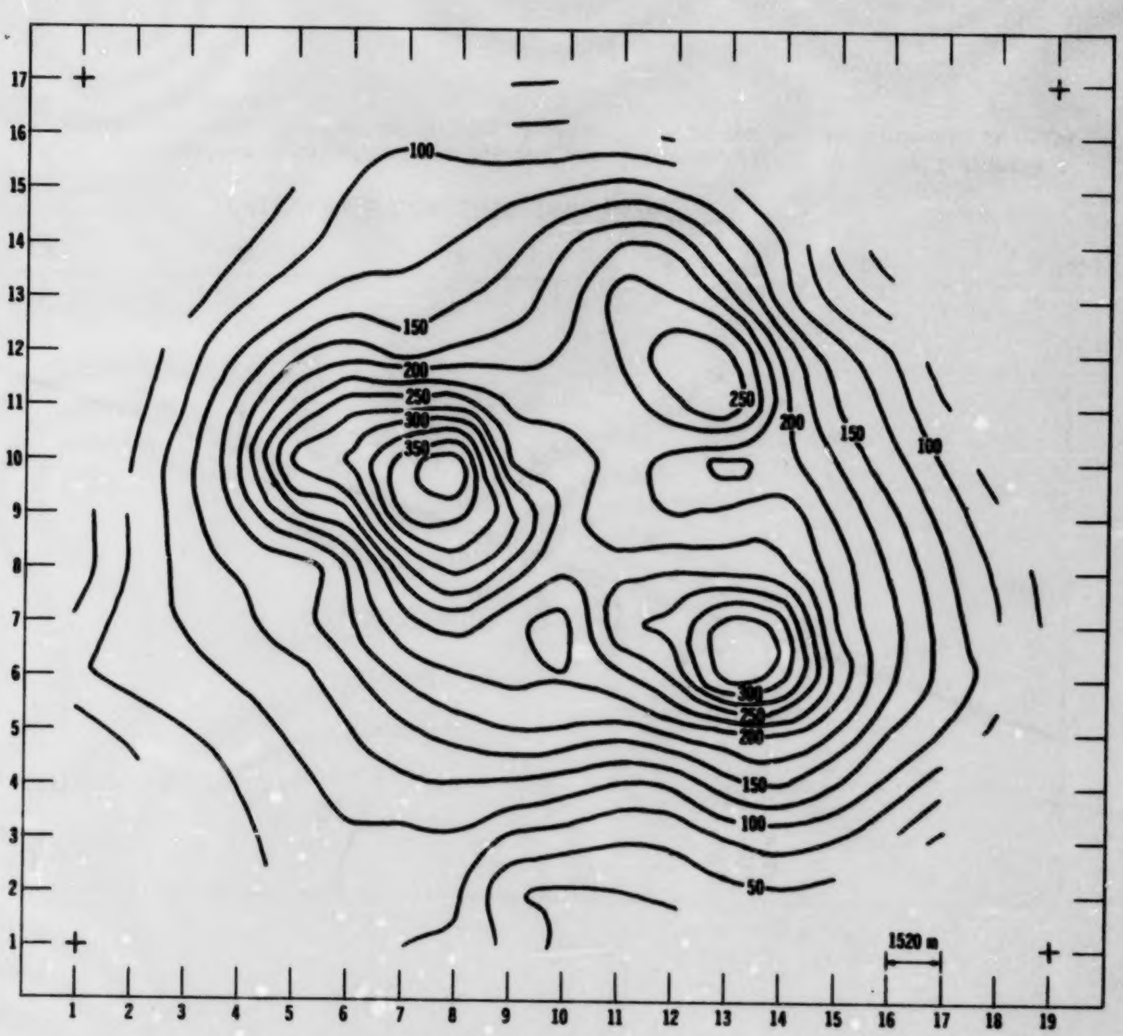
100
150
200
250
300
350
250
200
150
100
300
250
200
150
100
50
1520 m
1
2
3
4
5
6
7
8
9
10
11
12
13
14
15
16
17
18
19

Figure 6. Isopleths of computed average SO_2 concentration (μg/m^3) for period December 1, 1964, through February 28, 1965. For this calculation, wind speed was assumed constant with height and SO_2 half-life was assumed to be 30 minutes.

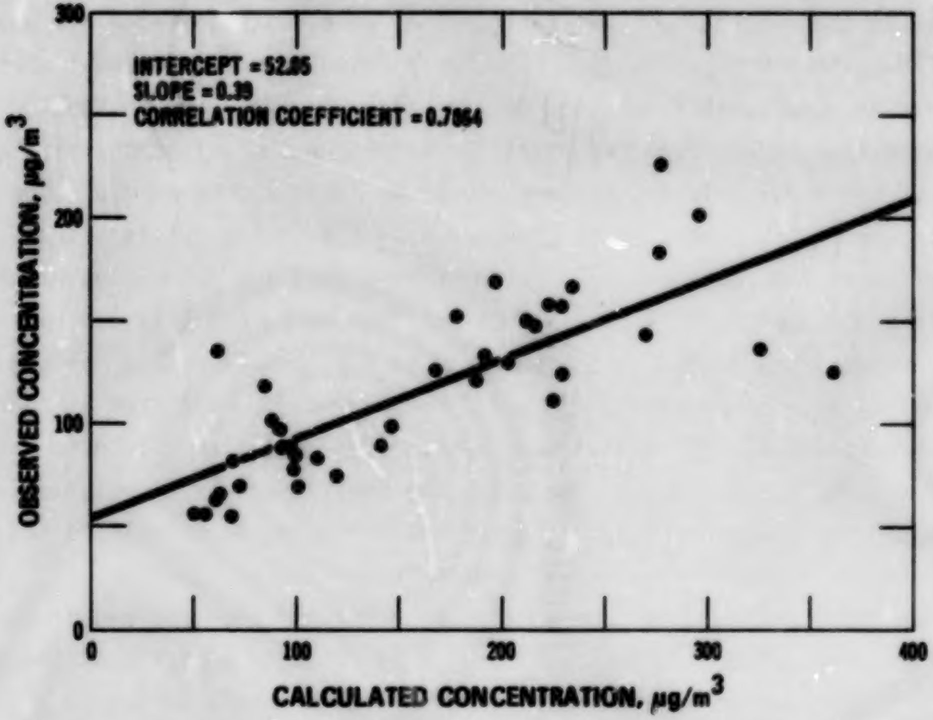

Figure 7. Regression line of observed versus calculated average SO_2 concentration ($\mu g/m^3$) for the period December 1, 1964, through February 28, 1965. For this calculation, wind speed was assumed constant with height and SO_2 half-life was assumed to be 30 minutes.

applications. Under these circumstances, the numerical properties, i.e., the relationship between model output and its numerous inputs, are only poorly understood. To improve understanding, the model is currently being subjected to an input-output sensitivity analysis.

The urgent practical need to apply the Martin-Tikvart model immediately and prior to further development and analysis has given rise, as an interim measure, to the concept of "calibrating" the model with observed air quality data (TRW Systems Group, 1969). As in the particular examples considered above for St. Louis, this involves determination of the least-squares regression line of observed concentration values on the values calculated by use of the model. If the scatter of points about the regression line is small enough for thelatter to be regarded as a statistically significant description of the relationship between the observed and calculated values, then, in other applications of the model to the same urban area and over the same climatological period, e.g., to estimate air quality with a different hypothetical source inventory, the model output would be adjusted at each receptor location according to the regression line equation. To determine whether the regression line is adequate, the coefficient of correlation, a measure of the data scatter about the regression line, is calculated and interpreted by standard statistical procedure.

Finally, some more obvious sources of error and shortcomings of the model should be noted. In the absence of a sensitivity analysis of the type mentioned, any attempt to provide a complete listing could amount to self-deception, and we therefore mention only the following:

(a) It is evident that emissions inventory estimates are inherently crude and subject to uncertainties. One shortcoming of the model in its present form is that it uses a constant average emissions inventory although significant variations must occur throughout the day, day-to-day and seasonally. The fact that the assumption of a diurnally constant emission rate may lead to overcalculation of concentrations has been previously noted by Clarke (1964) and Turner (1964), who indicated the need for a lower emission rate at night. That this is a source of overcalculation in the Martin-Tikvart model was demonstrated by some ad hoc calculations, although difficulty of developing a generally applicable objective scheme for specifying diurnal variability of emissions is apparent.

(b) The climatological data used in the model calculations must, in practice, frequently be obtained from a nearby airport weather station, and is a poor indication of urban meteorological conditions. Particular caution should be exercised in applying the model to any locales where the topography is at all complicated.

(c) The method proposed for estimating the mixing depth for use in the model calculations is very crude. Better modeling should result when data based on actual atmospheric soundings can be utilized. It is particularly desirable to refine the estimates of nighttime mixing depth as it may be shown, when the concentration calculations are separated by stability category, that the contribution from the nighttime stability category P_5 (when a 100 meter mixing depth is assumed) is frequently much greater than from all other stabilities even though P_5 only represents about 25% of the total observations.

REFERENCES

Bierly, E. W., and Hewson, E.W., 1962: Some restrictive meteorological conditions to be considered in the design of stacks. J. Appl. Meteorol., 1, 3, 383-390.

Briggs, G. A., 1969: Plume Rise. A.E. C. Critical Review Series, U.S. Atomic Energy Commission, Division of Technical Information

Calder, K. L., 1969: Some miscellaneous aspects of current urban pollution models, Symposium on multiple source urban diffusion models, Univ. of North carolina, Chapel Hill (To be published)

Clarke, J.F., 1964: A simple diffusion model for calculating point concentrations from multiple sources. APCA Journal, 14, 9, 347-352.

Clarke, J.F., 1969: Nocturnal urban boundary layer over Cincinnati, Ohio Monthly Weather Review, 97, 8, 582-589.

DeMarrais, G. A., 1959: Wind speed profiles at Brookhaven National Laboratory J. Appl. Meteorol., 16, 181-189.

Farmer, J.R., and Williams, J.D., 1966: Interstate Air Pollution Study, Phase II Project Report, III Air Quality Measurements, USDHEW, NAPCA, Cincinnati, Ohio.

Fortak, H., 1969: Numerical simulation of the temporal and spatial distributions of urban air pollution concentrations. Symposium on multiple source urban diffusion models, Univ. of North Carolina, Chapel Hill (To be published).

Gifford, F. A., 1961: Use of routine meteorological observations for estimating atmospheric dispersion. Nuclear Safety, 2, 4, 47-51.

Holland, J. Z., 1953: A meteorological survey of the Oak Ridge area. U.S. AEC Report ORO. 99, Tech.Inf. Serv., Oak Ridge, Tennessee.

Holzworth, G. C., 1967: Mixing depths, wind speeds, and air pollution potential for selected locations in the United States. J. Appl. Meteorol., 6, 6, 1039-1044.

Leavitt, J. A., 1960: Meteorological considerations in air quality planning. J. Air Poll. Contr. Assoc., 10, 3, 246-250.

Ozolins, G., and Smith, R., 1966: A Rapid Survey Technique for Estimating Community Air Pollution Emissions. U.S. Dept. of Health, Education, and Welfare, Public Health Service, National Air Pollution Control Administration, Raleigh, North Carolina, PHS Pub. No. 999-AP-29.

Pasquill, F., and Meade, P.J., 1958: A study of the average distribution of pollution around Staythorpe. *Int. J. Air Poll.*, 1, 60-70.

Pasquill, F., 1961: The estimation of the dispersion of windborne material *Meteorol. Mag.*, 90, 1063, 33-49.

Pasquill, F., 1962: *Atmospheric Diffusion*. Van Nostrand Co., New York.

Pooler, F., 1966: A tracer study of dispersion over a city. *J. Air Poll. Contr. Assoc.*, 16, 12, 677-681.

Szepsi, D.J., 1967: A model for the long-term distribution of pollutants around a single source. *IDOJARAS* (Budapest), 68, 257-69.

Szepsi, D.J., 1967: *Meteorological Conditions of the Turbulent Diffusion of Atmospheric Pollutants in Hungary*. Official Publications of the National Meteorological Institute, Vol. 32, Budapest.

TRW Systems Group, 1969: Air Quality Display Model. Contract No. PH 22-68-60 USDHEW, Public Health Service, National Air Pollution Control Administration, Washington, D.C.

Turner, D.B., 1961: Relationship between 24-hr. mean air quality measurements and meteorological factors in Nashville, Tennessee. *J. Air Poll. Contr. Assoc.*, *11*, 483-489.

Turner, D.B., 1964: A diffusion model for an urban area. *J. Appl. Meteorol.*, *3*, 83-91.

Turner, D.B., and Edmisten, N.G., 1968: St. Louis SO_2 dispersion model study - Description of basic data (Unpublished report, Division of Meteorology, NAPCA).

Turner, D.B., 1969: *Workbook of Atmospheric Dispersion Estimates*. USDHEW PHS, National Air Pollution Control Administration, Cincinnati, Ohio, PHS Pub. No. 999-AP-26.

Weber, E., 1970: Contribution to the residence time of sulfur dioxide in a polluted atmosphere. *J. Geophys. Res.*, 75, 15, 2909-2914.

Chapter II

A PROPOSED APPROACH ON MODELING TECHNIQUES FOR ECOLOGICAL PURPOSES USING DYNAMIC CRITERIA

A. Cardinale* - V. Gervasio - A. Marzocchi* - E. Nardelli***

*** Agip Nucleare, ENI Group**
**** ENI**

For presentation to the NATO/CCMS Panel on Modeling,
Paris, France, 26-27 July, 1971

A PROPOSED APPROACH ON MODELING TECHNIQUES FOR ECOLOGICAL PURPOSES USING DYNAMIC CRITERIA

SUMMARY

Purpose of this work is to show the possibility of describing complex problems quantitatively, such as those of ecological type, by using dynamic mathematical models which take as a starting point the works of Forrester and other on industrial dynamics.

This method consists in reducing any problem to a block diagram and in considering any correlations among the various compartments in mathematical terms.

In order to simplify the work, it has been useful to introduce the "key-substance" concept, defined as that reference substance existing in all compartments and constituting the exchange vehicle among them.

A living community may be described in terms of one or more "key-substances" such as Nitrogen for instance. An ecosystem may then be considered as the whole of compartments affected by a "key-substance" interchange.

When a "foreign" element, such as a pollutant, is introduced by any pathway in the ecosystem, such pollutant takes part in exchange mechanisms among the various compartments: the proposed mathematical model allows plotting pollutant concentration versus time in any compartment.

In order to make more clear the possibilities of such a method, an application dealing with the ecological chain affected by Iodine-131 is herein shown; Iodine-131 has been chosen since it is the critical radionuclide among fission products.

Characteristics and possibilities of general application of the proposed method are pointed out in the latter part of this work.

1. INTRODUCTION

One of the most complex natural sciences is that branch called ecology which deals with environmental biology.

The study of biotic communities and their interactions and the analysis of transfer mechanisms among populations of a same ecosystem require a systematic investigation as well as a setting-up of mathematical models allowing the quantitative description of the complex problems involved.

This work, then, has the purpose of proposing a mathematical model of dynamic type capable of describing an ecosystem's dynamics in quantitative terms.

A calculation method particularly fit for studying ecological chains and which takes as a starting point the works of Forrester(1) and others on the application of the systems theory to macroeconomics is proposed hereinafter.

2. METHODOLOGY

The calculation method is based on the well known compartment model outlining various systems components in a block diagram.

This method is full of applications in the most various fields of scientific research.

Wishing to describe, for instance, a productive community according to the systemsdynamics methodology, such a system may be considered composed of a compartment communicating with others complementary to it.

For the purpose of investigation this system can be subdivided into a good many subsystems including homogeneous elements reciprocally acting.

It is clear that the subdivision will be performed in accordance with criteria suggested by the knowledge of interaction mechanisms among the subsystems, the number of which is consequently proportional to the degree by which the aforementioned mechanisms are known.

The example shown in fig. 1 describes a human community in its productive activity together with the environment surrounding it.
In order to simplify the investigation, such a community may be considered as being subdivided into the following five subsystems:

1) Productive subsystem , including all human productive activities: industry, agriculture, etc. (the system is illustrated in fig. 1 by compartment n. 3)

2) Properties subsystem: embracing the whole of properties of which the human community is the consumer. (compartment n. 4)

3) Treatments subsystem (compartment n. 5)
In order to evaluate environmental pollution, the human activity may finally be considered as a waste production; consequently, adequate treatment measures are necessary especially for the most elevated stage of industrial development.

4) Chemical-Physical Environment, in which the productive community acts; this environment, disturbed by humans is constituted by air, water and soil and may be considered as the exchange medium of the community energy fluxes. (compartment n. 6)

5) Subsystem constituted by organisms living in the environment (man excluded) in which the productive community acts. (compartment n. 7)

Among the various subsystems, the interactions shown in fig. 1 exist; these may be expressed in mathematical terms once transfer constants or variation indexes are found.
It is intuitive that the same community may be represented by a set of subsystems different from those illustrated and that it can also be represented in mathematical form provided interactions among the various compartments are known.

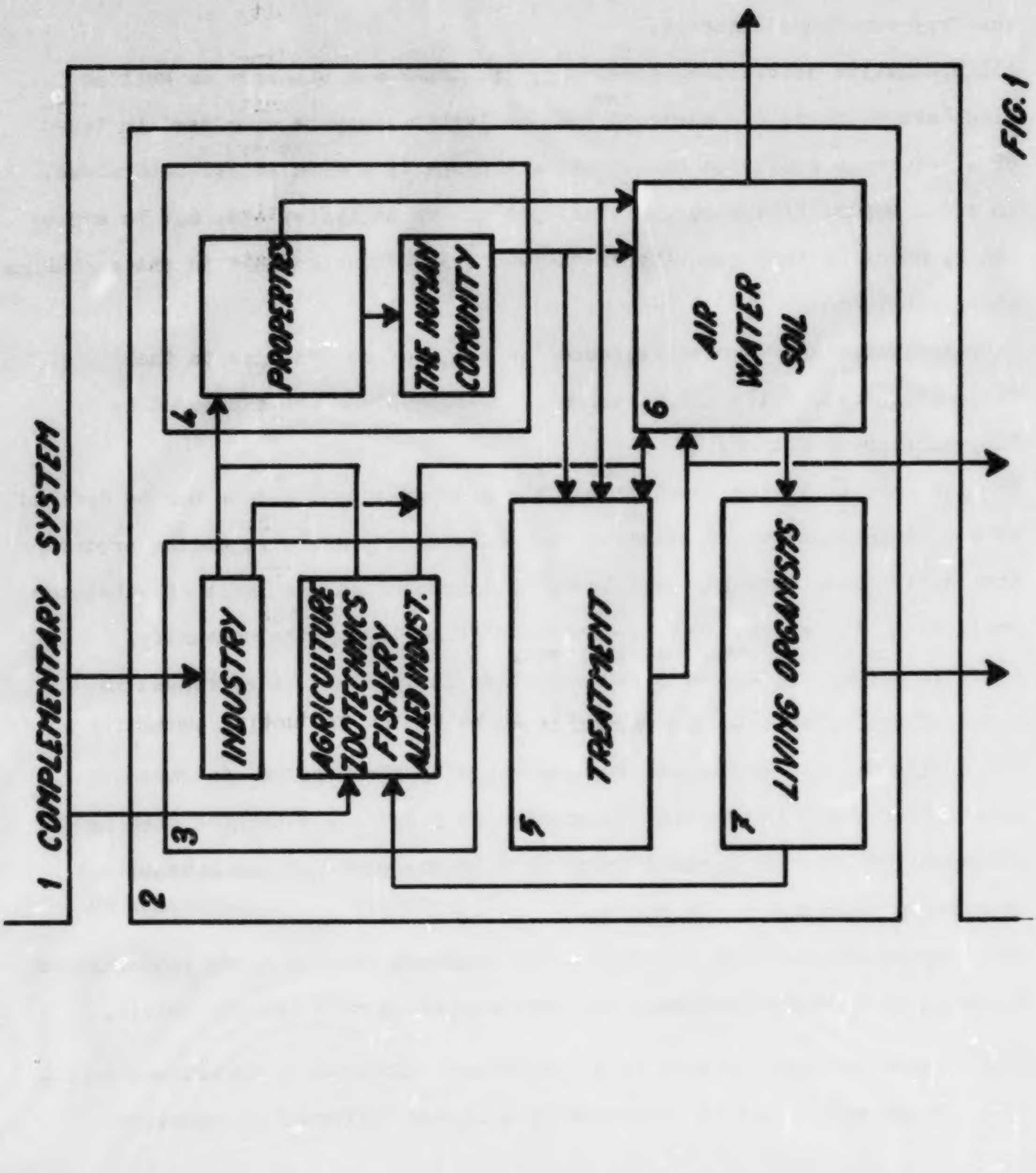
1 COMPLEMENTARY SYSTEM
2
3
INDUSTRY
AGRICULTURE
ZOOTECHNICS
FISHERY
ALLIED INDUST.
4
PROPERTIES
THE HUMAN COMMUNITY
5
TREATMENT
6
AIR
WATER
SOIL
7
LIVING ORGANISMS

FIG.1

In order to simplify the mathematical treatment it is useful to introduce the "key-substance" concept.

All productive activities, consuming, treatment and exchange as well as biosphere which is the abode of such activities, may be expressed in terms of a reference substance constituting a property common to all subsystems. In other words, living communities, productive activity, etc. may be expressed by means of that quantity of "key-substance" taking part in the exchanges among subsystems.

Each subsystem may then be expressed in terms of equivalence to the "key-substance", while interactions among subsystems are expressed by "key-substance" fluxes.

For the case of living communities, the aforesaid equivalence can be defined as a certain quantity of existing "key-substance", while regarding productive activities, such an equivalence is expressed as the ratio of substance produced to the amount of "key-substance" existing in the community.

In other words, all elements and variation indexes may be expressed in terms of equivalence to the "key-substance".

The choice of "key-substance" is determined by the type of system under examination. For the system illustrated in fig. 1, a substance such as Nitrogen, Carbon, etc., which takes part in the physical and biochemical transfer mechanisms can be chosen.

The "key-substance" then constitutes the exchange vehicle among compartments allowing an immediate mathematical representation with dynamic models.

The "key-substance" balance of a compartment affected by interchanges with other compartments can be expressed by a linear differential equation:

$$\frac{d\,y_1}{d\,\tau} = \frac{y_2}{\tau} - \frac{y_1}{\tau'}$$

where τ and τ' represent the "key-substance" transfer constants among compartments.

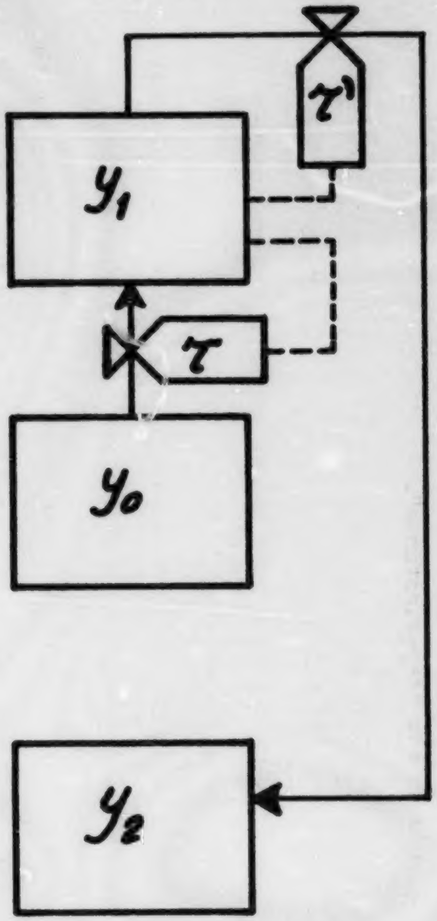
y_1
τ'
τ
y_0
y_2

$$\frac{dy_1}{dt} = \frac{y_1}{\tau} - \frac{y_1}{\tau'}$$

FIG 2

An example which best illustrates the above concepts is that of the food chains (fig. 3) where Nitrogen may be chosen as "key-substance".

It is of common knowledge that in such a chain Nitrogen is present in different aggregation levels: in fact it exists as an element in the atmosphere from where it is fixed in soil by nitrobacteria, and may exist in more aggregated forms such as proteins which are the most evolved forms of living components.

When a "foreign" element (fig. 3), such as a pollutant, is introduced in the ecosystem, it takes part in transfer mechanisms among the various components of the food chain finally reaching man.

The pollutant may be introduced in any compartment of the food chain; in fact it is not always introduced in the substratum constituted by air, water and soil: the use of chemical additives in poultry feed is an example of the introduction of a pollutant at a higher level of the food chain.

MASS BALANCE OF A FOREIGN ELEMENT INTRODUCED IN FOOD CHAINS

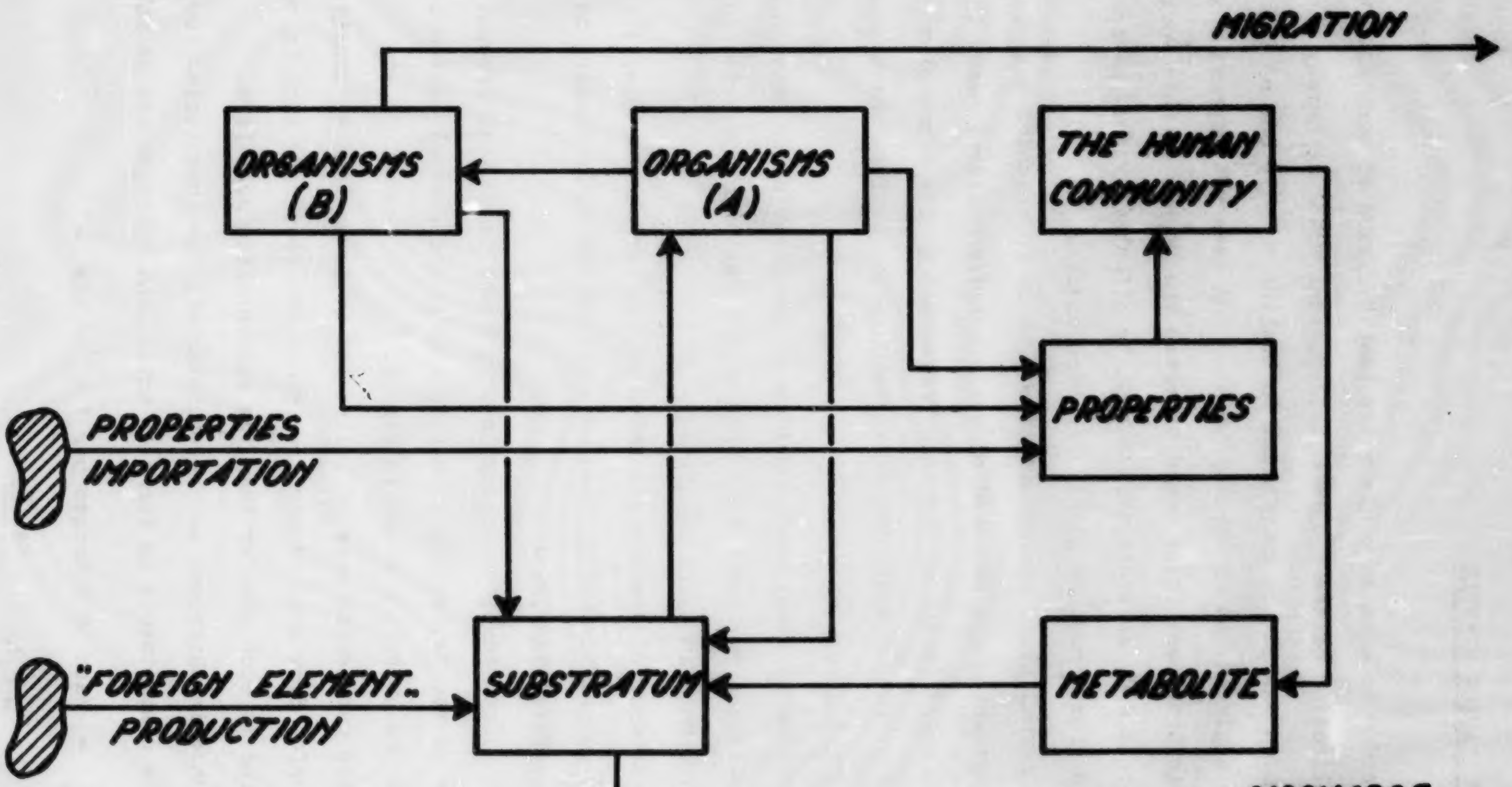
MIGRATION
ORGANISMS (B)
ORGANISMS (A)
THE HUMAN COMMUNITY
PROPERTIES
PROPERTIES IMPORTATION
"FOREIGN ELEMENT" PRODUCTION
SUBSTRATUM
METABOLITE
DISCHARGE

FIG. 3

3. APPLICATION EXAMPLE

In order to make more clear the possibilities of such a method, an application of the proposed mathematical model is hereby shown. Such an example is only meant to outline roughly one of the possible applications of systemsdynamics and does not represent a systematic treatment which would overstep the bounds of this work.

To this end, an ecological community affected by the gaseous effluents from a nuclear plant, has been chosen.

The normal plant operations give rise to radioactive material releases which are composed of various radionuclides; among these, Iodine-131 is one of the more "critical" in the sense given to this term by ICRP(2) (namely are "critical" those nuclides which cause the greatest injury to exposed individuals).

A systematic study must consider all possible paths through which a pollutant may reach man, when such a pollutant is released to the environment in which man lives.

In the case of atmospheric releases, as for our example, a simplified yet sufficiently drawn up model of the paths leading to man is illustrated in Fig. 4.

A well focused biecological study, which takes into account the fate of the pollutant, allows to reduce the general system of figure 4 to the subsystem shown in Fig. 5.

In the particular case of Iodine-131 it is useless to consider its transfer from soil to herbage, since the residence time in soil of Iodine is much greater than the radionuclide mean life.

By choosing Nitrogen as "key-substance", the inventories for the various compartments in terms of equivalent Nitrogen are as follows:

$$x_o = \text{Mass of Nitrogen per 1 } m^3 \text{ of air} =$$

$$= 0{,}94 \quad \frac{kg\ N_2}{m^3\ air}$$

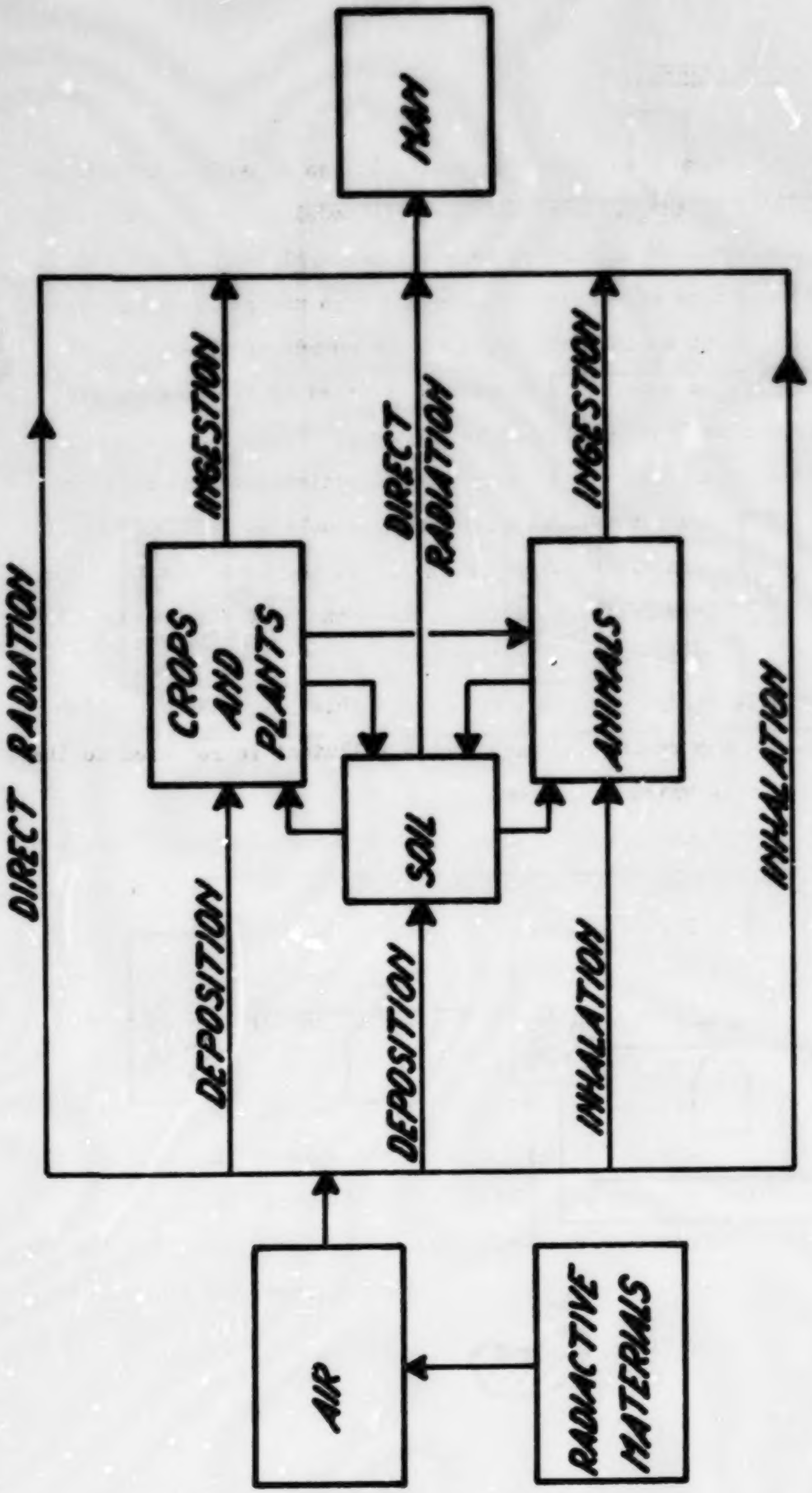
MAN
DIRECT RADIATION
INGESTION
DIRECT RADIATION
INGESTION
CROPS AND PLANTS
ANIMALS
SOIL
DEPOSITION
DEPOSITION
INHALATION
INHALATION
AIR
RADIACTIVE MATERIALS

FIG. 4

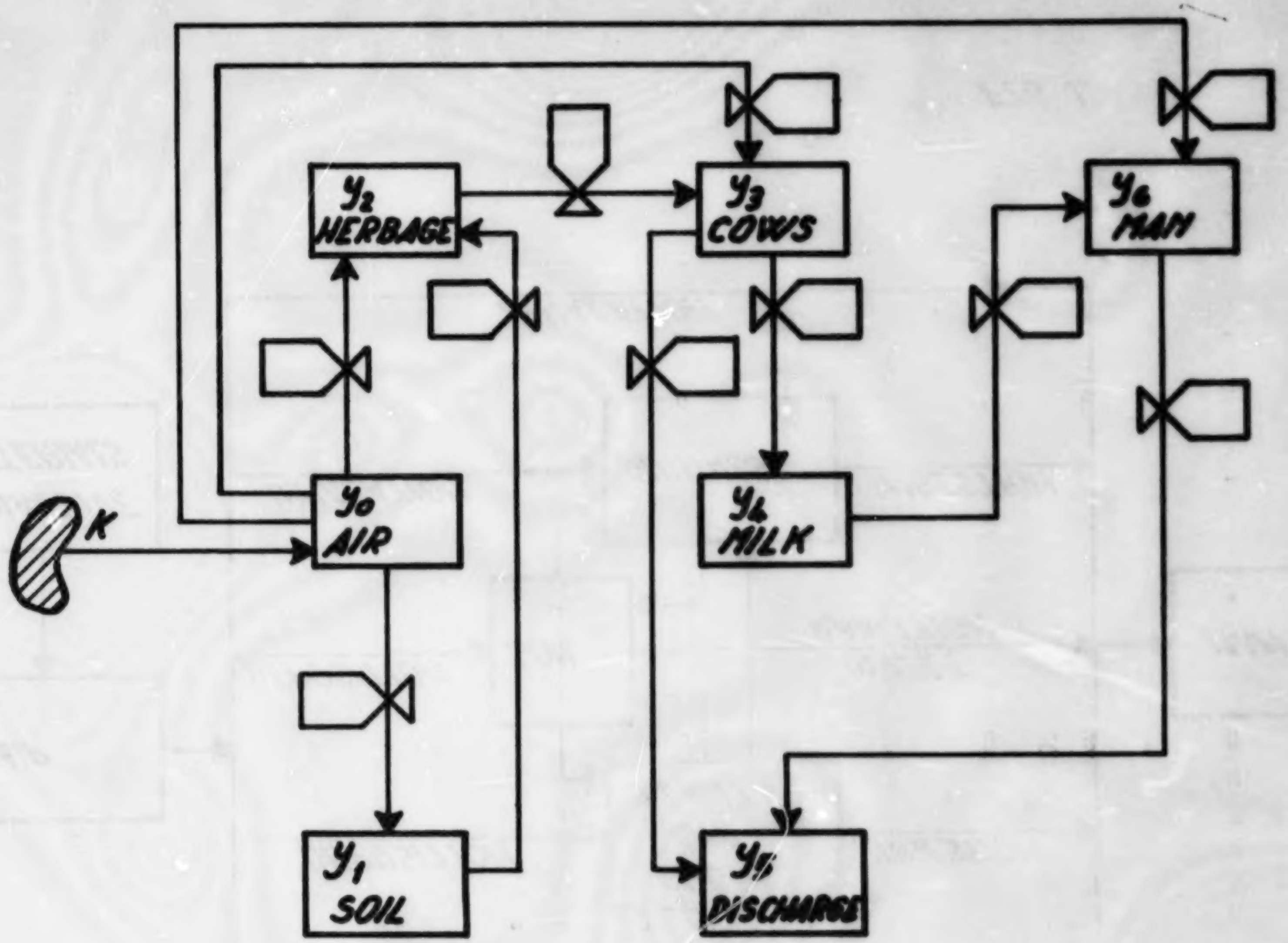
K
y_0 AIR
y_1 SOIL
y_2 HERBAGE
y_3 COWS
y_4 MILK
y_5 DISCHARGE
y_6 MAN

FIG. 5

x_2 = Mass of Nitrogen (4%) present in herbage daily injested (50 kg) by a cow(3) =
= 4% x 50 = 2 kg

x_3 = Mass of Nitrogen (3,2%) present in the standard cow (500 kg)(3) =
= 500 x 0,032 = 16 kg

x_4 = Mass of Nitrogen present in 1 kg of milk(3) =
= 0,033 kg

x_5 = Mass of Nitrogen present in 1 kg of cow excreta(3) =
= 0,012 kg

x'_5 = Mass of Nitrogen present in 1 kg of man excreta(4) =
= 0,01 kg

x_6 = Mass of Nitrogen (3%) present in the standard man (70 kg)(4) =
= 2,1 kg

The mass balance in each compartment is given by the following differential equations:

$$\frac{d\,y_o}{d\,t} = K - \left(\frac{1}{\tau_{o6}} + \frac{1}{\tau_{o3}} + \frac{1}{\tau_{o2}} + \frac{1}{\tau_r}\right) y_o = \qquad \text{AIR}$$

$$= K - \frac{y_o}{T_o}$$

$$\frac{d\,y_2}{d\,t} = \frac{y_o}{\tau_{o2}} - \left(\frac{1}{\tau_{23}} + \frac{1}{\tau_r}\right) y_2 = \qquad \text{HERBAGE}$$

$$= \frac{y_o}{\tau_{o2}} - \frac{y_2}{T_2}$$

$$\frac{d\,y_3}{d\,t} = \frac{y_o}{\tau_{o3}} + \frac{y_2}{\tau_{23}} - \left(\frac{1}{\tau_{35}} + \frac{1}{\tau_{34}} + \frac{1}{\tau_r} \right) y_3 = \qquad \text{COW}$$

$$= \frac{y_o}{\tau_{o3}} + \frac{y_2}{\tau_{23}} - \frac{y_3}{T_3}$$

$$\frac{d\,y_4}{d\,t} = \frac{y_3}{\tau_{34}} - \left(\frac{1}{\tau_{46}} + \frac{1}{\tau_r} \right) y_4 \qquad \text{MILK}$$

$$= \frac{y_3}{\tau_{34}} - \frac{y_4}{T_4}$$

$$\frac{d\,y_6}{d\,t} = \frac{y_o}{\tau_{o6}} + \frac{y_4}{\tau_{46}} - \left(\frac{1}{\tau_{65}} + \frac{1}{\tau_r} \right) y_6 \qquad \text{MAN}$$

$$= \frac{y_o}{\tau_{o6}} + \frac{y_4}{\tau_{46}} - \frac{y_6}{T_6}$$

where :

$y_o = \frac{\text{kg I-131}}{\text{kg air equivalent nitrogen}}$

$y_2 = \frac{\text{kg I-131}}{\text{kg herbage equivalent nitrogen}}$

$y_3 = \frac{\text{kg I-131}}{\text{kg cow equivalent nitrogen}}$

$y_4 = \frac{\text{kg I-131}}{\text{kg milk equivalent nitrogen}}$

$y_6 = \dfrac{\text{kg I-131}}{\text{kg man equivalent nitrogen}}$

$K = \dfrac{\text{kg I-131 daily supplied}}{\text{kg air equivalent nitrogen}}$

τ_{ik} = mean transfer life from the i^{th} to the k^{th} compartment [d]

T_k = effective mean life of excretion from k^{th} compartment [d]

τ_r = radioactive mean life [d]

Taking as reference the release of a 5 tons/day reprocessing plant (5) as being 0.15 Ci/d = $1.2 \cdot 10^{-9}$ kg d^{-1} of iodine-131 discharged to the atmosphere; assuming a dilution factor (6) of 10^{-6} m^{-3}, a daily input of I-131 = $K' = 1.2 \times 10^{-15}$ kg m^{-3} d^{-1} is obtained.

Expressing such quantity in terms of equivalence to the "key-substance" we have:

$$K = 1.3 \times 10^{-15} \quad \frac{\text{kg } d^{-1} \text{ I-131}}{\text{kg air equivalent nitrogen}}$$

The values of τ_{ik} and T_k to be used in the following equations, have been obtained on the basic of biecological data (3) (4).

$$\tau_{o6} = \frac{x_6}{\xi x_o} = 0.11 \text{ d}$$

where $\xi = 20\ m^3\ d^{-1}$ of air inhaled by a man

$$\tau_{o3} = \frac{x_3}{\gamma x_o} = 0.16 \text{ d}$$

where $\gamma = 109\ m^3\ d^{-1}$ of air inhaled by a cow

$$\tau_{o2} = \frac{x_2}{\eta x_o} = 3.5\ 10^{-5} \text{ d}$$

where $\eta = 6 \cdot 10^4$ kg/d of iodine deposited on 50 kg of herbage (corresponding to a surface of 70 m^2) per kg/m^3 of iodine in air, assuming 1 cm/s as the deposition velocity (7)

$$\tau_{23} = \frac{x_3}{\delta x_2} = 8 \quad [d]$$

where = 1 $[d^{-1}]$ daily grass ration of 50 kg injested by a cow

$$\tau_{35} = \frac{x_3}{\varepsilon x_5} = 67 \ [d]$$

where εx_5 = 0.24 kg d^{-1} equivalent Nitrogen daily excreted by a cow

$$\tau_{34} = \frac{x_3}{\xi x_4} = 32 \ [d]$$

where ξx_4 = 0.50 kg d^{-1} milk equivalent Nitrogen daily produced

$$\tau_{46} = \frac{x_6}{\nu x_4} = 63 \ [d]$$

where νx_4 = 0.033 kg d^{-1} of milk daily injested by a man

$$\tau_{65} = \frac{x_6}{\rho x'_5} = 70 \ [d]$$

where $\rho x'_5$ = 0.03 kg d^{-1} equivalent Nitrogen daily excreted by a man

$T_o = 3.5 \ 10^{-5} \ [d]$

$T_2 = 4.8 \ [d]$

$T_3 = 7.7 \ [d]$

$T_4 = 10 \ [d]$

$T_6 = 10 \ [d]$

At steady state, according to the hypothesis made, the following results are obtained:

$$\bar{y}_o = 4.5 \cdot 10^{-20} \quad \frac{\text{kg I-131}}{\text{kg air equivalent nitrogen}}$$

$$\bar{y}_2 = 6.3 \cdot 10^{-15} \quad \frac{\text{kg I-131}}{\text{50 kg herbage equivalent nitrogen}}$$

$$\bar{y}_3 = 6.1 \cdot 10^{-15} \quad \frac{\text{kg I-131}}{\text{Kg cow equivalent nitrogen}}$$

$$\bar{y}_4 = 1.9 \cdot 10^{-15} \quad \frac{\text{Kg I-131}}{\text{kg milk equivalent nitrogen}}$$

$$\bar{y}_6 = 3 \cdot 10^{-16} \quad \frac{\text{kg I-131}}{\text{Kg man equivalent nitrogen}}$$

These values correspond to the followings:

$$y^*_o = 4.2 \cdot 10^{-20} \quad \frac{\text{kg I-131}}{\text{m}^3 \text{ of air}}$$

$$y^*_2 = 6.3 \cdot 10^{-16} \quad \frac{\text{kg I-131}}{\text{kg of dry herbage}}$$

$$y^*_3 = 9.7 \cdot 10^{-14} \quad \frac{\text{kg I-131}}{\text{standard cow}}$$

$$y^*_4 = 6.3 \cdot 10^{-17} \quad \frac{\text{kg I-131}}{\text{kg of milk}}$$

$$y^*_6 = 6.3 \cdot 10^{-16} \quad \frac{\text{kg I-131}}{\text{standard man}}$$

from which it is possible to obtain concentration factors which are in a good agreement with the values found experimentally.

FINAL CONSIDERATIONS

Owing to its flexibility which makes it open to many extensions and adaptations, the proposed mathematical method is fit for various uses in the wide field of ecological disciplines.

Its main advantages can be summarized as follows:

1) Possibility of employment in digital and analog. computers to plot concentrations of the "foreign" element versus time.

   After all, this method provides large possibilities of a synthetic and non computational approach such as Fourier and Laplace transforms and convolution integrals; it also fits descriptions in terms of variables of state and transition matrices.

2) Ease of parametric analysis which allows the evaluation of the influence, as well as of the importance of the various factors.

3) Large possibilities of extending multicomponent systems by introducing the use of vector quantities: the "key-substance" as well as the pollutant may be represented by a "key-vector" and a "perturbation vector" respectively.

4) Possibilities of application of the model in transient conditions, besides the perturbation element (any variable input function), to the "key-substance also.

The authors are aware of having not exhausted in this concise paper all possibilities of systemsdynamics application to the wide field of ecological disciplines.

They simply feel hopeful of having given a small contribution to the systematic study of a discipline of basic importance to the human community, being convinced that such a study is open to wider and more fecund developments.

ACKNOWLEDGMENTS

This work takes as a starting point a seminar held by Dr. Ing. V. Gervasio in 25th May 1971 at the Italian Accademia dei Lincei.

The authors wish to acknowledge with thanks Dr. V. Garcia for the useful discussions and for supplying the bioecological data used in this work.

REFERENCES

(1) Forrester J.W. : "Principles of Systems", Wright Allen Press,

238 Main Street, Cambridge, Massachusetts, 1969

(2) "Principles of Environmental Monitoring to the Handling of Radioactive Materials" ICRP Publication n. 7, Pergamon Press, 1966

(3) R.Scott Russel : "Radioactive and Human Diet", Pergamon Press, 1966

(4) "Recommendations of the International Commission on Radiological Protection" ICRP Publication n. 2.

"Report of Committee II on Permissible Dose for Internal Radiation" Pergamon Press, 1959

(5) Atlantic Richfield Company Fuel Recovery Plant - Preliminary Site Evaluation, March 1969

(6) Cuoco A., Galvagni R., Pucciarelli L. e Scafe' R.

Determinazione delle concentrazioni di una nube radioattiva e delle contaminazioni del suolo secondo il metodo Pasquill-Gifford

CNEN - RT/PROT (65)10 - marzo 1965

(7) Beattie J.R.

An assessment of environmental hazard from fission product releases

AHSB (S) R 64 UKAEA (1963)

Chapter III

ESIMATION METHODS OF DISPERSION OF GASEOUS POLLUTANTS DOWNWIND INDUSTRIAL STACKS

R. Deniau and P. Mery

Division of Atmospheric Transfers
Electricite de France

For presentation to the Panel on Modeling, NATO/CCMS Pilot Project on Air Pollution, Paris, France, July 26-27, 1971.

Table of Contents

Page

1. Introduction III-6

2. Main Parameters in the Dispersion of Pollutants from an Isolated Stack III-6

2.1 Effluent Characteristics at the Chimney Exit III-7

2.2 Meteorological Parameters III-8

2.3 Characteristics of the Surroundings: Buildings and Topography III-13

2.3.1 Mechanical Effects III-13

2.3.2 Thermal Effects III-16

3. Usual Formula: Limits of Use III-18

3.1 Plume Rise Formula III-19

3.1.1 Theoretical Approach III-20

3.1.2 Phenomenological Approaches III-33

3.2 Formula: Diffusion of Plume Emitted by a Point Source III-48

3.2.1 Presentation of the Usual Diffusion Formula III-48

3.2.2 Simplified Formula for Practical Use "Critical" Wind Speed III-51

3.2.3 Conditions for Use III-52

3.2.4 Value of Diffusion Formula III-54

4. More Elaborate Methods for the Estimation of Pollution Downwind an Isolated Stack III-55

4.1 Experimentation In Situ III-55

4.2 Mathematical Models of Plume Diffusion III-57

4.2.1 Presentation of the Problem III-57

4.2.2 Examples of Resolution III-59

4.2.3 Value of Mathematical Models III-65

Page

4.3 Scale-Model Experiments III-66

4.3.1 Introduction III-66

4.3.2 Conditions of Similitude III-66

4.3.3 Modeling Facilities III-69

5. Conclusion III-70

List of Symbols

a	: thermal diffusivity	$L^2\ T^{-1}$
C	: concentration of a gaseous effluent (C_m: maximum concentration)	$M\ L^{-3}$
C_M	: absolute maximum concentration	$M\ L^{-3}$
C_p	: specific heat at constant pressure	$L^2\ T^{-2}\ {}^{o}C^{-1}$
C_y, C_z	: virtual diffusion coefficients of SUTTON	$L^{n/2}$
d	: stack diameter	L
g	: gravitational acceleration	$L\ T^{-2}$
h or H	: effective stack height, h_o: stack height, h: plume rise, h_{cr}; critical plume rise	L
k	: 1. mass diffusivity, k_x, k_y, k_z: diffusivities in the x-, y-, z- directions.	$L^2\ T^{-1}$
	2. von Karman's constant	dimensionless
	3. diffusion coefficient of PRIESTLEY	T^{-1}
K	: eddy diffusivity (K_1: mass; K_2: heat)	$L^2\ T^{-1}$
L	: MONIN and OBUKHOV length, or characteristic length	L
n	: SUTTON exponent	dimensionless
q_m	: emission rate of gaseous effluent	$M\ T^{-1}$
Q	: heat emission due to efflux of stack gases	$M\ L^2\ T^{-3}$
R	: radius (or characteristic length) of a plume R_o: internal; R_1: at the end of the first stage	L
r	: radial coordinate	L
s	: curve-linear abscissa	L
T	: average absolute temperature	t
u,v,w	: 1. speed components in the x-, y-, z- directions	$L\ T^{-1}$

2. speed component on the plume axis (p. III-75)

3. u: radial speed (p. III-26)

U : mean wind speed $L\ T^{-1}$

u_x, U_x: friction velocity

U_{cr}: critical wind speed

W_x or w_o : efflux velocity $L\ T^{-1}$

w_1: vertical velocity at the end of the first stage

w_m: vertical velocity on the plume axis

x_m: distance from the stack where $C = C_m$ L

z_o: 1. roughness height L

2. vertical distance between the stack and the virtual point source (p. III-29)

z_c or z_{max}: plume rise at the end of the second stage L

φ : instantaneous lateral deviation of wind direction dimensionless

φ_o : standard deviation of wind direction

Γ : adiabatic vertical temperature gradient $t\ L^{-1}$

ν : kinematic viscosity $L^2\ T^{-1}$

ρ : density $M\ L^{-3}$

σ_y, σ_z : standard deviations of lateral and vertical gaseous concentration distributions L

θ : potential temperature of effluent t

θ_e: potential temperature of ambient air

θ_o: potential temperature at the exit of stack

θ' : potential temperature excess of plume gases

I. Introduction

Most of the analytical methods used to determine pollution caused by a given source can only be applied to a few special cases which are seldom to be met in the lower atmosphere: flat ground, uniform roughness, constant wind and neutral conditions.

When dealing with the characteristics of gaseous pollutant sources, one has to cope with rather low ventilation shafts on top of buildings as well as with chimney stacks of modern thermal power plants about 200 m high.

The surroundings include as well as a high amount of parameters which, dealing with the diffusion of pollutants, may play an important part; they are: the meteorological conditions, the site where the stack is built and the natural or artificial obstructions around (hills and buildings).

A given analytical method cannot be applied to any complex situation without reducing its accuracy. Fortunately, it happens that some parameters may be neglected and then a reasonable answer may be brought. It also happens that the analytical method proves useless and it will be necessary to use more elaborate methods such as numerical or experimental models.

In this report we intend to describe different physical phenomena of plume dispersion (see part 2), then we shall review the methods used to determine the concentration field of pollutants around an isolated point source (power plant stacks). Part 3 deals with methods based on simple formula and there we particularly mention plume rise formula. Part 4 deals with more elaborate methods which are connected with research works.

It can be noticed that an adding process may be used in order to extend these methods to multi-source problems, at least when there is no aerodynamical interaction between the different sources (for instance: in-line stacks).

II. Main Parameters in the Dispersion of Pollutants from an Isolated Stack

Let us consider the development of the plume emitted by an isolated stack and spreading into the first 500 meters in the atmosphere above a flat free ground. Then the diffusion has two origins:

- the eddies due to the plume itself when leaving the chimney
- the eddies in the surrounding atmosphere

As Priestley and Scorer pointed out (1, 2), we may identify three stages in the development of plume.

First stage: The plume is almost vertical and the vertical component of its own velocity is higher than the horizontal velocity of the atmospheric wind.

This stage comes to an end when the vertical component of the plume veolcity is of the same magnitude as the wind velocity.

Second stage: The plume bends over and spreads out almost horizontally. This stage comes to an end when the vertical component of the plume velocity is of the same magnitude as the wind velocity fluctuations.

Third stage: It takes over after the plume has lost any effective independent motion and buoyancy; this is the stage of pure atmospheric diffusion.

Then comes out a plume model suitable for the study of phenomena affecting the dispersion of effluents.

During the first stage, the characteristics of the effluents at the exit of the chimney will have to play the most important part. On the contrary the characteristics of the atmosphere will be the only ones to interfere during the third stage.

In the presence of aerodynamical or thermal effects due to the topographical features or high buildings, the plume geometry may be deeply modified; this may happen at any stage.

2.1 Effluent Characteristics at the Chimney Exit

The physical parameters which will have an effect on the effluents at the chimney exit are as follows:

- d: stack diameter
- W: exit speed
- U: wind speed at the level of the top of the chimney

$\frac{\Delta \rho}{\rho_e}$: relative density discrepancy between effluents and atmosphere

Dimensional analysis provides the following equation:

$$z_1 = f\left(\frac{W}{U}, \frac{g\, d\, \Delta\rho/\rho}{U^2}, \frac{d}{h}\right)$$

in which:

z_1: effective height at the end of the first stage

h: chimney height

z_1 increases with $\frac{W}{U}$; for $\frac{W}{U} < 1.5$, there is no plume rise, because the effluents get mixed into the turbulent wake behind the chimney.

To the dynamic effect due to the exit speed of the effluent we must add the density effect; so in the case of hot gases, the height reached by the plume in its first stage will be increased, compared with the height reached by a plume emitted at the ambient temperature: so, z_1 increases with $\Delta\varrho/\varrho$.

On the opposite, with gases more dense than air, z_1 decreases with $\Delta\varrho/\varrho$.

The importance of buoyancy forces compared with inertial forces due to the atmospheric wind is often characterized by Froude's number:

$$F_r^2 = \frac{U^2}{g d \, \Delta\varrho/\varrho}$$

It is to be noted that z_1 increases with d and therefore with the stack section.

2.2 Meteorological Parameters (3, 4, 5)

Most of the dispersion problems take place in the atmospheric boundary layer whose thickness is about a few hundred meters; in this layer we may generally identify a region near the ground, named surface layer; its thickness is about a few ten meters and it is supposed that both shear stress and vertical heat flux are approximately constant with height.

In this shallow layer all the basic phenomena take place and give the atmospheric boundary layer its structure.

Above the surface layer, the so-called transition layer spreads up to the upper limit of the atmospheric boundary layer; the flow structure and the temperature profile still depend on the shear stress and heat flux on ground level; moreover Coriolis forces appear which could be neglected in the surface layer.

Then, the two characteristic parameters of the atmospheric boundary layer are:

$\frac{\partial U}{\partial z}$: speed gradient

$\frac{\partial T}{\partial z}$: temperature gradient

To those two parameters are connected small scale turbulent characteristics, that is to say turbulence caused by atmospheric phenomena which appear within a 10 kilometers horizontal distance. Obviously, turbulent fluctuations have periods varying from a few seconds to an hour; consequently, speed and direction mean values and turbulence depend on the sampling time. We generally consider sampling times appropriate for each particular case.

The geometry of a plume when observed in situ is generally due to the turbulence whose period is about the time taken for the plume to cover the distance from the source to the point of observation.

Concentration measurements will only be significant if we average the concentrations over an appropriate sampling time.

If we are interested in concentration measurements taken over much longer periods, we have to take into account changes in wind direction and wind speed.

Small scale atmospheric turbulence has two distinct origins; the first one is mechanical, the second is thermal.

According to the importance of a certain type of turbulence as opposed to the other one, the atmosphere may be stable, neutral or unstable.

The atmospheric stability is often characterized by the Richardson's number:

$$R_i = \frac{g}{T} \frac{\left(\frac{\partial T}{\partial z} + \Gamma\right)}{\left(\frac{\partial U}{\partial z}\right)^2}$$

$R_i < 0$: unstable atmosphere,

$R_i = 0$: neutral atmosphere,

$R_i > 0$: stable atmosphere.

In case of strong winds, important momentum transfers take place in the atmospheric boundary layer: then $\frac{\partial T}{\partial z}$, or vertical temperature gradient, tends toward the adiabatic lapse rate $-\Gamma$ (-1°/100 m) and Richardson's number becomes zero.

Surface roughnesses such as trees, buildings and terrain irregularities markedly affect the air flow.

Under these conditions, turbulence is predominantly mechanical.

It will be the same when the sky is cloudy and with moderate winds. For light winds, the atmospheric stability affects the nature of turbulence.

For instance, during a sunny day the ground becomes heated more quickly than the air above: as a result, the vertical temperature gradient grows negative and is inferior to the adiabatic lapse rate; the air layers nearest the ground become warmer than layers higher up, causing the atmosphere to become unstable and thus enhancing vertical mixing. Convective eddies appear. In light winds (2 m/s), eddies are essentially produced by thermal convection: their periods vary from a few minutes to some ten minutes and may be affected by the different thermal properties of the soil (albedo, emissivity, conductivity and diffusivity).

Obviously the predominance of turbulent convection depends on wind speed, and there are intermediate states in which thermal turbulence and mechanical turbulence are equally important.

During a clear night, when winds are light, the ground cools by radiation faster than the air above; an inversion then happens that is to say temperature increases with height. Richardson's number grows positive. Under these conditions the atmosphere is stable and the intensity of mixing is considerably lower.

The following figures clearly point out the influence of meteorological parameters upon the behaviour of a plume in a lapse of time of 24 hours.

1. Figure 1 shows a plume in intense solar heating and clear sky conditions. There is a very unstable stratification.

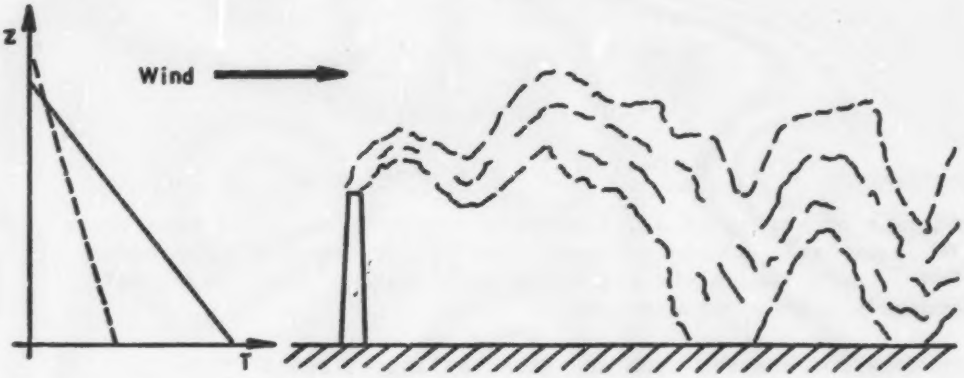

Fig. 1 : Conditions for strong instability

$$\frac{\partial T}{\partial z} < -1°\mathrm{C}/100\ \mathrm{m},\ \text{light wind,}$$

$$\frac{\partial T}{\partial z} = 1°\mathrm{C}/100\ \mathrm{m}\ ;\text{strong wind, adiabatic lapse rate.}$$

2. Figure 2 illustrates coming which occurs under high wind and near neutral stability conditions.

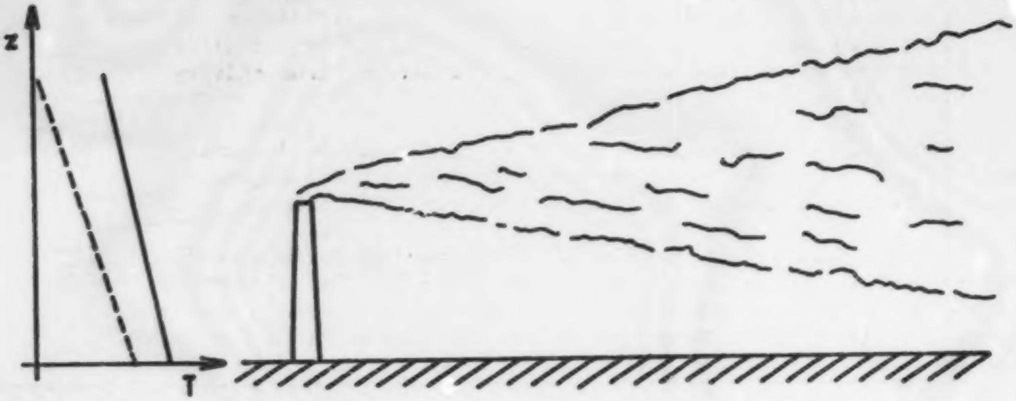

Figure 2: Near neutral stability conditions (high wind).

3. Figure 3 illustrates fanning which occurs under conditions of extreme stability.

This configuration exists during a nocturnal inversion although it may also be seen just before sunset and shortly after sunrise. The vertical component is suppressed more than the horizontal and thus the plume's horizontal width is typically greater than its vertical thickness.

This type of plume may undergo appreciable lateral fluctuation (meandering).

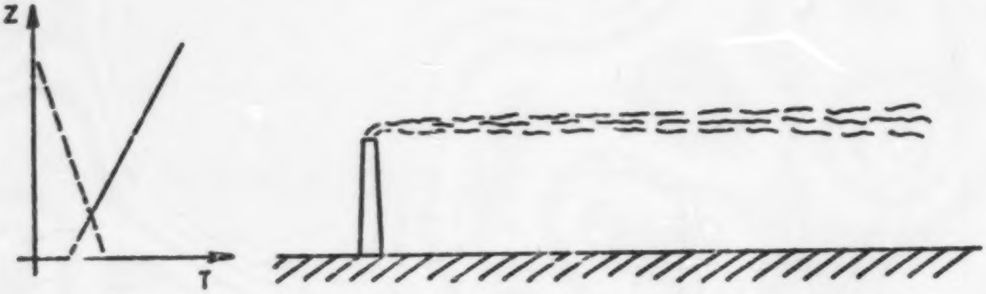

Figure 3: Extreme stability conditions ($\frac{\partial T}{\partial z} > -1^{\circ}C/100$ m, moderate wind).

4. Figure 4 shows a lofting plume which occurs when an inversion is building up. This type of plume may often be seen in the late afternoon or early evening. It is a most favorable case since part of the plume is rapidly dispersed upward and diffusion toward the ground is suppressed.

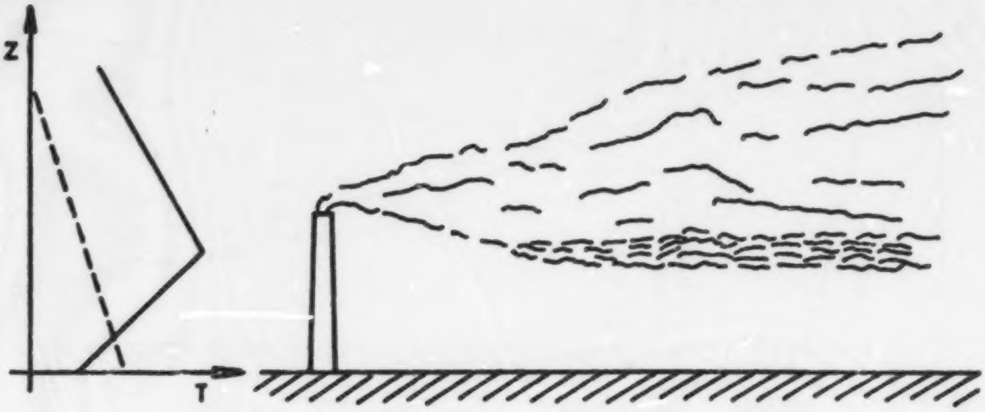

Figure 4: Inversion below, lapse aloft.

5. Figure 5 shows the fumigating plume; it can often be seen in the early morning, when the inversion is being destroyed from the ground upward. When instability reaches the level of the plume, the lower portions of the plume are brought to the ground rapidly, while the upper part may still remain intact; from the pollution point of view it is most unfavorable.

It may even happen that the whole plume is trapped into the unstable layer; this phenomenon is called "trapping"; the lower part of the stable layer acts as a lid.

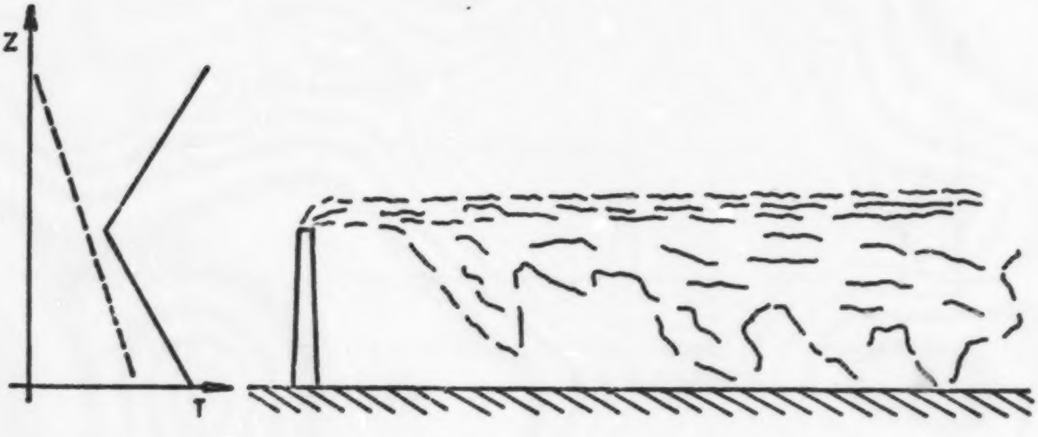

Figure 5: Lapse below, inversion aloft.

2.3 Characteristics of the Surroundings: Buildings and Topography

In the previous paragraph we dealt with the general effects of meteorological parameters and we made mention of the important influence of topography, buildings and other obstacles which are part of a stack surroundings.

This type of influence may be of either a mechanical or a thermal origin.

2.3-1 Mechanical effects

The influence of any obstruction to the wind can be noted upwind on a relatively short distance, about the size of the obstacle; it essentially appears as local variations in wind speed and direction; no important effects on turbulence can be noted.

Yet, behind the obstruction, turbulence as well as the average wind speed and direction are strongly affected.

For instance, turbulent wakes produced by sharp edged obstructions totally modify the flow structure.

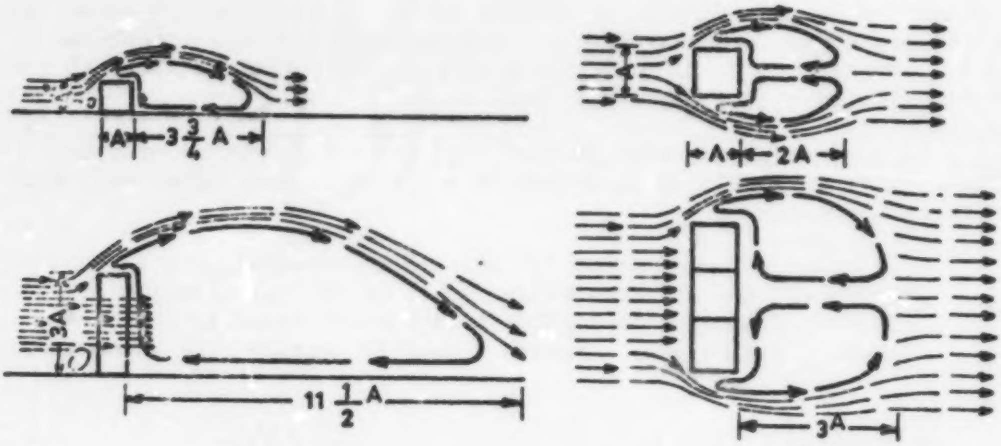

Figure 6: Variation of building air flow patterns with respect to transversal and vertical building dimensions (Evans (6)).

In situ studies as well as wind tunnel studies helped to investigate the effect of the shape of the obstructions upon the nature of turbulent wakes at the lee of them. These obstructions are usually parallelepipedical buildings.

As far as pollution is concerned this phenomenon is of the highest interest; obviously, dispersion out of a squat chimney on top of a building is totally different from dispersion out of a tall one.

In the first case, plume dispersion varies when the chimney protrudes from the apex of the roof or else when it does not. We usually agree to say that a minimum stack height corresponds to the turbulent wake thickness above the rood; consequently the chimney exit is situated above the highly perturbed area where plume entrainment and recirculation occur.

Yet, even in this last case, downwash may be observed; most authors agree that downwash is avoided when the stack height above ground is at least 2½ times the height of the building.

Among numerous studies dealing with that problem, we may quote those by Evans, Halitsky, Strom, Leutheuser and Vadot (6 to 10).

When considering high stacks (which satisfy the "2½ times rule") buildings act as surface roughnesses, that is to say turbulence generators: above a city, the average turbulent intensity of the flow is higher than above open areas.

Nevertheless, when obstructions are hills, cliffs or rocky salient edges, important pollution problems may appear even with tall stacks.

Scorer (11) and Strom (8) pointed out several models of separated flow or of turbulent wakes at the lee of hills of cliffs. Pollution is highly different according to the chimney location and height. Figures 7 to 9 illustrate this phenomenon.

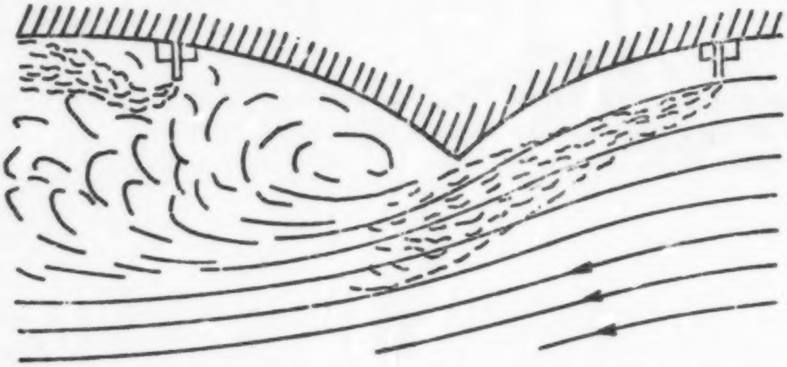

Figure 7: At the foot of a salient edged mountain (8).

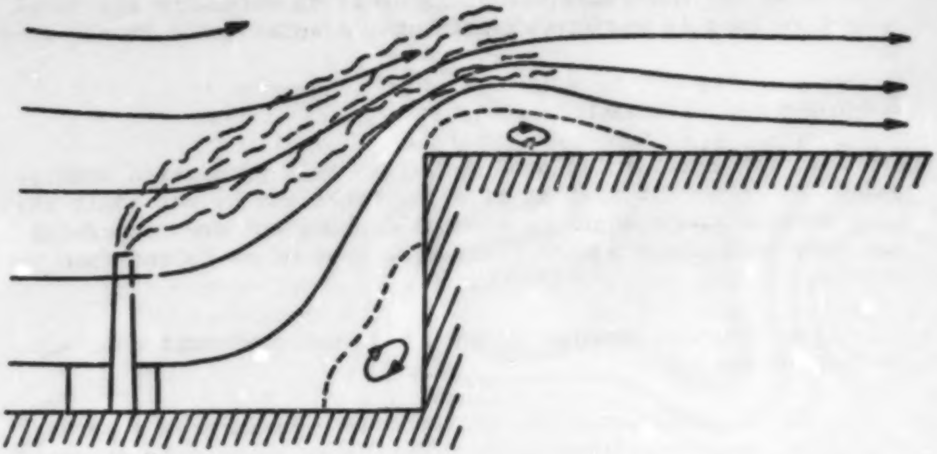

Figure 8: At the foot of a downwind cliff (11).

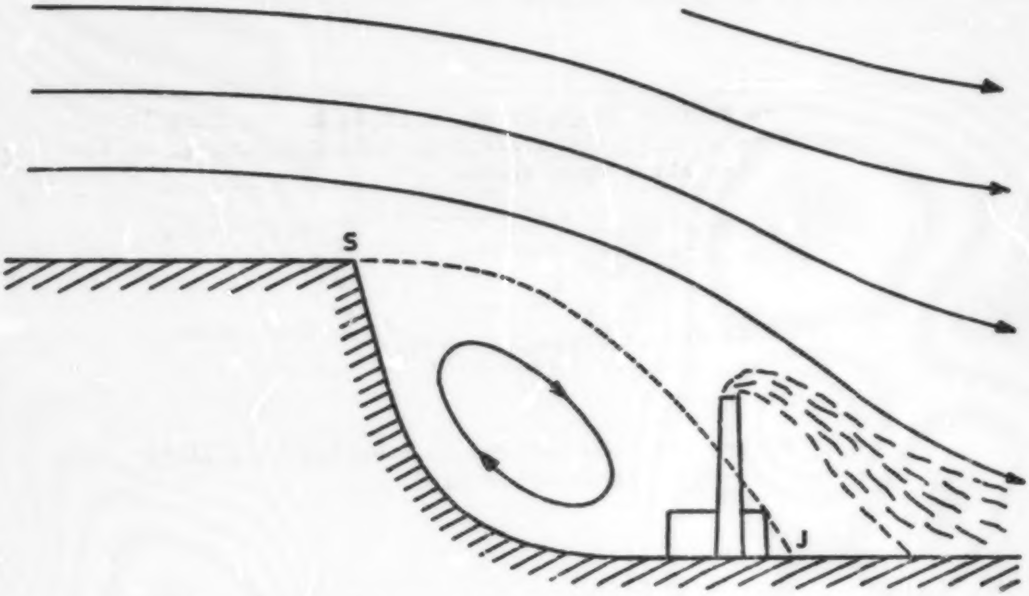

Figure 9: At the rear of a cliff eddy (11).

Modifications in the flow structure upwind or downwind a large obstruction cannot be taken into account by any analytical formula or any numerical model; in order to determine the stack height we have to perform experimental studies (wind tunnel experiments).

2.3-2 Thermal effects

In the case of isolated buildings heat production enables seldom an important thermal rise; nevertheless we may admit that in city centres temperature is about 5°C above country temperature. Any city area plays a part similar to that of an island (see below).

Experimental studies reveal that such a situation is apt to prevent pollution.

Thermal influences due to topography features are more important and the corresponding eddy scales may differ strongly.

It is so when dealing with shores and valleys.

2.3-2-1 Valleys (figure 10)

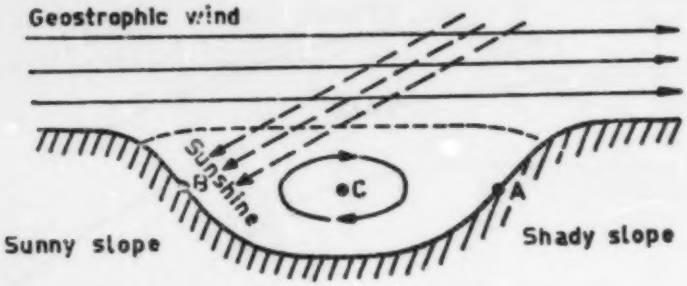

Figure 10: Flow pattern in a valley by a light geostrophic wind.

The air temperature of flow at A (shady slope) is different from the air temperature at B and C which are located at the same level, above the bottom of the valley; an anabatic wind is produced from A towards B.

A similar phenomenon may be noted in the direction of the valley; for instance when there is enough sunshine on the top part of the valley and when the down part is shady.

Geostrophic wind together with certain aerodynamic aspects (narrowing valleys) can make these phenomena highly complex.

2.3-2-2 Shores (figure 11)

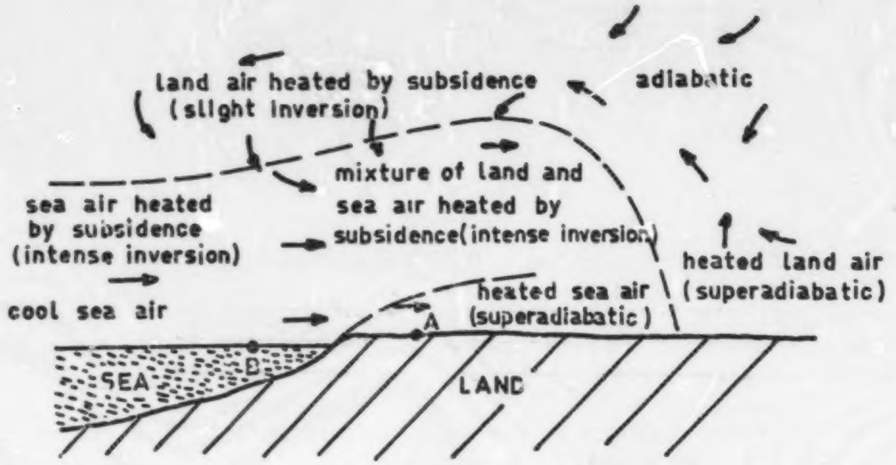
land air heated by subsidence
(slight inversion)
adiabatic
mixture of land and
sea air heated by
subsidence(intense inversion)
sea air heated
by subsidence
(intense inversion)
heated land air
(superadiabatic)
cool sea air
heated sea air
(superadiabatic)
A
B
SEA
LAND

Figure 11: Schematic representation of a sea breeze when the geostrophic wind is light (from Munn (4))

Early in the morning the sun starts heating the ground whereas water (lake or sea) remains cold: local circulation begins, characterized by an horizontal eddy the axis of which is parallel to the shore (subsidence above sea-level and uprising flow above ground-level).

In fact the situation grows much more complex because of a thermal boundary layer rising from the shore and in which the cold sea air gets heated by the ground; consequently, above A level two inversion layers get piled up.

At night everything is the other way round (land breeze). Lakes and islands may both be at the origin of a similar atmospheric, cellular-like circulation (uprising flow or subsidence at the center of the island or of the lake in daytime); in the case of a moderate wind, two inner boundary layers appear (see figure below); a few hundred meters inland from the downwind shore, two interfaces may lie above each other.

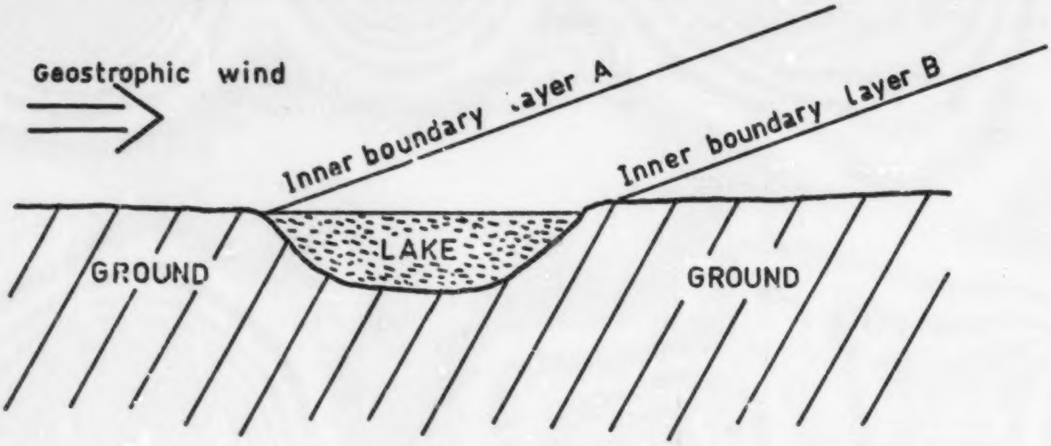

Figure 12: Flow pattern above a lake (from Munn(4)).

As far as pollution is concerned these thermal effects may have harmful influences since they produce intense inversions and privileged wind directions.

The study of these influences can be performed only by numerical and experimental models.

III. Usual Formula: Limits of Use

There are two steps in most of the methods used to determine the concentration rate of effluents emitted by stacks.

In the first step (see paragraph 3-1), we have to study the first two stages of the plume evolution, and we essentially try to determine the height it reaches at the end of the second stage which is called effective stack height.

The difference between effective stack height and real stack height is called plume rise.

In the second step (see paragraph 3-2), we have to study effluent dispersion during the third stage of the plume evolution.

The first two stages are supposed to be well known; consequently, we only consider S', a virtual upwind point source, higher than S, the real point source. The distance between S and S' will be called x_o, and h, the height of S' will be the sum of h_o, the height of S, and of Δh, the plume rise.

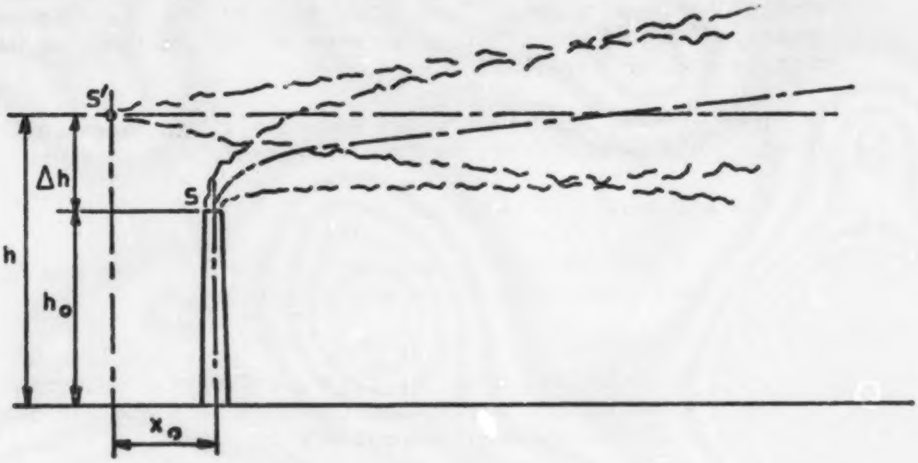

Figure 13: Plume model used in usual formula.

x_o is not very well known, but it does not really matter because it is not a great distance compared with logitudinal dimensions we are interested in.

3.1 Plume Rise Formula

Theoretically it is very difficult to determine plume rise because of the high number of parameters governing the flow in the first two stages of the plume development. One of the greatest difficulties lies in the convenient definition of the plume rise (see 3.1-2). Authors gave it various definitions; Davidson (12) indicates that his formula refers to a point when the plume slope is less than 0.1. Holland (13) indicates very generally that the height of rise may be considered as the height at which the plume levels off. Bosanquet (14) considers that the height of rise is the height at which the effects due to emission, i.e. buoyancy and momentum, have died away. We think that it is possible to state plume rise in a useful and accurate form, only when the atmosphere is stable or neutral: plume axis ends by being horizontal and plume rise is the height of the axis above the chimney top.

Most of the various theoretical or partially theoretical studies of the problem can be found in literature and they lead to formula or laws. In most of the cases, these formula are of no useful interest: the description of phenomena is too incomplete.

Yet there is a noticeable exception: that is the Priestley Study. Apart from that particular study, we can get useful formulae only by phenomenological studies (ss 3.1-2).

Nevertheless we shall examine a certain number of theoretical studies besides Priestley's because they enable us to get a better understanding of the physical aspects of the problems we have to cope with in those circumstances.

Then we shall consider a few essentially phenomenological studies, and we shall try to draw some useful conclusions.

3.1-1 Theoretical approach

3.1-1-1 Schmidt's approach is the simplest one and is well described in Sutton's book (3).

Its aim is to give the variation laws of w, the vertical speed of plume, and of the potential temperature difference between the plume and the surrounding air, with the vertical coordinate z.

In these conditions, the plume is supposed to have the shape of a cone the radius of which is:

$$R = R(z)$$

Then Schmidt assumes that:

(1) R is proportional to z: $R = k\,z$. It comes to accept a law of similitude for the lateral diffusion, considering a mixing length proportional to the radius.

(2) w and θ' are uniform in a given section of the plume, so they are totally dependent on z; of course, this assumption is the less verified as z is high.

(3) The laws Schmidt searched for are as follows:

$\theta' = \theta'_o z^{-m}$ and $w = w_o z^{-p}$, which adds a new limitation to his approach.

Then Schmidt uses on the one hand the conservation of the emitted energy Q, and, on the other hand, the theorem of kinetic energy applied to the elementary displacement mass unit.

We get then:

$$Q = \pi R^2 \rho \; w \; C_p \; \theta' = \text{constant}$$

$$\frac{d}{dz} \cdot \left[\frac{1}{2} w^2 \right] dz = g \alpha \theta' \, dz$$

with:

$$\alpha = - \frac{1}{\rho} \frac{d\rho}{d\theta'}$$

Buoyancy forces, the only external forces to be considered, are given by the $g\alpha\theta'$ term. If we suppose that α is constant (which is right only for small temperature differences) and if we neglect the ρ variation in the first equation, we come to:

$$z^{2-m-p} = \text{constant} \longrightarrow m + p = 2$$

$$\text{and} \quad z^{-2p-1} = z^{-m} \longrightarrow m = 2p + 1$$

We get: $m = \frac{5}{3}$ and $p = \frac{1}{3}$

So, the temperature discrepancy decreases much more quickly than the upward velocity w; the thermal effects can be neglected as opposed to the dynamic effects as the plume spreads up.

3.1-1-2 Sutton (3) comes to a similar conclusion but he a more elaborate process in which the rate of entrainment interferes: that is to say Q, the outside mass-flow of air coming in per unit surface through the lateral surface of the plume. By introducing 1, the Prandtl mixing length, he assumes that q is proportional to w', vertical velocity fluctuation, and consequently to:

$$1 \frac{d\,w}{d\,z}$$

If 1 is supposed to be proportional to R, (1 = c R), we get:

$$q = K \rho \, c \, R \, \frac{dw}{dz}$$

K and c are constant.

The equation of continuity in the plume is also a differential one:

$$R \frac{dw}{dz} + 2\ w\ \frac{dR}{dz} = 2\ R\ c\ \frac{dw}{dz}$$

This equation as well as the equation of conservation of Q, emitted energy per unit time, allows to find w and then θ' if the function $R = R(z)$ is known. Sutton then suggests the law: $R = R_o\ z\ 7/8$, which is based on observation results. The solution of the above equations is then:

$$w = w_o\ z^{\frac{2m}{1-2c}} \quad \text{in which} \quad m = \frac{7}{8}$$

Besides, the budget between potential energy and energy lost by dissipation allows us to write:

$$w^2 \propto gl \frac{\theta'}{\theta_o}$$

in which θ_o is the potential temperature of the atmosphere. Thanks to the last relation, the constant c may be identified:

$$c = \frac{7}{2}$$

So:

$$w = w_o z^{-0.29} \text{ and } \theta' = \theta'_o z^{-1.46}$$

w_o and θ'_o are emission characteristics.

These results are close to Schmidt's. Generally we must take wind speed U into account. With this object we may apply Schmidt's formula to w, but where z is replaced by s, curvi-linear abscissa; then, the plume rise is in inverse ratio to U^3 (plume rise means the height above the stack where the plume angle with the horizontal axis becomes less than 10°).

3.1-1-3 Scorer (11) also got Schmidt's results from simple considerations based on dimensional analysis. In his book entitled "Air Pollution" he assumes that the radius of the plume vertical section obeys the law: $R \propto z$, in the general case in which U differs from zero.

The conservation of Q, the emitted energy per unit time may be written:

$$Q = \pi R^2 \rho C_p U \theta' \propto R^2\theta' \Longrightarrow \theta' \propto z^{-2}$$

or:

$$m = 2$$

By writing the theorem of kinetic energy in the same way as above (see 3.1-1-1), we may conclude that:

$$p = \frac{1}{2}$$

So:

$$w \propto z^{-1/2}$$

We can easily find the equation of the trajectory of a particle and consequently of the plume. Indeen, the horizontal distance it covers is:

$x = U\,t$ (t is the time);

besides, the vertical distance is:

$$z \propto t^{2/3} \quad \text{as } w = \frac{dz}{dt} \propto z^{-1/2}$$

So, this equation is of the type:

$$z \propto x^{2/3}$$

In reality, it appears that it is never so, because though the law $R \propto z$ is approximately verified--at least when the atmosphere is neutral and not very turbulent--we notice that the atmospheric turbulence governs quickly the evolution of the plume, so that this equation describes nothing but the first stage of the evolution and is proved to be of no practical interest to determine the plume rise.

3.1-1-4 Briggs (16) studied the problem by only using dimensional analysis; he selected some of the most significant physical parameters.

Therefore, in the formula he suggests, the emission conditions of hot gases only appear through the parameter F, given by the relation:

$$F = \frac{gQ}{\pi\,(\rho C_p T)_a}$$

in which $(\rho C_p T)_a$ is the value of the product $\rho C_p T$ for the ambient atmosphere.

In fact:

$$F \# g \frac{\theta'}{\theta_o} w R^2$$

where θ_o is the potential temperature of emitted gases.

$\frac{F}{U^3}$ has the dimension of a length and will be written L.

The atmosphere (besides U, the wind speed) is characterized by s, a single stability parameter:

$$s = \frac{g}{\theta_a} \frac{\partial \theta_a}{\partial z}$$

- For the transition stage of the plume, Briggs suggests the following formula:

$$z = 2 F^{\frac{1}{3}} \frac{x^{\frac{2}{3}}}{U}$$

which takes into account the above mentioned law (see 3.1-1-3).

We chall see further that Bringfelt experimentally proved the law to be correct for $250 < x < 500$ m.

- In the case of stable calm air, the plume rise formula is readily found to be:

$$\Delta h = 4.7 F^{\frac{1}{4}} s^{-\frac{3}{8}}$$

4.7, the proportionality coefficient, comes out of a compromise between the experimental results of several authors (Crawford and Leonard (17), Morton and Alii (18).

- In the case of windy stable air, the formula turns out to be different:

$$\Delta h = 2.6 \left(\frac{F}{Us}\right)^{1/3}$$

The coefficient 2.6 also comes out of experiments, in particular at the T.V.A. (colbert Power Plant).

- In the case of neutral atmosphere, Briggs also suggests the inequality:

$$\Delta h > 400 \frac{F}{U^3}$$

(This formula and the preceding ones may be applied in any coherent unity system.)

Thanks to dimensional analysis we get back a plume rise which is in inverse ratio to U^3 (see Sutton 3.1-1-2). Unfortunately, that formula seems to be inapplicable; Whaley (19) stressed the point that it may lead to inacceptable deviations compared with usual formulae. Yet, the value of dimensional analysis is not to be questioned; in reality, it happens that the number of characteristic parameters in the atmosphere is too low in this case because of the essential part played by turbulence; it must be added that Briggs had first introduced two supplementary parameters: h the stack-height and u, the friction velocity; their suppression is precisely what seems to be improper.

On the contrary, formulae for stable cases are much more useful; they seem to give acceptable values when we try to determine Δh.

This author does not set up formulae in the case of unstable atmosphere.

3.1-1-5 Moore (CEGB)(20) discusses the implication of the physical aspects of plumes. Behaviour of plumes differed whether they remained continuous or broke down during the early stages after emission. He even pointed out and stressed an intermediate case: that of the plume, breaking down into lumps that remain separate for a time, then that merge together.

A breaking down plume doesn't behave in the same way as a continuous one; a larger surface area of the hot effluent is exposed to the environment, thus increasing the rate of entrainment of cool air and hence increasing the rate of dissipation of buoyancy; consequently, plume rise may be considerably decreased. His formulae may not be used in practice because some of his constants lack precision; yet it is worth noting that Moore comes back to Brigg's law of the plume evolution in the case of a continuous plume emitted in a stable atmosphere. Scriven (21) believes that the breaking down of plumes may explain some important deviations between experimental results and the classical plume rise formulae. Though low values of emission characteristics (speed and temperature) and of stack diameter, are circumstances particularly favorable to the apparition of that type of phenomenon in stable or near stable atmosphere, the plumes emitted by thermal power plants may also be concerned. The theoretical approach of such a problem is particularly complex because a three-dimensional plume has to be taken into account.

3.1-1-6 Priestley's theoretical approach (1, 22 to 25)

It is by far the most complete and interesting study. We may even say that Priestley's works (1, 22 to 25) are the basic ground of the works achieved at C.E.G.B. in that field: in fact, Lucas, Moore and Spurr (24) completed them so as to materialize them in a practical formula. Numerous scientists used them even in U.S.S.R.; among them, we mention Danovitch, Zeiger (26) and Berlyand (27).

Concerning the first stage of the plume, the theory starts with general elementary equations written in cylindrical coordinates.

$$\frac{\partial}{\partial z}(r\,w\,\rho) + \frac{\partial}{\partial r}(r\,u\,\rho) = 0 \quad \text{(Equation of continuity)}$$

$$\frac{\partial}{\partial r}\left(\frac{1}{2} r\,u\,w^2\rho\right) + \frac{\partial}{\partial z}\left(\frac{1}{2} r\,w^3\rho\right) = w\,\frac{\partial(r\tau)}{\partial r} + \rho g\,\frac{\theta' r w}{\theta_e}$$

(Equation of conservation of vertical momentum)

$$\frac{\partial}{\partial r}(r\,\theta'\,u\rho) + \frac{\partial}{\partial z}(r\,w\,\theta'\rho) = \frac{1}{c_p}\,\frac{\partial}{\partial r}(r\,q_r) - rw\,\frac{\partial\theta_e}{\partial z}\,\rho$$

(Equation of conservation of heat)

In these equations:

u: radial component of speed of plume gases;

τ : vertical shearing stress:

q_r: radial heat flux;

θ and θ_o: potential temperatures in plume and atmosphere.

$\theta' = \theta - \theta_o$;

(these equations are set up in Appendix I)

If we take into account the boundary conditions for $r \rightarrow \infty$, which impose that $r\,q_r$, $r\tau$, w, θ' tend to zero and that $r\rho u$ remains finite, we may integrate those equations over

$$\frac{d}{dz}\int_0^{\infty} r\, w^2 \rho \; dr = \frac{g}{\theta_e}\int_0^{\infty} r\; \theta' \rho \; dr$$

$$\frac{d}{dz}\int_0^{\infty} r\, w^3 \rho \; dr = \frac{g}{\theta_e}\int_0^{\infty} r\, w\, \theta' \rho \; dr - \int_0^{\infty} r \tau \frac{\partial w}{\partial r} \; dr$$

$$\frac{d}{dz}\int_0^{\infty} (r\, w\, \rho\, \theta')\; dr = -\frac{\partial \theta_e}{\partial z}\int_0^{\infty} r\, w\, \rho \; dr$$

If we want to go on with the integration, we must now introduce a first hypothesis: the radial distributions of w, θ' and τ are supposed to remain similar, that is to say we introduce three functions: f, h and j, which are totally independent of z and which are defined as follows:

$$w = w_m\, f\left(\frac{r}{R}\right) \quad \theta' = \theta'_m h\left(\frac{r}{R}\right) \quad \tau = \tfrac{1}{2} \rho\, x_m^2 \; j\left(\frac{r}{R}\right)$$

In these expressions, w_m and θ'_m are the values of w and θ' on the plume axis and R is a characteristic radial dimension which is in fact the plume radius.

Then, the equations turn out to be:

$$\frac{d}{dz}\left(R^2\, w_m^2\right) = a\, R^2\, \frac{\theta'_m}{\theta_e}\, g$$

$$\frac{d}{dz}\left(R^2\, w_m^3\right) = b\, R^2\, w_m\, \frac{\theta'_m}{\theta_e}\, g - c\, R\, w_m^3$$

$$\frac{d}{dz}\left(R^2\, w_m\, \theta'_m\right) = - d\, R^2\, w_m\, \frac{\partial \theta_e}{\partial z}$$

There a, b, c and d are numerical expressions where only the functions f, h and j interfere. So:

$$a = \frac{\int_0^\infty x\, h\,(x)\, dx}{\int_0^\infty x\, f^2\,(x)\, dx} \qquad \text{with} \qquad x = \frac{r}{R}$$

We may say that these equations are more complete than Schmidt's or Sutton's for instance; they take into account the degree of stability of the atmosphere through the term:

$$\frac{\partial\, \theta_e}{\partial\, z}$$

which equals zero in a neutral atmosphere.

Here we only detail the resolution of this last case, though the computation has been made for all cases of stability. If we suppose that the functions f and h are gaussian and indentical:

$$f\,(x) = h\,(x) = e^{-\frac{x^2}{2}}$$

we find that: $a = d = 2$ and $b = 3$.

Then we eliminate the terms containing $\frac{\theta'_m}{\theta_e}$ in the first two equations; we come to:

$$2\, c\, w^3\, R = w^3 \frac{d\, R^2}{dz} = 2\, R\, w^3 \frac{dR}{dz}$$

(we suppress now the m subscript).

Therefore $R = cz$ by assuming $R = o$ for $z = o$.

This law is no longer a hypothesis but a property which is the more satisfied as w and θ are nearer to gaussian distributions.

The integration of the system presents no difficulty; we write the last equation as follows:

$$R^2 w \theta' = A$$

with:

$$A = \frac{Q}{\pi \rho C_p}$$

The general solution is:

$$w = \left(\frac{3 A g}{2 \theta_o c^2 z} + \frac{B}{z3} \right)^{\frac{1}{3}}$$

$$\theta' = \frac{A}{c^2 z^2} \left(\frac{3 A g}{2 \theta_o c^2 z} + \frac{B}{z^3} \right)^{-\frac{1}{3}}$$

B is a constant whose value is determined by the following boundary condition:

$B = {w_o}^3 {z_o}^3 - \frac{3 A g}{2 \theta_o c^2} {z_o}^2$ where $z_o = \frac{R_o}{c}$ and R_o

is the inner radius of the stack.

In the second stage of its evolution, the plume is described by a system of two equations:

$$\frac{d w}{dt} = \frac{g \theta'}{\theta_e} - k w$$

$$\frac{d \theta}{dt} = - k \theta'$$

in which the k coefficient is called "turbulent mixing rate" and accounts for the exchanges due to turbulence (see Appendix 2).

In reality the mixing rate is proportional to the ratio of a turbulent diffusivity to the square of a length: Priestley suggests:

$$k = \frac{8 K}{{R_1}^2}$$

in which R_1 is the radius of the plume, at the end of the first stage.

The integration of the above system can be easily achieved. If we use index 1 for values related to the end of the first stage, the laws of the evolution of θ' and w with time are:

$$\theta' = \theta'_1 e^{-k\,(t - t_1)}$$

$$w' = \left[w_1 + \frac{g\,\theta'_1}{\theta_e}\,(t = t_1) \right] e - k\,(t - t_1)$$

The integration of the last equation from $t = t_1$ to $t = \infty$ gives us the ceiling height of the plume, and therefore the plume rise:

$$z_{max} = z_1 + \frac{w_1}{k} + g\,\frac{\theta'_1}{k^2\theta_e}$$

Then, we must determine w_1 and z_1. To do so, we write that, at the transition point between the first two stages, the general solution we made out before when dealing with the first stage, has to satisfy also the system of equations which describes the second stage. Therefore, we may write, when α is the ratio:

$$\frac{3\,A\,g}{2\,\theta_e c^2}$$

$$w_1^3 = \frac{\alpha}{z_1} + w_o^3\,\frac{z_o^3}{z_1^3} - \alpha\,\frac{x_o^3}{z_1^3} \quad \text{(first stage solution)}$$

and:

$$\frac{d\,w_1}{dz_1} = \frac{g\,\theta'_1}{\theta_e\,w_1} - k \quad \text{(second stage).}$$

In the second equation we replace θ'_1 by $\frac{A}{R_1^2 w_1}$ and we get after multiplicating both members by $3\,w_1^2$:

$$3\,w_1^2\,\frac{d\,w_1}{dz_1} = \frac{2\alpha}{z_1^2} - 3\,w_1^2 k \qquad (R_1^2 = c^2 z_1^2)$$

Concerning the first equation, we obtain after a differentiation with respect to z:

$$3 w_1^2 \frac{dw_1}{dz_1} = \frac{\alpha}{z_1^4} (3 z_o^2 - z_1^2) - \frac{3 w_o^3 z_o^3}{z_1^4}$$

The identification of the right-hand members of these two last equations gives a third degree equation in z_1^2 which is due to Spurr (23).

$$z_1^6 - a z_1^2 - b = o$$

with:

$$a = \frac{\alpha}{k^3} = - \frac{3 A g}{2 k^3 \theta_o c^2} \quad \text{and} \quad b = \frac{B}{k^3} =$$

$$w_o^3 \frac{z_o^3}{k^3} - \frac{3 A g}{2 \theta_o c^2} \frac{z_o^2}{k^3}$$

An approximate solution of that equation is given by Lucas, Moore and Spurr (24).

For $a^3 > b^2$ ....$z_1 = (1.075 \pm 0.075) a^{1/4}$

For $a^3 < b^2$ ....$z_1 = (1.075 \pm 0.075) b^{1/6}$

For $a^3 = b^2$ ....$z_1 = 1.15 b^{1/6} = 1.15 a^{1/6}$

It is easy to get w_1 and one shows that:

$w_1 = k z_1$ (see Appendix 3)

The final results enables us to write z_{max} in terms of z_1:

$$z_{max} = 2 z_1 + \frac{2 a}{z_1^3} \quad \text{(see Appendix 3)}$$

Then we only have to replace z_1 by one of its approximate expressions and we get a plume rise formula in which there are only a and b.

In normal operations of power stations, the condition $a^3 > b^2$ is generally satisfied so that b does not appear in the final expression:

$$z_{max} = (2.68 \pm 0.05) a^{1/4}$$

The condition $a^3 > b^2$ is verified when the following conditions are verified:

$$\begin{cases} w_o \; U < \frac{3}{2} \, g \, \frac{\theta_o - \theta_{eo}}{\theta_{eo}} \; x_{k\,N} \\ z_o^2 \ll z_1^2 \end{cases}$$

($x_{k\,N}$ will be determined later)

Theoretically, the problem is then solved when dealing with neutral atmosphere but the above formula is not yet practically utilizable because a includes k and c which have not yet been determined.

Priestley (1) then makes two supplementary assumptions:

(1) He assumes that c^2 is proportional to U

$$c^2 = \frac{U}{U_c} \quad \text{(see Appendix 4)}$$

U_c is a characteristic speed to which Priestley assigns a standard value $U_{cs} = 4.27$ m/s (14 ft/s).

(2) In the second stage, he assumes that the evolution of the plume radius with x, horizontal distance, is an exponential function determined by:

$$\frac{1}{R} \; \frac{dR}{dx} = \frac{1}{2 \, x_{kN}}$$

x_{kN} is a characteristic distance to which Priestley assigns a standard value: $x_{kN} = 305$ m (1000 ft).

In these conditions, k is given by the equation:

$$k = \frac{U}{x_{kN}} \quad \text{(see Appendix 4)}$$

The formula giving the plume rise is then:

$$\Delta h = z_c \; \# \; 2 \cdot 68 \left(\frac{3 \, g \, 10^6}{2 \, \theta_{eo} \, \pi \, \rho_e \, C_p} \right)^{1/4} U_c^{1/4} \, x_{kN}^{3/4} \, Q^{1/4} \, U^{-1}$$

When $\theta_{eo} = 283^{o}K$, this last formula may be written:

$$\Delta h = z_c = 5700\,\beta Q^{\frac{1}{4}}\,U^{-1}$$

(z_c in m, U in m/s and Q in MW).

The coefficient β equals 1 when U_c and x_{kN} are actually equal to their standard values. When it is not so, we have

$$\beta = \left[\frac{x_{kN}}{x_{ks}}\right]^{3/4}\left[\frac{U_c}{U_{cs}}\right]^{\frac{1}{4}}$$

In the case of stable and unstable atmospheres, Lucas, Moore and Spurr come to a new formula which is identical with the former one: the only difference comes from the introduction of a multiplicative factor (which is called γ) which varies with the degree of instability of the atmosphere and with the ratio:

$$\frac{x_k}{x_{kN}}$$

The definition of x_k is the same as that of x_{kN}, but x_k is related to a given stability condition, whereas x_{kN} is defined in the case of a neutral atmosphere.

3.1-2 Phenomenological approaches

There are no less than 15 or 20 empiric formulae to calculate the rise of plume effluents. None has been universally accepted primarily because it has been impossible to establish the validity of any one from experiments whose observation and measurement techniques and whose experimental conditions (such as: characteristics of pollutant sources, atmospheric conditions) differ appreciably (see tables 1, 2, 3, 6 and 8).

As the number of experiments is getting quite important, several authors have been trying for five years to make a statistical analysis of all the experiments so as to obtain a formula which would give the best average of all the results.

We shall limit our study to the works of a few authors who take into account a great number of experimental results relating to various types of stacks; they are: Moore, Lucas, Hamilton (28), Brummage (29), Bringfelt (36), Moses and Carson (31), Whaley (19).

Because the sets of data used by these authors are not necessarily the same, or because data from different sources are not weighed in the same manner, their final conclusions often vary.

Besides, we may notice, too, two other difficulties which are:

- plume rise definition (see 3.1-1)
- the influence of the emitted heat flux

Among the points of agreement, there is essentially the formulation of plume rise which may be generally written:

$$\Delta h = \text{"constant"} \times Q^{a} \times U^{b}$$

Then we shall attempt to point out the most interesting conclusions which may appear in these various studies.

3.1-2-1 Brummage (29) comes to a formula as follows:

$$\Delta h = 0.175 \frac{Q^{\frac{1}{2}}}{U^{3/4}} \qquad \text{Q in calories/s and U in m/s}$$

$$\text{or: } \Delta h = 86 \frac{Q^{\frac{1}{2}}}{U^{3/4}} \qquad \text{Q in MW and U in m/s}$$

This formula is built from Lucas' experiments (28) and from Bosanquet's (14) , Stewart's (34), Rauch's (see table 2).

In reality, data relating to the site of Duisburg represent more or less 75% of the total, which considerably limits the value of this statistical analysis. Then Brummage's formula (usually known as "Concawe formula") is most significant for Duisburg's tests which are usually charged with the following facts:

- the Rauch data, which dominate the Concawe analysis consist of measurements which reached 500m downwind on only 10 per cent of the occasions when the plumes were photographed: consequently, we cannot be sure at all that the maximum plume rise was then reached.

- the rates of heat emission are low: between 1 and 10 MW. Consequently it seems difficult to extend that formula to stacks whose rates of heat emission exceed 10 MW.

3.1-2-2 Lucas, Moore, Spurr (24) suggest a formula as follows:

$$\Delta h = \alpha \frac{Q^{\frac{1}{4}}}{U} \qquad \text{(see above)}$$

This formula was proved quite satisfactory for the stacks of four British Power Plants (table 3).

α was assumed to vary according to the power plant site, the atmospheric stability conditions and the type of stack.

Besides Lucas gives a formula as follows:

$$\alpha = 475 + 2/3\ (h_o - 100) \text{ in } m^2 \cdot s^{-1} \cdot MW^{-1/4}$$

in which:

$h_o = 50$ to 150 m is the real height of the stack.

Gartrell (31) (T.V.A.) and Rauch's (33) (Duisburg) have been compared to the estimations obtained by using this formula (table 3).

In all these comparisons, Lucas et al tried to determine the plume rise as the height above the chimney at which the mean plume axis levels off. When the observation distance was not too short, they extrapolated the mean path of the plume to a distance of about 2 kilometers. Then they got the results indicated in table 3. the values of in that table vary from 300 to 580.

By examining these data, Hamilton showed that there was a significant correlation between α and the stack-height, provided one excludes the values for Duisburg.

Scriven (21) tried to explain this divergence from Duisburg's estimates, by showing that the ratio of the stack diameter to the stack height was much smaller than at any of the other plants, and that such a small ratio contributed to increase the tendency of the plume to break up into discrete puffs, which according to Moore (20) could result in lower plume rise (see 3.1-1-5).

Then important diverging points as regards the meaning of the tests, appear between C.E.G.B. results (lucas et al) and Concawe's (Brummage).

3.1-2-3 Bringfelt (30) suggests several formula:

$$\Delta h = \frac{103}{U}\ Q^{0.39} \text{ when } x = 250 \text{ m}$$

$$\Delta h = \frac{167}{U}\ Q^{0.36} \text{ when } x = 500 \text{ m}$$

$$\Delta h = \frac{224}{U}\ Q^{0.34} \text{ when } x = 1000 \text{ m}$$

Q is expressed in MW.

These formulae are based on a great number of experiments (see table 4).

For x distances between 250 m and 500 m, Bringfelt finds that the plume develops downwind according to a $x^{2/3}$ law.

Between 500 and 1000 m, it seems that the law can no longer be verified because the atmospheric turbulence plays a more important part.

The results obtained 1000 m downwind seem to be 70% inferior to those we got with Lucas formula for heat emissions of 33.5 MW (see table 5). Bringfelt thinks these variations are due to several circumstances.

- Lucas' formula is available only when distances exceed one kilometer.
- Lucas uses wind speed at the level of the effective height of plume instead of using it at the top of the stack.

The comparisons with the Concawe formula (table 5) give us consistent values at a distance of 500 m, and when the heat emissions are inferior to 10 MW. It seems to be normal because the Concawe formula is almost entirely based on Duisburg's results. (Observations made at a distance of 500 m from the stack.)

On the other hand, we notice that when the heat emissions exceed 33.5 MW, it is the 1000 m formula which gives the best agreement with the Concawe formula.

According to Bringfelt we notice that the Concawe formula was established in order to give the maximum rise at a distance of 500 m for a heat emission of 6.7 MW and at about 1500 m for a heat emission of 33.5 MW.

3.1-2-4 Moses and Carson (31) suggest three formulae:

$$\Delta h = 0.029 \frac{W_s}{U} d + 5.3 \frac{\sqrt{Q}}{U} \qquad (1)$$

$$\Delta h = 1.96 \frac{W_s}{U} d + 3.06 \frac{\sqrt{Q}}{U} + 11 \qquad (2)$$

$$\Delta h = 5.32 \frac{\sqrt{Q}}{U} \qquad (3)$$

in which Q is expressed in Kcal/s, d and Δh in meters, U in m/s. They only consider the first equation.

In order to take the atmospheric stability into account, they suggested a more general formula:

$$\Delta h = A \left[- 0.029 \frac{W_s}{U} d + 5.35 \frac{\sqrt{Q}}{U} \right] \qquad (4)$$

in which:

A = 1.08 neutral atmosphere

A = 2.65 unstable atmosphere

A = 0.68 stable atmosphere

Table 6 and 7 sum up all the data used by Moses and Carson.

The data relating to experiments in stable or unstable atmosphere are not very numerous and, moreover, they only refer to rather small stacks: then, the general formula (4) is not very significant and it can't be easily extrapolated to high stacks.

In table 7, most of the data come from Duisburg (about 50% of the total); consequently the results Moses and Carson could get are rather close to the Concawe's.

$$\Delta h = 5.32 \frac{\sqrt{Q}}{U} \qquad \text{(Moses and Carson)}$$

$$\Delta h = 5.53 \frac{\sqrt{Q}}{U^{3/4}} \qquad \text{(Concawe)}$$

Q is expressed in Kcal/s.

Or:

$$\frac{(\Delta h) \text{ Conc.}}{(\Delta h) \text{ Moses}} \; \# \; 1.04 \, U^{\frac{1}{4}}$$

Moses and Carson formula then seems to give plume rises lower than Concawe's, because of the 3/4 speed exponent: the difference increases with the speed.

3.1-2-5 Another synthesis was achieved in 1969 by Whaley (19); it completes the precedent mentioned analysis. Whaley used the data of table 8. He distinguished 7 classes of data, according to the rate of heat emission.

He also estimated that Δh is in inverse ratio to U and he considered, for each class, the curve $\Delta h/Q$ versus 1/U. The best regression line was calculated for any of these categories; n, the exponent of Q, was then estimated so as to get a single curve for the whole of the various classes. Then, Whaley got the "C C R L -2" formula.

$$\Delta h = 262 - \frac{Q^{\frac{1}{4}}}{U} \qquad Q \text{ in MW.}$$

Then, he compared the results obtained by using Concawe, Lucas, Moses - Carson, C C R L -2 formulae and data different from those he used to get his formula (table 9). The observed plume rises related to distances between 400 and 2500 m. Whaley extrapolated them to distances of 1000 m and 20000 m. He thought that the discrepancies between the various formulae essentially came from the distance to the stack at which the plume rise was observed.

As far as rates of heat emission lower than 10 MW are concerned, the Concawe formula fits well the experimental results.

On the opposite, when the rates of heat emission are higher than 10 MW, the C E G B formula (compared with data obtained at 2000 m) and Whaley's formula (compared with data obtained at 1000 m) seem to be more available. Moses and Carson formula may provide reasonable results, too.

As a conclusion, we may say that in all the above mentioned studies, it seems to be convenient to distinquish between formulae built on far distant observations from stacks and formulae built on short distant observations. Lucas, Whaley and Bringfelt formulae are probably the only ones to take it into account.

Lucas suggests a formula in which plume rise is observed at a distance of about 2 kilometers from the plant, which seems to correspond to the point at which the plume axis is practically horizontal.

Bringfelt suggests several formulae according to the distance of observation; he does not consider any definition of maximum plume rise.

Whaley uses a definition of plume rise slightly different from Lucas': he says that the maximum height-of-rise is reached by the visible plume when the density effects and the initial momentum stop to contribute to the rising of the plume axis. Such a definition implies that the differential coefficient of the height of plume axis (considered as a function of the distance x) becomes constant or reaches a minimum: Whaley estimates that point between 450 and 1200 m.

In Concawe, Moses and Carson formulae, there is no definition of plume rise.

This lack of uniformity is an essential factor in the differences among the various formulae. As far as we know it seems to be rather difficult to promote a universal formula which could be applied to any stack, whatever their dimensions or conditions of emission may be. As Whaley did--though we try to find a different formula for any different type--we believe that it is convenient to classify the various tests and experimental results according to the criteria of rate of heat emission: first we notice that we may indifferently speak about heat emission or mass flow when only power plants are concerned, because their exit temperatures always are not strongly different from 110 or 120°C.

In this last case, Lucas' formula could be accepted, the coefficient is taken equal to 500 (Q being expressed in MW). The precision of this formula would then average ± 20%. Such a precision certainly decreases as wind speed decreases and reaches a value we might estimate to be 3 m/s. There is no contribution of wind speeds inferior to that value practically in most tests (table 5) as Brummage pointed out.

As for the advisability of a classification according to an atmospheric stability criteria, we must say that such a classification is deprived of any kind of interest when we come to consider higher wind speed; Strom (35) estimates that 3 m/s is the limit under which atmospheric stability effects prevail over the effects due to mechanical turbulence; it is probably one of the reasons why the various authors did not consider any possible measurement below 3 m/s. Unfortunately, when we calculate the so-called "dangerous" or "critical" speeds in air pollution (see paragraph 3.2), the values we must take into account often are close to that limit and sometimes do not reach it: the result found under those circumstances are not significant.

Table 1

Summary of Techniques Used for Plume Measurements (Bringfelt (30))

Original Article	Measurement of Plume Rise	Distance Interval m	Measurement of Wind Speed	Measurement of Stability
BOSANQUET (1950)	Projection on a screen	30-244	Not described	Not made
HOLLAND X-10 (1953)	Ground photography	unknown	From tower near chimney top level	From tower beneath top level
WATTS BAR	Projection on screen	unknown	From tower beneath top level	See above
THOMAS (1954)	Theodolite-readings	unknown	From tower near top level	See above
STEWART (1954)	^{41}A - concentrations with balloon carried Geiger-counters	350-650	See above	See above
CSANADY (1961)	Ground photography	50-300	Timing of plume details	Not made
MOSES-STROM (1961)	See above	30-60	From tower near top level	From tower at plume level
WEDIN (1962)	Fluorescent ZnCd-sulphide particles collected from aeroplane	3000-20000	Pilot balloons gave wind profile	Wire-sonde and radio-sonde
LUCAS (1963)	Tracking of hydrogen-filled balloons with rangefinder	300-1800	Timing of balloons in plume	Not made
RAUCH (1964)	Ground photography	50-500	Plume details on photographs	Balloon-carried thermograph

Table 1

Summary of Techniques Used for Plume Rise Measurements (Bringfelt (30))

Original Article	Measurement of Plume Rise	Distance Interval m	Measurement of Wind Speed	Measurement of Stability
GARTRELL (1964)	SO_2-concentrations from helicopter	800-3000	Pilot balloons gave wind profile	Thermistor on helicopter
LFAVITT (1965)	Ground photography and localization by theodolite and helicopter	200-2000	See above	See above
HAMILTON (1967)	Modified cloud height search light	400	From tower near top level	From tower near top level
TILBURY				
NORTHFLEET	Plume cross-section with laser	1800	See above	See above
BRINGFELT (1968)	Photography from aeroplane	50-750	Plume details on photographs	Thermistor on aeroplane

Table 2

Sources of Plume Rise Data Used by Brummage (Concawe)
Brummage (29)

Authors	Stability Category	Efflux rate $Nm^3 s^{-1}$	Exit Velocity $m\ s^{-1}$	Temperature Difference ^oK	Heat Flux $cal.s^{-1}x10^o$	Wind Speed ms^{-1}	No. of Observations
Lucas, Moore, Spurr (1963)	neutral	24-122	3,3-17	130	1,0-5,1	4,4-10,5	13
	various	101-405	3,75-15	120	4-16	3-10,5	14
Bosanquet (1957)	unknown	4,1-35,3	3,7-11,0	25-116	0,07-1,58	3-10,0	8
Stewart, Gale, Crooks (1954)	neutral	69	14,6	50	1,16	4,2-12,3	27
	slightly-unstable	69	14,6	50	1,16	4,4-8,0	12
Rauch (Duisburg) (1964)	neutral	36-76	5,2-11,5	99-125	1,25-3,25	2,1-9,7	137
	slightly-unstable	28-78	4,0-11,4	98-121	1,10-2,95	1,6-10,5	159
	fairly-stable	46-76	5,8-11,1	100-115	1,40-2,95	2,5-9,3	35
Rauch (Darmstadt)	neutral	7-11	3,4-5,5	270-298	0,65-1,1	4,1-9,2	33

Table 3

Values of for Different Plants
(Hamilton (28)

$$\Delta h = \alpha \frac{Q^{1/4}}{U}$$

Plant	Mean value of α $m^2 s^{-1}$ $MW^{-1/4}$	Distance of measurements m	Number of stacks	Stack height m	Stack diameter m	Heat emission MW	Exit velocity $m\ s^{-1}$
Castle Donington Power Station	580	1100-1800	2	128	7	17-67	4-15
Northfleet Power Station	400	1200-2500	2	150	6	10-60	3-20
Tilbury Power Station	400	400	2	100	7	20-60	5-15
Colbert Power Station (TVA)	450	1600	4	90	5	30	14
Earley Power Station	460	1100-1800	2	75	3,5	3-25	2-18
Harwell	400	110-970	1	60	3,5	3,5	10
Bosanquet 1, 2, and 3	450	90-240	?	?	?	0,2 and 4,2	8-11
Duisburg Power Station	300	100-800	1	125	3,5	4-12	4-12

Table 4

Distribution of Q, U and ΔT Used by Bringfelt (30)

N	Q MW	N	u m/s	N	ΔT $^{\circ}C$
4	<3	0	<3	7	<50
71	3-12,9	7	3-3,9	27	50-99
6	13-24,9	20	4-4,9	93	100-199
48	25-59,9	77	5-8,9	3	200-499
2	⩾60	19	9-11,9	1	⩾500
		8	12-15,9		

ΔT is the initial temperature difference in $^{\circ}C$ between chimney gases and outer air. N gives numbers of observations.

Table 5
(Bringfelt (30))

Calculated Plume Rises for Some Values of Heat Flux and Wind Speed

Heat flux MW	Wind speed $m\ s^{-1}$	Plume Rise, m				
				Bringfelt		
		Lucas Formula	Concawe Formula	250 m	500 m	1000 m
6,7	4	214	70	54	83	107
	8	107	43	27	41	54
	10	86	37	22	33	43
16,7	4	268	119	77	115	146
	8	134	73	39	58	73
	10	107	63	31	46	58
3,5	4	312	178	101	148	185
	8	156	110	51	74	92
	10	125	94	41	59	74

Table 6

Ranges of Stack and Meteorological Parameters Used by Moses and Carson (31)

Station	Wind speed m/s	Exit Velocity m/s	Heat flux k cal/s	Stack height m	Stack diameter m
Argonne I	7,3-1,0	13,2-4,7	12,7-2,0	34	0,44
Arbonne II	10,3-3,1	14,0-4,56	34,4-3,3	34	0,44
Harwell	11,7-3	9,90	1215-1215	61	3,46
Duisberg	10,5-1,6	12,1-3,5	2475-979	125	3,50
Gernsheim	9,2-1,5	5,3-2,2	1003-384	75	2,30

Tennessee Valley Authority

Widow's Creek	6,6-1,5	24,5-22,9	1,79-1,57.10^4	153	6,34
Gallatin	8,2-1,6	16,4-14,8	1,77-1,5.10^4	153	7,63
Paradise	11,3-2,3	19,2-15,3	2,46-1,7.10^4	183	7,93

Table 7

Summary of Data Sources Used by Moses and Carson

Station	Stable	Neutral	Unstable	Total
Argonne I	19	10	6	35
Argonne II	26	6	102	134
Harwell	8	27	11	46
Duisburg	51	328		379
Gernsheim	10	33		43
Bosanquet		7		7
Widow's Creek	1	9		10
Gallatin	2	24		26
Paradise	4	26		30

Table 8

Sources of Plume Rise Data Used by Whaley (19)

Reference	Number of Observations	Stability Category	Efflux velocity range m s^{-1}	Wind velocity m s^{-1}	Heat flux range 10^3 Kcal/s
Carpenter et al (1967)	62 7	neutral stable	14,8-24,5	0,6-11,3	15,0-24,6
Lucas, Moore, Spurr (1963)	13 14	neutral stable	2,0-18,0	3,0-10,5	0,7-16,0
Stewart, Gale, Crooks (1954)	26	neutral	9,9	3,0-10,5	1,2
Rauch (1964)	329	neutral stable	2,2-12,0	1,6-10,5	0,6-3,3

Table 9

Comparison of Measured and Extrapolated Plume Rise With Calculated Values (Whaley (19))

Heat flux $Qx10^{-3}$ (Q in Kcal /s)	Wind Velocity m/s	Measured and Extrapolated Plume Rise: Measured Z_x m	Measured x m	Extrapolated Z_{1000} m	Extrapolated Z_{2000} m	Calculated Plume Rise: Concawe $\frac{Q^{\frac{1}{2}}}{5,53U}$	Lucas $Z_{2000} = 116\frac{Q^{\frac{1}{4}}}{U}$	Moses/Strom $\frac{Q}{5,32U}^{\frac{1}{2}}$	CCRL-2 $Z_{1000} = 66,4\frac{Q^{\frac{1}{4}}}{U}$	Observations
1,25	4	97	400-1200	97	156	69	173	47	99	
2,5	3,5	147	400-1200	91	147	108	235	76	135	
4,06	7,2	82	1200-2500	51	82	80	129	47	74	
4,06	10,2	107	1200-2500	107	173	62	91	33	52	
7,89	4,2	182	1200-2500	113	167	167	261	118	149	
7,89	7,2	182	1200-2500	113	182	112	152	66	87	
7,89	10,2	105	1200-2500	65	105	86	108	46	61	The data are from:
7,89	16,2	68	1200-2500	42	68	61	68	29	39	
8,5	4,5	180	400-1200	180	290	165	248	109	142	
8,5	6,1	146	400-1200	146	236	131	183	80	105	-Bartrell, Thomas, Carpenter (1964)
8,5	9,5	120	400-1200	120	193	94	118	52	67	
9,56	2,0	450	1200-2500	279	450	321	577	260	329	
11,9	4,2	167	1200-2500	104	167	205	288	138	164	
11,9	7,2	162	1200-2500	100	162	137	168	81	96	
11,9	10,2	100	1200-2500	62	100	106	119	57	68	-Carpenter et al (1967)
11,9	13,0	85	1200-2500	53	85	88	93	45	53	
11,9	16,2	60	1200-2500	37	60	75	75	36	43	
15,7	2,0	510	1200-2500	316	510	412	652	333	370	
15,7	6,0	220	1200-2500	136	220	181	217	111	123	-Hamilton (1967)
15,7	8,0	165	1200-2500	102	165	146	163	83	93	
15,7	10	96	1200-2500	60	96	123	130	67	74	
15,7	12	80	1200-2500	50	80	107	109	56	62	
15,7	16	120	1200-2500	74	120	87	82	42	46	
17,6	0,6	1025	400-1200	1025	1653	1074	2232	1177	1273	
17,6	1,4	777	400-1200	777	1253	570	957	504	545	
17,7	6,6	103	400-1200	103	166	179	203	107	116	
18,4	11,3	70	400-1200	70	113	123	121	64	68	
24,6	5,2	106	400-1200	106	171	252	282	160	160	

3.2 - FORMULAE: DIFFUSION OF PLUME EMITTED BY A POINT SOURCE

3.2-1 - Presentation of the usual diffusion formulae

One may consider four formulae are used in making practical estimates of ground level concentrations C (x,y,o, H). They are, in chronological order:

1) BOSANQUET and PEARSON formula (1936): [36]

$$C\ (x,\ y,\ o,\ H) = \frac{q_m}{\sqrt{2\pi}\ pqx^2\ U} \exp\left[-\frac{1}{2}\left(\frac{y}{qx}\right)^2 - \frac{H}{px} \right]$$

2) SUTTON formula (1947) : [3]

$$C\ (x,\ y,\ o,\ H) = \frac{2\ q_m}{C_y\ C_z\ x^{2-n}\ U\pi} \exp\left[-\frac{1}{x^{2-n}} \left(\frac{y^2}{C_y^2} + \frac{H^2}{C_z^2}\right) \right]$$

3) CALDER formula (1952) : [37]

$$C\ (x,\ y,\ o,\ H) = \frac{q_m\ U}{2\ k^2\ a\ U_*^2\ x^2} \exp\left[-\frac{U}{k\ U_* x} \left(\frac{y}{a} + H\right) \right]$$

4) PASQUILL formula (1959) : [38]

$$C\ (x,\ y,\ o,\ H) = \frac{q_m}{\pi \sigma_y\ \sigma_z\ U} \exp\left[-\frac{1}{2}\left(\frac{y}{\sigma_y}\right)^2 - \frac{1}{2}\left(\frac{H}{\sigma_z}\right)^2 \right]$$

We may notice that in all these formulae the concentrations are distributed according to exponential laws. They may be written in a general way:

$$C\ (x,\ y,\ o,\ H) = A \exp \left[- \left(\frac{y}{\sqrt{2}\,\sigma_y} \right)^r - \left(\frac{H}{\sqrt{2}\,\sigma_z} \right)^s \right]$$

The available formulae by which σ_y, σ_z, are expressed semi-theoretically, in terms of parameters related to the turbulence, are summarized in the following table.

	σ_y	σ_z	r	s
BOSANQUET & PEARSON	$q\ x$	$\sqrt{2}\ p\ x$	2	1
SUTTON	$\frac{1}{\sqrt{2}} C_y\ x^{\frac{2-n}{2}}$	$\frac{1}{\sqrt{2}} C_z\ x^{\frac{2-n}{2}}$	2	2
CALDER	$\frac{\sqrt{2}\ a\ k\ U_*\ x}{U}$	$\frac{\sqrt{2}\ k\ U_*\ x}{U}$	1	1
PASQUILL	σ_y	σ_z	2	2

In these formulae, the source coordinates are x,y, and H. q_m is the emitted mass rate, H is the effective height in which we have included Δh, the plume-rise; σ_y and σ_z are the lateral and vertical standard deviations of the pollutant distribution.

U_* is the fraction velocity given by: $U_*\#(kU_z))/(\log(z/z_o))$

where z is a characteristic length of the surface layer, and where z_o is the roughness height.

C_y and C_z are called SUTTON diffusion coefficients, n is a turbulence parameter determined by the vertical profile of mean wind speed, q is an empiric coefficient, p is the numerical coefficient in an assumed form of the vertical diffusion coefficient ($k_z = p\ Uz$), a is the ratio of the lateral velocity fluctuation to the vertical one, k is the VON KARMAN's constant ($k = 0.4$).

Formulae developed by CALDER, BOSANQUET and PEARSON are all strictly applicable only in neutral conditions of stability.

BOSANQUET and PEARSON suggested $p = 0.005$ and $q = 0.08$. CALDER recommended $a = 2$ at the ground level but he gave no indications at all about the variation with z of such a coefficient, and his formula turns out to be practically useless.

SUTTON's formula, which was very often used, is but a particular aspect of PASQUILL's formula; yet it does not explain the standard deviations σ_y and σ_z. These two formulae might be used in any stable case with the appropriate values of the coefficients σ_y, σ_z, C_y, C_z and u. Consequently, PASQUILL suggests tables which indicate the various laws of variations $\sigma_y(x)$ and $\sigma_z(x)$ for six categories or stability (classified from A to F according to the increasing order of stability).

SUTTON, whose formula rests on the hypothesis concerning the form of the lagrangian correlation coefficient [see TAYLOR, ref. 39] assumes that $C_y = C_z$ when $z \geqslant 25$ m. The variations of C_z, C_y and u with z and of the atmospheric stability conditions are indicated in the following table:

Stability condition	n	z Height above ground level (m)			
		25	50	75	100
unstable	0.20	0.21	0.17	0.16	0.12
neutral	0.25	0.12	0.10	0.09	0.07
slightly stable	0.33	0.08	0.06	0.05	0.04
very stable	0.50	0.06	0.05	0.04	0.03

SUTTON diffusion coefficients at PORTON; sampling time: 3 minutes.

$(C_y = C_z)$

Numerous authors: HOLLAND at Oak Ridge [13], SINGER and SMITH at Brookhaven [40], FRIEDMAN at Round Hill [41], have also determined numerical values of SUTTON coefficients. There may be important differences, which may reach 200 per cent, among the corresponding values, though the sampling times were about the same.

3.2-2 - Simplified formulae for practical use. "Critical" wind speed.

Generally, one is interested in knowing the manimum concentration C_m at ground level for given emission conditions. This maximum is obviously situated under the plum axis; then one only has to determine the value x_m of x which cancels the differential coefficient:

$$\frac{d\,C\,(x,\,o,\,o,\,H)}{dx}$$

The expression of C_m is: $C_m = C\,(x_m,\,o,\,o,\,H)$. Then, we get from SUTTON formula:

$$x_m = \left(\frac{H}{C_z}\right)^{\frac{2}{2-n}} \qquad \text{and} \qquad C_m = \frac{2\,q_m}{\pi e\,U\,H^2}\;\frac{C_z}{C_y}$$

Finally, it is of some interest to know the various stages in the evolution of the maximum concentration when the emission conditions change, so as to determine C_M, the maximum absolute concentration. As we may express C_m as a function of U (wind speed) and q_m (mass flow), one will only try to get C_M as the partial differential coefficient with respect to U. The corresponding value of U is called critical wind speed U_{cr} (or dangerous wind speed).

So, from the general expression of plume rise formula we get:

$$\Delta h = K\,Q^a\,U^b \qquad \text{(cf. 3.1-2)}$$

or:

$$H = h_o + K\,Q^a\,U^b$$

By using the above example, we find:

$$U_c = \left[\frac{-\,h_o}{K\,Q^a\,(2b+1)}\right]^{\frac{1}{b}}$$

We get the expression of C_M by introducing the value U_c in H and then in C_m. When the wind speed equals U_{cr}, the plume rise is then given by the following relation:

$$\Delta h = (\Delta h)_{cr} = -\frac{h_o}{2b + 1} \quad \text{(in which we always have } b <- \frac{1}{2}\text{)}$$

NOTES: The idea of critical wind speed is intuitively suggested by a simple way of reasoning as follows; we suppose that there is no wind speed at all; the plume rise without ever bending over; Δh is unlimited. There are no concentrations at ground-level. In the same way, if we suppose that the wind speed is unlimited Δh would not exist but there would be no concentrations at ground level because the flow rate of pollutant would remain limited. Between these two opposites there is a certain wind speed for which the ground concentration takes a maximum value.

3.2-3 - Conditions for use.

Plume diffusion formulae such as the SUTTON one enable us to get rather a good approach to the concentration field in the simplest case. That is to say when the three following conditions are encountered:

1) Pollutant source (stack) is isolated.

2) Pollutant emission is known and continuous; all the atmospheric stability conditions are steady.

3) The site we consider is rather flat and its ground level roughness is not important (no high buildings in the source vicinity).

The accuracy of the estimations which are then provided depends on the atmospheric stability: for instance, TURNER [42], says that the standard deviation σ_z, indicating the state of stability, may be known, with an accuracy of 100 per cent in the three following circumstances:

1) In any case of stability, but for travel distances (x) inferior to a few hundred meters.

2) In neutral or slightly unstab[illegible]tions, and for distances inferior to a few kilometers.

3) In the case of an unstable lower layer (o-1000 m) with a strong inversion above it, for distances which may exceed 10 kilometers.

In any other circumstance (and especially for important distances) the estimation of σ_z is worse.

As for the errors due to the estimation of σ_y, we think that they are closely linked to the question of concentration sampling times. The standard deviation σ_y is much more sensitive than σ_z to an increase of the sampling times because the horizontal wind fluctuations may introduce an important dispersion of the plume at large distances downwind. We may particularly notice it by light wind and stable condition because low frequency horizontal fluctuations (cf. 2.2) may be then observed. This effect is markedly reduced when vertical diffusion is considered especially when the stability conditions do not change repidly. The plume meanderings which occur can be considered as virtual and vertical displacements of the source. On the one hand, these displacements are not generally very important and, on the other hand, the field interested by plume diffusion is more limited vertically than horizontally; consequently the variations at ground level are the less sensitive as the distance downwind is greater.

Many people considered sampling times inferior to an hour, and in any case, the very principle of the utilization of diffusion formulae to know the average concentration for a greater lapse of time (about 24 hours) is groundless. In effect, these formulae make us suppose that the distribution of wind speed fluctuations are normal for a given wind direction and such an hypothesis is groundless in most cases, In other words, the standard deviation σ_y does not take into account fluctuations whose periods exceed an hour.

Besides we shall find the same kind of limit when dealing with turbulent diffusivities (see 4.2).

This limitation related to sampling times is not the only one. We may also mention a few ones particular to these formulae:

1) They only give normal or exponential distributions of concentrations. It happens that, in certain circumstances, they are totally inadequate to the actual distributions; the most typical case being the fumigation: in his workbook of Atmospheric Dispersion Estimates, TURNER has no other possibility that to keep the normal distribution of concentrations in the upper stable part of plume, and to admit that in it's lower unstable part, there is a uniform concentration distribution down to the ground. This last concentration is given by the conservation law of the emitted mass rate (see fig. 14).

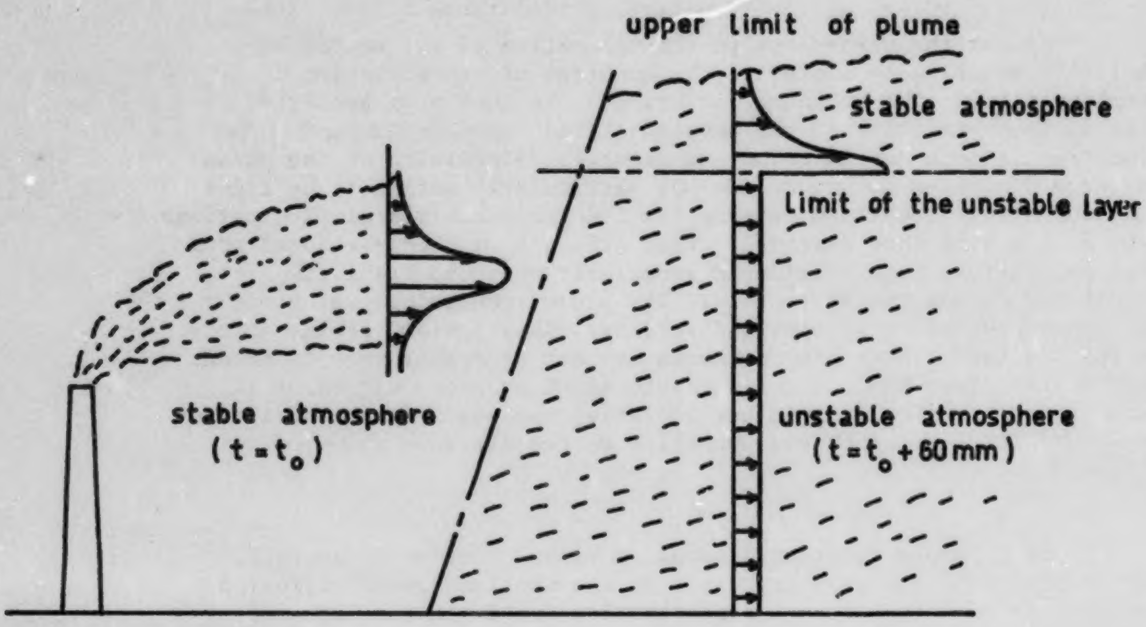

2) If these formulae may be considered as accurate enough, it is not so when we consider those we get out by differentiation. We have previously noted that when we try to determine a critical speed or an absolute maximum of concentrations at ground level we come to differentiate the law giving C(x, o, o, H), first with respect to x and then with respect to U. Consequently we believe that the value of the absolute maxima we may get out of such a process is very doubtful.

3.2-4 - Value of diffusion formulae.

First of all, these formulae have the merit of being of a very simple use. Because they take into account the mass conservation law and suggest continuous solutions in x, y, and z, maximum on the plume axis and always tending to 0 for infinite values of the variables, all we have to do is to adjust them, thanks to the functions σ_y (x) and σ_z (x) so as to be able or at least try to describe reasonably the possible field of concentrations. Besides we had the opportunity to simulate in a wind tunnel, diffusion in neutral atmosphere over a flat ground: the distributions of concentrations were measured with a good accuracy (2 to 3%) and offered valuable "gaussian" profiles (fig. 15), except that the plume was reflected on the ground.

In conclusion, the major deficiency of these formulae appears when trying to estimate correctly the standard deviations σ_y (x) and σ_z (x). Besides, they give only particular solutions that cannot account for the vertical variations of wind speed and turbulent diffusivities.

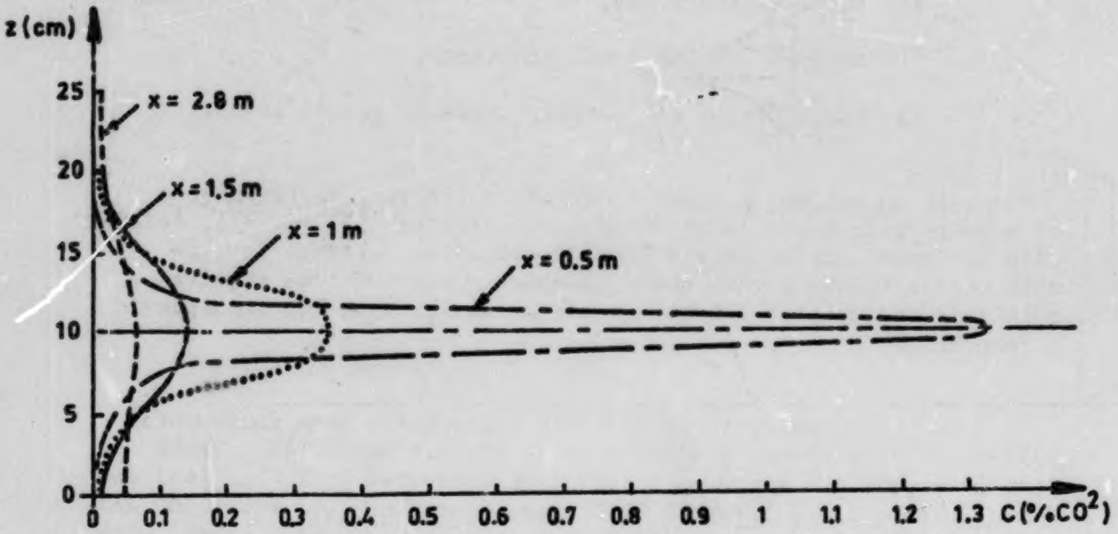

Fig. 15: VERTICAL DISTRIBUTIONS OBTAINED AT CHATOU IN WIND TUNNEL

(U = 8 m/s, emission of CO_2)

4 - MORE ELABORATE METHODS FOR THE ESTIMATION OF POLLUTION DOWNWIND AN ISOLATED STACK

4.1 - EXPERIMENTATION IN SITU

Experiments in situ on plume dispersal have the advantage of being conducted under the actual conditions of atmosphere and stack operation and in the presence of buildings, topography, and all other details of the real situation.

We have already pointed out (see 2.2) that in the determination of a plume we had to consider the characteristic parameters of the source on the one hand side and, on the other hand side, the characteristic parameters of the meteorological situation.

If we may consider that the operating conditions of a source do not vary throughout the year (for instance in the case of a modern power plant), it is not so when we consider the meteorological parameter. Consequently, the systematic exploration of a given site necessarily includes a great number of measurements during a lapse of time of about one year. We have to determine:

- the shape of the plume,
- the temperature and speed gradients,
- the distribution of concentrations at ground level.

It is not our subject to dwell on the various techniques of measurement; there is an abundant literature [43, 46, 47], dealing with the expoloration of the lower atmospheric layers. Yet, we must stress the fact that these systematic explorations require much time and people, because of the variability of the atmospheric parameters.

As an example, it is possible to indicate some fundamental full-scale measurement studies such as PRAIRIE GRASS [43], GREEN GLOW [44], and the more applied studies conducted by T.V.A. [45] and CEGB [28]; in the only GREEN GLOW experiment, the 200, 800, 1600 and 3200 acres contained 5 towers, 8 degrees apart from each other, with 15 samplers for each tower.

Obviously, for a new installation in the design stage, it is impossible to make any measurement, at least it would be very expensive. Some authors think that pollutant sources situated at the same height as the chimney can be very helpful; in the case of very high stacks this technique is not easily feasible.

In such a case we must then turn to other methods (wind tunnel experiments, numerical models, analytical formulae).

In the case of an already existing power plant, the measurement of the meteorological parameters can be achieved together with concentration measurements at ground level or in altitude.

Usually we can do with concentrations at ground level and we try to formulate correlations between the various pollution levels and the various meteorological characteristics.

When a sufficiently wide range of conditions has been measured an empirical relation between concentration and meteorological parameters can be established.

Nevertheless, it seems that measurements in situ are more interesting when they are part of more orientated experiments, complementarily with other methods. We may distinguish two different aspects:

- the determination of the micrometeorological characteristics of a given site;
- a short term forecast of these characteristics.

Under its first aspect, the experiment in situ enables us to characterize the most frequent meteorological conditions: knowledge of these conditions is necessary to the application of analytical or numerical methods and wind tunnel experiments (see 4.2).

Under its second aspect, we have to estimate, by a short term forecast, the pollution risks in a given site, from directly available data, such as:

- Value of meteorological parameters at ground level,
- Pollution rates (including emission data),
- Large scale weather conditions,
- Large scale weahter forecast.

4.2 - MATHEMATICAL MODELS OF PLUME DIFFUSION

4.2-1 - Presentation of the problem.

We must calculate C(x, y, z), the concentration field of a plume during the third stage of its evolution. Most of the models now in use are based on the turbulent diffusivity concept. In other words, they consist in solving an equation that can be written in rectangular co-ordinates as follows:

$$\frac{dC}{dt} = \frac{\partial C}{\partial t} + u\frac{\partial C}{\partial x} + v\frac{\partial C}{\partial y} + w\frac{\partial C}{\partial z} = \frac{\partial}{\partial x}\left(k_x\frac{\partial C}{\partial x}\right) + \frac{\partial}{\partial y}\left(k_y\frac{\partial C}{\partial y}\right) + \frac{\partial}{\partial z}\left(k_z\frac{\partial C}{\partial y}\right) \qquad (1)$$

with u, v, w: mean components of the speed of the effluent particles, k_x, k_y, k_z: turbulent diffusivities in the directions Ox, Oy, Oz.

We must stress here, two objections against the turbulent diffusivity concept. First, this concept assumes that a certain analogy exists between turbulent transfers and molecular transfers, which is not particularly satisfying. Secondly, RICHARDSON pointed out that these diffusivities are not universal parameters but are connected to the scale of turbulence.

In other words, a mathematical model of diffusion using turbulent diffusivities cannot account but for turbulent motions whose periods are inferior to a certain value T_o. We shall have to remember it when we want to compare the results given by a mathematical model to those given by experiments in situ, from concentrations sampled over a duration which may exceed T_o (see 4.2-2-1).

As we are generally only interested in steady flows and in two-dimensional speed fields, the term $\frac{\partial c}{\partial t}$ of equation (1) equals zero as well as v, and k_y, the lateral diffusivity is independent of y. Besides, we may neglect longitudinal diffusion compared with the transport term:

$$u \frac{\partial C}{\partial x}$$

The previous general equation then turns out to be:

$$u \frac{\partial C}{\partial x} + w \frac{\partial C}{\partial z} = k_y \frac{\partial^2 C}{\partial y^2} + \frac{\partial}{\partial z} \left(k_z \frac{\partial C}{\partial z}\right) \qquad (2)$$

with the following boundary conditions:

When $x = o$, $C(x,y,z) = C_o \, \delta(y) \, \delta(z - h)$ (δ : DIRAC function)

When $z = o$, $k_z \frac{\partial C}{\partial z} = o$ (zero flux condition at the surface of the ground).

When $x, |y|, z \longrightarrow \infty$ $C(x, y, z) \longrightarrow 0$

Besides, the concentration distribution is symmetrical with respect to the vertical plane containing the source; we may write:

$$C = C(x, |y|, z)$$

The various models only differ in the way, more or less elaborate, we introduce the values u, w, k_y and k_z, or in the way we solve the equation (2). The last point concerns essentially the assumptions on the form of the searched solution. As for the introduction of speeds and diffusivities, there are various procedures: the most simple one consists in considering constant coefficients or coefficients universally depending on z only; the most complicate one consists in solving a physico-numerical model of the atmospheric boundary layer.

In this last case, speeds and diffusivities are calculated from the large scale characteristics of the atmosphere as well as the local characteristics such as: roughness and heat flux at ground level, topography features. Several models of the atmospheric boundary layers exist, but the general problem is far from being solved. We believe that the introduction of one of these models might give us interesting results when we consider the effect of a certain topography. For instance, we might quote that of ESTOQUE and BHUMRALKAR [48]: they calculated the modifications brought to a universal profile of speed and temperature by the presence of an "island" characterized by different roughness and temperature at ground level. We might add that in this respect, the introduction of results checked or completed by wind tunnel or water channel modelling is highly recommendable.

The elaboration of boundary layer models is not anywise essential as regards the resolution of equation (2): the degree of complexity in the functions of x and z describing u, w, k_y and k_z has no effect upon its linear character; if this complexity has practical consequences on its numerical resolution, it does not modify its principle.

4.2-2 - Examples of resolution. *

4.2-2-1 - The U.S.S.R. model.

This model was used to establish the regulations, now in use in U.S.S.R., concerning the emission conditons of gaseous and solid effluents in the atmosphere. We owe it to BERLYAND, GUENIKHOVITCH and ONIKUL [27[. We can consider it as a semi-empirical model because the solution of the equation (2) is sought for as follows:

$$C\ (x,\ y,\ z) = \frac{q\ (x,z)}{2\sqrt{\pi}\ k_o\ x}\, e^{-\frac{y^2}{4\ k_o\ x}} \qquad (3)$$

We may simultaneously write: $k_y = k_o\ u$ in which k_o = constant.

---

* We indicate the existence of a certain number of analytical resolutions prior to the use of numerical methods (DAVIES study [49] and SMITH study [50] among them).

Consequently it is quite easy to simplify the equation, and we get:

$$u \frac{\partial q}{\partial x} + w \frac{\partial q}{\partial z} = \frac{\partial}{\partial z} \left(k_z \frac{\partial q}{\partial z} \right) \qquad (4)$$

The term $k_y \frac{\partial^2 C}{\partial y^2}$ being then equal to $u \frac{\partial C}{\partial x} - u \frac{\partial q}{\partial x} \frac{1}{2\sqrt{\pi k_o x}} e^{-\frac{y^2}{4 k_o x}}$

and the term $\frac{1}{2\sqrt{\pi k_o x}} e^{-\frac{y^2}{4 k_o x}}$ appears as a multiplicative factor.

of the two members. It comes to admit that the lateral distribution of concentrations is gaussian and to accept the law: $\sigma_y = \sqrt{2 k_o x}$ (**) or also to assume the coefficients n and C_y in SUTTON formula have the following values: $N = 1$ (value corresponding to a very stable atmosphere).
$C_y = 2k_o$

The resolution of equation (4) is then achieved thanks to the following laws for u, w and k_z:

$$u = u_1 \frac{\mathrm{Log} \frac{z}{z_o}}{\mathrm{Log} \frac{z_1}{z_o}}$$

$k_z = V + k_1 z$ when $z \leq h'$

$k_z = k_2$ (constant) when $z > h'$

$w = o$ (except for calculation of deposition of particulate matter which requires a special flux condition at ground level).

** This assumption is suggested by the statistical theory of turbulence in which we write: $k_o = \frac{1}{2} \frac{d\sigma 2}{dx}$

In these laws, u_1 is the wind speed at $z = 1$ m, z_o is a roughness height and ν is the air kinematic viscosity. The constants k_1 and k_2 (which determine the thickness of the surface layer) are experimentally determined.

The authors have published numerous results; they suggest formulae that give the value of the maximum concentration at ground level. By assuming for k_z a more complex variation law with z, they managed to take into account the possible existence of an inversion layer whose height and thickness are supposed to be known.

As we have already mentioned (see 4.2-1) the results provided by this model are of some value only if the scale of turbulence does not exceed a certain limit: T_o. The authors think the possible limit is about 2 or 3 minutes: in the case of superior sampling time, the measurements indicate concentrations lower than the calculated ones (in U.S.S.R. ordinary concentration measurements of pollutants are integrated over about 20 minutes).

In order to compare the results we get thanks to the model and to the experiements in situ, we should make theoretically, during each sampling duration, a great number of measurements of the deviation φ of the wind direction from its value: this mean direction is represented by the axis Ox, in the model. Then we whould determine the probability density ω (φ) of φ during the sampling duration. If the sampling was made at ground level at the point (x, y) it gives an experimental value $\overline{C}$ (x, y, o) which is related to the calculated one C (x, y, o) through the relation:

$$\overline{C}\,(x,y,o) = \int_{-\frac{\pi}{2}}^{+\frac{\pi}{2}} C(x,y - x\sin\varphi\,,\,o)\;\omega\,(\varphi)\,d\varphi \qquad (5)$$

Having regard to the form of the solution (equation 3), we may write this relation as follows:

$$\overline{C}\,(x,y,o) = \int_{-\frac{\pi}{2}}^{+\frac{\pi}{2}} C(x,o,o)\; e^{-\frac{(y - x\sin\varphi)^2}{4\,k_o\,x}}\;\omega\,(\varphi)\,d\varphi$$

We may justify such a method as follows: because turbulent diffusivities cannot take into account all the scales of turbulence, we have better not try to outspread the scale they represent and try to limit it to 2 or 3 minutes. The model then describes a "stable" plume, that is to say a plume which is not submitted to horizontal fluctuations of a wide amplitude. If we have to take these fluctuations into account, that is to say if we consider large scale eddies existing in the atmosphere, we then use equation (5), which in reality conveys a principle of superposition.

Practically, the $\omega(\varphi)$ function is supposed to be a GAUSS function:

$$\omega(\varphi) = \frac{1}{\varphi_o \sqrt{2\pi}} e^{-\frac{\varphi^2}{2\varphi_o^2}}$$

Then it is easy to show that the method of superposition translated by equation (5), comes to consider a x-variation of the lateral diffusivity, More exactly, if we consider the type of solution we are looking for in the mathematical model, it would be the same if we introduced in the model, instead of k_o, a certain length $\tilde{k}_o$, determined by the relation:

$$\tilde{k}_o = k_o + \frac{1}{2} x \ \varphi_o^2$$

When the values of x are large enough, we may neglect k_o compared with $\frac{1}{2} x \varphi_o^2$; it means that the plume meandering plays an important part, more important that the lateral diffusion inside the plume itself.

The determination of φ_o, which we may also call "standard wind deviation" was often measured in situ in U.S.S.R.

4.2-2-2 - Japanese models.

Nowadays there are two types of Japanese models: the ITO model issued in 1966 [51] and the HINO one issued in 1967 and 1968 [52].

Unfortunately most of the HINO publications are written in Japanese and have not yet been translated; consequently a strict analysis has been impossible.

The ITO model only deals with the two-dimensional problem because it only solves the following equation:

$$u \frac{\partial C}{\partial x} = \frac{\partial}{\partial z} \left(k_z \frac{\partial C}{\partial z} \right)$$

This equation may only be applied to a plume emitted by a linear source varying from + ∞ to - ∞ on the axis y' 0 y. In reality, this equation is the same as equation (4) in which we wrote:

$w = 0$
$q = C$

The solution indicates the concentration in a plume centerline downwind a point source, only after being multiplied by a coefficient K (x) imposed by the law of conservation of mass. It is then necessary to introduce a new hypothesis about the lateral distribution of concentrations, so as to determine K (x).

If we admit that the distribution obeys a GAUSS law charaterized by a standard deviation σ_y such as $\sigma_y = \sqrt{2 k_o x}$, we may then write:

$$K (x) = \frac{1}{2 \sqrt{\pi k_o x}}$$

and we get expression (3) for the plume concentration. The ITO model then brings us back to the U.S.S.R. model as regards the carrying out of equation (2). It only differs from it in the laws k_z (z) and u (z), for ITO writes:

$$u = \frac{u_*}{k} f \left(\frac{z}{L} \right) ,$$

$$k_z = \frac{k L u_*}{f' \left(\frac{z}{L} \right)}$$

in which:

u_* = friction velocity;

k = VON KARMAN's constant;

L = MONIN and OBUKHOV stability length.

The function $f(\frac{z}{L})$ has three various forms. Very near the ground, within the vegetation canopies, f is an exponential law. Higher up, but when $z \preccurlyeq L$, f is a "log linear" law. Still higher up, it is a linear law.

The comparison between the results given by this model and the results we might get out of experiments is limited to a few experiments in situ (in the case of stable atmosphere) for GREEN GLOW project (see 4.1) and ITO does not give any general precision about the validity of his model.

- HINO model seems to be of a much more general interest than the previous ones; it solves the three-dimensional problem by taking into account the mechanical effects due to topography. Equation (1) turns out to be written:

$$u\left(\frac{\partial C}{\partial \xi} - \frac{\partial h}{\partial \xi}\frac{\partial C}{\partial \zeta}\right) + v\left(\frac{\partial C}{\partial \eta} - \frac{\partial h}{\partial \eta}\frac{\partial C}{\partial \zeta}\right) + w\frac{\partial C}{\partial \zeta} = \frac{\partial}{\partial \eta}\left(k_y \frac{\partial C}{\partial \eta} - k_y \frac{\partial h}{\partial \xi}\frac{\partial C}{\partial \zeta}\frac{\partial C}{\partial \xi}\right.$$

$$\left. - \frac{\partial h}{\partial \eta}\left[\frac{\partial}{\partial \zeta}\left(k_y \frac{\partial C}{\partial \eta}\right)\right] + \left(\frac{\partial h}{\partial \eta}\right)^2 \frac{\partial}{\partial \zeta}\left(k_y \frac{\partial C}{\partial \zeta}\right) + \frac{\partial}{\partial \zeta}\left(k_z \frac{\partial C}{\partial \zeta}\right) \qquad (6)\right.$$

in which: $\xi = x$

$\eta = y$

$\zeta = z - h\,(x, y)$ in which $h\,(x, y)$ = ground elevation.

The boundary conditon at the ground level becomes:

$$\frac{\partial C}{\partial \zeta} = 0 \text{ when } \zeta = 0$$

We notice that equation (6) is very general; longitudinal diffusion alone is neglected. Of course, the speed compone determined by the preliminary resolution of an aerodynamical model of the lower layers. Besides, the equations describing the surface layer are very much simplified. As regards the functions u (ζ) and k_z (ζ), their expressions on flat ground are the same as those given by ITO, f being a "log linear" law. On hilly ground, HINO suggests to use some power-law for k_z (ζ):

$$k_z\ (\zeta) = A\ \ \zeta^{\,m}\ |\vec{V}|$$

As for lateral diffusivity, k_y, it is supposed to be proportional to the speed and to a n-power of the abscissa:

$$k_y\ (\xi) = B\ \ \xi^{\,n}\ |\vec{V}|$$

HINO gives precise results obtained from a hilly ground, 200 m to 700 m high. He assumes atmosphere is neutral and he takes m = 0.85 and n = 1. It is interesting to note an appreciable increase in pollution at ground level downwind, a rather low hill (210 m) under the plume centerline, and 2 kilometers from the source (the source itself was 400 m high). The comparison between these results and those given by an aerodynamical model seems to be satisfactory enough, especially if we take into account a necessary correction because of the two different sampling times corresponding to the two methods: according to the author his numerical model was corresponding to 10 minutes sampling times whereas the wind tunnel experiments were corresponding to sampling times ranging from 3 to 5 minutes.

4.2-3 - Value of mathematical models.

A mathematical numerical model is a fast-working convenient and rather cheap tool particularly adapted when all we have to do is to get a first estimate of pollution. Yet, we have stressed the fact that it cannot totally get rid of experimental results when dealing with φ_o, standard wind deviation used by the Soviets, as well as when dealing with the importance of topography (important thermal and mechanical effects).

These models stand out as tools of a high accuracy, if they are rightly and sufficiently completed and verified with numerous experimentations. In spite of rising objections, the notion of turbulent diffusivity has been already considered of a very satisfactory practice when we had to describe a diffusion experiment inside a circular duct by means of a two-dimensional model [53]. Atmospheric flows are certainly more difficult to describe because their turbulence spectrum is far wider.

Yet, we think that the point of view adopted in that respect by the Soviet model is very interesting; in FRANCE, the determination in situ of standard wind deviations (φ_0) should not be a real problem.

So, when they are combined with the results of various experiments, numerical models of diffusion can then be particularly appreciated to extrapolate other experimental results. Finally, we may then avoid over-numerous experiments which, sometimes, cannot even be yet made.

4-3 - SCALE-MODEL EXPERIMENTS

4.3-1 - Introduction

In comparison with experimentation in situ, scale-model experiments are cheaper and save handwork. They have also a time advantage since the conditions of the experiment may be changed at will and consequently they are more precise in determining the influence of given conditions. The experimental model then turns out to be the indispensable complement of experimentation in situ and of mathematical models.

From a practical point of view, we may use it as an analogical computer for which the input data are the characteristics of pollutant sources and of lower atmospheric layers, and for which the output data are the pollution rates at ground level and in altitude.

From a fundamental point of view, modelling enables us to reach a better understanding of turbulent transfers in the lower atmospheric layers (in relation to experimentations in situ and mathematical models).

Of course, scale-model experiments on stacs gas plumes suffer from the same types of defects as model experiments in other fields, because the prototype phenomena will probably not be completely scaled and may be only partially scaled in the model.

Yet we must say that we usually know how and in which way scale effects act: the model overestimates often the pollution rates. Lateral dispersion is essentially interested by those effects: it is then possible to correct them as we did when dealing with numerical models (see 4.2-2-1).

4.3-2 - Conditions of similitude

In this paragraph we do not intend to develop a detailed study of the conditions of similitude; complete studies have been made in that field; the reader who feels concerned with that problem can read from [54] to [59].

We only indicate a few leading ideas on the particular problem of effluent dispersion from an isolated stack.

We have already indicated that in this particular case, two categories of variables may interfere:

- the category of variables characterizing the source of pollutant (source geometry, speed and temperature at the emission, nature of the pollutant).
- the category of variables characterizing the lower atmospheric layers (speed and temperature gradients, turbulence, nature of site).

In the most general case, when the two categories of variables have the same importance, the achievement of experimental models requires geometric and kinematic similitudes together with the equality of a certain number of dimensionless parameters characterizing the phenomena we are interested in.

Those parameters can be read in the following table:

Dimensionless parameters	Characteristic ratio
1. Wind flow or effluent flow.	
REYNOLDS number	
UL/ν	$\frac{\text{Inertial force}}{\text{(viscous force)}}$
FROUDE number	
$U/gL \left(\frac{\Delta\rho}{\rho}\right) \frac{1}{2}$	$\frac{\text{Inertial force}}{\text{Buoyancy force}}$
2. Transfer processes	
PRANDTL number	
ν/a	$\frac{\text{Momentum transfer rate}}{\text{Heat transfer rate}}$
SCHMIDT number	
ν/k	$\frac{\text{Momentum transfer rate}}{\text{Mass diffusion rate}}$

In this table, the letters have the following meaning:

U: characteristic speed of air;

L: characteristic length;

ν: kinematic viscosity;

g: acceleration of gravity;

ρ: mass density;

Δρ mass density discrepancy (between air layers or between pollutant and ambient air);

a : thermal diffusivity;

k: mass diffusivity.

We must remark that the above mentioned dimensionless parameters can only be applied to small scale atmospheric phenomena (that is to say to types of motion whose vertical scales do not range higher than about 200 m). Obviously it is impossible to reach a strict similitude; it is practically impossible to respect both FROUDE number and REYNOLDS number. Yet, experiments show that when we consider the nature of the ground (rough and with obstacles), the wind flow is not highly affected by an important variation of REYNOLDS number, if its value is superior to a critical value depending on the particular case.

Consequently, it is possible to respect FROUDE number to the detriment of REYNOLDS number; an approximate similitude is then perfectly justified: it leads us to achieve a flow of turbulent boundary layer at a low speed over a heated or cooled plate. Then we can show that it is possible to reproduce, more or less in similitude, speed and temperature gradients, turbulent structure (essentially in the range of important eddies, which is the most significant for pollution at a large distance).

As far as flow out of stack is concerned, it turns out to show that the influence of REYNOLDS number on the turbulent structure of the jet is not important when it is superior to 2,000: approached similitude is then still possible; it leads to a low speed flow of a jet made of air and helium (when the effluent is lighter than air) or made of air and freon (when the effluent is heavier than air).

4.3-3 - Modelling facilities

Usually two techniques may be used to simulate atmospheric dispersion.

- Aerodynamic wind tunnel,
- Water channel.

The aerodynamic model, probably may be more easily applied to the simulation of turbulent characteristics of atmospheric flows: then it is advised to use it as far as not neutral atmospheric conditons are concerned. In effect, thermal gradients in the surface layer cannot be reproduced in a water channel through heating or cooling the lower plate: the heat transfer process at the wall is not the same at all in water as in air, because of the much higher value of the PRANDTL number (about 7 in water opposite to 0.7 in air) which introduces physically an important decrease of the part played by the so-called "logarithmic zone".

Yet the hydraulic model may be used to simulate neutral atmospheres and is recommended to simulate calm atmospheres.

Informations about both techniques as well as measurement facilities are given in references [54] to [59].

5 - CONCLUSION

The general problem of prevention of atmospheric pollution due to the exploitation of thermal plants has two different aspects: that of optimizing the conditions of effluent emission in the atmosphere (it usually ends up by determining the characteristics of high stacks yet to be built) and that of forecasting the risks of pollution in the surroundings of an operating plant.

In the first case, we have to be as objective as possible in the estimation of the efficiency, from the pollution point of view, of an isolated stack or of a group of stacks; it requires a good knowledge of small scale atmospheric movements, that is to say affecting distances from 5 to 10 kilometers. Research field has mainly to deal with aerology and micrometeorology.

In the second case, on the opposite, we have to forecast the various meteorological conditons which are connected to large scale movements as well as to small scale movements. In order to increase the efficiency of the forecast, we need knowing a relation between large scale and small scale movements.

Once again, it is important to stress the fact that the various techniques of estimating pollutant dispersion at ground level, from an isolated source or not, are not sufficient to solve both problems. The confusion of these two aspects and of the corresponding meteorological scales (time and space scales) leads us to several errors, the most frequent being the application of diffusion formulae to important pollution sampling times, about one day or even one month (see 3.2-1) whereas the validity of such formulae should be limited to sampling times which would not exceed the time taken by the plume to reach the considered point.

Whereas forecasting techniques are still under-developed, estimation techniques have already been the subject of a constant research, theoretically as well as experimentally (laboratory and in situ experiment). More than the previous ones, they are concerned with the mechanic of fluids, because samll scale atmospheric flows have numerious analogies with turbulent boundary layer flows.

Besides, it is perfectly groundless to set against each other the different approaches of pollution estimations (mathematical models, scale model experiments and in situ experiments): these approaches have to be considered as complementary and we hope this idea has been pointed out sufficiently in this paper.

APPENDICES

APPENDIX 1 - EQUATIONS OF THE FIRST STAGE OF PLUME

When we write the basic equations, ρ is considered as constant in any term in which buoyancy forces have no effect.

Equation of vertical motion

As a consequence of plume symmetry, we use the cylindrical co-ordinates. So the θ- terms are eliminated and this equation may be written:

$$\rho u \frac{\partial w}{\partial r} + \rho w \frac{\partial w}{\partial z} = \frac{1}{r} \frac{\partial}{\partial r} (r \tau) + \rho g_z$$

in which:

$$\rho g_z = \rho g \frac{\theta'}{\theta_e}$$

After multiplying each member by rw, we get:

$$rw\, u \rho \frac{\partial w}{\partial r} + w^2 \frac{\partial (r\, w \rho)}{\partial z} = w \frac{\partial}{\partial r} (r \tau) + \rho g_z$$

Now, we may add the following term to the first member of this equation, since the value of this term is zero as a consequence of the equation of continuity:

$$\frac{1}{2} w^2 \left[\frac{\partial}{\partial z} (r\, w\, \rho) + \frac{\partial}{\partial r} (r\, u\, \rho) \right] ,$$

Then it is obvious that the first member may be considered as the development of:

$$\frac{\partial}{\partial r}\left(\frac{1}{2} r u w^2 \rho\right) + \frac{\partial}{\partial z}\left(\frac{1}{2} r w^3 \rho\right)$$ (what was to be demonstrated).

Equation of conservation of heat

The general equation is:

$$C_p \frac{DT}{Dt} = -k \nabla T = -\operatorname{div} \vec{q}$$

Here, it may be written:

$$\rho C_p \left(u \frac{\partial T}{\partial r} + w \frac{\partial T}{\partial z}\right) = -\frac{1}{r} \frac{\partial}{\partial r}(r q_r)$$

or else, by taking into account the equation of continuity:

$$\frac{\partial}{\partial r}(\rho u T r) + \frac{\partial}{\partial z}(\rho w T r) = -\frac{1}{C_p} \frac{\partial}{\partial r}(r q_r)$$

The equation remains accurate when T is replaced by the potential temperature $\theta = \theta_e + \theta'$. We find the equation we were seeking for by developing the first member: the $\frac{\partial \theta_e}{\partial r}$ term disappears as well as the θ_e- term which is equal to zero because of the equation of continuity.

APPENDIX 2 - EQUATIONS OF THE SECOND STAGE OF PLUME

A standard way of taking into account turbulent transfers in the second stage of plume is the introduction of turbulent diffusivities K. (K_1 for momentum transfer and K_2 for heat transfer). So, the local equation of motion may be expressed in the following w by using the cylindrical co-ordinates where the z-axis is the plume axis:

$$\frac{dw}{dt} = \frac{\theta'}{\theta_e} \rho g - K_1 \frac{1}{r} \frac{\partial}{\partial r} \left(r \frac{\partial w}{\partial r} \right)$$

($\frac{\partial K_1}{\partial r}$ is supposed to be non-existent).

Then, we write:

$w = w_m f(x)$

$\theta' = \theta'_m f(x)$

$x = \frac{r}{R}$

and we integrate the last equation over x from zero to infinite:

$$\frac{d(w_m f)}{dt} dx = \frac{g \theta'_m}{\theta_e} \int_0^\infty f dx - \frac{K_1 w_m}{R^2} \int_0^\infty \frac{1}{x} \frac{d}{dx} \left(x \frac{df}{dx} \right) dx$$

Now: $\frac{d(w_m f)}{dt} = f \frac{dw_m}{dt}$ since $\frac{df}{dt} = 0$

Then:

$$\frac{dw_m}{dt}\int_0^{\infty} f(x)\,dx = g\,\frac{\theta'_m}{\theta_o}\int_0^{\infty} f(x)\,dx - \frac{K_1\,w_m}{R^2}\int_0^{\infty}\frac{1}{x}\,\frac{d}{dx}\left(x\,\frac{df}{dx}\right)dx$$

or else, when we write:

$$C_1 = \frac{\displaystyle\int_0^{\infty}\frac{1}{x}\,\frac{d}{dx}\left(x\,\frac{df}{dx}\right)dx}{\displaystyle\int_0^{\infty} f(x)\,dx}$$

$$\frac{d\,w_m}{dt} = g\,\frac{\theta'_m}{\theta_o} - \frac{K\,C_1}{R^2}\,w_m$$

We then come to the first equation of the system describing the second stage, by suppressing the index m and by writing:

$$k = \frac{K\,C_1}{R^2}$$

By assuming $K_1 = K_2$ we then settle the equation of conservation of heat as follows:

$$\frac{d\theta}{dt} = -k\theta'$$

APPENDIX - 3 DETERMINATION OF w_1 AND z_{max}

To prove that: $w_1 = kz_1$:

The solution of the first stage provides the following expression of w_1:

$$w_1^3 = \frac{1}{z_1^3}\left[(z_1^2 - z_o^2)\,\alpha + w_o^3\, z_o^3\right]$$

but z_1 verifies the equation:

$$k^3\, z_1^6 = (z_1^2 - z_o^2)\,\alpha + w_o^3\, z_o^3$$

therefore:

$$w_1^3 = k^3\, z_1^3 \quad \text{and} \quad w_1 = kz_1$$

To prove that:

$$z_{max} = 2\, z_1 + \frac{2\, a}{3\, z_1^3}$$

The starting point is:

$$z_{max} = z_1 + \frac{w_1}{k} + g\,\frac{\theta'_1}{k^2\,\theta_e}$$

Or:

$$z_{max} = 2\ z_1 + g\ \frac{\theta'_1}{k^2\ \theta_e}$$

if we take the previous result into account.

We know that:

$$\theta'_1 = \frac{A}{R_1^{\ 2}\ w_1}$$

(equation of conservation of heat)

and that:

$$R_1 = c\ z_1$$

Therefore:

$$g\ \frac{\theta'_1}{k^2\ \theta_e} = g\ \frac{A}{c^2\ k^3\ z_1^{\ 3}\ \theta_e} = \frac{2}{3}\ \frac{\alpha}{k^3\ z_1^{\ 3}} = \frac{2\ a}{3\ z_1^{\ 3}}$$

APPENDIX 4 - PHYSICAL INTERPRETATION OF PARAMETERS c AND x_{k_N}

1) $c^2 = \dfrac{U}{U_c}$

In the first stage, the plume section is supposed to be elliptical with dispersion R_1 and R_2 along the principal axes (R_1 in the direction of the speed U). PRIESTLEY assumes that:

$R_1 = c_1\ z$ and $R_2 = c_2\ z$

in which:

$c_1 = c'_1\ U$ and c_2 = constant.

Therefore:

$$R = \sqrt{R_1 R_2} \propto U^{1/2}$$

2) To prove that: $k = \dfrac{U}{x_{kN}}$:

We apply EULER's theorem to a definite volume determined by a "slice" of plume, the thickness of which is ds. (s is the curvilinear abscissa along the plume axis (see figure). We suppose that the values u, w, and θ are uniform in a given section of the plume. We then get:

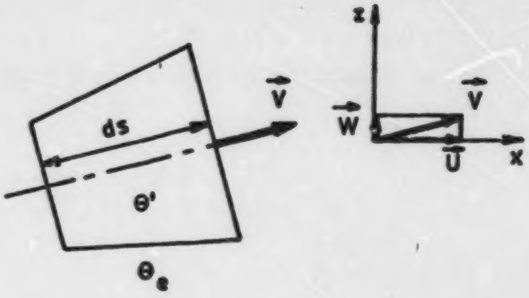

$$\frac{\partial}{\partial s}(\pi r^2 v w) = \pi r^2 g \frac{\theta'}{\theta_e}$$

Or: (we neglect $\frac{\partial e}{\partial s}$)

$$\frac{d}{dt}(\pi r^2 v w) = \pi r^2 g \frac{\theta'}{\theta_e} v$$

As $w \ll U$, we may replace v by U and after simplifying by U, we have:

$$\frac{2}{r}\frac{dr}{dt} w + \frac{dw}{dt} = g \frac{\theta'}{\theta_e}$$

The equation of conservation of heat, which may be written:

$$\frac{d}{dt}(\pi r^2 v \theta) = 2\pi r \frac{dr}{dt} v \theta_e$$

then turns out to be:

$$\frac{2}{r}\frac{dr}{dt}\theta' + \frac{d\theta}{dt} = 0$$

The equations of the second stage are then written:

$$k w + \frac{dw}{dt} = g \frac{\theta'}{\theta_e}$$

$$k \theta' + \frac{d\theta}{dt} = 0$$

These equations can only be compatible with the previous ones when:

$$k = \frac{2}{r}\frac{dr}{dt}$$

from which: $k = \frac{2\,U}{r}\frac{dr}{dx}$, and if we write $\frac{1}{r}\frac{dr}{dx} = \frac{1}{2\,x_{kN}}$
it comes:

$$\boxed{k = \frac{U}{x_{kN}}}$$

REFERENCES

1 - PRIESTLEY (C.H.B.). A Working Theory of the Bent-Over Plume of Hot Gas J.R. Met. Soc., 82 (1956), 165.

2 - SCORER (R.S.). The Rise of Bent-Over Hot Plumes. Advances in Geophysics 6, (1959), 399.

3 - SUTTON (O.G.). Micrometeorology (MacGraw Hill, New York) (1953).

4 - MUNN (R.E.). Descriptive Micrometeorology. (Academic Press, New York) (1966).

5 - LAIKHTMAN (D.L.). Physics of the Boundary Layer of the Atmosphere (Traduit du Russe). Israel Program for Scientific Translation, Jerusalem; (1964).

6 - EVANS (B.H.). Natural Air Flow Around Buildings. Research Report 59, Texas Engng. Exp. Station (1957).

7 - HALITSKY (J.). Diffusion of Vented Gas Around Buildings. J. Air Pollution Control Assoc., 12 (2), 74 (1962).

8 - STROM (G.H.). Atmospheric Dispersion of Stack Effluents. Air Pollution, 1, 118 (1962).

9 - LEUTHEUSER (H.J.) - LORD(G.R.). Minimum Stack Heights for Apartment Buildings. TP 6602, Department of Mechanical Engng. Univeristy of Tronto (1966).

10 - VADOT (L.). Etude de la Diffusion des Panaches de Fumée dans l'Atmosphere. Publ. C.I.T.E.P.A. Paris (1965).

11 - SCORER (R.S.). Air Pollution. Pergamon Press, Londres (1968).

12 - DAVIDSON (W.F.). The Dispersion and Spreading of Gases and Dust from Chimneys. Trans. Conf. on Industrial Wastes, 14th Annual Meeting (Nov. 18, 1949).

13 - HOLLAND (J.Z.). A Meteorological Survey of the Oak Ridge Area. U.S. Atomic Energy Commission Report ORO - 99, 554 (1953).

14 - BOSANQUET (C.H.). The rise of a Hot waste Gas Plume. J. Inst. of Fuel 30, 197, 322 (1957).

15 - SCHMIDT (W.). Turbulente Ausbreitung eines Stromes Erhitzter Luft. Zeitung. angew. Math. Mech. 21, 265 et 351 (1941).

16 - BRIGGS (G.A.). A Plume Rise Model Compared with Observations. J. Air Pollution Control Assoc., 15, 433 (1965).

17 - CRAWFORD (T.V.) - LEONARD (A.S.), Obeservations of Buoyant Plumes in Calm, Stable Stratified Air. J. Appl. Meteorol. 1, 251 (1962).

18 - MORTON (B.R.) - TAYLOR (G.I.) - TURNER (J.S.). Turbulent Gravitational Convection from Maintained and Instantaneous Sources. Proc. Roy. Soc., London, A, 234, 1 - 23 (1956).

19 - WHALEY (H.). A Proposed Canadian Standard for Estimating Atmospheric Dispersion of Combustion Source Pollution from Chimneys. Atm. Environment. 3, 177 (1969).

20 - MOORE (D.J.). Physical Aspects of Plume Models. Air and Water Pollution. Int. J. 10, 411 (1966).

21 - SCRIVEN (R.A.). On the Breakdown of Chimney Plumes Into Discrete Puffs. Air and Water Pollution. Int. J. 10, 419 (1966).

22 - PRIESTLEY (C.H.B.) - BALL (F.K.). Continuous Convection from an Isolated Source. Quart. J. R. Met. Soc. 81, 144 (1955).

23 - SPURR (G.). The Bent-Over Plume of Gas Quart. J. R. Met. Soc. 83, 269 (1957).

24 - LUCAS (D.H.) - MOORE (D.J.) - SPURR (G.). The Rise of Hot Plumes from Chinmeys. Air and Water Pollution Int. J. 7, 473 (1963).

25 - PRIESTLEY (C.H.B.). Buoyant Motion in a Turbulent Environment. Australian J. of Physics. 6, 279 (1953).

26 - DANOVITCH (A.M.) - ZEIGER (S.G.). Determination de la Hauteur d'Ascension d'un Effluent Chaud dans l'Atmosphere. Institut d'Hydrologie et de Meteorologie de Leningrad Serie 18, 201 - Traduction E.D.F n° 1281 (Etudes et Recherches).

27 - BERLYAND. Trudy n° 158 de l'Observatoire Central de Geophysique de Leningrad p. 3, 22, 32 (1964).

28 - MOORE (D.J.) - LUCAS (D.H.) - HAMILTON (P.M.). Symposium on Chimney Plume Rise and Dispersion. Atm. Envir. 1, 351 (1967).

29 - BRUMMAGE (K.G.). The Calculation of Atmospheric Dispersion from a Stack. Atm. Envir. 2, 197 (1968).

30 - BRINGFELT. Plume Rise Measurements at Industrial Chimneys. Atm. Envir. 2, 575 (1968).

31 - MOSES (H.) - CARSON (J.E.). Stack Design Parameters Influencing Plume Rise. J. Air Pollution Control Assoc. 18, (7), 454 (1968).

32 - GARTREL (F.E.) et al. Full Scale Dispersion of Stack Gases. Summary Report Tennessee Valley Authority - Chatanooga, Tennessee (1964).

33 - RAUCH (H.) - Zur Schornstein - Uberhohung - Beitr. Phys. Atmos. 37, 132 (1964).

34 - STEWART (N.G.) et el. The Atmospheric Diffusion of Gases Discharged from the Chimney of the HARWELL Reactor BEPD. Int. J. Air Pollution 1, 87 (1957).

35 - STROM (G.H.) et el. Effects of Meteorological and Engineering Factors on Stack Plume Rise. Feature Article - Nuclear Safety, 6 (1), Fall (1964).

36 - BOSANQUET (C.H.) - PEARSON (J.L.). The Spread of Smoke and Gases from Chimneys. Trans. Faraday Soc. 32, 1249 (1936).

37 - CALDER (K.L.). Some Recent British Work on the Problem of Diffusion in the Lower Atmosphere. Proc. U.S. Tech. Conf. Air Poll. 782. New York, MacGraw Hill (1952).

37 - PASQUILL (F.). The Estimation of the Dispersion of Windborne Material. Meteorol. Mag. 90, 1063, 33 (1961).

39 - TAYLOR (G.I.). Diffusion by Continuous Movements. Proc. London Math Soc. 20, 196 (1921).

40 - SMITH (M.E.) - SINGER (I.A.). Proc. 3rd Nat'l. Air Poll. Symposium, Pasadena, California, p. 80 (1955).

41 - FRIEDMAN (D.G.). J. Meteorol. 10, 372 (1953).

42 - TURNER (D.B.). Workbook of Atmospheric Dispersion Estimates. U.S. Department of Health, Education and Welfare. Cincinnati, Ohio (1967).

43 - BARAD (M.L.). Project Prairie Grass, A Field Program in Diffusion. Geophys. Res. Paper, 59, vols. 1 and 2 (1958).

44 - BARAD (M.L.). (ed). The Green Glow Diffusion Program, vols. 1 and 2, Geophy. Res. Paper, n° 73.

45 - LEAVITT (J.) - CARPENTER) (S.B.) - THOMAS (F.W.). An Interim Report on Full-Scale Study of Plume Rise at Large Electric Generating Stations - Ann. Meet. Air Poll. Control Assoc., Toronto (June 1965).

46 - LETTAU (H.H.) - DAVIDSON (B.) (ed). Exploring the Atmosphere's First Mile - vols. 1 and 2. Pergamon Press, Londres (1957).

47 - STERN (A.C.) (ed). Air Pollution - Academic Press, New York.

48 - ESTOQUE (M.A.) - BHUMRALKAR (C.M.). Theoretical Studies of the Atmospheric Boundary Layer, Technical Report - E.C.O.M. - 67G2 - F. Atmospheric Sc. Laboratory, FORT HUACHUCA, Arizona (1968).

49 - DAVIES (D.R.). Three Dimensional Turbulence and Evaporation in the Lower Atmosphere. Quart. J. of Mech. and App. Math. 3, 51 (1950).

50 - SMITH (F.B.). The Diffusion of Smoke from a Continuous Elevated Point Source into a Turbulent Atmosphere. J. of Fluid Mechanics. 2, 49 (1957).

51 - ITO (S.). Atmospheric Diffusion in the Earth's Boundary Layer. Geophys. Magazine, 33 (1) - (1966).

52 - HINO (M.). Computer Experiment on Smoke Diffusion over a Complicated Topography. Atmosph. Environ. 2, 541 (1968).

53 - CASEAU (P.) - DENIAU (R.). Diffusion dan un Tuyau (Comm. a la Soc. Hydr. de France). La Houille Blanche 3, 259 (1969).

54 - STROM (G.H.). Scale Model Wind Tunnel Studies on Atmosphere Diffusion Pheonomena, Proceedings on the Seventh Hydraulics Conference (1958).

55 - SUQUET (F.). Similitude des Phenomenes de Pollution Atmospherique, SOGREAH, Grenoble (1965).

56 - CERMAK (J.E.) et al. Simulation of Atmospheric Motion by Wind Tunnel Flows, Tech report n° CER 66 JEC - WAS - EJP - CJB - HC - RNM - SI - 17, Fluid Dynamics and Diffusion Laboratory, Colorado State University (1966).

57 - ARMITT (J.) - COUNIHAM (J.). The Simulation of the Atmospheric Boundary Layer in a Wind Tunnel, Atm. Environ., 2 (1968).

58 - MERY (P.). Reproduction en Similitude de la Diffusion dans la Conche Limite Atmospherique, La Houille Blanche, 4, 327 (1969).

59 - MAC VEHIL (G.E.) - LUDWIG (G.R.) - SUNDARAM (T.R.). On the Feasibility of Modeling Small Scale Atmospheric Motions. Cornell Aeronautical Laboratory, Report n° ZB. 2328 - P - 1, Buffalo, New York (1957).

Chapter IV

PRACTICAL APPROACHES FOR SOLUTION OF SOME PROBLEMS IN CONNECTION WITH THE ESTIMATION OF AIR POLLUTION BY STACK EFFLUENTS

R. DENIAU and P. MERY
Division of Atmospheric Transfers
ELECTRICITE DE FRANCE

For presentation to the Panel on Modeling, NATO/CCMS Pilot Project on Air Pollution, Paris, France, July 26-27, 1971

1 - INTRODUCTION

The prevention of atmospheric pollution represents a serious problem for a power industry as E.D.F. because of the phenomenal growth in electric power use and production. Increases in size of individual generating units and total capacity at single locations have induced the power industry to adopt in some cases tall stacks in an effort to maintain reasonable air quality at ground level near the power plants.

From a practical point of view, it is evident that at the present time, theoretical models are not accurate enough and in most of the cases, do not allow to justify the height of a stack.

After the presentation of an estimation method based on the works of PASQUILL, we intend to expose the solutions to some problems encountered when trying to develop better diffusion models with which one would determine ground level concentrations of pollutants emitted by large power plants.

2 - A SIMPLE PRACTICAL METHOD FOR ESTIMATING THE DAILY MAXIMUM LEVEL CONCENTRATIONS NEAR A POINT SOURCE OF GASEOUS POLLUTANTS

A method now in use by E.D.F. for the estimation of SO_2 ground level concentrations in the vicinity of a power plant concerns only daily mean values. It consists namely in adding tri-hourly values calculated every 3 hours by PASQUILL's method over a large period. Each calculation uses the following data provided by an available meteorological station : wind speed and direction at level 11 m, cloud cover (from 1 to 8 1/8th). The results given by the PASQUILL's formula (10 minutes mean values) must be extrapolated to give tri-hourly mean values as follows : it is supposed that a simple 0.5 coefficient would be available and that these so -calculated tri-hourly mean values concern a 20 degrees angle whose bisectrix would be the wind direction . The last assumption cannot be sactifactorily introduced since it consists in assuming always the same angular width for the actual plumes, without considering the influence of the atmospheric conditions and especially the influence of the stability categories.

Nevertheless, this assumption provides a great simplification for the calculations : the x - y plane is divided into 18 angles, eight of them or less being polluted during a given day. The daily calculations require 18 x 100 memories, most of them being equal to zero (if we suppose that the r - axis of each angle has been divided into 100 parts). Additions are made automatically and then it is easy to determine the highest of the 1800 values which is finally divided by 8 to give a maximum daily mean value.

In order to reduce the calculation time, only a limited number of different computations is performed at the beginning of the program : the wind speed range is consequently reduced to a limited set of discrete values (6 for instance).Considered with the 6 stability categories, they lead to 36 computation cases. In fact, this number reaches a higher value such as 72 or 108 if one considers two or three different chimney heights to take into account the main topography features of the power plant surroundings.

In addition to the approximations introduced by the application of the PASQUILL's formula, with the above outlined assumptions, the present method has to cope with the following doubtful points :

- Choice of a plume rise formula : this is a general problem for all the calculations. The formula which is used is LUCAS's one, which seemed to be the most accurate to describe plumes emitted by large power plants.

- Choice of wind speed profiles to determine the wind speed at the top of the chimney ; the law which has been used is a power law with a 0.25 coefficient for unstable and neutral cases and with a 0.5 coefficient for stable cases.

- Choice of an uniform height for the topography in a given 20 degrees angle.

3 - MATHEMATICAL DISPERSION MODEL

The main deficiencies of the usual diffusion formulae (SUTTON, PASQUILL ...) are as follows :

- uncertainties about the extrapolation of the parameters σ_y (x) and σ_z (x) for distances exceeding 1000 m ;

- assumption of an uniform vertical velocity profile.

The model which is proposed below does not present the last deficiency : it takes into account vertical velocity and diffusivity profiles. Moreover, it uses turbulent diffusivities k_y and k_z instead of the standard deviations σ_y and σ_z .

3.1 - DESCRIPTION OF THE DISPERSION MODEL

The fundamental parabolic equation of turbulent diffusion may be written as follows :

$$(1) \quad \frac{\partial C}{\partial t} + u \frac{\partial C}{\partial x} + v \frac{\partial C}{\partial y} + w \frac{\partial C}{\partial z} = \frac{\partial}{\partial x} k_x \frac{\partial C}{\partial x} + \frac{\partial}{\partial y} k_y \frac{\partial C}{\partial y} + \frac{\partial}{\partial z} k_z \frac{\partial C}{\partial z}$$

where C is the concentration and u, v, w are the speed components of the particle in the x, y and z directions, and where k_x , k_y and k_z are the turbulent diffusivities in the same directions.

This equation can be reduced by neglecting the term

$$\frac{\partial}{\partial x} k_x \frac{\partial C}{\partial x}$$

compared with the term $u \dfrac{\partial C}{\partial x}$, and by assuming a steady state and the k_y coefficient independent of y . It becomes :

$$(2) \qquad u \frac{\partial C}{\partial x} + w \frac{\partial C}{\partial z} = k_y \frac{\partial^2 C}{\partial y^2} + \frac{\partial}{\partial z} k_z \frac{\partial^2 C}{\partial z^2}$$

The boundary conditions are :

1) $x = 0$: $C(x, y, z) = C_o \; \delta(y) \; \delta(z - H)$

(δ = Dirac function, H = effective height of the chimney)

2) $z = 0$: $k_z \dfrac{\partial C}{\partial z} = 0$ (zero - flux condition)

3) $x, |y|, z \longrightarrow \infty$: $C(x, y, z) \longrightarrow 0$.

The following properties of the solution may be noticed :

1. $C(x, y, z, Ku) = C\left(\frac{x}{K}, y, z, u\right)$

An accurate solution for a given velocity profile can be easily deduced from another solution which has been already found for a similar profile .

2. The last equation may be written :

$$u \frac{\partial C}{\partial x} + \left(w - \frac{\partial k_z}{\partial z} \right) \frac{\partial^2 C}{\partial z} = k_y \frac{\partial^2 C}{\partial y^2} + k_z \frac{\partial^2 C}{\partial z^2} \tag{3}$$

In other words, the $\frac{\partial k_z}{\partial z}$ term can be considered in the same manner as a vertical velocity.

3. $C(x, y, z) = C(x, -y, z)$

The solving method consists in expanding a given boundary solution for $x = 0$ in a FOURIER series without sine-terms : each function $C(x_0, y, z_0)$ is considered as a periodic y-function in the $\left(\frac{-L}{2}, \frac{L}{2}\right)$ interval, where L is a given length, large compared with the lateral dimensions of the plume ($L = 2$ km for instance). Then $C\left(x, \frac{L}{2}, z\right)$ can be neglected and the boundary condition for $y \to \infty$ can be changed into a zero-flux condition. So, we may write :

$$(4) \qquad C\,(x,\,y,\,z) \;\#\; \sum_{n=0}^{N} A_n\,(x\,,\,z)\,\cos\,2\pi n\,\frac{y}{L}$$

where $(N + 1)$ is the total number of harmonics, each of them verifying the following equation :

$$(5) \qquad u\,\frac{\partial A_n}{\partial x} + \left(w - \frac{\partial k_z}{\partial z}\right)\frac{\partial A_n}{\partial z} + \omega^2_n\,k_y\,A_n = k_z\,\frac{\partial^2 A_n}{\partial z^2}$$

with $\omega_n = 2\pi\,\frac{n}{L}$.

About the initial condition $(x = 0)$, we assume the solution is known near the source and can be written at $x = x_0$:

$$C_0\,(\,x_0,\,y,\,z) = C_1\,(x_0,\,y)\,.\,C_2\,(x_0,\,z - H)$$

where C_1 and C_2 may be Gaussian functions or cosine functions which must only verify the continuity condition :

$$\iint_{x=x_0} u\,(z)\,.\,C\,(x_0,\,y,\,z)\,dy\,dz = q \quad \text{(volume rate of the source)}$$

The expansion of the C_0 function provides the initial values of each harmonic A_n . This expansion must use 20 harmonics because of the narrow width of the plume at $x = x_0$.

Each harmonic is then separately calculated from equation (5), the A_n (x, z) values are stored for the final reconstruction of the solution.

The numerical method is a finite-difference one (CRANK - NICHOLSON). The grid has 200 steps in the x-direction and 80 steps in the z-direction : the grid spacing in the z-direction is variable, so as to take into account the gradients near the ground as fairly as possible, the values of u, k_y and k_z being numerically introduced for each location in the z-direction.

3.2 - EXAMPLE OF CALCULATION

This example points out the influence of the surface boundary layer on the atmospheric dispersion. The vertical velocity and diffusivity profiles are as follows :

$$u = \frac{u_*}{K} \log \frac{z}{z_0} \qquad \text{when} \quad z < 100 \text{ m}$$

$$u = 5 \text{ m/s} \qquad \text{when} \quad z > 100 \text{ m}$$

$$k_z = k_y = 0{,}1\, z \qquad \text{when} \quad z < 100 \text{ m}$$

$$k_z = k_y = 10 \text{ m}^2/\text{s} \qquad \text{when} \quad z > 100 \text{ m}$$

With K = von Karman constant,

u_* = friction velocity # 0.25 m/s

z_0 = roughness length # 2.5 cm.

Figure 1 shows the ground level concentration distribution on the x-axis (under the plume axis).

Figures 2a and 2b show ground level isopleths. In these figures, the results are compared with the results which would have been found if assuming uniform vertical velocity and diffusivity profiles ($u = 5$ m/s and $k_y = k_z = 10 \text{ m}^2/\text{s}$). It can be seen that the no surface boundary layer assumption leads to an under-estimation of the ground level pollution.

Fig.1

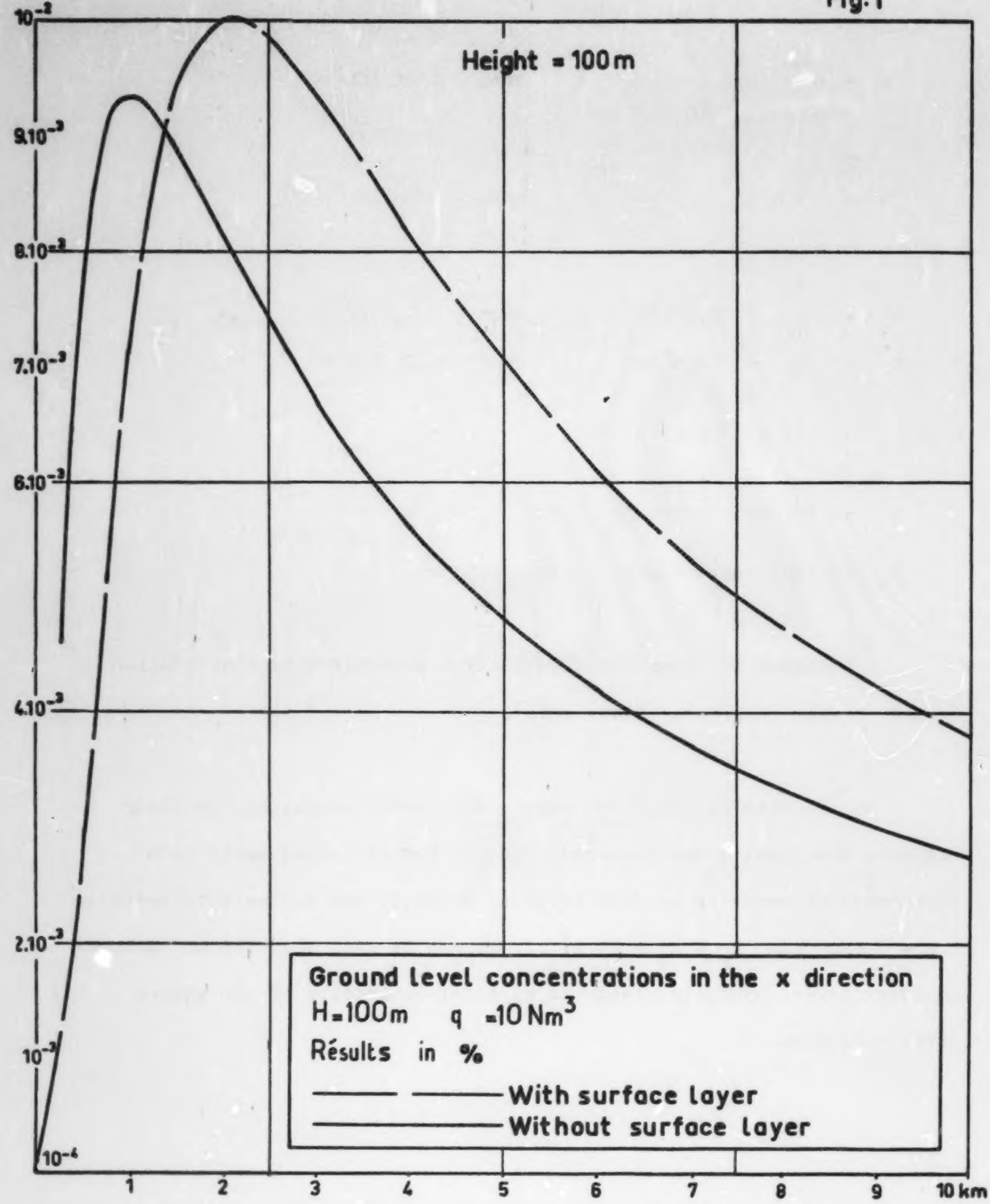

Fig. 1 - GROUND LEVEL CONCENTRATIONS IN THE X-DIRECTON WITH A POINT SOURCE LOCATED ABOVE THE GROUND AT A 100 m HEIGHT

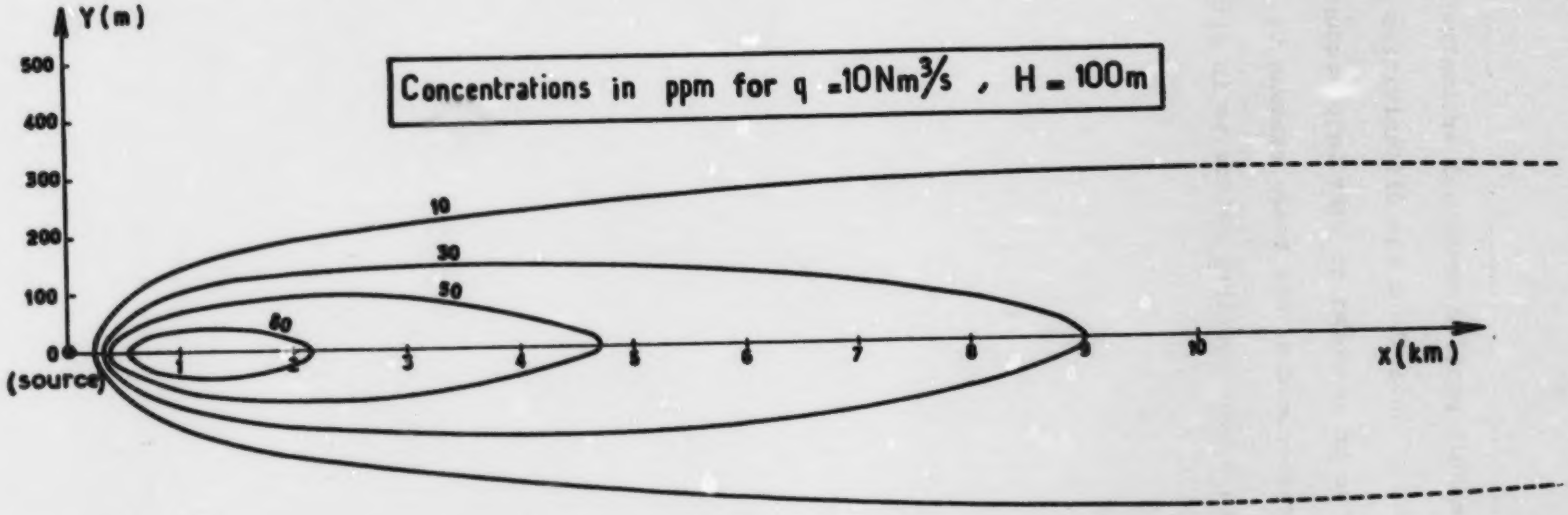

FIG.2a_ Ground level isopleths (Without surface layer)

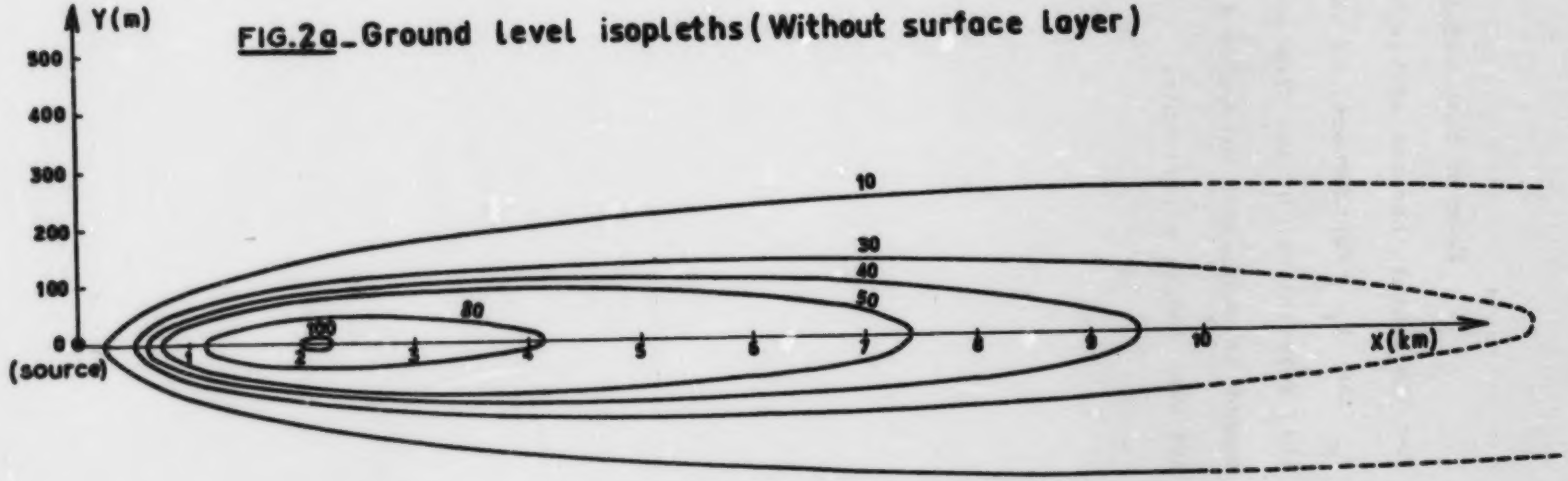

FIG.2b_ Ground level isopleths (With surface layer)

However this model cannot provide practical estimations for the moment, because of the lack of data about the diffusivities k_y and k_z . Furthermore, it has to be improved to take into account the x-variations of the flow characteristics. For these reasons it cannot be considered otherwise than a complementary method to in situ and wind tunnel experiments.

4 - WIND TUNNEL EXPERIMENTS

4.1 - GENERALITIES

The ability to model atmospheric phenomena is of great practical value because information can be obtained by direct laboratory measurements much quicker and cheaper than by extensive field programs. A great advantage of a model is that it permits the possibility to control and systematically vary different independant parameters, which is important not only in the applied problems of structure design or contamination prediction, but also in fundamental studies on turbulence, heat transfer and other flow phenomena.

Till ten years ago, industrial stacks were not very high and often were located on buildings. So, in most of the cases it was possible to neglect the atmospheric turbulence compared with the turbulence created by the surroundings (buildings and very local topography). One had to deal with problems of aerodynamics, that is to determine the height of the chimney in order to escape to the turbulent wakes.

For some years high stacks have been appeared, and it is now necessary to take into account the local atmospheric conditions and especially the velocity and temperature gradients and turbulence structure.

Numerous authors (MAC VEHIL et al., 1967 ; MERY, 1969 ; CERMAK et al., 1966) have shown that a complete simulation of atmospheric phenomena is not possible and that one is obliged to realize an approximate model. The restrictions which inhibit this simulation stem mainly from the nature of the study problem. In our case, we limited ourselves to the simulation of the atmospheric surface layer which is agreed to have transfer problems of the same nature as in the wall region of a turbulent boundary layer on a flat plate. In effect, the transitional zone of the atmospheric boundary layer appears to have only a qualitative analogy with the outer region of a wind tunnel boundary layer. In other words, we try to simulate an atmospheric layer, the horizontal and vertical dimensions of which are respectively 10 km and 100 m and where only small scale turbulence can be taken into account, assuming as a principle that the atmospheric transition region will be approximately reproduced if this layer near the ground is fairly well simulated.

In the atmosphere, flows have high REYNOLDS numbers which is why it is of the greatest importance to realize a very thick boundary layer. However for this boundary layer to be naturally developed on a flat plate, it is necessary to build a very long and expensive wind tunnel. Yet, some authors (COUNIHAN, 1969 ; LLOYD, 1967 ; MAC VEHIL et al., 1967) tried to provide different experimental sets in order to reduce the size of their facilities.

Most experimental sets can be classified into two categories : one which attempts to create, by completely artificial means, a flow with specific mean and turbulent characteristics, and another which tries to accelerate the thickening of the turbulent boundary layer by vortex generators and/or by important roughnesses. Presented in this paper is a method of the second type, which attempts to thicken the boundary layer by the injection of air into a restricted area, a short distance before the beginning of a test plate. The boundary layer as disturbed was intended to recover with the characteristics of a natural boundary layer, only thicker than a purely natural boundary layer.

4.2 - A METHOD OF BOUNDARY LAYER THICKENING BY THE INJECTION OF AIR AT THE BEGINNING OF A TEST PLATE

4.2-1 - Experimental set

A wind tunnel with a 1.20 x 1.00 m^2 cross section, of the open circuit type was employed. At the channel intake was a settling chamber with grids and a convergent, the ratio of which was 16. The test plate (10 m long) designed of stratified polyester could be heated by hot air circulation, while the movable ceiling, also of the same material, made it possible to cancel the pressure gradient. Turbulence intensity at the channel center was 0.3 %, and in the last measurement section ($x = 9.20$ m), the flow was verified as bidimensional. Air injection took place at the beginning of the channel through a porous plate, the ductloss of which was important enough to assume a good distribution of the injected air (fig.3).

For each section of the channel we first measured the characteristics of the boundary layer without injection, then we measured the same characteristics in the boundary layer with upstream injection.

4.2-2 - Analysis and discussion of data

The injection method was first studied by M. DREVILLON (1968) in another wind tunnel. The latter demonstrated that it was possible to thicken the boundary layer by three or four times with adequate injection rates. For injection rates of $A = 0.000$, 0.036, 0.0112, he obtained boundary layer thicknesses of 0.14, 0.28 and 0.42 m.

Fig. 3

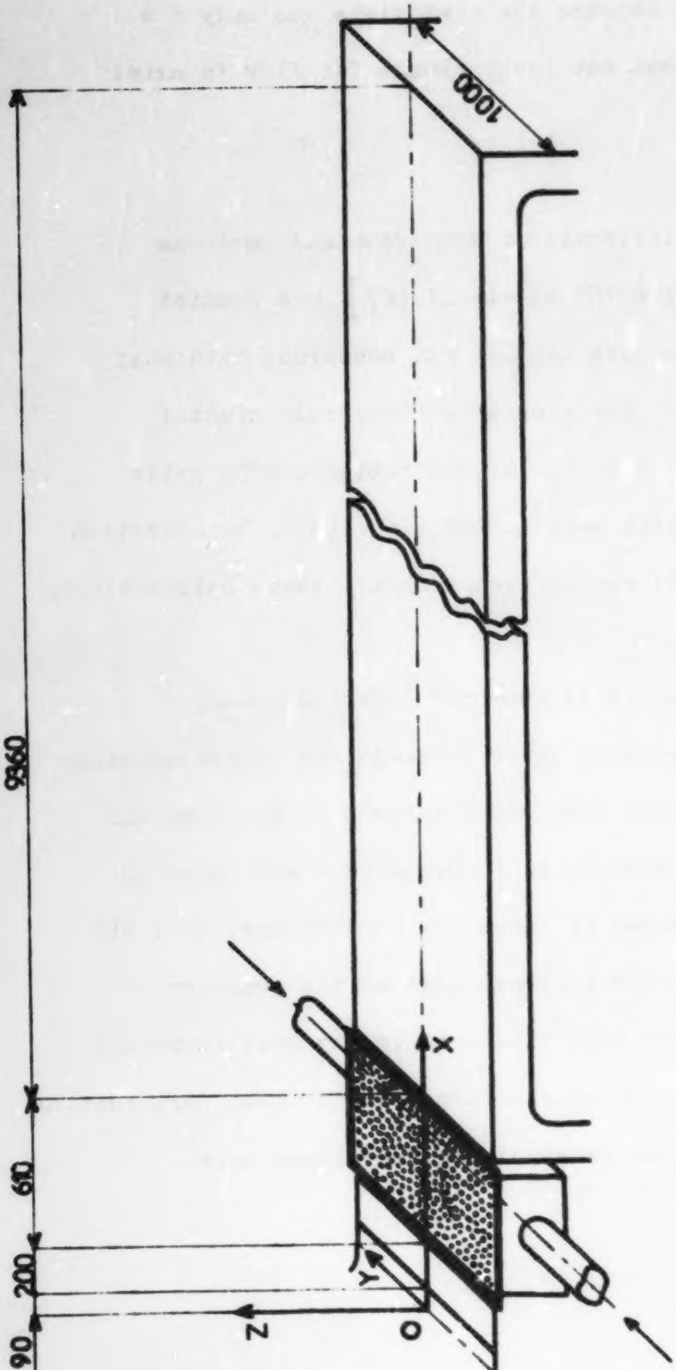
1000
9360
610
200
90
X
Y
Z
O

Fig. 3 - TEST PLATE

However, the modest dimensions of his device did not allow the boundary layer to restabilize because the test plate was only 6 m long and because the channel was not large enough for flow to exist as purely bidimensional.

In the existing litterature, we have found numerous authors [i.e. CRAVEN (1960) ; FAVRE et al. (1966)] who studied injection or suction, but they were usually not concerned with what happened far downstream of the injection zone. They only studied the influences of injection on the C_f or the protection of walls by injection where hot flows were used (GOLDSTEIN, 1965). An exception can be made for BRADSHAW (1968) who derived boundary layer calculations.

After a certain distance from the injection zone, BRADSHAW concluded that the boundary layer presents the characteristics of a natural boundary layer, only that its thickness is altered. Our results showed, using an injection rate of 0.036 ($U = 6.50$ m/s) to achieve a boundary layer thickness of twice the natural one, that his conclusion can be accepted for the internal zone of the boundary layer. Furthermore, we discerned that this zone is the most important element for the simulation of atmospheric phenomena but that perturbation seems to have an influence on the external boundary layer zone.

Far from the injection zone results about mean velocity profiles are in good agreement with the logarithmic law of a natural boundary layer and, with the exception of the external zone, the turbulence intensities tend as anticipated to take on the characteristics of a natural boundary layer (fig. 4, 5, 6). For the REYNOLDS stresses (fig. 7), equilibrium appears to be realized for the entire layer. Turbulence spectra taken at a height of $z = 0.2\delta$ and at $x = 9.20$ m along the test plate in the thickened boundary layer are similar to those discerned in a natural boundary layer, which appears to confirm that equilibrium is obtained at least in the thickened wall region of boundary layer.

When we compare the turbulence characteristics of our flow with the equivalent ones at the corresponding atmospheric heights, we find that they are less intense -a turbulence intensity of 5 % in simulation compared to one of 10 to 15 % in the real atmosphere- which is why in the future it will be necessary to simulate the roughness of the soil. And perhaps the use of a roughened plate would not only increase turbulence intensities but would also thicken the boundary layer for given injection rates. Furthermore, equilibrium would be reached at a shorter distance from injection.

Fig. 4

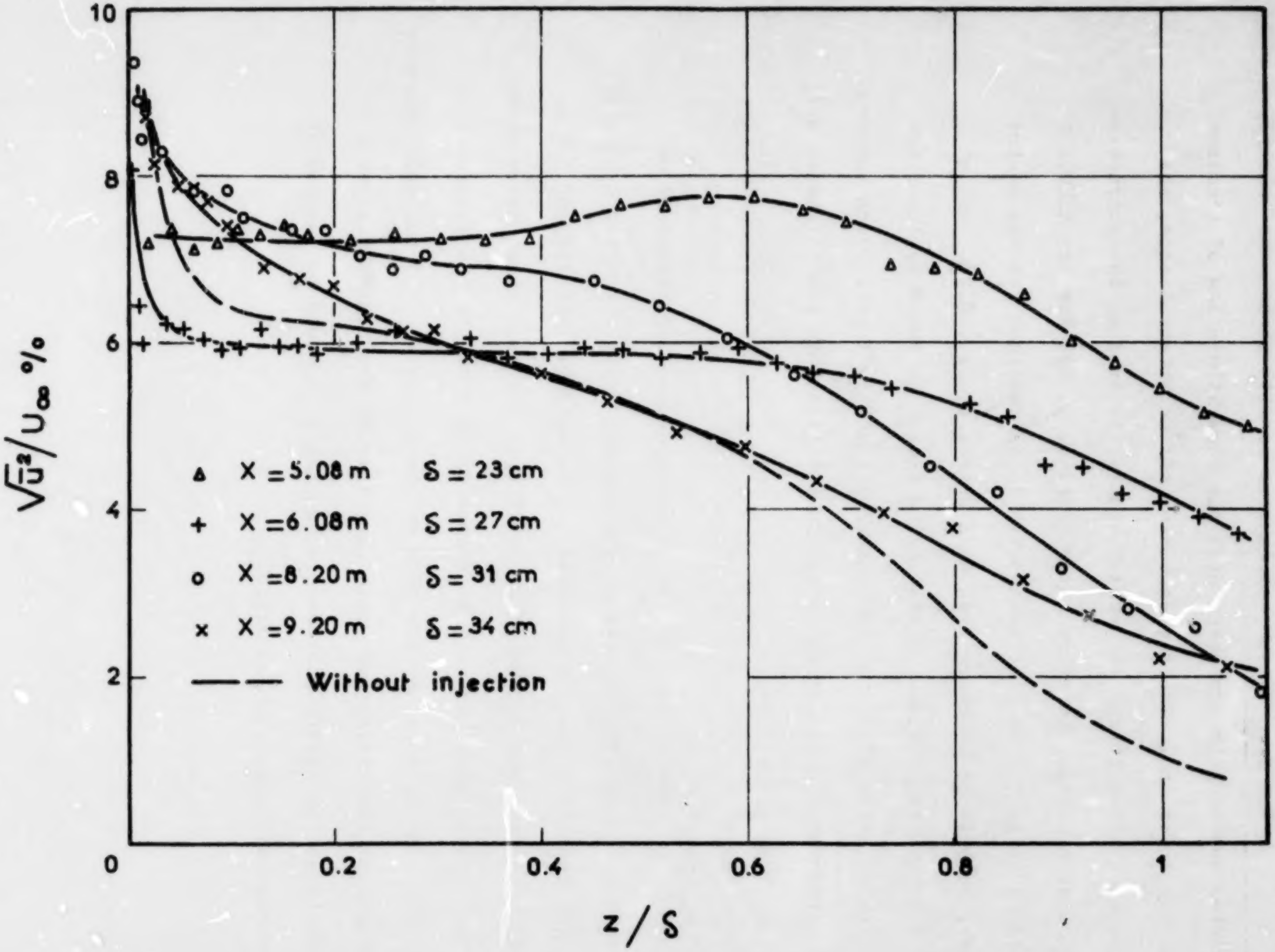

Fig. 4 - LONGITUDINAL TURBULENCE INTENSITY PROFILES

Fig. 5

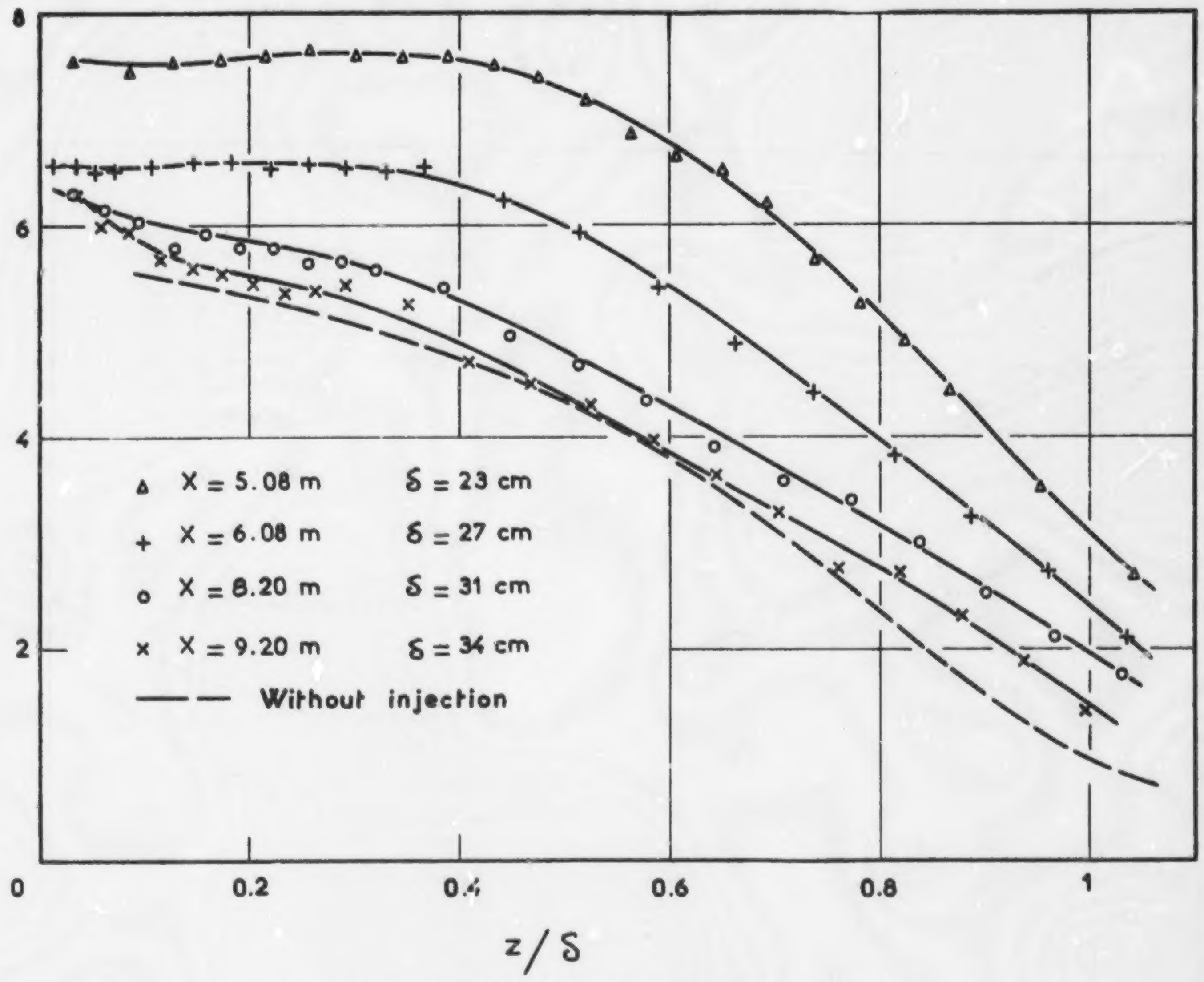

Fig. 5 - LATERAL TURBULENCE INTENSITY PROFILES

Fig.6

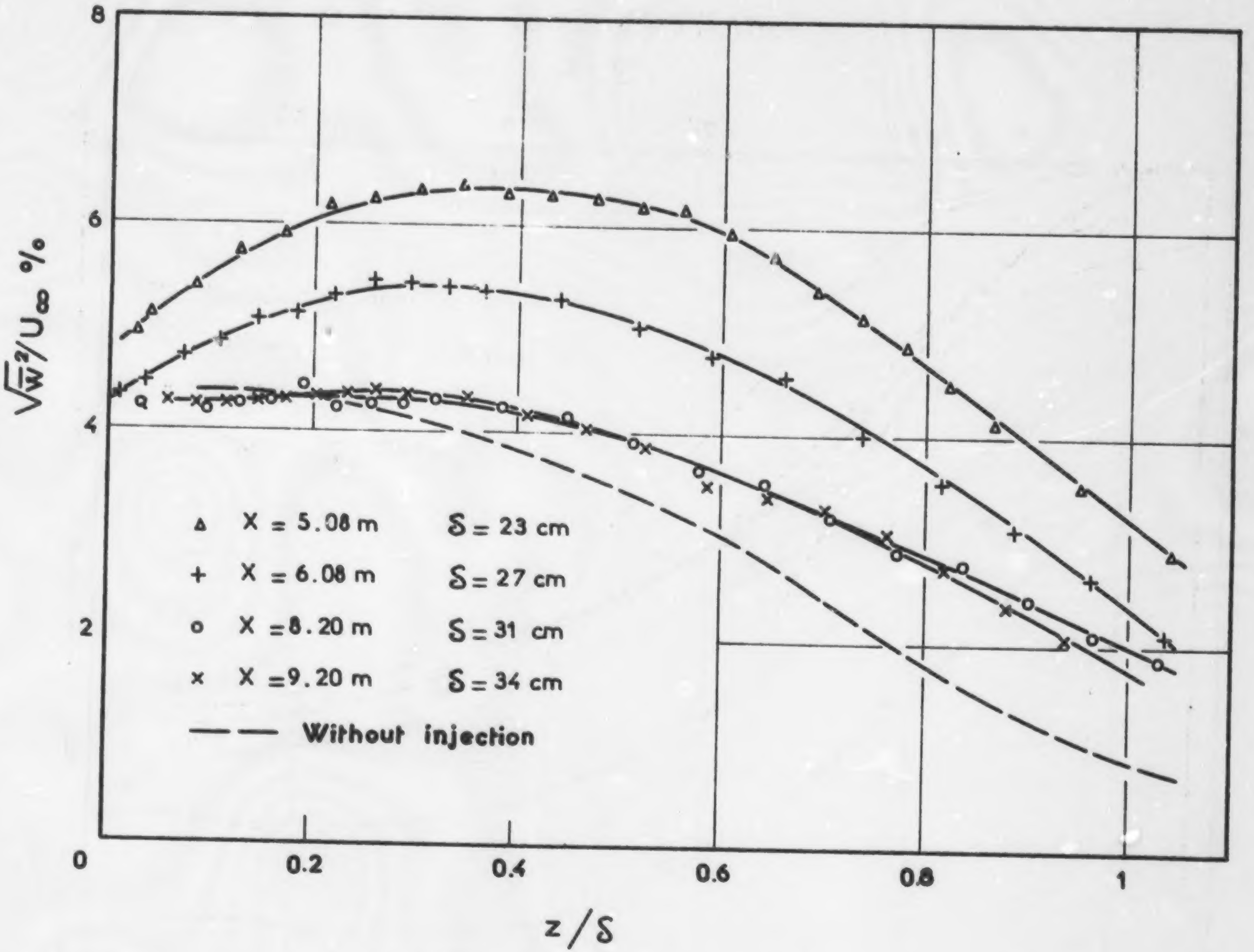

Fig. 6 - VERTICAL TURBULENCE INTENSITY PROFILES

Fig.7

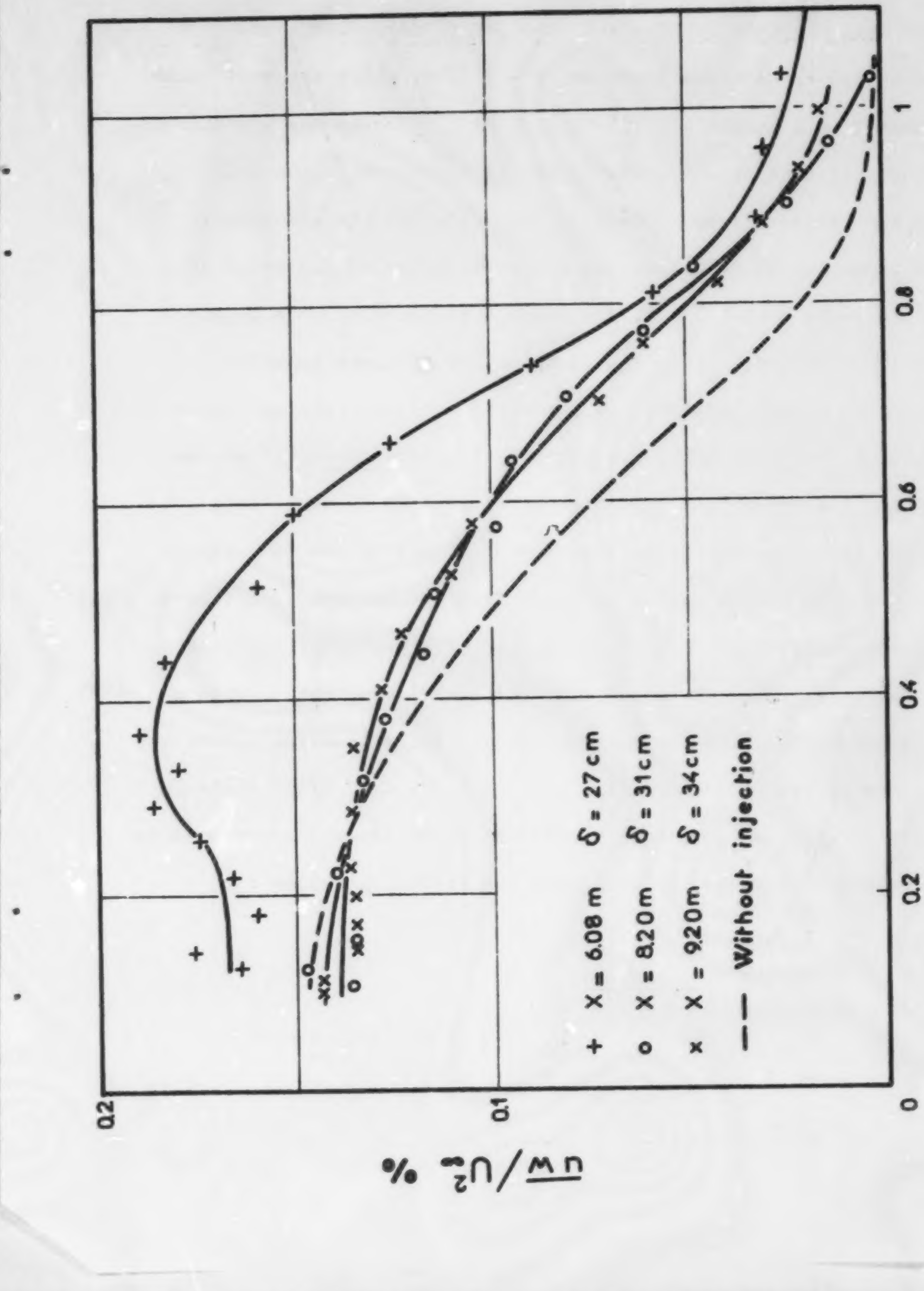

Fig. 7 - REYNOLDS STRESS PROFILES

Turbulence spectra (fig. 8, 9) were measured and then compared with the data of BUSH and PANOFSKY (1968), FICHTL and MAC VEHIL (1969). Data was taken at $x = 9.20$ m. along the test plate and measured at a height of $z/\delta = 0.2$ which corresponds approximately, taking into account the accuracy of the measurements, to half of the constant stress layer. Accepting the idea that the atmospheric surface layer is 50 m thick, the geometric scale of the model can be deduced to be about 1/350. The atmospheric spectra were measured at heights of between 15 and 46 m, the first of these heights corresponding approximately to 1/3 of the surface layer and the second corresponding to practically its upper limit. Good agreement exists between the laboratory and the atmospheric spectral values, which are traced in a representation lending importance to the most energy carrying structures. Differences result from the influence of viscosity on the small structures of the wind tunnel (for reduced frequencies higher than 3), which is to say that the tunnel does not provide a large enough REYNOLDS number to simulate the whole inertial convective range found in the atmosphere (the -2/3 law). If the 1/350 scale is held into account, a comparison between the wave lengths corresponding to the maxima of the spectra indicates the following values :

- in the wind tunnel :

$\lambda_{mu} = 385$ m $\qquad \lambda_{mw} = 75$ m for $z = 25$ m

Fig.8

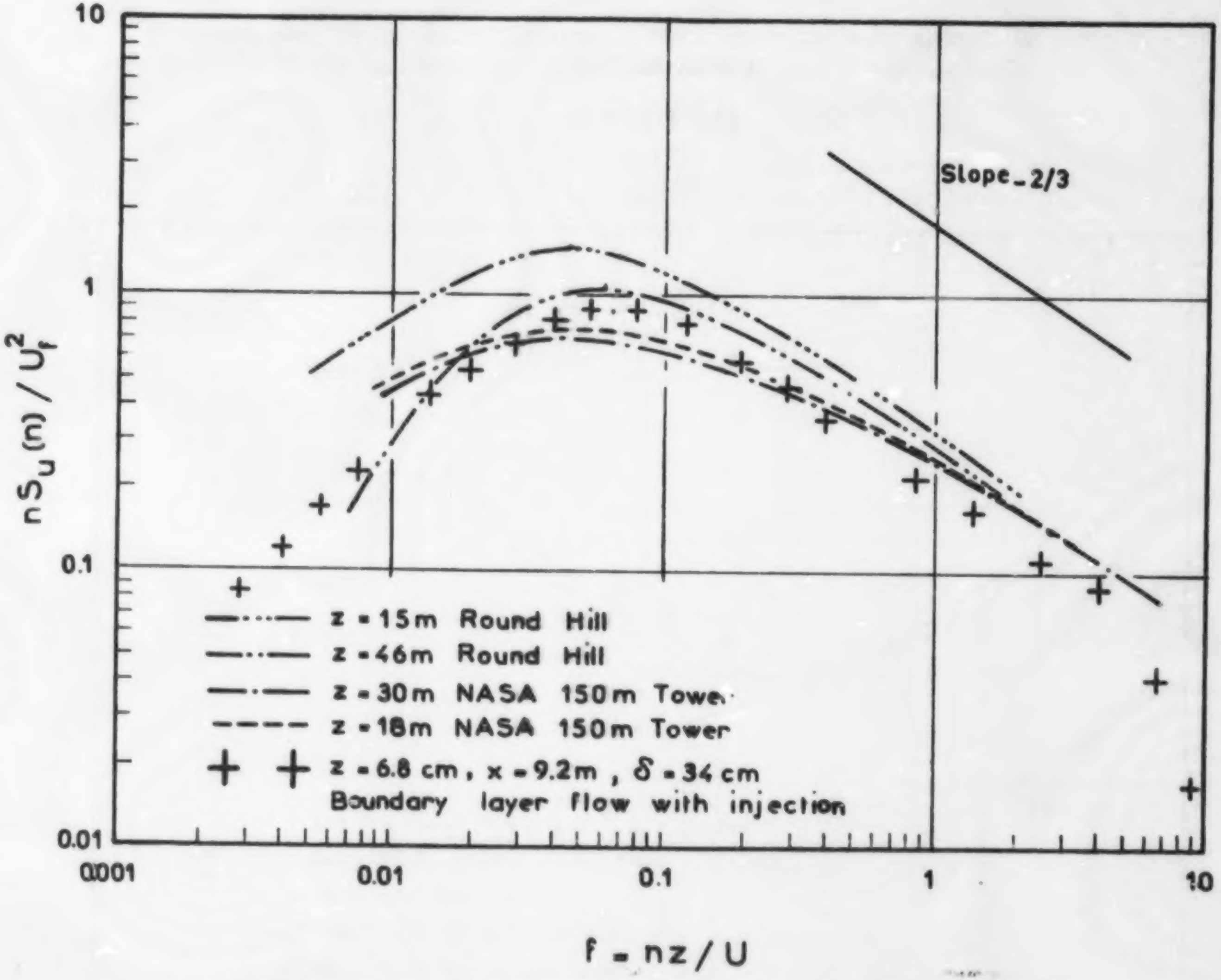

Fig. 8 - COMPARISON OF LONGITUDINAL FLUCTUATION SPECTRA IN THE ATMOSPHERIC BOUNDARY LAYER AND THE TURBULENT BOUNDARY LAYER WITH INJECTION

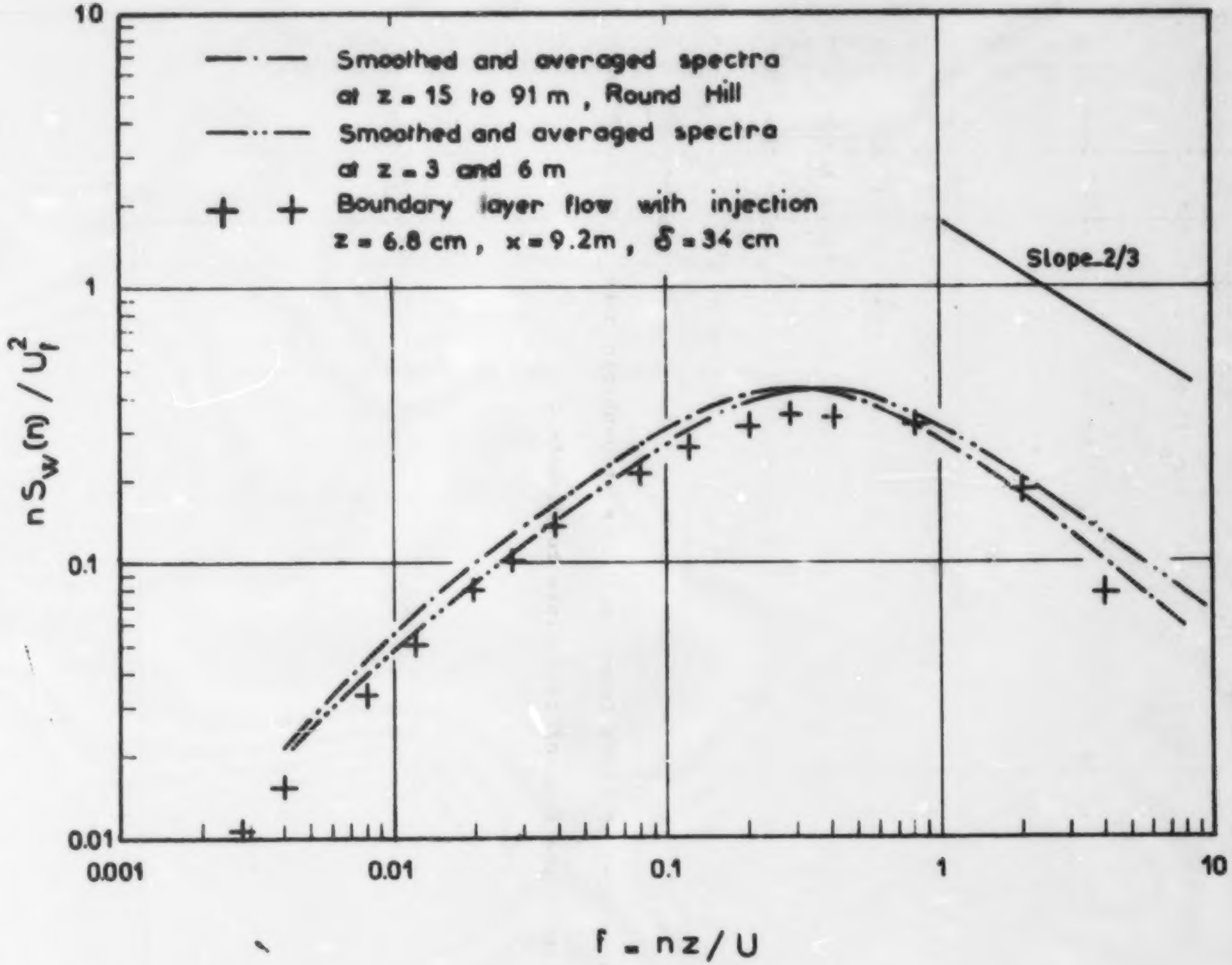

Fig. 9 - COMPARISON OF VERTICAL FLUCTUATION SPECTRA IN THE ATMOSPHERIC BOUNDARY LAYER AND THE TURBULENT BOUNDARY LAYER WITH INJECTION

Fig.9

- in the atmosphere :

$$350 \text{ m} < \lambda_{mu} < 750 \text{ m} \quad \text{for} \quad 15 \text{ m} < z < 46 \text{ m}$$

$\lambda_{mw} = 75$ m for $z = 25$ m, if we assume that, like BUSH and PANOFSKY (1968), f_{mw} is constant for $z < 50$ m.

In conclusion, our results show that the injection of air upstream of a boundary layer presents an interesting method for the thickening of this layer and therefore of simulating the atmospheric surface layer. In addition, we noticed after a certain distance (9.20 m) that the boundary layer recovers, at least in the inner zone, the characteristics of a natural turbulent boundary layer. The comparison of the spectra of these layers with the atmospheric ones is encouraging in spite of the lack of test plate roughnesses.

To develop a method to achieve a better simulation of the atmospheric surface layer, the following projects will be undertaken :

1) a study of the influence of different roughnesses,

2) a study of the evolution of spectra as a function of height, so as to obtain a more complete comparison with atmosphere data,

3) a study of stable and unstable stratified flows by cooling or heating the floor.

These studies are connected with the project of a large diffusion wind tunnel whose floor could be heated and cooled. So as to work with scales higher than 1/1000, the dimensions of the test section must be very important : length : 40 m, width : 8 m, height : 3 m. Nevertheless, the above method of thickening the boundary layer provides a substantial economy for the length of the test section.

This wind tunnel must be a closed circuit one, to prevent external wind influences and to allow ambiant temperature and humidity controls ; fig. 10 shows more details concerning this project.

Fig.10

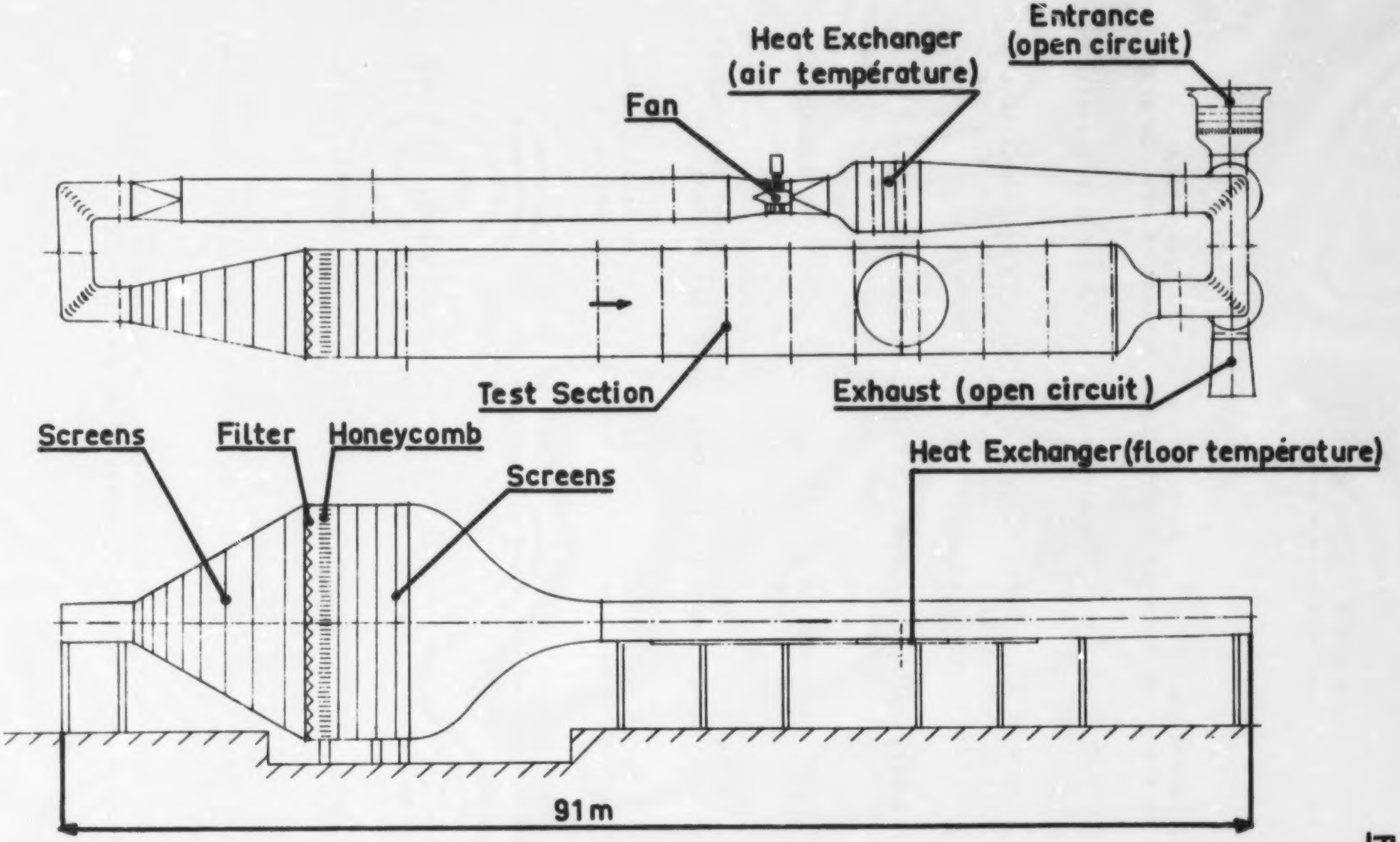
Entrance (open circuit)
Heat Exchanger (air température)
Fan
Test Section
Exhaust (open circuit)
Screens
Filter
Honeycomb
Screens
Heat Exchanger(floor température)
91m

Fig. 10 - DIFFUSION WIND TUNNEL PROJECT

REFERENCES

BRADSHAW P., FERISS D.H. (1968), The effect of initial conditions on the development of turbulent boundary layer. A.R.C. current papers, CP N°986.

BUSH N.E., PANOFSKY H.A. (1968), Recent spectra of atmospheric turbulence. J. Roy. Met. Soc., 94, pp. 132-148.

CERMAK J.E., SANDBORN V.A., PLATE E.J., BINDER G.H. (1966), Simulation of atmospheric motion by wind tunnel flows. Technical Report CER. 66, Fluid dynamics and diffusion laboratory, Colorado State University.

COUNIHAN J. (1969), An improved method of simulating an atmospheric boundary layer in a wind tunnel. Atmospheric Environment, 3, pp. 197-214.

CRAVEN A.J. (1960), Boundary layer with suction or injection. College of Aeronautics, Cranfield U.K., Rep. 136.

DREVILLON M., SCHON J.P. (1968), Caractéristiques turbulentes des couches limites soufflées. Rapport E.C.L. - E.D.F. , Fev. 1968 .

FAVRE A., DUMAS R., VEROLLET E., COANTIC M. (1966), Couche limite turbulente sur parci poreuse avec aspiration. Journal de Mécanique, 5,1 .

FICHTL G.H., MAC VEHIL G.E. (1969). Longitudinal and lateral spectra of turbulence in the atmospheric boundary layer. A.G.A.R.D. Conference Proceedings N° 48 Munich.

GOLDSTEIN R.J. (1965), Film cooling effectiveness with injection through a porous section. Trans. A.S.M.E., Series C, pp. 353-364.

LLOYD A.R. (1967), The generation of shear flow in a wind tunnel, Quart. J. Roy. Met. Soc., 93, pp. 79-96.

MAC VEHIL G.E., LUDWIG G.R., SUNDARAM T.R. (1967), On the feasibility of modeling small scale atmospheric motions. Cornell Aeronautical Laboratory, Rep. N° ZB. 2328-P-1, Buffalo, N.Y. .

MERY P. (1969), Reproduction en similitude de la diffusion dans la couche limite atmospherique. La Houille Blanche, N° 4, pp. 327-344.

Chapter V

MATHEMATICAL-METEOROLOGICAL MODELING OF AIR QUALITY IN THE UNTERMAIN REGION (FRANKFURT)

Prof. Heinz Fortak
Institute for Theoretical Meteorology
Free University of Berlin

For presentation to the Panel on Modeling, NATO/CCMS Pilot Project on Air Pollution, Paris, France, July 26-27, 1971

MATHEMATICAL-METEOROLOGICAL MODELING OF AIR QUALITY IN THE UNTERMAIN REGION (FRANKFURT)

(status and further plannings)

Objective

On the basis of a complete emission inventory of air pollutant substances and of frequency statistics of meteorological diffusion conditions the frequency distributions of concentrations of air pollutants shall be computed by means of a mathematical-meteorological multi-source model for each grid point of a grid net extended over the region. The properties of the frequency distributions are of importance for the solution of immission-orientated plannings. This procedure of a mathematical simulation of the immission climatology of an industrial agglomeration area has been successfully applied for the first time to the city of Bremen and realized by means of an appropriate measuring programme.

Particularities of the Untermain-Region

Whereas no principal differences are existing in the conditions in Bremen with regard to the emission inventory, the meteorological conditions on the one hand and the topographical conditions in the Frankfurt-Untermain Region on the other hand differ so much from those in Bremen that a relatively large number of new models must be developed. From the meteorological side the following problems are arising:

1. The wind field within the diffusion layer cannot be considered homogeneous in a larger number of cases. Horizontal divergences and convergences combined with associated meso-scale systems of vertical motion cause a more intensive transportation of the pollutants into higher layers and/or a more intensive accumulation in the diffusion layer, according to certain prevailing conditions.

2. Weather situations having weak gradient and small eddy flux with inversion conditions occur so frequently in the region that a special model of these conditions in required. Local small-scale circulation systems have to be particularly considered.

   With respect to the topographical conditions the existence of the Taunus is of great significance with respect to the formation of flows and distribution conditions if corresponding wind directions exist aloft.

These are essential differences in conparison with the conditions in Bremen. There it was verified that the wind field within the distribution layer could be considered as sufficiently homogeneous for the modeling. Since weather situations with weak gradient and small eddy flux as well as those with distinct low inversions occur so rarely that they are of little importance in the computed immission climatology we have not accounted for them in our model. The area of the city of Bremen is flat, therefore no models were developed for rough terrain.

Models in the first phase

In the Untermain-Region weather situations frequently exist in which the wind field within the diffusion layer may be considered as sufficiently homogeneous for the whole area and in which, due to the particular wind direction, the influence of the topography may be neglected. For these weather situations the application of the model developed for Bremen is justified.

The model strategy is, therefore, the following: for the development of the immission climatology four models are used:

1. The model of Bremen for homogeneous, tropographically undisturbed wind conditions. The existence of layers preventing vertical exchange caused by inversions is already included in this model.
2. Diffusion model for meso and/or submeso-scale wind systems in which divergent and/or convergent flow conditions are considered.
3. Diffusion model for weather situations with weak gradient and small eddy flux, especially for cases when it is calm and under the influence of very low inversions.
4. Diffusion model for topographically influenced flow and diffusion conditions.

The first phase of the model development is concerned with the application of an improved version of the model, developed for Bremen, to the Untermain Region.

A prerequisite for the application of the model is the existence of the emission invertory and of meteorological diffusion statistics for those weather conditions to which the Bremen model may be applied. The work in both areas has been started by another authority but has not yet been completed to the point that the model computation can be started.

However, in the meantime an improved version of the original Bremen model has been developed and successfully used in models for the Köln area. The improvements are the following:

1. The emission sources of the residential combustion are normed by means of an appropriate procedure, i.e. two-dimensional numerical filtering on a characteristic horizontal scale, which is in accordance with the scale of correspondingly filtered immission fields.

. The method of the dispersion of equal probability of the plumes in the given 10 vectors of wind direction is introduced consequently and modified lateral dispersions occurred was defined.

3. Lateral and vertical dispersions have been recently determined for the conditions of European towns on the basis of the experiments obtained with the Bremen model.

4. Tests to replace the non-Fickian diffusion theory, which is used in the Bremen model, by a simplified version of the Fickian diffusion theory (K-theory) in order to save computation time on the computers, have been successful. The result has to be attributed to the fact that modelings of an immission climatology are long-term processes to which the application of the K-theory seems to be justified.

The work on point 4 has not progressed to the point that a completely new programming of the multi-source models seems to be suitable at this time. On the contrary, the original model will be applied with the modifications 1 to 3 as soon as emission inventory and meteorological data are avaliable.

Models of the second phase

Models are developed for non-homogeneous meso and/or sub-meso-scale wind systems associated with vertical wind fields as well as models for weather situations with weak gradient and small eddy flux and/or calm weather situations with distince inversion.

No models for non-homogeneous wind fields exist at the present time in the literature. Simple approaches in which the stationary "plume" model is relinguished and trajectory-oriented "puff" models are used instead should also be successful when applied to a multi-source problem although the required computation time will probably be extraordinarily long. Preliminary studies are necessary and have already been started in order to achieve success by means of the K-theory. The determination of the relevant exchange coefficients requires a lot of effort. In a certain way these exchange coefficients have been linked with the dispersions of the non-Fickian theory and in addition related to the deformation of the wind field. However, it will still require a great deal of effort in order to develop a reliable model for non-homogeneous wind systems.

According to their nature, models for calm weather situations and weather situations with weak gradient and small eddy flux are stationary models. Here it is, the concentration of air pollutants increasing with the time in case of stationary emission, which entails extremely high concentration values. Therefore, these weather situations are of relatively great importance in the immission climatology.

A mathematical model for the single source under these conditions has been developed and can be applied directly to a multi-source problem. If we know the ascent velocity of the plume and any sudden change in the angle of ascent in case of a weak wind aloft, as well as the height of a existing inversion, the model permits to compute the timely development of a concentration in the three-dimensional space. It is a "puff" model which is continuously brought to a "plume" model when the wind velocity as well as the diffusion time are sufficiently large. However, at present it is not possible to obtain, the dispersion parameters for these conditions. Probably systematic measurements will have to be made in this region.

In this second phase the development of models for sensitivity studies will be particularly important in order to estimate the influence of parameters which cannot be determined with certainty and to consider it in the immission climatology.

Beginnings have already been made.

Models in the third phase

One of the most difficult parts of the model development is the one in which the influence of the surface topography on the formation of the flow and diffusion conditions has to be considered. It seems that the treatment of the aerodynamic overflow of a smooth, finitely wide mountain ridge, under consideration of the friction conditions of the ground and any flow direction, will soon be successful in this project. Since the large-scale wind conditions can be considered as known, it is hoped that the modification in the wind field caused by the Taunus can be calculated theoretically. A thorough verification of the results by comparisons with measured wind fields will be indispensable.

The problem of the diffusion of air pollutants in this non-homogeneous wind field caused by the topography is the same as already described. Here also, the applicaiton of the K-theory will be the most practical solution, however, considerable mathematic and physical problems will have to be solved.

The final model for the immission climatology

An essential task for the meteorologist will be to classify the weather situations (hourly values) in such a way that there will be no doubt which section of the model has to be used. The computation of all cases with those sections of the models which have to be used entails, the same as in the Bremen model, the computation of the frequency distributions of concentrations of air pollutant substances for each grid point of the region in a distance of 500 m. Average values of different times (daily average means of a period) as well as other statistical dimension figures can easily be determined and represented on charts.

The verification of the computed values by means of a specific measuring porgramme at "strategically" planned measuring points will, as in Bremen, permit one to adapt the parameters of the model to the special conditions in the region, and thus a means would be avaliable for immission-orientated plannings in the region.

Chapter VI

DEPENDENCE OF POLLUTANT CONCENTRATION ON THE SPATIAL VARIATION OF A CROSSWIND LINE SOURCE

April, 1971

Suha Selamoglu*

Mechanical Engineering Department
The Middle East Technical University
Ankara, Turkey

* On assignment to the NATO/CCMS Panel on Modeling by the Turkish Scientific and Technical Research Council

Summary

In the calculations of pollutant concentration due to distributed point and/or surface sources it is sometimes convenient to approximate part of the sources with an infinite, uniform line source. By this artifice, the problem may be reduced to a two-dimensional one. However, in order for the approximation to be of any use, the actual source distribution should be fairly uniform in the direction of the substitute line source.

The effect of nonuniformity appears as a variation in the crosswind direction of the pollutant concentration. This variation may quantitatively be estimated by assuming a nonuniform line source whose strength is appropriately determined to represent the actual distribution.

In what follows a crosswind line source of varying strength is considered. The resulting pollutant concentration is obtained in a form to reveal its dependence on the derivatives of the line source strength. It is seen that, when the source distribution depends weakly on the crosswind coordinate, the line source may be assumed to have a uniform distribution whose value is that at the point directly upwind from the receptor.

The approximation has been previously proposed by Calder [1]. The present analysis provides a basis for justification.

Analysis

Suppose that the pollutant sources emit at steady-state along the line $x=0$, $z=H$ according to the distribution $Q(y)$ per unit length in the interval $-a \le y \le a$. Assuming that the pollutant concentration due to a continuous point source may be represented sufficiently well by a biaxial Gaussian distribution, and that the line source may be realized by an integration over the independent (i.e., noninterfering) point sources $Q(y)dy$, one can write for the concentration at the receptor

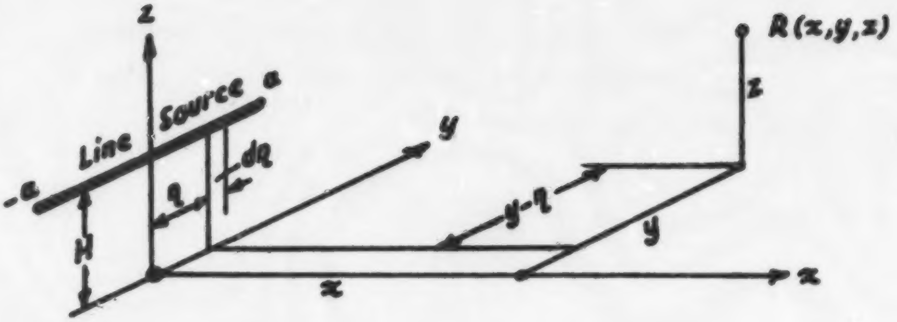

Figure 1

point $R(x,y,z)$ downwind of the line source (Fig. 1)

$$\chi(x,y,z;H)=\frac{\exp\left\{-\left[\frac{z-H}{\sqrt{2}\sigma_z(x)}\right]^2\right\}+\exp\left\{-\left[\frac{z+H}{\sqrt{2}\sigma_z(x)}\right]^2\right\}}{2\pi u\ \sigma_y(x)\sigma_z(x)}\int_{-a}^{a}Q(\eta)\exp\left\{-\left[\frac{y-\eta}{\sqrt{2}\sigma_y(x)}\right]^2\right\}d\eta. \tag{1}$$

In Eq.(1) the effect of the ground surface on the concentration distribution was accounted for by an image source along $z=-H$, $x=0$. Introducing a function $A(x,z;H)$ defined as

$$A(x,z;H)=\frac{\exp\left\{-\left[\frac{z-H}{\sqrt{2}\sigma_z(x)}\right]^2\right\}+\exp\left\{-\left[\frac{z+H}{\sqrt{2}\sigma_z(x)}\right]^2\right\}}{2\pi u\ \sigma_z(x)}, \tag{2}$$

one can write from (1)

$$\chi(x,y,z;H)=\frac{A(x,z;H)}{\sigma_y(x)}\int_{-a}^{a}Q(\eta)\exp\left\{-\left[\frac{y-\eta}{\sqrt{2}\sigma_y(x)}\right]^2\right\}d\eta. \tag{3}$$

By the variable transformation

$$\frac{y-\eta}{\sqrt{2}\sigma_y(x)}=t \tag{4}$$

the expression may be put into the form

$$\chi(x,y,z;H)=\sqrt{2}A(x,z;H)\int_{t_1}^{t_2}Q(y+\sqrt{2}\sigma_y t)e^{-t^2}dt, \tag{5}$$

where

$$t_1=-\frac{a+y}{\sqrt{2}\sigma_y}\quad , \quad t_2=\frac{a-y}{\sqrt{2}\sigma_y} \tag{6}$$

Expanding Q into a Taylor series about y ,

$$\chi(x,y,z;H)=\sqrt{2}A(x,z;H)\int_{t_1}^{t_2}\sum_{n=0}^{\infty}\frac{(\sqrt{2}\sigma_y)^n}{n!}t^n e^{-t^2}Q^{(n)}(y)dt. \tag{7}$$

If one assumes that the conditions of continuity and convergence are fulfilled one can interchange the orders of integration and summation to obtain

$$\chi(x,y,z;H)=A(x,z;H)\sum_{n=0}^{\infty}\frac{2^{\frac{n+1}{2}}\sigma_y^n}{n!}Q^{(n)}(y)\int_{t_1}^{t_2}t^n e^{-t^2}dt. \tag{8}$$

Let $i_n(x,y)$ be defined as

$$i_n(x,y)=\int_{t_1}^{t_2}t^n e^{-t^2}dt. \tag{9}$$

Then,

$$\chi(x,y,z;H)=A(x,z;H)\sum_{n=0}^{\infty}\frac{2^{\frac{n+1}{2}}}{n!}[\sigma_y(x)]^n Q^{(n)}(y)\,i_n(x,y). \tag{10}$$

Now let the extent of the line source distribution be so large that $a/\sqrt{2}\sigma_y$ tends to infinity. Then,

$$\lim_{a/\sqrt{2}\sigma_y\to\infty} i_n(x,y)=\int_{-\infty}^{\infty}t^n e^{-t^2}dt\left\{\begin{array}{ll}=\dfrac{1\cdot3\cdot5\cdot\ldots\cdot(2k-1)}{2^k}\sqrt{\pi}, & \text{if } n=2k\\ =0 & , \text{if } n=2k+1\end{array}\right\} \tag{11}$$

where k is an integer. The pollutant concentration in this case is found as

$$\chi_\infty(x,y,z;H)=\sqrt{2\pi}\,A(x,z;H)\sum_{k=0}^{\infty}\frac{[\sigma_y(x)]^{2k}Q^{(2k)}(y)}{2^k k!}. \tag{12}$$

Its transverse derivative, on the other hand,

$$\frac{\partial}{\partial y}\chi_\infty(x,y,z;H)=\sqrt{2\pi}\,A(x,z;H)\sum_{k=0}^{\infty}\frac{[\sigma_y(x)]^{2k}Q^{(2k+1)}(y)}{2^k k!}. \tag{13}$$

For the evaluation of χ_∞ or $\partial\chi_\infty/\partial y$ at ground level and along x-axis one has merely to set $z=0$ and $y=0$, respectively. It should be borne in mind that the above limiting values are restricted to the range of downwind distances x for which $a/\sqrt{2}\sigma_y(x)$ is very large. Otherwise, the expression (10) should be used.

The relative variation of χ_∞ in the crosswind direction is indicative of how strongly χ_∞ depends on the distribution

$Q(y)$. Let a mean source strength $Q_m(y)$ be defined by

$$\chi_\infty(x,y,z;H) = \sqrt{2\pi}\, A(x,z;H)\, Q_m(y). \tag{14}$$

Combining (14) with (5) $Q_m(y)$ may be calculated from

$$Q_m(y) = \frac{1}{\sqrt{\pi}} \int_{-\infty}^{\infty} Q(y+\sqrt{2}\sigma_y t)\, e^{-t^2} dt. \tag{15}$$

Hence, the relative crosswind variation of the concentration due to an infinite line source is obtained as

$$\frac{1}{\chi_\infty} \cdot \frac{\partial \chi_\infty}{\partial y} = \frac{1}{Q_m(y)} \sum_{k=0}^{\infty} \frac{[\sigma_y(x)]^{2k}\, Q^{(2k+1)}(y)}{2^k\, k!}. \tag{16}$$

As should be expected, the variation depends only on the derivatives of the source strength; it vanishes if Q is constant. The effect of the higher derivatives becomes weaker quickly because of the factorial in the denominator of each term.

Examples

In the examples to follow it is assumed that the source is practically of infinite extent. q is a constant with appropriate dimension.

1. Linear distribution:

$$Q = Q_0 + qy \quad , \quad Q_m = Q_0 + qy, \tag{17a,b}$$

$$\frac{1}{\chi_\infty} \cdot \frac{\partial \chi_\infty}{\partial y} = \frac{q}{Q_m}. \tag{17c}$$

2. Quadratic distribution:

$$Q = Q_0 + qy^2 \quad , \quad Q_m = Q_0 + q(y^2 + \sigma_y^2), \tag{18a,b}$$

$$\frac{1}{\chi_\infty} \cdot \frac{\partial \chi_\infty}{\partial y} = \frac{2qy}{Q_m}. \tag{18c}$$

3. Cubic distribution:

$$Q = Q_0 + qy^3 \quad , \quad Q_m = Q_0 + qy(y^2 + 3\sigma_y^2). \tag{19a,b}$$

$$\frac{1}{\chi_\infty} \cdot \frac{\partial \chi_\infty}{\partial y} = \frac{3q(y^2 + \sigma_y^2)}{Q_m}. \tag{19c}$$

4. Trigonometric distribution:

$$Q = Q_0 + q \left\{ \begin{matrix} \cos \\ \sin \end{matrix} \right\} y, \quad Q_m = Q_0 + e^{-\frac{\sigma_y^2}{2}} q \left\{ \begin{matrix} \cos \\ \sin \end{matrix} \right\} y, \tag{20a,b}$$

$$\frac{1}{\chi_\infty} \cdot \frac{\partial \chi_\infty}{\partial y} = \left\{ \begin{matrix} - \\ + \end{matrix} \right\} \frac{q}{Q_m} \left\{ \begin{matrix} \sin \\ \cos \end{matrix} \right\} y \sum_{k=0}^{\infty} (-1)^k \frac{\sigma_y^{2k}}{2^k k!}. \tag{20c}$$

It may be seen that the relative variations vanish along x-axis for even source distribution, whereas they are proportional to q/Q_m for odd distributions.

Conclusion

When the nonuniformity in the line source distribution is not too strong the crosswind variation of the pollutant concentration may be neglected. If the nonuniformity term containing the factor q is looked upon as a perturbation on the mean source distribution Q_m then the variation of the concentration is seen to be proportional to the perturbation parameter q/Q_m.

When an area source distribution may be expressed in terms of a series of crosswind line sources, and when the variation of the source strength is small relative to its mean value, the resulting variation in the pollutant concentration is then also small.

In the calculation of the climatological pollutant concentration due to area sources the crosswind variation as represented by $\sigma_y(x)$ drops out as a result of the long-time averaging relative to the wind direction [1] . But when the short-time averaged concentration is required the crosswind variation due to area sources distributed over a large area may also be neglected if the nonuniformity in the source distribution is not too large, i.e., if $q \ll Q_m$.

Reference

[1] K. L. Calder, "A Narrow Plume Simplification for Multiple Source Urban Pollution Models", Dec., 1969, not published.

Chapter VII

MODIFICATIONS TO THE CLIMATOLOGICAL AIR POLLUTION MODEL FOR ANKARA

April, 1971

Suha Selamoglu*

Mechanical Engineering Department
The Middle East Technical University
Ankara, Turkey

---

* On assignment to the NATO/CCMS Panel on Modeling by the Turkish Scientific and Technical Research Council

MODIFICATIONS TO THE CLIMATOLOGICAL AIR POLLUTION MODEL FOR ANKARA

The climatological air pollution study of Ankara is currently being made on computer by the use of Calder's climatological dispersion model [1]. The compatibility of the model to Ankara may be discussed only after the numerical results are obtained and compared with the observed pollution data. On the other hand, certain facts about the model as well as about the peculiarities of the city stimulate ideas which may help improve the efficiency of the model. In the following these ideas will be explained in order to make the ground for critisism and discussion. They should be thought of as being possible modifications to the current model based on Calder's paper. The fundamentals of the current model will be assumed known and not explained here unless needed.

1. The "Gaussian plume" formula for a steady, continuous point source at an effective height H and evaluated at the ground level $z=0$ is given by

$$\chi(x,y,0;H)=\frac{Q}{u}\cdot\frac{2\,e^{-\left[\frac{H}{\sqrt{2}\,\sigma_z(x)}\right]^2}}{\sqrt{2\pi}\,\sigma_z(x)}\cdot\frac{e^{-\left[\frac{y}{\sqrt{2}\,\sigma_y(x)}\right]^2}}{\sqrt{2\pi}\,\sigma_y(x)} \qquad (1)$$

where u is wind speed, $\sigma_y(x)$, $\sigma_z(x)$ are the crosswind and vertical dispersion functions, respectively, and χ is the pollutant concentration.

In the process of averaging over wind directions the factor $\exp\left\{-[y/\sqrt{2}\sigma_y(x)]^2/\sqrt{2\pi}\sigma_y\right\}$ is integrated to yield $1/x$, so that

$$\bar{\chi}=\frac{Q}{ux}\cdot\sqrt{\frac{2}{\pi}}\cdot\frac{e^{-\left[\frac{H}{\sqrt{2}\sigma_z(x)}\right]^2}}{\sigma_z(x)} \qquad (2)$$

appears as the average pollutant concentration within a wind sector for unit wind frequency. This may also be written as

$$\chi=\frac{Q}{u}\cdot\frac{1}{x}\cdot C(x), \qquad (3)$$

where

$$C(x) = \sqrt{\frac{2}{\pi}} \cdot \frac{e^{-\left[\frac{H}{\sqrt{2}\,\sigma_z(x)}\right]^2}}{\sigma_z(x)} \tag{4}$$

is the one-dimensional Gaussian plume formula at ground level per unit source and unit wind traveling time. The last expression has the following general behavior: It has practically zero value between $x=0$ and $x=x_1$, increases rapidly to a maximum C_{max} at $x=x_m$, then decreases back to a negligible value at approximately $x=x_2$. A log-normal plot of the function (i.e., C vs. $\log x$) shows that it is possible to approximate $C(x)$ by four straight line segments OABCD (Figs. 1a ,1b).

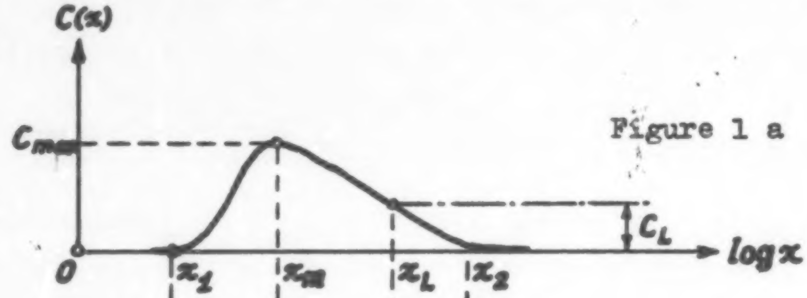

Figure 1 a

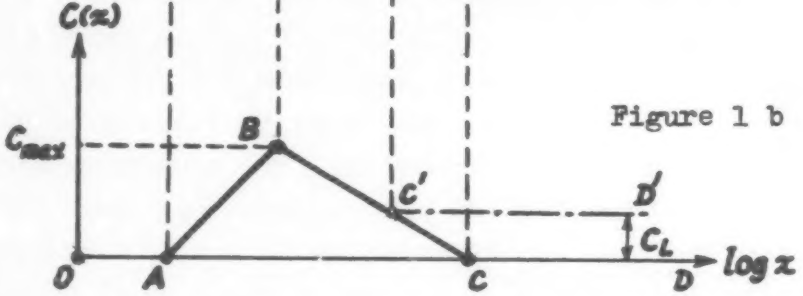

Figure 1 b

Namely,

$$\left.\begin{array}{llll} \text{OA :} & 0 \leq x \leq x_1 , & C(x)=0 \\ \text{AB :} & x_1 \leq x \leq x_m , & C(x)= C_{max}\dfrac{\log(x/x_1)}{\log(x_m/x)} \\ \text{BC :} & x_m \leq x \leq x_2 , & C(x) = C_{max}\dfrac{\log(x_2/x)}{\log(x/x_m)} \\ \text{CD :} & x_2 \leq x , & C(x)=0 \end{array}\right\} \tag{5}$$

In case that a mixing layer exists so that the concentration may be assumed uniform beyond $x = x_L$ the modification to the above is simply to superimpose

C'D' : $x_L \leq x$, $C(x) = C(x_L) = C_L$ (providing $x_1 \leq x_L \leq x_2$). (6)

Note that it is only necessary to evaluate x_1, x_m, x_2, x_L and C_{max} for all stability categories once and for all, but it is not necessary to introduce the dispersion function $\sigma_z(x)$ and the exponential function. This simplifies the computer work without causing a great error.

2. The factor $1/x$ that appears in the $\bar{\chi}$ expression reflects the crosswind dispersion effect in an approximate fashion. All area sources within the wind direction sector of $2\pi/16$ (= $22^\circ 30'$) contribute into the concentration at the vertex with a dispersive attenuation which is inversely proportional to x .

Instead of looking at the area sources as representative point sources at the weighted centers of the areas, one can consider equally spaced crosswind line sources that are distributed in such a way that the resultant effect is approximately equivalent to that of the original area source distribution. At a given receptor point the concentration is to be calculated by adding up the contributions from each line source located upwind of the receptor. It can be shown [2] that the ground level concentration at the receptor located at $R(x,y,0)$ due to an infinite crosswind line source at $x=0$, $z=H$ whose distribution is given as $Q(y)$ is

$$\chi_L(x,y,0;H) = C(x) \sum_{n=0}^{\infty} \frac{[\sigma_y(x)]^{2n}}{2^n n!} Q^{(2n)}(y) \qquad (7)$$

Now, it will be assumed that $Q(y)$ is a weak function of y , so that only the first term in the above series may be retained. Consequently, the concentration at the given point is the sum over x_k of all χ_L due to the crosswind line sources of uniform strength $Q_k(y)$, located at $x=x_k$, $z=H_k$:

$$\chi(x,y,0) = \sum_{k} \frac{Q_k(y)}{u} C_k(x-x_k) , \tag{8}$$

where

$$C(x-x_k) = \sqrt{\frac{2}{\pi}} \; \frac{e^{-\left[\frac{H_k}{\sqrt{2}\sigma_z(x-x_k)}\right]^2}}{\sigma_z(x-x_k)} . \tag{9}$$

The procedure replaces the summation over all area source elements within a sector of width $\pi/8$ with a summation over k along a unit strip in the upwind direction from the receptor (Fig. 2).

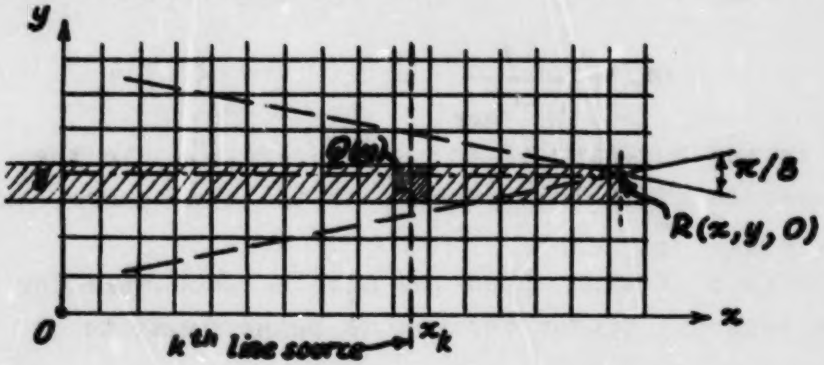

Figure 2

The approximation for $C(x)$ given in 1. by the relations (5) and (6) may be utilized here also to simplify the calculations.

3. Space heating is the major source of air pollution in Ankara. The correlation between the emission strength and the meteorological parameters such as temperature and wind speed is strong enough to be noticed even by an inexperienced observer. The assumption that the source strengths are constant at their seasonal averages may cause serious error. The correlation may be introduced to the model in many ways. The following is a possible method based on the assumption of linear relation of the emission factors to the meteorological deviations.

Let T_c be the critical temperature above which practically no space heating is required, T the average temperature for a given time interval, and Q the seasonal average emission factor. One can then substitute Q' for Q in the concentration formula. Q' is defined as

$$\left.\begin{array}{lll} Q' = m_T\, Q(T_c - T) & \text{when} & T < T_c\ , \\ Q' = 0 & \text{when} & T_c \leq T\ . \end{array}\right\} \qquad (10)$$

The constant coefficient m_T should be so determined that the seasonal average of Q' coincides with Q , i.e.,

$$\int_{\Delta t} m_T\, Q(T_c - T)\,dt = Q\Delta t \quad , \ T < T_c\ , \qquad (11)$$

or

$$m_T = \frac{1}{T_c - T_{ave}} \qquad (12)$$

where Δt is the duration of the season and T_{ave} is the seasonal average of the temperature of the atmosphere, excluding the values above T_c .

The effect of wind speed may also be accounted for by means of a separate factor defined as being equal to

$$\left.\begin{array}{lll} 1 + m_W\,(u - u_c) & \text{when} & u_c \leq u\ , \\ 1 & \text{when} & u \leq u_c\ , \end{array}\right\} \qquad (13)$$

where m_W and u_c are constants to be chosen suitably in order to obtain a best fit.

Thus, the new emission factor, $\bar{Q}$, to replace the old Q , becomes

$$\left.\begin{array}{lll} \bar{Q} = Q\,\dfrac{T_c - T}{T_c - T_{ave}}\,[1 + m_W(u - u_c)] & \text{when} & T < T_c\ ,\ u_c < u \\ \bar{Q} = Q\,\dfrac{T_c - T}{T_c - T_{ave}} & \text{when} & T < T_c\ ,\ u \leq u_c \\ \bar{Q} = 0 & \text{when} & T_c \leq T. \end{array}\right\} \qquad (14)$$

It may be noticed that certain amount of calibration is possible in the end results by suitable choices of T_c , u_c and m_W. The proposed method calls for further splitting of the joint frequency function as to the occurrence of temperature and wind speed within certain intervals. The number of intervals needs not be large; two or three intervals may suffice.

4. In the current model the mixing depth, L, is assumed constant over the entire city area. The elevation from sea level varies in Ankara within 300 meters. This may cause significant deviations in the calculated concentration values from the actual ones. The upper lid of the mixing layer may be assumed to be a plane -most probably a horizontal one- so that the value L, which is to be measured between the upper lid and the ground, varies as the elevation of the ground does.

As a simple device, one may choose to vary L according to the relation

$$L = L_0 - m_L (h - h_0) \tag{15}$$

where h is the elevation from sea level of the receptor point, L_0 is the mixing depth at the reference station with elevation h_0, and m_L is an adjustable constant correction factor. The limiting distance x_L may be determined, as previously, by ignoring the topography of the ground.

Summarizing, it is hoped that the model may be made more elastic by introducing a number of adjustable parameters into the system. Certain simplifications in the computer work may also be effected without causing serious deviations from the original model. The success of the proposed modifications largely depends on the choice of the arbitrary parameters.

References

[1] K. L. Calder, "A Climatological Model for Multiple Source Urban Air Pollution", 1970, to be published.

[2] S. Selamoglu, "Dependence of Pollutant Concentration on the Spatial Variation of a Crosswind Line Source", 1971, see elsewhere in this Proceedings.

Chapter VIII

PHYSICAL AND CHEMICAL TRANSFORMATIONS IN AIR POLLUTION MODELING

June, 1971

Suha Selamoglu*

Mechanical Engineering Department
The Middle East Technical University
Ankara, Turkey

For presentation to the NATO/CCMS Panel on Modeling,
2nd meeting, Paris, France, July 26-28, 1971

---

* On assignment to the NATO/CCMS Panel on Modeling by the Turkish Scientific and Technical Research Council

VIII-2

PHYSICAL AND CHEMICAL TRANSFORMATIONS IN AIR POLLUTION MODELING

All constituents of the atmosphere - whether these be of natural or artificial origin - undergo continual transformations which alter their physical, chemical and nuclear structures. Because of the formidable complexity of the subject it will be discussed in the following on a very general basis.

If the atmosphere is considered as a thermodynamic system it is an open, strongly dynamic one. All kinds of energy and mass transfer take place between the atmosphere and its surroundings, namely the earth and the space where radiation of solar and cosmic origin plays the prominent role. Chemical, as well as nuclear, interactions occur during these transfers to such an extent that the collection of the whole of atmospheric phenomena cannot adequately be studied in an isolated fashion. The atmosphere is, within itself, involved in the similar kinds of interactions. Photochemical and chemical reactions, phase transformations are some of them.

Each process within the atmosphere may be associated with a rate which indicates how fast it proceeds. The rate of a process is affected by a series of interwoven factors such as the temperature, pressure and the water content of the atmosphere, the intensity of solar radiation, the motion of the atmosphere and, furthermore, the existence and the extent of other phenomena. Incidentally, temperature is a very important parameter. In chemical reactions the reaction rate may be doubled by a small temperature change in the order of 10°C. One should expect great variations of form and speed in a physical or chemical process depending on many factors. As a result, for example, the residence time for aerosols vary between days near the ground and years in the stratosphere; or the half life of sulphur dioxide may show a wide variation.

The fact that the product of a previous transformation may play an intermediate or sometimes catalytic role in a new transformation dictates the consideration of almost all phenomena together. In a rigorous treatment one must include all rate processes. Consider, for example, sulphur dioxide. It undergoes various physical and chemical processes whose rates depend on humidity of air, concentration of particulates and hydrocarbons in air, and sunlight. Furthermore, if H_2S is present it undergoes a photochemical reaction to contribute as a source of SO_2. Atomic oxygen, which also reacts with SO_2, is produced by photodissociation of NO_2. Hence, NO_2 and along with it other nitrogen compounds in air enter into the picture. This example alone is indicative of the very complicated nature of the problem.

It would be relatively easy to determine the steady equilibrium composition of the atmosphere at a given set of values of temperature, pressure and radiation intensity. But the system is inherently under nonequilibrium conditions. Rate processes render the problem time dependent. The first step in a quantitative approach should, therefore, be to discriminate very carefully between the significant and the negligible factors and to set up certain limitations in order to seek for a manageable model of the system. Certain results from reaction kinetics, used in a more general sense to encompass all transformations, may be helpful here to reduce the complexity of the problem. For example, very fast and very slow transformations, with characteristic times lying outside of the time domain of interest, may be treated differently. The former types follow very closely the processes of moderate rate, hence, may be assumed to have reached equilibrium. The latter, i.e. very slow processes, may be omitted altogether since they do not contribute sensibly to the concentration of species within the time interval concerned. One of the most important part of the task is certainly to analyze the transformations so as to reveal their true steps, for otherwise the rate determination would be in error. It is then necessary to find, or at least to compare, the rate constants governing each process. Only after that the aforenamed simplifications can be confidently made.

Another complication arises from the fact that the thermodynamic and fluiddynamic parameters do also vary, dependently to some degree on the above processes. Temperature is one of them. It would bring considerable simplification if the transformations are regarded as an independent part of the problem. Because in that case temperature, pressure, velocity, radiation intensity and various other factors could be taken as constant external parameters. This can only be done at the expense of reliability of the results, but otherwise the problem may even be unmanageable. For instance, a photoreaction depends on a certain wavelength of the sun's radiation whose intensity is strongly affected by the concentrations of other substances in various levels of the atmosphere including water in the form of gas or cloud.

In a reasonable first approach the collection of processes should be kept at a minimum by narrowing the interest to the phenomena that take place within the mixing layer of the atmosphere where processes are more likely, and within a relatively short time interval to be significant from the local air pollution standpoint. Very near to the source of pollution the problem is again complicated by the fact that the distribution of species concerned is not sufficiently uniform. The limitations set on time and space should be in conformity. In a long-term tracing of a certain pollutant in the atmosphere it may be necessary to take the processes outside of the mixing layer into account.

It was previously mentioned that all transformations may be regarded as rate processes, a familiar example of which being chemical reaction. Transformation, in this broad sense, is an event whereby certain new substances appear at the expense of the disappearance of an original substance. From this standpoint the physical and chemical transformations are alike. The terminology of chemistry may adequately be used for both kinds.

The chemical equation for a binary reaction suffices to describe most transformations. The transformations that involve implicitly more than two "reactants" may in many cases be split up into a succession of binary transformations if the kinetic mechanism of the process is taken into account. Hence, one can represent the jth transformation by an equation of the form

$$\mu_1^j A_1 + \mu_2^j A_2 \longrightarrow \nu_3^j A_3 + \nu_4^j A_4 + \cdots \quad . \tag{1}$$

Here A_1 is the species whose transformation is in question, A_2 is either another species or energy in the form of light quanta, A_3 , A_4, etc. are the products of the transformation, μ's and ν's are the stoichiometric coefficients. If the transformation is spontaneous, i.e. without the need for an extra agent as in spontaneous dissociation of a molecular gas, then $\mu_2 = 0$. The transformation should be regarded as a sink mechanism for the species on the left and as a source for the others.

After all possible simplifications and reductions there will remain n independent transformations of the above form that are significant for the problem at hand. A's may appear on either side of the equations, i.e. a substance may play the role of a "reactant" in some transformations while it is the product of certain others. Closure is necessary for the set of these n equations. In other words, they should exhaust all transformations which have significant roles in controlling the concentrations of all species included in the system.

Equations (1) do not provide the concentrations of the species involved. They merely indicate the relative quantities of the species entering or leaving the transformation. The rates at which the transformations occur should be obtained from phenomenological rate equations. If c_l denotes the instantaneous concentration of the species A_l then its time rate of change may be found from an expression like

$$\dot{c}_l = \sum_{j=1}^{n} k_j f_j(c_1, c_2, \ldots, c_m). \tag{2}$$

Here k_j is the rate factor (specific reaction velocity constant) for the jth transformation. The form of the functions depends upon the particular transformation. In general, the number of unknown concentrations, m , is greater than the number of equations, M . The deficiency is remedied by reducing the number of unknowns using the stoichiometric factors in each transformation. k_j are functions of temperature. If temperature is to be taken as a variable of the problem then an energy equation for the atmosphere should also be written to determine its temperature. The "heat of reaction" associated with each transformation should appear in this equation either as a heat input or heat loss depending on whether the transformation is exothermic or endothermic. Many transformations involving pollutant components take place in a dilute mixture. It is then possible to neglect the contribution of the "heat of reaction" for those transformations to the overall heat balance of the atmosphere.

The integration of the set of equations (2) will involve the initial concentrations of the species. All sources and sinks external to and independent from the system should also be known and their rates of production or absorption of the corresponding species should be included to the right-hand side of equations (2). It should further be emphasized here that the reliability of the solution depends very strongly on the precision in the knowledge of the rate factors. Once the concentrations have been related to time, they may be combined with the formulation of a given air pollution problem to study the change of pollutant concentrations in space and time.

The preceding discussion can only spotlight certain aspects of the inherently very complex and exceedingly broad subject of physical and chemical transformations in the atmosphere, and the possible ways of approach in order to include them in air pollution work. The task requires, and deserves too, a serious and conscientious effort to be made by workers from a variety of related fields.

Bibliography

1. H.B. Callen, Thermodynamics, Wiley, 1960.

2. I. Prigogine, Thermodynamics of Irreversible Processes, Wiley, 1965.

3. M. Boudart, Kinetics of Chemical Processes, Prentice-Hall, Inc., 1968.

Chapter IX

REPRESENTATION OF GROUND SURFACE EFFECT BY SURFACE SOURCE DISTRIBUTION IN ATMOSPHERIC DIFFUSION OF POLLUTANTS

March, 1971

Suha Selamoglu*

Mechanical Engineering Department
The Middle East Technical University
Ankara, Turkey

*** On assignment to the NATO/CCMS Panel on Modeling by the Turkish Scientific and Technical Research Council**

REPRESENTATION OF GROUND SURFACE EFFECT BY SURFACE SOURCE DISTRIBUTION IN ATMOSPHERIC DIFFUSION OF POLLUTANTS

Introduction

The diffusion of pollutants due to atmospheric turbulence is a complex pheromenon. Empirical and semiempirical models to represent the variation of pollutant concentration in space and time have been proposed. The most widely accepted of all is the Gaussian model which suits best to analytical work.

The Gaussian model is the exact solution of the linear diffusion problem which may be one-, two-, or three-dimensional. However, the analogy between linear diffusion and nonlinear turbulence is not very intimate. In order to maintain simplicity in analytical work one is forced to make assumptions which do not correspond to the real physical situation.

Starting with the triaxial Gaussian puff formula, these points are discussed in the following. The interest is then focused on how to deal with an impenetrable plane boundary. A new method is developed and compared with the conventional method of image.

"Gaussian puff" formula

The analogy between turbulent mixing and molecular diffusion is partly real, partly artificial. The most important points to be aware of are: (1) the difference in scale (i.e., macroscopic mixing versus microscopic diffusion) and (2) the dependence of mixing on the scale of turbulence, hence on the dimensions of the field. Nevertheless, if the analogy is accepted then the governing equation of diffusion of a "puff" (sudden, localized release of inert, airborne material into the atmosphere) consisting of a mass q of pollutant released at time $t=0$ at point $P(\bar{\xi}_0)$ is

$$\frac{d\chi}{dt} = \nabla\cdot(\bar{K}\cdot\nabla\chi) \tag{1}$$

with the conditions

$$\left.\begin{aligned} \chi &= 0 \begin{cases} R \to \infty, & t \geqslant 0 \\ R > 0, & t < 0 \end{cases} \\ \int_{v_R} \chi \, dv &= q \begin{cases} R \to \infty, & t \geqslant 0 \\ R \to 0, & t \to 0 \end{cases} \end{aligned}\right\} \qquad \text{(1a)}$$

Here, $\chi(x,y,z,t)$ is the pollutant concentration, $\bar{\bar{K}}$ is diffusivity tensor, v_R is the sphere of radius R, and $R=|\vec{r}-\vec{\rho}_0|$, $\vec{r}=\vec{r}(x,y,z)$, $\vec{\rho}_0=\vec{\rho}_0(\xi_0,\eta_0,\zeta_0)$.

If there is no convection then $d\chi/dt=\partial\chi/\partial t$. Assuming a homogeneous, infinite atmosphere $\bar{\bar{K}}$ is independent of $\vec{r}$ but it must depend on time since the mixing varies as the dimension of the puff changes. Hence,

$$\frac{\partial \chi}{\partial t} = \left[\bar{\bar{K}}(t)\cdot\nabla\right]\cdot\nabla\chi \,. \qquad (2)$$

Selecting a vertical z-axis $\bar{\bar{K}}(t)$ may be diagonalized with components K_x, K_y, K_z. The only anisotropy to be expected in a calm atmosphere is in K_z; but for later development, where there will be assumed a horizontal wind in x-direction, all three components should be taken to be different. The equation now becomes

$$\frac{\partial \chi}{\partial t} = K_x(t)\frac{\partial^2\chi}{\partial x^2} + K_y(t)\frac{\partial^2\chi}{\partial y^2} + K_z(t)\frac{\partial^2\chi}{\partial z^2}\,, \qquad (3)$$

with the solution

$$\chi(x,y,z,t) = \frac{q}{(2\pi)^{3/2}}\,\frac{\exp\left[-\left(\frac{x-\xi_0}{\sqrt{2}\,\sigma_x}\right)^2-\left(\frac{y-\eta_0}{\sqrt{2}\,\sigma_y}\right)^2-\left(\frac{z-\zeta_0}{\sqrt{2}\,\sigma_z}\right)^2\right]}{\sigma_x(t)\,\sigma_y(t)\,\sigma_z(t)}\,, \qquad (4)$$

where $\sigma(t)$'s are related to $K(t)$'s through the relation

$$K(t) = \frac{d}{dt}\left\{\frac{1}{2}\left[\sigma(t)\right]^2\right\}. \qquad (5)$$

When the atmosphere is in translation as a whole so that point P which is originally located at $\vec{\rho}_0(\xi_0,\eta_0,\zeta_0)$ moves, on the average, along a curve $\vec{\rho}(t)=\vec{\rho}\left[\xi(t),\eta(t),\zeta(t)\right]$, the solution may then be written as [1]

$$\chi(x,y,z,t) = \frac{q}{(2\pi)^{3/2}}\,\frac{\exp\left\{-\left[\frac{x-\xi(t)}{\sqrt{2}\,\sigma_x(t)}\right]^2-\left[\frac{y-\eta(t)}{\sqrt{2}\,\sigma_y(t)}\right]^2-\left[\frac{z-\zeta(t)}{\sqrt{2}\,\sigma_z(t)}\right]^2\right\}}{\sigma_x(t)\,\sigma_y(t)\,\sigma_z(t)}\,. \qquad (6)$$

The case of continuous emission from a fixed point, which may be chosen without loss of generality as the origin of the coordinate axes, at a rate $q(t)$ per unit time may be treated approximately by integrating (6) written for infinitesimal puffs. The approximation is due to the fact that the trajectory $\vec{\rho}(t)$ is not the same for the entire atmosphere. Hence the concentration due to a source which continuously emits starting at $t=-\infty$ and up to the present time t is

$$\chi_c(x,y,z,t)=\int_{-\infty}^{t}\frac{q(\tau)d\tau}{(2\pi)^{3/2}}\;\frac{\exp\left\{-\left[\frac{x-\xi(t-\tau)}{\sqrt{2}\sigma_x(t-\tau)}\right]^2-\left[\frac{y-\eta(t-\tau)}{\sqrt{2}\sigma_y(t-\tau)}\right]^2-\left[\frac{z-\zeta(t-\tau)}{\sqrt{2}\sigma_z(t-\tau)}\right]^2\right\}}{\sigma_x(\tau)\,\sigma_y(\tau)\,\sigma_z(\tau)}, \quad (7)$$

or, by an obvious transformation of the dummy variable, it is

$$\chi_c(x,y,z,t)=\int_{0}^{\infty}\frac{q(t-\tau)d\tau}{(2\pi)^{3/2}}\;\frac{\exp\left\{-\left[\frac{x-\xi(\tau)}{\sqrt{2}\sigma_x(\tau)}\right]^2-\left[\frac{y-\eta(\tau)}{\sqrt{2}\sigma_y(\tau)}\right]^2-\left[\frac{z-\zeta(\tau)}{\sqrt{2}\sigma_z(\tau)}\right]^2\right\}}{\sigma_x(\tau)\sigma_y(\tau)\sigma_z(\tau)}. \quad (8)$$

Clearly, the concentration distribution (8) due to a continuous source is not Gaussian. But if the diffusion in x-direction is neglected it may be put into a biaxial Gaussian form by a limiting process as $\sigma_x(\tau)$ tends to zero [1]. Solving τ from $\xi(\tau)$ so that

$$\tau=\tau(\xi)\ ,\ d\tau=\frac{d\xi}{\xi'(\tau)} \quad (9)$$

one obtains

$$\lim_{\sigma_x\to 0}\frac{\exp\left\{-\left[\frac{x-\xi}{\sqrt{2}\sigma_x[\tau(\xi)]}\right]^2\right\}}{(2\pi)^{1/2}\;\sigma_x[\tau(\xi)]}=\delta(x-\xi) \quad (10)$$

where δ denotes the Dirac's "delta function". Thus the integral operation (8) simply effects the substitution $\xi=x$ in the integrand:

$$\lim_{\sigma_x\to 0}\chi_c(x,y,z,t)=\frac{q[t-\tau(x)]}{2\pi\;\xi'[\tau(x)]}\;\frac{\exp\left\{-\left(\frac{y-\eta[\tau(x)]}{\sqrt{2}\sigma_y[\tau(x)]}\right)^2-\left(\frac{z-\zeta[\tau(x)]}{\sqrt{2}\sigma_z[\tau(x)]}\right)^2\right\}}{\sigma_y[\tau(x)]\;\sigma_z[\tau(x)]}. \quad (11)$$

The last expression yields the conventional biaxial Gaussian distribution

$$\chi_0(x,y,z,t)=\frac{Q}{2\pi u\,\sigma_y(x)\sigma_z(x)}\;\exp\left\{-\left[\frac{y}{\sqrt{2}\sigma_y(x)}\right]^2-\left[\frac{z-H}{\sqrt{2}\sigma_z(x)}\right]^2\right\} \quad (12)$$

with the following assumptions:

$$\begin{aligned} q\left[t-\tau(x)\right] &= Q = \text{const.} \\ \xi'\left[\tau(x)\right] &= u = \text{const. (wind velocity)} \\ \zeta\left[\tau(x)\right] &= H = \text{const. (effective stack height)} \\ \eta\left[\tau(x)\right] &= 0 \end{aligned} \tag{13}$$

The assumption $\sigma_x(\tau)\to 0$ may be justified only for sufficiently large τ , or sufficiently far downwind from the source, since in this case $\sigma_x[\tau(x)] \ll x$ and the definition in measuring the x- coordinate may be sacrificed up to a small relative amount of the order of σ_x/x. However, near the source the assumption cannot be justified. On the other hand, the assumptions $\eta=0$, $\zeta=H$, $\xi'=u$ amount to saying that the wind has a constant direction parallel to x-axis and has constant magnitude.

The effect of ground surface

When there is an impermeable, nonabsorbing, solid, infinite, plane boundary at $z=0$ the linear diffusion equation (3) is satisfied by adding the mirror image of the source relative to the boundary. There are, however, certain difficulties in accepting this method.

1. The actual problem is nonlinear; superposition does not hold.

2. The trajectory of the center of the puff determined by $\xi(\tau)$, $\eta(\tau)$, $\zeta(\tau)$ are altered by the existence of the boundary.

3. Apart from the deviations -due to nonlinearity- of the concentration from the Gaussian distribution (11) or (12), the combination of two identical sources $2H$ apart along z-axis is not physically representative of the actual phenomenon. The diffusion is predominantly due to turbulence in the air. The velocity of the air should vanish at the boundary. Whereas, in the method of image the velocity is also reflected at the boundary. In the following, a new method to account for the boundary effect is developed. Although it is also based on superposition, the effect of the ground surface is considered from a more realistic point of view.

The quantity of pollutant that reached the ground surface may be thought of as trapped within the roughness elements and then released as if emitted from a new source which is distributed on the ground surface. The strength of this fictitious surface source, which is supposed to emit symmetrically with respect to $z=0$, should then be taken twice the net flux of pollutant that would cross $z=0$ plane if there were no physical boundary there.

Determination of fictitious source distribution

The flux of pollutant is due primarily to turbulent diffusion and convection since the molecular diffusion is negligible. Denoting the flux vector by $\vec{F}(f_x,f_y,f_z)$ and the velocity vector by $\vec{V}(u,v,w)$ one can write

$$\vec{F} = \chi_0 \vec{V} - \bar{\bar{K}} \cdot \nabla \chi_0 \tag{14}$$

where $\chi_0(x,y,z,t)$ is the pollutant concentration (density) due to the given source in an unbounded atmosphere, i.e., without the effect of the ground surface.

$\vec{F}$ is consistent with the continuity equation with convection

$$\frac{\partial \chi_0}{\partial t} = -\nabla\cdot\vec{F} = -\vec{V}\cdot\nabla\chi_0 - \chi_0 \nabla\cdot\vec{V} + \nabla\cdot(\bar{\bar{K}}\cdot\nabla\chi_0), \tag{15}$$

or, since $\nabla\cdot\vec{V}=0$ (incompressible air flow),

$$\frac{d\chi_0}{dt} = \frac{\partial\chi_0}{\partial t} + \vec{V}\cdot\nabla\chi_0 = \nabla\cdot(\bar{\bar{K}}\cdot\nabla\chi_0) \tag{16}$$

which is the starting equation, (1).

The strength of the fictitious source distribution on the ground surface will then be

$$\frac{1}{2}q(x,y) = -f_z(x,y,0) = \left[-\chi_0 w + K_z \frac{\partial \chi_0}{\partial z}\right]_{z=0},$$
$$q(x,y) = 2K_z\left(\frac{\partial\chi_0}{\partial z}\right)_{z=0} \tag{17}$$

for K_z is a function of z only and $w=0$ for $z=0$.

(17) is generally valid for any concentration function χ_0 and diffusion constant K_z. Consider now a steady, biaxial Gaussian distribution due to a point source of strength Q_p at

point $(0,0,H)$. Then,

$$\chi_{p_0}(x,y,z)=\frac{Q_p}{2\pi\, u(x)\sigma_y(x)\sigma_z(x)}\, exp\left\{-\left[\frac{y}{\sqrt{2}\sigma_y(x)}\right]^2-\left[\frac{z-H}{\sqrt{2}\sigma_z(x)}\right]^2\right\}. \qquad (18)$$

By the use of relation (5) and noting that $\frac{d\sigma(t)}{dt}=u(x)\frac{d\sigma(x)}{dx}$,

$$K_z(x)=u(x)\sigma_z'(x)\sigma_z(x), \qquad (19)$$

and finally,

$$q_p(x,y)=\frac{Q_p H\sigma_z'(x)}{\pi\sigma_y(x)[\sigma_z(x)]^2}\, exp\left\{-\left[\frac{y}{\sqrt{2}\sigma_y(x)}\right]^2-\left[\frac{H}{\sqrt{2}\sigma_z(x)}\right]^2\right\},\ x\geqslant 0. \qquad (20)$$

In case of a line source along $x=0$, $z=H$ of strength Q_L

$$\chi_{L_0}(x,z)=\frac{Q_L}{\sqrt{2\pi}\, u(x)\sigma_z(x)}\, exp\left\{-\left[\frac{z-H}{\sqrt{2}\sigma_z(x)}\right]^2\right\}, \qquad (21)$$

$$q_L(x)=\sqrt{\frac{2}{\pi}}\,\frac{Q_L H\sigma_z'(x)}{[\sigma_z(x)]^2}\, exp\left\{-\left[\frac{H}{\sqrt{2}\sigma_z(x)}\right]^2\right\},\ x\geqslant 0. \qquad (22)$$

Both q_p and q_L are defined for nonnegative x. They vanish when $x\leqslant 0$ since q_y, σ_z vanish for $x\leqslant 0$.

Pollutant concentration

The concentrations $\chi_{p_1}(x,y,z)$, $\chi_{L_1}(x,z)$ due to $q_p(x,y)$, $q_L(x)$, respectively, will be found by superposition. Assuming that Gauss distribution is valid also for the diffusion of pollutants emitted from the ground surface one can write in case of a point source (see Fig. 1)

$$\chi_{p_1}(x,y,z)=\int_0^x d\xi\int_{-\infty}^{\infty}\frac{q_p(\xi,\eta)\,d\eta}{2\pi u(x)\sigma_y(x-\xi)\sigma_z(x-\xi)}\, exp\left\{-\left[\frac{y-\eta}{\sqrt{2}\sigma_y(x-\xi)}\right]^2-\left[\frac{z}{\sqrt{2}\sigma_z(x-\xi)}\right]^2\right\}, \qquad (23)$$

and, in case of a line source,

$$\chi_{L_1}(x,z)=\int_0^x\frac{q_L(\xi)\,d\xi}{\sqrt{2\pi}\,u(x)\sigma_z(x-\xi)}\, exp\left\{-\left[\frac{z}{\sqrt{2}\sigma_z(x-\xi)}\right]^2\right\}. \qquad (24)$$

Inserting the explicit expressions for q_p, q_L from (20), (22) one obtains, for a point source at $(0,0,H)$,

$$\chi_{p_1}(x,y,z)=\frac{Q_p H}{2\pi^2 u(x)}\int_0^x\frac{[\sigma_z'(\xi)/\sigma_z(\xi)]\,d\xi}{\sigma_y(\xi)\sigma_y(x-\xi)\sigma_z(x)\sigma_z(x-\xi)}\ \cdot$$

$$\cdot\, exp\left\{-\left[\frac{H}{\sqrt{2}\sigma_z(\xi)}\right]^2-\left[\frac{z}{\sqrt{2}\sigma_z(x-\xi)}\right]^2\right\}\left\{\int_{-\infty}^{\infty} exp\left\{-\left[\frac{\eta}{\sqrt{2}\sigma_y(\xi)}\right]^2-\left[\frac{y-\eta}{\sqrt{2}\sigma_y(x-\xi)}\right]^2\right\}d\eta\right\}. \qquad (25)$$

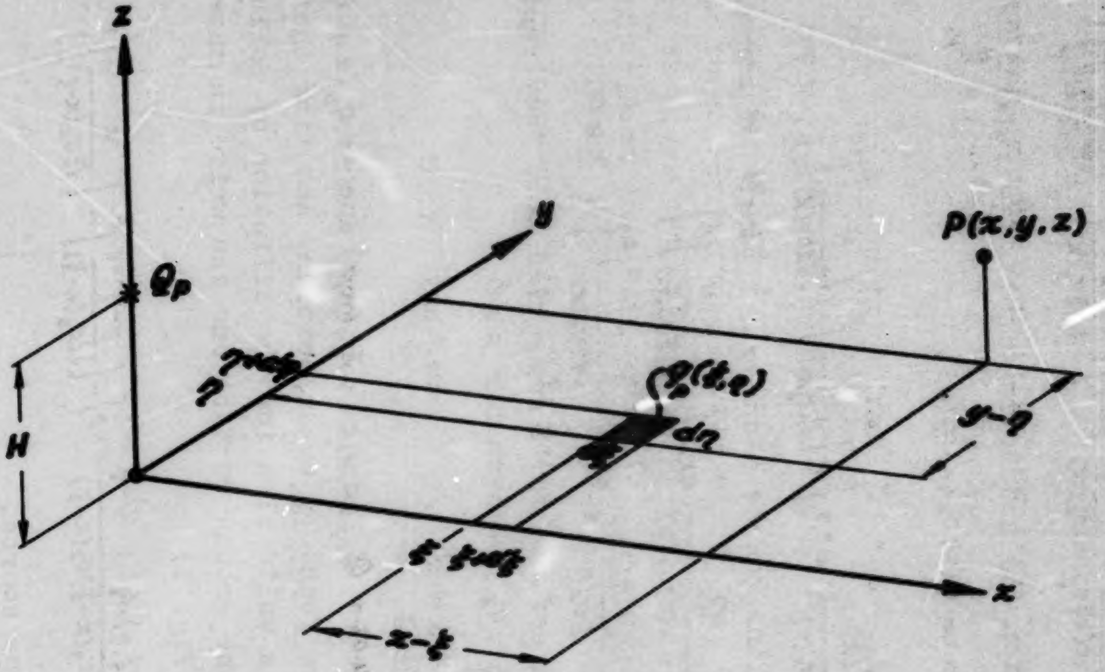
z
Q_p
H
η
η+dη
y
P(x,y,z)
Q_p(ξ,η)
dη
dξ
y−η
ξ
ξ+dξ
x−ξ
x

Figure. 1

Coordinate Layout

and, for a line source along $x=0$, $z=H$,

$$\chi_{L1}(x,z)=\frac{Q_L H}{\pi u(x)}\int_0^x \frac{[\sigma_z'(\xi)/\sigma_z(\xi)]\,d\xi}{\sigma_z(\xi)\,\sigma_z(x-\xi)}\exp\left\{-\left[\frac{H}{\sqrt{2}\,\sigma_z(\xi)}\right]^2-\left[\frac{z}{\sqrt{2}\,\sigma_z(x-\xi)}\right]^2\right\}\cdot \qquad (26)$$

The actual concentrations taking into account the effect of the ground surface will then be found by adding up χ_{p_0} and χ_{p1} or χ_{L0} and χ_{L1} :

$$\chi_p(x,y,z)=\chi_{p_0}(x,y,z)+\chi_{p1}(x,y,z) \text{(point source)} , \qquad (27)$$

$$\chi_L(x,z)=\chi_{L0}(x,z)+\chi_{L1}(x,z) \quad \text{(line source)} . \qquad (28)$$

One might think that the method just described could be repeated in order to seek for a better representation of the nonlinear behavior of the problem. However, the substitution of χ for χ_0 in expression (17) gives the same result since $(\partial\chi_{p1}/\partial z)_{z=0}=0$, $(\partial\chi_{L1}/\partial z)_{z=0}=0$.

It can be shown that χ_p and χ_L satisfy the continuity requirements

$$\int_0^\infty dz\int_{-\infty}^\infty \chi_p\, u\, dy=Q_p \ , \qquad \text{for any} \quad x\geq 0 \qquad (30)$$

$$\int_0^\infty \chi_L\, u\, dz=Q_L \ , \qquad \text{for any} \quad x\geq 0 \qquad (31)$$

Applying the divergence theorem to $\nabla\cdot\vec{F}$ within a volume defined by $0\leq\xi\leq x$, $-\infty\leq\eta\leq\infty$, $\zeta\geq 0$, and noting that $\nabla\cdot\vec{F}=0$ at steady state one obtains

$$-\int_0^\infty d\zeta\int_{-\infty}^\infty f_x(0,\eta,\zeta)\,d\eta-\int_0^x d\xi\int_{-\infty}^\infty f_z(\xi,\eta,0)\,d\eta+\int_0^\infty d\zeta\int_{-\infty}^\infty f_x(x,\eta,\zeta)\,d\eta=0. \qquad (32)$$

The contribution of the closing surfaces at $\eta=\pm\infty$ and $\zeta=\infty$ are zero since f_y , f_z vanish exponentially at infinity. On the other hand,

$$\int_0^\infty d\zeta\int_{-\infty}^\infty f_x(0,\eta,\zeta)\,d\eta=Q_p \qquad (33)$$

and from (14) for $K_x=0$,

$$f_x(x,\eta,\zeta)=\chi_{p_0}(x,\eta,\zeta)\,u(x)\,. \qquad (34)$$

It can be seen further that

$$\int_0^\infty d\zeta \int_{-\infty}^{\infty} \chi_{p_1}(x,\eta,\zeta)\, u(x)\, d\eta = \frac{1}{2}\int_0^x d\xi \int_{-\infty}^{\infty} q_p(\xi,\eta)\, d\eta = -\int_0^x d\xi \int_{-\infty}^{\infty} f_z(\xi,\eta,0)\, d\eta . \quad (35)$$

Making use of (33), (34), (35) in (32) one finally arrives at

$$\int_0^\infty d\zeta \int_{-\infty}^{\infty} [\chi_{p_0}(x,\eta,\zeta) + \chi_{p_1}(x,\eta,\zeta)]\, u(x)\, d\eta = Q_p \quad (36)$$

which is exactly (30).

Numerical results

In order to compare the method described above and the conventional image source method computer use was necessary. In the calculations five stability categories were considered in accordance with the Pasquill-Gifford definition (M = 1, 2, 3, 4, 5 corresponding to categories A, B, C, D, E)[2]. σ_y and σ_z were calculated from simple exponential expressions of the general form

$$\sigma(x) = a x^b + c \quad (37)$$

where x and σ are in meters and the values of a, b and c were taken from Table 1 (see Ref. [3]).

Three effective stack heights were chosen : 10m, 30m and 100m. The pollutant concentrations were calculated along x-axis for simplicity in the calculations. In the case of a point source

$$\frac{u}{Q_p}\chi_{p_0}(x,0,0) = \frac{\exp\left\{-\left[\frac{H}{\sqrt{2}\sigma_z(x)}\right]^2\right\}}{2\pi\sigma_y(x)\sigma_z(x)} , \quad (38)$$

$$\frac{u}{Q_p}\chi_{p_1}(x,0,0) = \frac{H}{2\pi^2}\int_0^x \frac{[\sigma_z'(\xi)/\sigma_z(\xi)]\exp\left\{-\left[\frac{H}{\sqrt{2}\sigma_z(x)}\right]^2\right\}}{\sigma_y(\xi)\sigma_y(x-\xi)\sigma_z(\xi)\sigma_z(x-\xi)} \cdot$$

$$\cdot\left(\int_{-\infty}^{\infty} \exp\left\{-\left[\frac{\eta}{\sqrt{2}\sigma_y(\xi)}\right]^2 - \left[\frac{\eta}{\sqrt{2}\sigma_y(x-\xi)}\right]^2\right\} d\eta\right) d\xi . \quad (39)$$

The second integral in (39) yields

$$\int_{-\infty}^{\infty} \exp\left\{-\left[\frac{\eta}{\sqrt{2}\sigma_y(\xi)}\right]^2 - \left[\frac{\eta}{\sqrt{2}\sigma_y(x-\xi)}\right]^2\right\} d\eta = \sqrt{\frac{2\pi}{[\sigma_y(\xi)]^2 + [\sigma_y(x-\xi)]^2}}\, \sigma_y(x)\sigma_y(x-\xi) . \quad (40)$$

Table 1

Constants in the expressions for σ_y and σ_z

M		$\sigma_z = a.x^b+c$ (*)			$\sigma_y = a.x^b+c$ (**)
		$x \leqslant 100$	$100 \leqslant x \leqslant 1000$	$1000 \leqslant x$	
1	a	0.174	0.001	0.001	0.385
	b	0.936	1.890	1.890	0.89
	c	0.00	9.60	9.60	0.00
2	a	0.143	0.048	0.048	0.284
	b	0.922	1.110	1.110	0.90
	c	0.00	2.00	2.00	0.00
3	a	0.123	0.119	0.119	0.187
	b	0.905	0.915	0.915	0.915
	c	0.00	0.00	0.00	0.00
4	a	0.080	0.187	2.610	0.123
	b	0.881	0.755	0.450	0.915
	c	0.00	-1.40	-25.50	0.00
5	a	0.060	0.135	52.600	0.092
	b	0.854	0.745	0.150	0.915
	c	0.00	-1.10	-126.00	0.00

(*) The values were taken from Ref. [3].

(**) Determined by best fit by eye neglecting curvature in the log-log plot.

Thus

$$\frac{u}{Q_p}\chi_{p_1}(x,0,0)=\frac{H}{\pi\sqrt{2\pi}}\int_0^x \frac{[\sigma_z'(\xi)/\sigma_z(\xi)]\exp\left\{-\left[\frac{H}{\sqrt{2}\sigma_z(\xi)}\right]^2\right\}}{\sqrt{[\sigma_y(\xi)]^2+[\sigma_y(x-\xi)]^2}\cdot\sigma_z(\xi)\sigma_z(x-\xi)}\,d\xi \qquad (41)$$

The total concentrations were determined by summing χ_{p_0} and χ_{p_1} while the image method gives, by symmetry,

$$\chi_{p_{Im}}(x,y,0)=2\chi_{p_0}(x,y,0). \qquad (42)$$

Line source, on the other hand, gives simpler expressions.

$$\frac{u}{Q_L}\chi_{L_0}(x,0)=\frac{1}{\sqrt{2\pi}\,\sigma_z(x)}\exp\left\{-\left[\frac{H}{\sqrt{2}\sigma_z(x)}\right]^2\right\}, \qquad (43)$$

$$\frac{u}{Q_L}\chi_{L_1}(x,0)=\frac{H}{\pi}\int_0^x\frac{[\sigma_z'(\xi)/\sigma_z(\xi)]}{\sigma_z(\xi)\sigma_z(x-\xi)}\exp\left\{-\left[\frac{H}{\sqrt{2}\sigma_z(\xi)}\right]^2\right\}d\xi. \qquad (44)$$

Again, $\chi_L(x,0)$ was obtained by adding (43) to (44). The image method yields

$$\chi_{L_{Im}}(x,0)=2\chi_{L_0}(x,0). \qquad (45)$$

Since the convergence of the integrals at their upper limits is poor for computer calculation, they were truncated near the upper limit and the truncated portion was approximated by assuming $\sigma_y(\xi)$ and $\sigma_z(\xi)$ to be constant. The intervals of integration by the trapezoidal rule were arranged as a geometrical sequence in decreasing steps toward the source.

The results are collected in Figures 2 to 6 each for a different stability category.

Discussion

As the figures clearly show the two methods yield markedly different results although their general trends are essentially the same. The distributed source method gives consistently larger concentrations than the image method. This result is natural since the new method does not permit a vertical velocity component for the diffusing pollutant so that the diffusion in the vertical is slowed down.

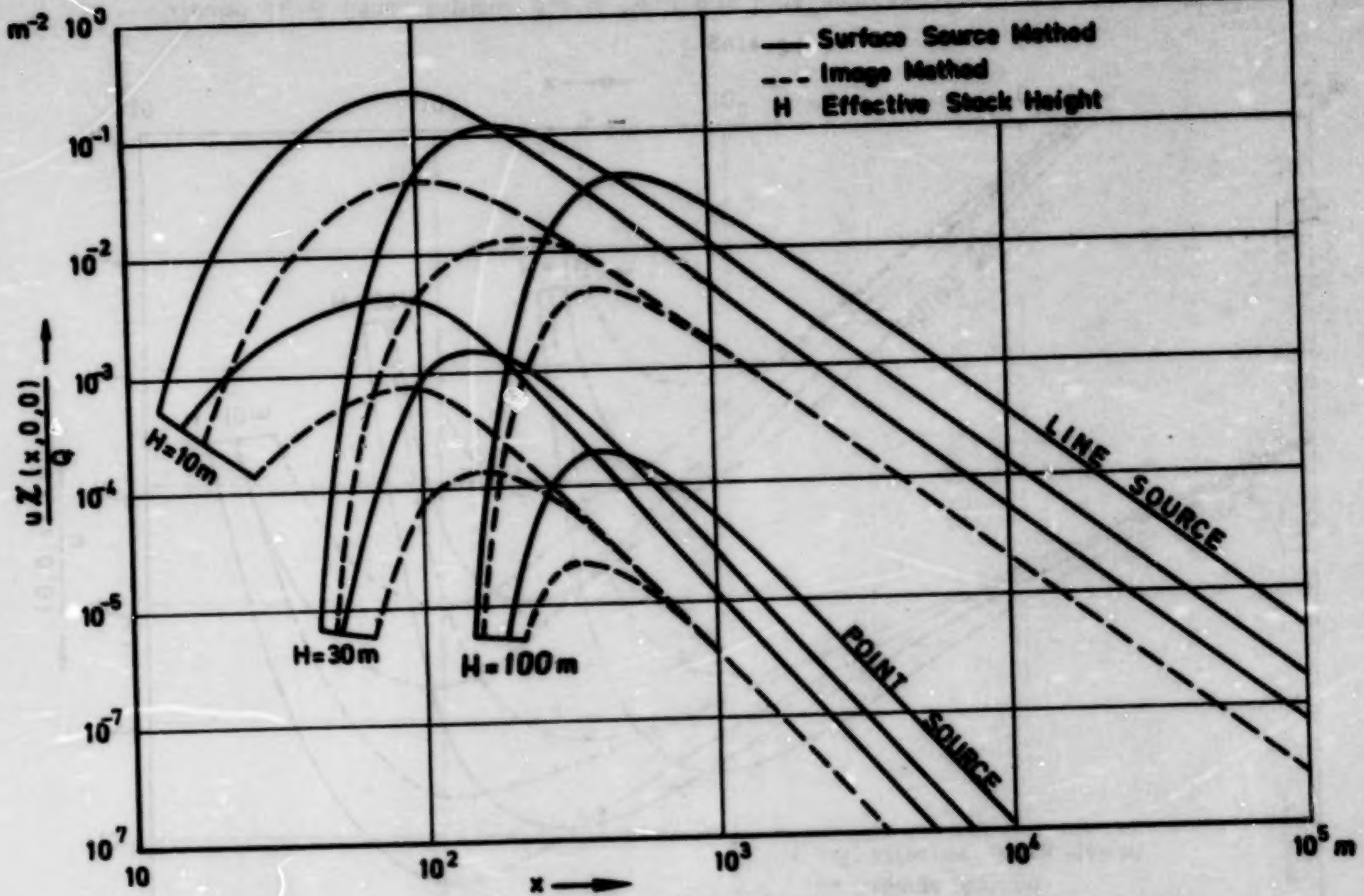

Figure 2

Ground Level Concentrations due to Point and Line Sources–Stability Category M = 1

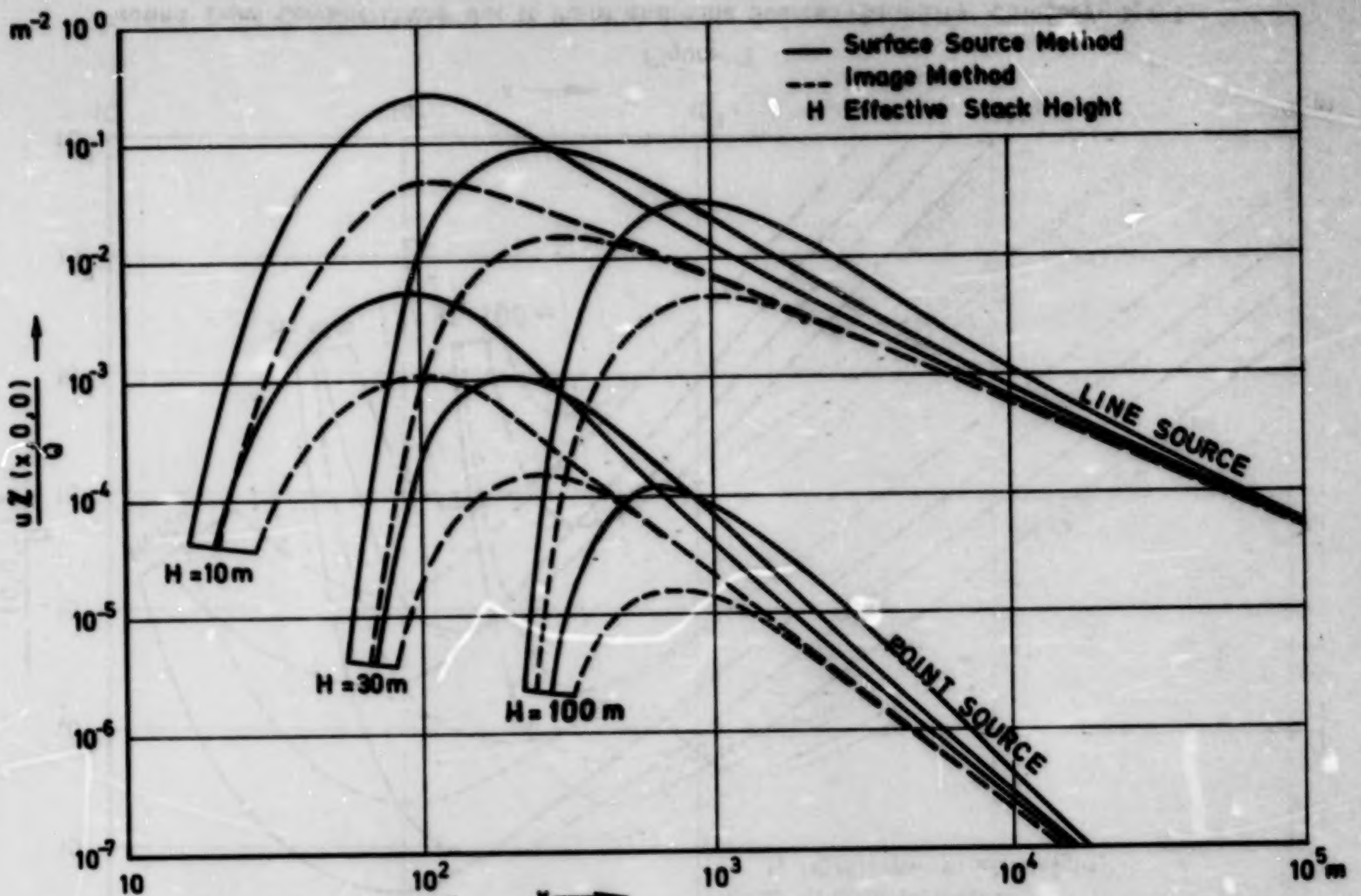

Figure 3

Ground Level Concentrations due to Point and Line Sources—Stability Category M = 2

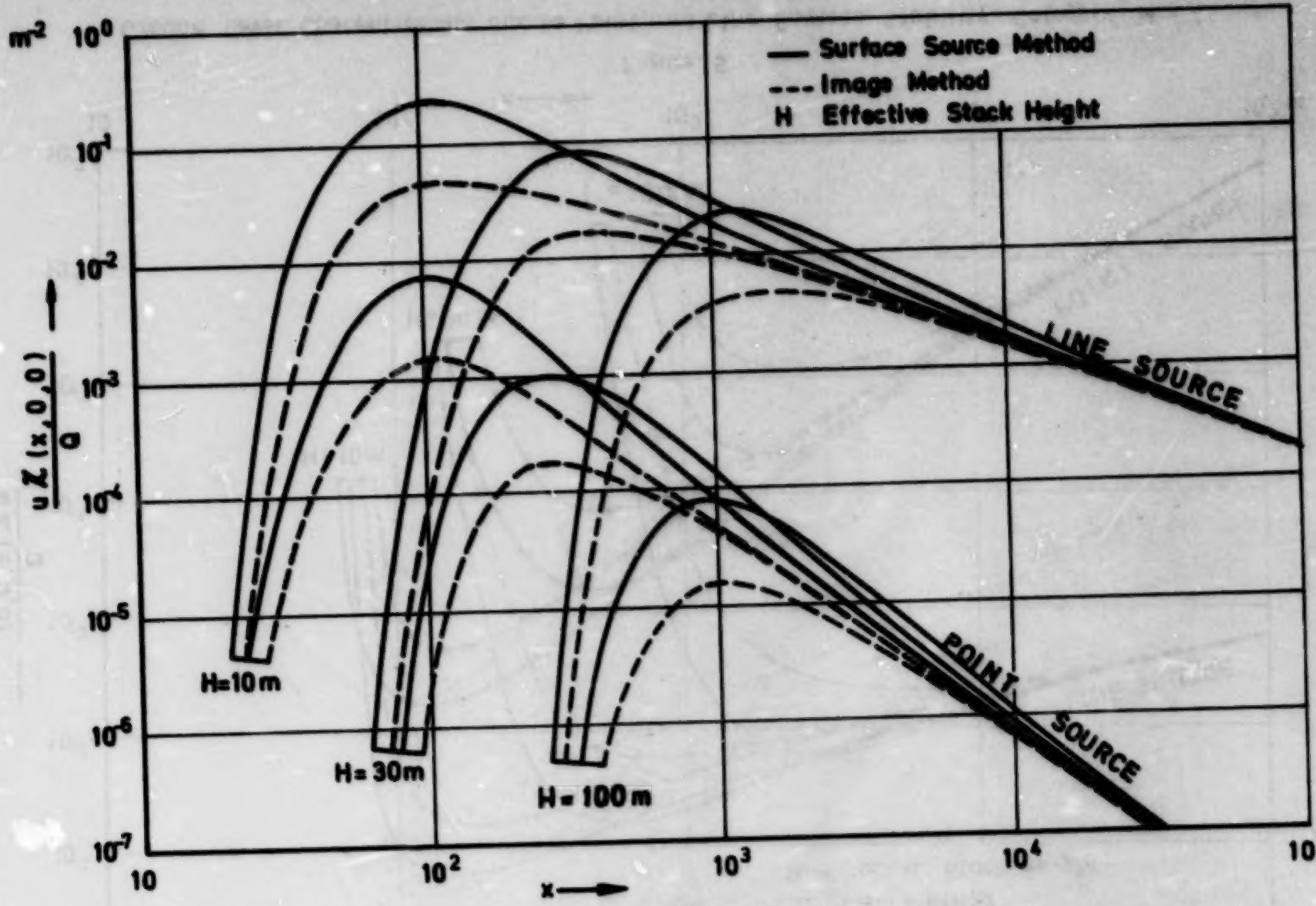

Figure 4

Ground Level Concentrations due to Point and Line Sources–Stability Category M = 3

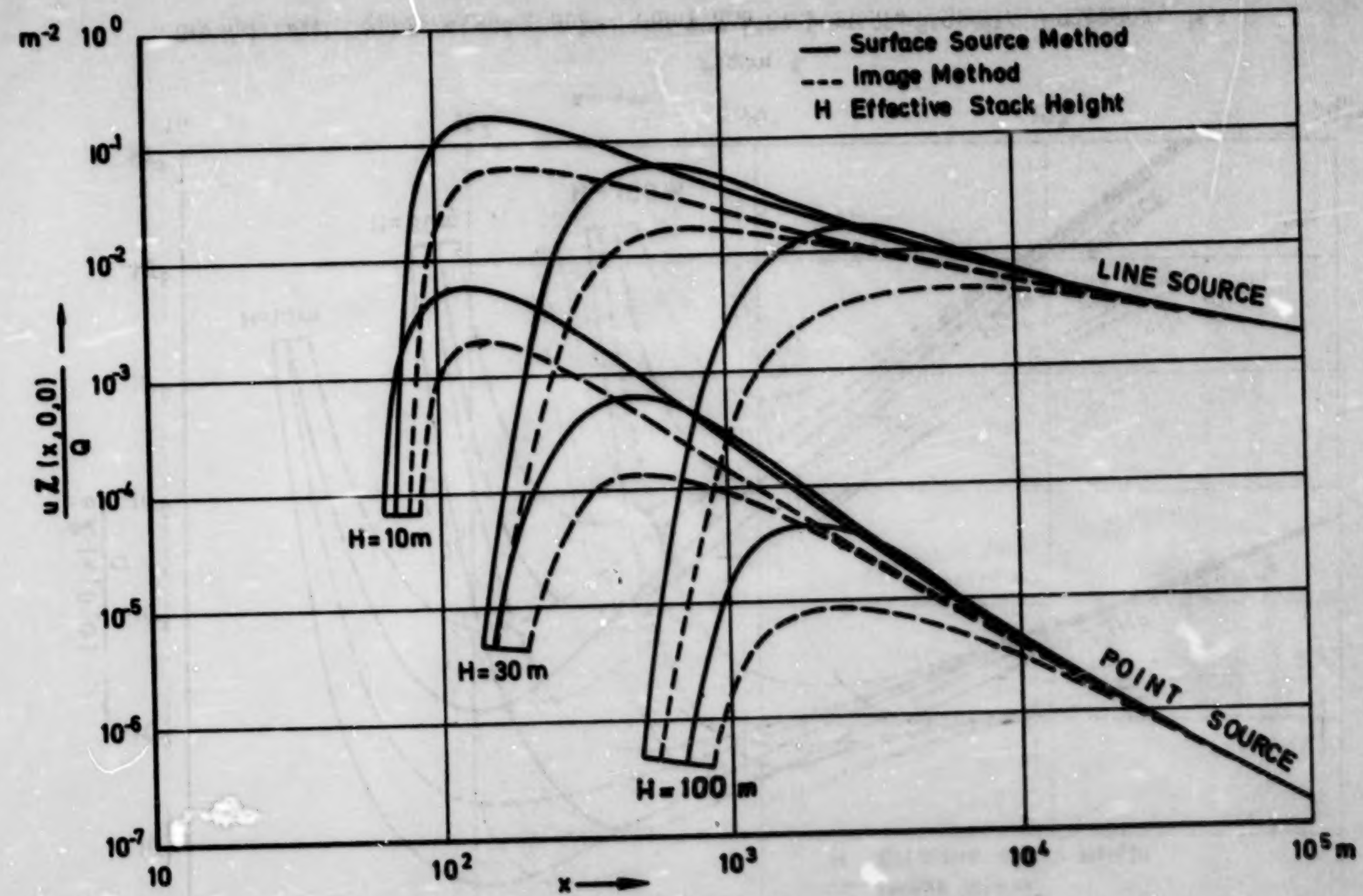

Figure 5

Ground Level Concentrations due to Point and Line Sources–Stability Category M = 4

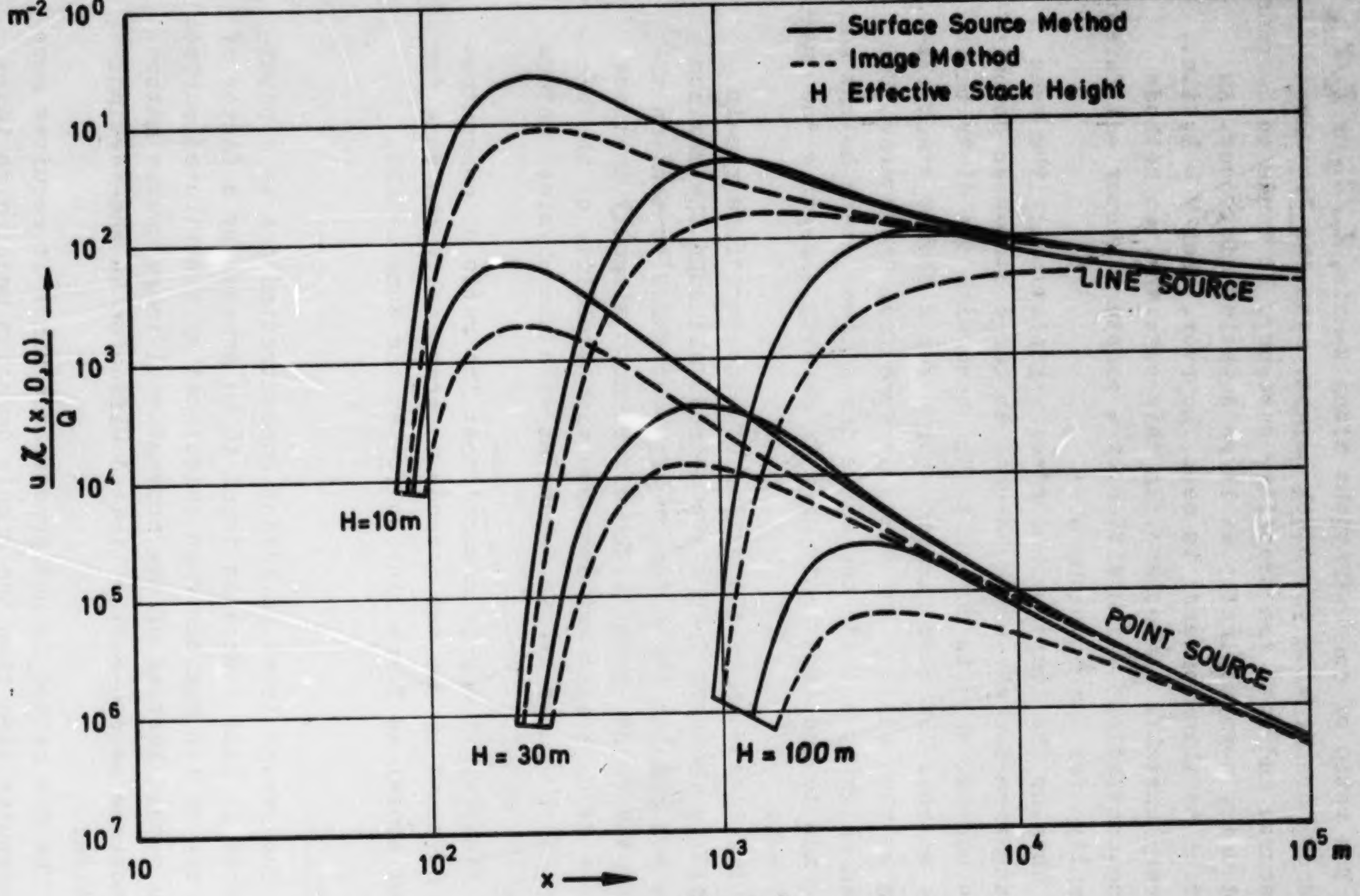

Figure 6

Ground Level Concentrations due to Point and Line Sources–Stability Category M = 5

The ratio of concentrations along x-axis, χ_p/χ_{pIm} or χ_L/χ_{LIm} vary considerably with the stack height, with the distance from source and with the stability category. It tends to decrease toward unity asymptotically at large downwind distances. An exception to this tendency is seen, however, when M = 1, i.e., in a very unstable atmosphere. In this case the two methods give concentrations which differ by a constant factor -different from unity- for large values of x.

Whereas the image method gives asymptotically the same concentration for all stack heights at large distances downwind of the source, this is not quite the case with the distributed source method. The concentration curve for a higher stack elevation is much smaller for some distance from the source. But it then slightly exceeds the curve for a lower stack height and then tends to the same limit as x increases, excepting the case with M = 1.

The locations of the maxima of concentrations remain essentially the same in the two methods although the maximum values are greater (by a factor of about three to ten) in the distributed source method. The differences slightly increase with the stack height and decrease with stability of the atmosphere. Both trends are in agreement with the physical nature of the new model.

Finally, it may be noticed that the ratio of concentrations obtained by the two methods is practically the same for a point source as for a line source at the same height.

Conclusion

The ground level pollutant concentration due to a point or crosswind line source is found to be greater by a factor of up to ten at its maximum when calculated by distributed surface source method instead of the conventional image source method. The increase is due to the limited diffusion in the vertical direction.

The new method is not practicable since it requires much more computer time than the simple Gaussian model with image source does. It is of interest, however, in showing that the problem of turbulent diffusion of pollutants in the atmosphere may admit different solutions as the method of approach is varied toward obtaining a more meaningful physical model.

References

[1] H. Fortak, "Bodenimmisionsverteilungen im Lee eines Schornsteins für den Fall beliebiger Formen der Rauchfahnenachse", Institut für theoretische Meteorologie, der freien Universität Berlin, Berlin, 1969.

[2] F. Pasquill, Atmospheric Diffusion, D. Van Nostrand, New York, 1962.

[3] K. L. Calder, "A Climatological Model for Multiple Source Urban Air Pollution", Report, N. A. P. C. A., September, 1970.

Chapter X

SIMILARITY CRITERIA FOR THE APPLICATION
OF PHYSICAL MODELS
FOR THE STUDY OF AIR POLLUTION METEOROLOGY

William H. Snyder*
Division of Meteorology
National Environmental Research Center
Environmental Protection Agency
Research Triangle Park, North Carolina 27711

For presentation to the Panel on Modeling, NATO/CCMS Pilot Project on Air Pollution, Paris, France, July 26-27, 1971

*On assignment from the National Oceanic and Atmospheric Administration, U.S. Department of Commerce.

ABSTRACT

Similarity criteria for modeling atmospheric flows in air and water are reviewed. It is shown that five nondimensional parameters plus nondimensional boundary conditions must be matched in model and prototype. The neglect of the Rossby number can lead to serious errors in modeling of diffusion in a prototype with a length scale greater than about five kilometers. The Reynolds number, the Peclet number and Reynolds-Schmidt product criteria may be neglected if the model flow is of sufficiently high Reynolds number. The Froude number criterion appears to be the most important. The complete specification of boundary conditions is found to be nebulous, but is discussed in some detail. Both air and water appear to be suitable fluids to use as modeling media.

INTRODUCTION

The present mathematical models of turbulent diffusion in the lower atmospheric layer tend to ignore the fundamental fluid-dynamical processes involved in the dispersion of materials. This results from the memory size of the latest computer being far too small to keep track of the large number of "eddies" in a turbulent flow. Corrsin (1961), in speculating on the future role of large computing machines in following the consequences of the Navier-Stokes equations under random initial conditions, estimated a required memory size of $\sim 10^{13}$ bits, then asked if "the foregoing estimate is enough to suggest the use of analog instead of digital computation; in particular, how about an analog consisting of a _tank of water_?" (emphasis added). In spite of the tremendous advances in computer memories in the past decade, Corrsin's remark is still appropriate.

Physical models of various aspects of atmospheric motion have been described in the literature many times. The necessity of studying the dispersion of atmospheric pollutants, especially in urban areas, has further directed thoughts of meteorologists towards physical modeling.

Many factors affect the dispersion of pollutants in the atmosphere; thermal effects, the topography, the rotation of the earth, etc. Physical model studies are desirable mostly because essential variables can be controlled at will, and the time and expense involved are greatly reduced from that required in full scale studies. It is not usual, however, for all the factors influencing atmospheric dispersion to be included in a model. Normally, the similarity criteria employed are conflicting in some sense; it may be necessary to model one physical process at the expense of not being able to model another.

This paper reviews the similarity criteria on physical modeling relevant to air pollution meteorology and evaluates the usefulness of such models from both scientific and engineering viewpoints.* Air and water are most commonly used as media for the simulation of atmospheric motions. The potentials of both of these fluids are reviewed here.

For correct modeling, certain nondimensional parameters in the prototype must be duplicated in the model[1]. Almost invariably, duplication of these nondimensional parameters is impractical or impossible. Hence, a decision must be made as to which parameters are dominant. The less important ones must be ignored. This decision will generally depend upon the scale in which the investigator is interested. For example, when studying the upper air flow above a city, the waffle-like topography may be treated as surface roughness. The heat island effect may be modeled by using a heated plate. If the city is large enough, Coriolis forces may be important. If, however, the interest is in dispersion in the immediate vicinity of buildings, the topography cannot be treated as surface roughness. The heat island effect would require a detailed distribution of heat sources, and Coriolis forces could be ignored because the aerodynamic effects of the flow around the buildings would dominate.

REQUIREMENTS FOR RIGOROUS SIMULATION OF ATMOSPHERIC BOUNDARY LAYER

The equations of motion are the starting point for the similarity analysis. With the earth as a reference frame rotating at an angular velocity Ω, the fluid motion is described by the following equations (Lumley and Panofsky, 1964):

--- Conservation of Momentum

$$\frac{\partial U_i}{\partial t} + \frac{U_j \partial U_i}{\partial x_j} + 2\epsilon_{ijk} U_k \Omega_j = -\frac{1}{\rho_o} \frac{\partial \delta P}{\partial x_i} + \frac{g}{T_o} \delta T \delta_{3i} + \frac{\nu \partial^2 U_i}{\partial x_k \partial x_k} \tag{1}$$

--- Continuity

$$\frac{\partial U_i}{\partial x_i} = 0 \tag{2}$$

--- Energy

$$\frac{\partial \delta T}{\partial t} + \frac{\partial \delta T}{\partial x_i} U_i = \kappa \frac{\partial^2 \delta T}{\partial x_i \partial x_i} \qquad (i = 1, 2, 3) \tag{3}$$

where the x_3 axis is taken vertically upward, U_i is instantaneous velocity, δP and δT are deviations of pressure and temperature from those of a neutral atmosphere, ρ_o and T_o are density and temperature of a neutral atmosphere (function of height), ν is kinematic viscosity, κ is thermal diffusivity, ϵ_{ijk} is the alternating tensor, and δ_{ij} is Kronecker's delta.

The assumptions made in deriving the above equations are:

1) the atmosphere is composed of a perfect gas of constant composition,

2) the deviations of pressure, temperature, and density are small compared with the neutral values,

3) the density is independent of the fluctuating pressure (small Mach number),

4) variations of ν and κ are negligible,

5) the generation of heat through viscous stresses is negligible, and

6) there are no sources of any kind.

The second step in the similarity analysis is to nondimensionalize the equations of motion through the use of appropriate reference quantities. Reference quantities assumed to be supplied through the boundary conditions are: L, length; U_R, velocity; ρ_R, density; δT_R, temperature deviation; and Ω_R, angular velocity. The dimensionless variables are

$$x_i' = \frac{x_i}{L} \qquad U_i' = \frac{U_i}{U_R}$$

$$t' = \frac{U_R}{L} t \qquad \rho' = \frac{\rho_o}{\rho_R}$$

$$\delta P' = \frac{\delta P}{\rho_R U_R^2} \qquad \delta T' = \frac{\delta T}{\delta T_R}$$

$$\Omega_j' = \frac{\Omega_j}{\Omega_R}$$

Using these definitions to nondimensionalize equations (1), (2), and (3) yields

$$\frac{\partial U_i'}{\partial t'} + U_j' \frac{\partial U_i'}{\partial x_j'} + \frac{2}{Ro} \varepsilon_{ijk} U_k' \Omega_j' = -\frac{1}{\rho'} \frac{\partial \delta P'}{\partial x_i'} + \frac{1}{Fr^2} \delta T' \delta_{3i} + \frac{1}{Re} \frac{\partial^2 U_i'}{\partial x_j' \partial x_j'} \qquad (4)$$

$$\frac{\partial U_i'}{\partial x_i'} = 0 \qquad (5)$$

and

$$\frac{\partial \delta T'}{\partial t'} + U_i' \frac{\partial \delta T'}{\partial x_i'} = \frac{1}{Pe} \frac{\partial^2 \delta T'}{\partial x_i' \partial x_i'} \qquad (6)$$

where $Ro \equiv U_R/L\Omega_R$ is the Rossby number,

$Fr \equiv U_R/(gL\delta T_R/T_o)^{1/2}$ is the densimetric Froude number,

$Re \equiv U_R L/\nu$ is the Reynolds number,

and, $Pe \equiv U_R L/\kappa$ is the Peclet number.

Concerning the philosophy of modeling, equations (4), (5), and (6) with appropriate boundary conditions completely determine the flow. The question of uniqueness of solutions of the Navier-Stokes equations is avoided here (see Lumley, 1970). These five equations contain five unknowns, U_1', U_2', U_3', $\delta P'$, and $\delta T'$, so that, in principle, their solutions may be determined. Any two flows within the same general category (i.e., in so far as they are governed by the above equations) will be similar if and only if they are described by identical solutions to the given set of equations (4), (5), and (6). Solutions to this set of equations will be identical if and only if the coefficients Ro, Fr, Re, and Pe, and the nondimensional boundary conditions are identical (Birkhoff, 1950; Batchelor, 1953). The final statement, then, as it applies to physical modeling of atmospheric motions becomes: any atmospheric flow which can be described by equations (4), (5), and (6) may be modeled by any other flow which can also be described by the same set of equations, provided that the Rossby, Froude, Reynolds, and Peclet numbers are identical, and provided that the nondimensional boundary conditions (to be discussed later) are identical.

Equations (4), (5), and (6) as shown apply to both laminar and turbulent flows. It is not necessary to determine a priori whether the flow is laminar or turbulent or to write separate expressions for the two types of flows; the various parameters and boundary conditions will determine whether the flow is laminar or turbulent. Consideration of the turbulent flow equations will not introduce any new dimensionless parameters.

Thus far, only the requirements for similarity of flow patterns have been discussed. The dispersion of a pollutant within the system will now be considered. The contaminant is assumed to be completely passive in the sense that it is without effect on the governing equations.

Prediction of the dispersion of this contaminant in space and time is desired. Since a passive contaminant is specified, its dynamic behavior must be the same as that of the air; hence, the similarity criteria describing its dynamic behavior have already been specified. One additional parameter, however, remains to be specified. This is obtained through nondimensionalization of the molecular diffusion equation:

$$\frac{\partial\chi}{\partial t} + U_i \frac{\partial\chi}{\partial x_i} = \alpha \frac{\partial^2\chi}{\partial x_i \partial x_i} \quad , \tag{7}$$

where χ represents the instantaneous concentration and α is the molecular mass diffusivity. Nondimensionalization of this equation requires $\chi' \equiv \chi/\chi_R$, and yields

$$\frac{\partial\chi'}{\partial t'} + U_i' \frac{\partial\chi'}{\partial x_i'} = \frac{1}{\mathrm{ReSc}} \frac{\partial^2\chi'}{\partial x_i' \partial x_i'} \tag{8}$$

where $Sc \equiv \nu/\alpha$ is the Schmidt number.

To summarize, equations (4), (5), (6), and (8) form a complete set of equations which govern the dispersion of a dynamically passive contaminant in the atmosphere and in a model. If and only if the nondimensional coefficients in these equations and the boundary conditions are identical, the dispersion of the contaminant in a model will be identical to that in the atmosphere.

It is generally impossible to satisfy these criteria when the ratio of the length scales (i.e., prototype to model) is greater than about 10. As an example consider the Reynolds and Froude numbers:

$$Re = \frac{U_R L}{\nu} \quad , \quad Fr = \frac{U_R}{\sqrt{gL\delta T_R/T_o}} \quad .$$

If one models in a wind tunnel, the values of ν and g are identical to values in the atmosphere, and T is roughly the same. Thus, decreasing the length scale by 10 requires an increase of 10 in the velocity to satisfy the Reynolds number criterion. Considering the Froude number, L decreased by 10 and U_R increased by 10 implies that δT must be increased by a factor of 1000, which is, of course, highly impractical. In general, a length scale reduction much greater than 10 is desired.

A factor of 15 in the Reynolds number may be gained by modeling with water as the fluid medium, but then the Peclet number and Reynolds number criteria cannot be satisfied simultaneously. The Peclet number can be written as the product of the Reynolds number and the Prandtl number. Even if the Reynolds number can be matched, the Prandtl number cannot, because it is a fluid property and differs by a factor of 10 between air and water.

Many examples of this type can be shown. All modelers recognize that rigorous modeling with significant reduction of scale is impossible.

THE DIMENSIONLESS PARAMETERS

It may be that, under certain circumstances, some of the criteria may be relaxed. In the first example, if the atmospheric flow were of neutral stability, the Froude number would be infinite. This is easily accomplished by making the model flow isothermal. (The vertical dimension of a typical wind tunnel is small enough that the temperature differences between isothermal and strictly neutral conditions is extremely small. Hence, "neutral" and "isothermal" are used interchangeably when referring to wind tunnel flows.) Hence, both Reynolds number and Froude number criteria may be satisfied simultaneously.

It is instructive now to examine the nondimensional parameters in detail.

THE ROSSBY NUMBER, $U_R/L\Omega_R$

The Rossby number represents the ratio of advective or local accelerations to Coriolis accelerations. Local accelerations may result from unsteadiness or nonuniformities in the velocity field. Coriolis accelerations, of course, result from the fact that the earth rotates. The importance of the Rossby number criterion for modeling of atmospheric diffusion is described as follows.

In the planetary boundary layer, or "Ekman" layer, which extends from the earth's surface to a height of one to two km, the combined effect of the Coriolis acceleration, the pressure gradient, and surface friction cause the wind vector to change direction or spiral with increasing height from the surface. The geostrophic wind is parallel to the isobars, whereas the surface wind blows to the left across the isobars, typically at an angle of 20° to 40°. The maximum rate of change of wind direction with height occurs at the surface.

Imagine a cloud of material released at ground level in an Ekman layer and suppose that the dispersion is of the gradient type, i.e., describable in terms of K-theory. This behavior is illustrated in Figure 1. The surface wind is directly into the paper. The crosswind velocity profile is as shown. The initial cloud (Step 1) being small, is transported mainly by the surface wind. Its size increases mainly by turbulent dispersion (Step 2). At this point, the upper levels of the cloud will be advected in a different direction from that of the surface wind. Hence, the cloud is tilted by the crosswind (Step 3), and the simultaneous turbulent diffusion (Step 4) increases the width of the cloud at ground level over what it would have been by turbulent diffusion alone. In fact, the center of gravity of a slice of the cloud at ground level will not follow the surface wind.

The Coriolis accelerations cause the spiraling wind. The Rossby number describes the relative importance of the Coriolis accelerations when compared with advective, or local, accelerations. Evidently, if the Rossby number is large, Coriolis accelerations are small, so that enhanced dispersion due to directional wind shear may be ignored. Equivalently, a near infinite Rossby number is automatically matched in a model.

To date all wind and water tunnel modelers have assumed the Rossby number to be large and discarded the terms involving it in the equations of

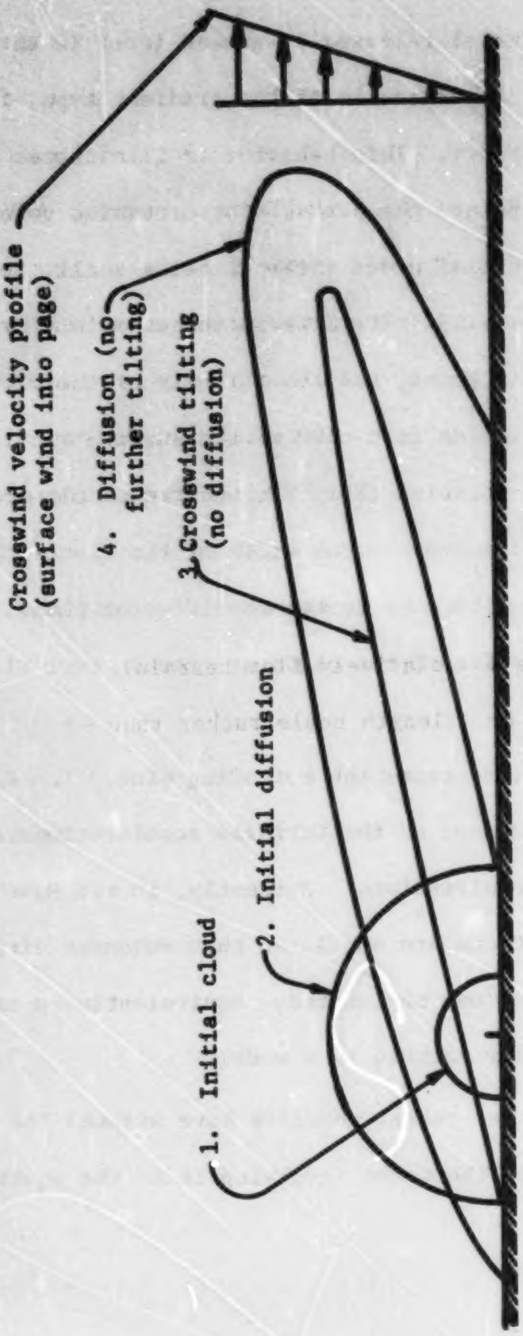
1. Initial cloud
2. Initial diffusion
3. Crosswind tilting (no diffusion)
4. Diffusion (no further tilting)
Crosswind velocity profile (surface wind into page)

Figure 1. Schematic of Diffusion in Ekman Layer

motion or, equivalently, ignored that particular parameter as a criterion for modeling. Cermak, et. al. (1966) made the rather broad statement that, provided the typical length in the horizontal plane is less than 150 kilometers, the Rossby number can generally be eliminated from the requirements for similarity. Hidy (1967) made similar statements. McVehil, et. al. (1967) ignored the Rossby number when modeling atmospheric motions on the scale of one kilometer in the vertical and several tens of kilometers in the horizontal. Ukeguchi, et. al. (1967) claimed that the cut-off was 40 to 50 km. Mery (1969) claimed that the Coriolis force may be neglected if the characteristic length is less than 15 kilometers. The present discussion shows that the cut-off point is on the order of five kilometers for modeling diffusion under appropriate atmospheric conditions (i.e., neutral or stable conditions in relatively flat terrain).

The criterion is based on a length scale rather than on the Rossby number itself because the angular rotation of the earth, Ω_o, is a constant ($Ro = U_R/L\Omega_o$), and the characteristic velocity of the atmospheric flow does not vary by more than an order of magnitude, so that the characteristic length is primarily responsible for determining the Rossby number.

Several papers have examined the effect of crosswind shear on dispersion. Pasquill (1962) measured horizontal spread both in the longitudinal and crosswind directions for medium range dispersion. He was apparently the first to consider the effect of crosswind shear. His data, however, were insufficient to allow firm conclusions to be drawn about the relative importance of turbulence and shear in promoting horizontal spread.

Saffman (1962) was the first to analyze this effect in the atmosphere. He used the classical diffusion equation, applied the concentration - moment method of Aris (1956), and obtained solutions for the longitudinal spread (he did not consider turning of wind with height, although similar considerations are involved). For an unbounded (semi-infinite) flow, ground level source (puff), and linear velocity profile he found $\sigma_x \alpha t^{3/2}$ (σ_x is streamwise puff width; t is time). For a completely unbounded flow, Smith (1965) showed that $\sigma_x \alpha t^{3/2}$.

Since the contribution to the spread from the turbulence alone is $\sigma_x \alpha t^{1/2}$, the shear effect will eventually dominate the dispersion process. These solutions are valid only for constant diffusivity and large times; they do not provide any indication of the early development. Hence, they are of no help in determining at what distance the shear effect becomes dominant.

Tyldesley and Wallington (1965) used a numerical scheme and an analog computer to study the effect of crosswind shear on dispersion. They used an 8-step Ekman spiral except with the surface wind 22 1/2° from the geostrophic wind. They claimed that the 3/2 power law does not apply because the crosswind shear is not constant with height. Their estimates indicate that the wind shear becomes dominant around 4 to 6 kilometers from the source. For much larger distances, the turbulence will again dominate because the shear goes to zero for large heights.

Hogstrom (1964) and Smith (1965) used statistical approaches to the crosswind shear problem. A homogeneous field of turbulence, a mean wind speed which was constant with height, and a crosswind component which varied linearly with height were assumed. They obtained expressions valid for all times of travel, but did not estimate times or distances at which the shear would dominate.

Csanady (1969) attempted to confirm analytically the numerical results of Tyldesley and Wallington. Because of analytical difficulties, he confined his investigation to a slice at ground level of a cloud released from a source at ground level. He found that, indeed, the centroid of the slice at ground level did not follow the surface wind. By the time the cloud occupied 1/3 of the Ekman layer ($\sim$600m) its distance from a line parallel to the surface wind was of order 10 km. The contribution to the spread from the turbulence and from the shear were found to be equal at one kilometer from the source. He estimated that, in the actual atmosphere, the shear effect would overtake the turbulence effect at 3 to 4 kilometers from the source. He shows that for small times, $\sigma_y \alpha t^{1/2}$ (i.e., turbulent diffusion dominates). For intermediate times, $\sigma_y \alpha t^{3/2}$ (i.e., shear-induced diffusion dominates). For large times, $\sigma_y \alpha t^{1/2}$ again, because the cloud height is the same as the Ekman layer depth, and the flow is, in effect, bounded (σ_y is cross-streamwise puff width).

Thus far, no diffusion experiments have been reported that have been specifically designed to examine the relative effects of turbulence and shear, but Pasquill (1969) has recently reexamined two independent studies which contain information of interest in this connection. He looked at Hogstrom's (1964) data on the behavior of smoke puffs released from an elevated source under neutral and stable atmospheric conditions. The data for the crosswind spread show the onset of a more rapid than linear growth at 2.5 kilometers. These data are somewhat misleading because they indicate the total puff width rather than the width at a given level. Hence, they indicate the bodily distortion (tilting) of the puff but do not show directly the enhanced spread at a given level. Pasquill concluded in accounting for this that the enhanced spread at a given level as a result of shear becomes important around 5 kilometers from the source.

In analyzing the Hanford data of Fuquay, Simpson, and Hinds (1964) (continuous ground release of a tracer), Pasquill concluded that the effect on spread at ground level under stable atmospheric conditions appeared to have set in significantly at about 12.8 kilometers. He summarized:

> "...a bodily crosswind distortion of the plume from a point source (either elevated or on the ground) sets in between 2 and 3 km. However, the form of the crosswind growth curves suggests strongly that the communication of the distortion to the spread at a given level was not of practical importance below about 5 km in the case of the elevated source and about 12 km in the case of the ground level source. Thereafter the implication is that the shear contribution is dominant."

It is evident that, if it is desired to model diffusion in a prototype with a length scale greater than about 5 km, under neutral or stable atmospheric conditions, in relatively flat terrain, the Rossby criterion should be considered.

THE REYNOLDS NUMBER, $U_R L/\nu$

The Reynolds number represents the ratio of inertial to viscous forces. It imposes very strong limitations on rigorous simulation; it is the most abused criterion in models of atmospheric flows. The scale reductions commonly used result in model Reynolds numbers three to four orders of magnitude smaller than found in the atmosphere. The viscous forces are thus relatively more important in the model than they are in the prototype. If strict adherence to the Reynolds number criterion were required, no atmospheric flows could be modeled.

Various arguments have been presented which attempt to justify the use of smaller Reynolds numbers in a model (i.e., to justify the neglect of the Reynolds number criterion). These arguments may be divided into three general categories; the laminar flow analogy, Reynolds number independence, and dissipation scaling. Each of these is discussed below.

The Laminar Flow Analogy: Abe (1941) was the first to introduce this concept. If the instantaneous velocity, temperature, and pressure in equation (1) are written as the sum of mean and fluctuating parts ($U_i = \overline{U}_i + u_i$), and the equation is then averaged, the following equation is obtained (after minor manipulation):

$$\frac{\partial \overline{U}_i}{\partial t} + \overline{U}_j \frac{\partial \overline{U}_i}{\partial x_j} + 2\epsilon_{ijk}\Omega_j \overline{U}_k = - \frac{1}{\rho_o} \frac{\partial \overline{\delta P}}{\partial x_i} + \frac{g}{T_o} \overline{\delta T}\, \delta_{3i} + \nu \frac{\partial^2 \overline{U}_i}{\partial x_j \partial x_j} + \frac{\partial \overline{u_i u_j}}{\partial x_j} \; . \quad (9)$$

An eddy viscosity is defined to relate the Reynolds stress to the mean velocity, $-(\overline{u_i u_j}) = K \frac{\partial \overline{U}_i}{\partial x_j}$. The nondimensional equation is then

$$\frac{\partial \overline{U}'_i}{\partial t'} + U'_j \frac{\partial \overline{U}'_i}{\partial x'_j} + \frac{2}{Ro} \epsilon_{ijk} \overline{U}'_K \Omega'_j = - \frac{1}{\rho'} \frac{\partial \overline{\delta P}'}{\partial x'_i} + \frac{1}{Fr^2} \overline{\delta T}' \delta_{3i} + \frac{1}{Re} \frac{\partial^2 \overline{U}'_i}{\partial x'_j \partial x'_j} + \frac{1}{Re_K} \frac{\partial^2 \overline{U}'_i}{\partial x'_j \partial x'_j} \quad , \quad (10)$$

where $Re_K \equiv \frac{U_R L}{K}$ is called a "turbulent" Reynolds number. Now, K/ν is of order 10^3, so that the term containing the turbulent Reynolds number is much larger than the term containing the ordinary Reynolds number. If the nondimensional equation for laminar flow were now written, it would appear identical to equation (10), with the exception that the term containing the turbulent Reynolds number would be absent. Assume the prototype flow is turbulent, the model flow is laminar, the scale ratio is of the order $1{:}10^3$, and U_R is the same order of magnitude in model and prototype. Then

$$(Re)_{model} \cong (Re_K)_{prototype}.$$

Hence, the similarity may be established by modeling a turbulent prototype flow by a laminar model flow when the scale ratio is on the order of $1{:}10^3$, all else being equal in a nondimensional sense.

This scheme is fundamentally incorrect for the same reasons that K-theories are fundamentally incorrect. Eddy sizes scale with distance from the ground, with the size of the obstacle, or, generally, with the scale of substantial variation of the mean flow. Diffusion is a flow property not a fluid property. The laminar flow analogy assumes unrealistically that eddy sizes are very small compared with the scale of variation of the property being diffused. Perhaps under very restrictive conditions when there exists a small upper bound to the sizes of atmospheric eddies (i.e., extremely stable conditions) there may be some realistic modeling possibilities, but the chances of that being the case without any doubt are small.

Perhaps qualitative use of this technique is the answer to those (nondiffusive) problems where the spread of a contaminant is controlled primarily by advective transport (mean flow). Two previous experimental studies give guidance here. Abe (1941) attempted to model the flow around Mt. Fuji, Japan, at a scale ratio of 1:50,000 using this analogy. Cermak et.al (1966) claimed that "the model flow patterns obtained were not even qualitatively close to those observed in actual field tests" (the original paper was not available for verification). Cermak and Peterka (1965) made a second study of the wind field over Point Arguello, California (a peninsula jutting into the Pacific Ocean). Cermak, et.al. (1966) claimed that:

> "Comparison of the surface flow directions and smoke traces for neutral and inversion flows established an excellent agreement in wind flow patterns over the Point Arguello area for flows approaching from the northwest."

After careful study of the figures presented, the author of this paper is not convinced of the validity of this statement. Large scatter in the field data on concentration levels prevented firm conclusions concerning diffusion characteristics of the two flow fields. Rather surprisingly, a logarithmic plot of concentration versus downwind distance showed that rates of decrease of concentration with distance were grossly similar in model and prototype. In view of the dissimilarity in surface flow patterns, this agreement is regarded as fortuitous.

Since kinematic viscosity is a fluid property, it is not an adjustable parameter. Turbulent eddy viscosity varies strongly with height, stability, and direction. These two severely limit the use of this laminar-turbulent analogy for physical modeling. Mathematical modeling techniques are superior to physical modeling techniques in the sense that K is a controllable variable in the mathematical model (e.g., a function of height, stability and direction). K is not a controllable variable in this sense in the physical model.

Reynolds Number Independence: This approach is based on the hypothesis that in the absence of thermal and Coriolis effects and for a specified flow system whose boundary conditions are expressed nondimensionally in terms of a characteristic length, L, and velocity, U_R, the flow structure is similar at all sufficiently high Reynolds numbers (Townsend, 1956). Most nondimensional mean-value functions depend only upon nondimensional space and time variables and not upon the Reynolds number, provided it is large enough. Exceptions are those functions which are concerned with the very small scale structure of the turbulence, (i.e., those responsible for the viscous dissipation of energy). The viscosity has very little effect on the main structure of the turbulence; its major effect is limited to setting the size of the small eddies which convert mechanical energy to heat.

This hypothesis of Reynolds number independence was put forth by Townsend (1956). Townsend called it Reynolds number similarity. There now exists a large amount of experimental evidence supporting this principle. Townsend stated it simply "geometrically similar flows are similar at all sufficiently high Reynolds numbers." This is an extremely fortunate phenomenon from the standpoint of modeling. The gross structure of the turbulence is similar over a very wide range of Reynolds numbers. This concept is used by nearly all modelers.

To obtain a better idea of the contributions to dispersion from the various scales of turbulence, it is convenient to examine the spectral form of the Taylor (1921) diffusion equation. Taylor's expression for the mean-square fluid particle displacement in a stationary homogeneous turbulence is given by

$$\overline{y^2(T)} = 2\overline{v^2}\int_0^T\int_0^t \rho(\xi)\, d\xi\, dt \qquad (11)$$

where $\overline{v^2}$ is the variance of particle velocities, $\rho(\xi)$ is the Lagrangian autocorrelation of particle velocities with time separation ξ, and T is the time of particle travel from the source. Batchelor (1949) applied the Fourier-transform relation between the autocorrelation, $\rho(\xi)$, and the corresponding Lagrangian spectrum function, F_L (n) (normalized) to obtain

$$\overline{y^2}(T) = \overline{v^2}T^2\int_0^\infty F_L(n)\left[\frac{\text{Sin }(\pi nT)}{\pi nT}\right]^2 dn, \qquad (12)$$

where n is the frequency. The squared term under the integral is a filter function which is very small when n<1/T and virtually unity when n<1/(10T). Thus, for very small travel times, the filter function is virtually unity, so that all scales of turbulence contribute to the dispersion with the same weight that they contribute to the total energy. For larger travel times, the larger scales of turbulence progressively dominate the dispersion process. This means that eddies with diameter smaller than about one-tenth the plume width do not significantly effect the spread of the plume; only those eddies with diameter about the same size as the width of the plume and larger substantially increase its width.

For a given class of turbulent flow, an increase of the Reynolds number increases the range of the high frequency end of the spectrum. It is instructive here to examine the trends observed experimentally and theoretically in grid-generated turbulence. A good measure of the width of a turbulent energy spectrum is the ratio of the integral scale, I, to the Kolmogoroff microscale, η. It may be shown, through arguments presented by Corrsin (1963), that this ratio is

$$\frac{I}{\eta} \propto Re^{3/4}, \qquad (13)$$

where Re is the grid Reynolds number (based upon upstream velocity, U, and mesh size, M). Ideally, both I and η would be reduced in the same proportion in a model (i.e., the geometrical scale ratio), so that the width (number of "decades") of the spectra would be identical in model and prototype. It is clear, however, that this would require identical Reynolds numbers in model and prototype. Equation (13) may be used to estimate the comparative widths of model and prototype spectra:

$$\frac{(I/\eta)_m}{(I/\eta)_p} = \left(\frac{Re_m}{Re_p}\right)^{3/4} = \left(\frac{L_m}{L_p}\right)^{3/4} , \qquad (14)$$

assuming that the ratio of flow speed to viscosity is roughly the same in model and prototype. Hence, at a scale ratio of 1:1000, a seven-decade-wide atmospheric spectrum is "modeled" by a 4-1/2-decade-wide laboratory spectrum. This appears to be a drastic reduction in spectral width, but observations of grid-generated flows show that only the high frequency end of the spectrum is cut out, so that this reduction in spectral width has insignificant effects. It is found empirically that I/M (M is the mesh size) at a fixed distance downstream of a grid is nearly independent of Reynolds number (Corrsin, 1963). Similarly, it may be expected in other flow geometries that I/L (L is a characteristic length in the flow, for example, the mesh size or the height of a building) at corresponding geometrical locations will be roughly independent of Reynolds number, i.e.,

$$\frac{I_p}{L_p} \approx \frac{I_m}{L_m} . \qquad (15)$$

Indeed, the integral scale is found to be roughly half the size of the characteristic length and independent of Reynolds number in a wide variety of classes of flows.

Combining equations (13) and (15) yields

$$\frac{\eta_p}{\eta_m} \approx \frac{I_p}{I_m}\left(\frac{L_m}{L_p}\right)^{3/4} \approx \left(\frac{L_p}{L_m}\right)^{1/4} . \qquad (16)$$

In summary, integral scales reduce with the first power of the geometrical scale ratio (as desired), whereas Kolmogoroff microscales reduce with only the one-fourth power of the geometrical scale ratio.

A practical example here will make the point clear. The Kolmogoroff microscale in the atmosphere is about one millimeter between 1 and 100 meters above ground (Lumley and Panofsky, 1964). As indicated by equation (14), at a scale ratio of 1:500, the spectral width in a model would be approximately two orders of magnitude smaller than desired. The Kolmogoroff microscale in the model would be about 100 times larger than required by rigorous similarity. This would correspond to a Kolmogoroff microscale of ten centimeters in the atmosphere. It is difficult to imagine a practical atmospheric diffusion problem where eddies smaller than ten centimeters would contribute significantly to the spread of a contaminant.

It should be noted that the arguments beginning with equation (13) have been concerned with Eulerian scales and spectra, whereas they would best have been posed in terms of Lagrangian coordinates, as required in equation (12). However, it is reasonable to assume that if the Eulerian spectra and scales of model and prototype are similar, then so will be the Lagrangian spectra and scales; more appropriately, if Eulerian spectra differ in certain respects between model and prototype, then the Lagrangian spectra will be dissimilar in like fashion. Hence, conclusions drawn in the Eulerian framework are expected to be valid in the Lagrangian framework (to at least within the same order of magnitude).

Concerning puff (relative) diffusion, the problem is somewhat different. Corrsin (1961a) has argued that the principal contribution to two-particle relative diffusion comes from eddies of roughly the same size as the particle pair separation. This contrasts with single particle diffusion, where the principal contribution comes from the large eddies. Hence, puff diffusion in a model will depend much more strongly upon the model Reynolds number. Intuitively, it appears that reasonable results would be obtained if the Kolmogoroff microscale were small compared with the initial puff width.

The discussion of the Reynolds number criterion in the modeling literature normally centers around sharp-edged geometry where it is usually stated that the mean flow patterns will not be much affected by changing the Reynolds number. While this is true, it does not make full use of the concept. Most mean-value functions, including those describing the main turbulence structure will be nearly independent of Reynolds number, providing it is sufficiently high, the only exceptions being those discussed above.

The question is: how high must the Reynolds number be to be high enough? A precise answer would depend upon the geometrical shape of the boundaries, the accuracy desired, the type of information desired from the model, and possibly other effects (e.g., those characterized by the Rossby and Froude numbers). The answer to this question is reasonably well known for simple flow classes such as jets and cylinder wakes, but is largely unknown for models of atmospheric motions.

Only a few systematic studies have been made on Reynolds number independence relating to atmospheric modeling. Golden (1961) measured the concentration patterns above the roof of model cubes in a wind tunnel. Buoyant and neutrally buoyant effluent was discharged into the air stream from a flush vent in the center of the cube. Two sizes of cubes were used to vary the Reynolds number from 3000 to 57000. The nondimensional concentration isopleths above the roof showed only slight variations over the entire range of Reynolds numbers with neutrally buoyant effluent and with an effluent-to-free-stream velocity ratio of unity. However, the maximum concentration on the roof itself was found to vary strongly with Reynolds numbers less than 11,000, but to be invariant with Reynolds numbers between 11,000 and 94,000. Thus, a critical Reynolds number may be defined, which, with this type of geometry, appears to be 11,000.

A study by Smith (1951) may be regarded as a test of Reynolds number independence. He investigated the size of the wake created by both model and prototype sharp-edged buildings. He assumed that the flow was independent of Reynolds number effects if the ratio of length of the cavity region to the building height was the same in both model and prototype. In the prototype tests, he found this ratio to be constant for Reynolds numbers (based upon an appropriate characteristic length) between about 2×10^4 and 2×10^6. Moreover, in the model tests, he found the ratio to be constant for various block models over a range of Reynolds numbers from 2×10^4 to 2×10^5. This demonstrates that his choice of the characteristic length was very appropriate.

Critical Reynolds numbers for other geometrical shapes remain to be determined. A study by Halitsky, et al. (1963) on a reactor shell (a hemisphere fitted on a vertical cylinder) indicated a critical Reynolds number greater than 79,000. The separation point, and, hence, the pressure distribution for rounded buildings is affected by the Reynolds number. Generally speaking, the more streamlined is the object, the larger is the critical Reynolds number.

Dissipation Scaling: A hypothesis on the similarity of the detailed turbulence structure of model and prototype flows was proposed by Nemoto (1968). Again, a basic assumption is that thermal and Coriolis effects are negligible. He reasoned that mean flow patterns of both model and prototype would be similar if the turbulent structure of the two flows were geometrically similar. Two assumptions were made:

1) the turbulence of both model and prototype flows was "locally isotropic" (Kolmogoroff, 1941),

2) the Kolmogoroff velocity, υ and microscale, η, characterize the turbulence at each point in the flow.

Assumption 1 is satisfied if the Reynolds number is very large (Hinze, 1959). Using assumption 2, Nemoto reasoned that the turbulence structures of model and prototype flows would be similar when

$$\frac{\eta_m}{\eta_p} = \frac{L_m}{L_p} \qquad (17)$$

and

$$\frac{\upsilon_m}{\upsilon_p} = \frac{U_{Rm}}{U_{Rp}} \quad , \qquad (18)$$

where the subscripts m and p refer to model and prototype respectively. From the definitions of η and υ, the following equation may be established:

$$\varepsilon = \frac{\upsilon^3}{\eta} \qquad (19)$$

From equations (17), (18), and (19) it may be deduced that:

$$\frac{U_{Rm}}{U_{Rp}} = \left(\frac{\varepsilon_m}{\varepsilon_p}\right)^{1\backslash 3}\left(\frac{L_m}{L_p}\right)^{1\backslash 3} \qquad (20)$$

Equation (20) is the similarity criterion proposed by Nemoto. He has also shown how the above relationship may be obtained from a peculiar dimensionalization of the turbulent energy equation.

It is agreed that the turbulence structures of model and prototype flows would be similar if equations (17) and (18) could be satisfied. However, it is impossible to satisfy equation (17) using typical length scale reductions (i.e., 1:300 to 1:1000). Measurements of the Kolmogoroff microscale in the atmosphere indicate that $\eta \sim 1$ mm between 1 m and 100 m above ground (Lumley and Panofsky, 1964). Typical values of η in laboratory flows are 0.075 mm (Wyngaard, 1967), and 0.5 mm (Snyder and Lumley, 1971). Measurements in very high Reynolds number laboratory flows (Kistler and Vrebalovich, 1966) show that the smallest Kolmogoroff microscale which can reasonably be generated in the laboratory is 0.05 mm. Thus, the largest ratio of microscales is of order 20, which is far short of the typical ratio required (i.e., 300 to 1000).

Generally speaking, the satisfaction of equation (17) requires identical Reynolds numbers of the model and prototype flows, as shown in the discussion of Reynolds number independence. This is also easily shown by the usual nondimensionalization of the turbulent energy equation (Cermak, et al., 1966).

THE PECLET NUMBER AND THE REYNOLDS-SCHMIDT PRODUCT

The Peclet number is most easily discussed by writing it as

$$Pe = \frac{U_R L}{\kappa} = \frac{U_R L}{\nu} \frac{\nu}{\kappa} = Re \cdot Pr.$$

where Pr is the Prandtl number.

The Reynolds-Schmidt product may be written as

$$\frac{U_R L}{\alpha} = \frac{U_R L}{\nu} \frac{\nu}{\alpha} = \mathrm{Re} \cdot \mathrm{Sc}.$$

Both of these dimensionless parameters have the same form (i.e., the product of a Reynolds number and a ratio of molecular transport coefficients). Both the Prandtl and Schmidt numbers are fluid properties and not flow properties. The Prandtl number is the ratio of the momentum diffusivity (kinematic viscosity) to the thermal diffusivity. The Schmidt number is the ratio of the momentum diffusivity to mass diffusivity.

For air, the Prandtl number does not vary strongly with temperature. When air is used as the medium for modeling, the Prandtl number is nearly the same in model and prototype, and, if the Reynolds numbers were the same, the Peclet number criterion would be nearly satisfied. However, if water is used as the medium for modeling, the Prandtl number at ordinary room temperatures is a factor of about 10 larger than it is in air, and it varies rather greatly with temperature. Thus, from the standpoint of rigorous similarity, it does not appear that water would be a suitable medium in which to do model studies.

The Schmidt number for most gases in air is about one. Thus, the Schmidt number for an effluent plume (which contains only minor fractions of gases other than air) diffusing in the atmosphere is about one. If air is used as the medium for modeling, the Schmidt number (for nearly any foreign gas introduced) will be nearly the same in model and prototype.

If, at the same time, the Reynolds number were the same, the Reynolds-Schmidt product criterion would be nearly satisfied.

When water is used as the medium for modeling, salt water or alcohol are typically used to simulate the buoyancy of a plu[illegible] The Schmidt number for sodium chloride or alcohol in water is approximately [illegible]00. Thus, it appears that strict similarity using water as the modeling medium would be difficult to obtain.

The basic problem, however, in matching of the Peclet number or Reynolds-Schmidt product, is not in the Prandtl or Schmidt numbers, but rather in the Reynolds number. Arguments similar to those constructed for Reynolds number independence may be used to justify the neglect of the Peclet number and Reynolds-Schmidt product as modeling criteria. The term on the right hand side of equation (6) represents the molecular diffusion of heat. The term on the right hand side of equation (8) represents the molecular diffusion of mass. In this connection, both heat and mass are regarded as passive scalar contaminants. If the flow is of a sufficiently high Reynolds number, then the main structure of the turbulence will be almost totally responsible for the transport of the contaminant (heat or mass). Molecular diffusion will contribute very little to the bulk contaminant transfer; its main function is to smooth out the very small scale discontinuities of concentration or temperature (i.e., it acts as a high pass filter on the concentration or temperature fluctuations). Indeed, arguments of this nature have been used to postulate the form of concentration or temperature spectra at large wave numbers (see Pao, 1965). The main effect of thermal or mass diffusivity is confined to setting the high wavenumber cutoff of the temperature or concentration spectrum. Since turbulent diffusion strongly dominates molecular diffusion in turbulent air flows, especially at high Reynolds numbers, and since molecular diffusion is even less important for Prandtl or Schmidt numbers larger than unity, the effect of not matching the Prandtl or Schmidt numbers of the prototype in the model is unimportant. Generally speaking, the Peclet number and Reynolds-Schmidt product may be neglected as modeling criteria if the flow exhibits Reynolds number independence. Both air and water are suitable media for modeling, from this standpoint.

THE FROUDE NUMBER, $U_R/(gL\delta T_R/T_o)^{1/2}$

The square of the Froude number represents the ratio of inertial forces to buoyancy forces. A large value of the Froude number implies that buoyancy forces are small compared to inertial forces. Thus, thermal effects become important as the Froude number approaches unity. Batchelor (1953) has shown how this parameter is related to the Richardson number. In the absence of a clearly defined length in the atmospheric boundary layer, it is convenient to replace U_R/L by a respresentative velocity gradient and $\delta T_R/L$ by a representative temperature gradient. Substitution of these gradients into the expression for the Froude number yields.

$$Fr^2 = \frac{U_R^2}{L^2}\,\frac{L}{\delta T_R}\,\frac{T_o}{g} = \frac{T_o}{g}\,\frac{(\partial\overline{U}/\partial z)_R^2}{(\partial\delta T/\partial z)_R} .$$

Thus, the Froude number may be regarded as the inverse square root of a Richardson number. It is also related to the Monin-Obukhov length (1954). Although any of these parameters may be used as similarity criteria, the Froude number is used here because it appeared naturally through the non-dimensionalization of equation (1). Batchelor (1953) has also discussed the conditions under which this parameter is the sole governing criterion for dynamical similarity of motions of a perfect gas atmosphere. The Froude number is not, by itself, a difficult parameter to duplicate in a physical model. It is likely to be the most important individual parameter to be matched when the model is to simulate atmospheric diffusion. When the modeling medium is air, provisions must be made for heating or cooling of the air stream to obtain the temperature startification. However, in order to match small Froude numbers of the prototype in a model with a typical scale reduction (i.e., 1:300 to 1:1000), and in order to maintain reasonable temperatures (i.e., maximum temperatures difference of 200°C) in the model, it is necessary to decrease the mean flow speed. To match the Reynolds number between the model and prototype requires that the mean flow speed be increased. This conflict is resolved by matching the Froude number while insuring that a Reynolds-number-independent flow is established. This is not always possible.

When considering water as the medium for modeling, it is necessary to redefine the Froude number, since in its present form, it is applicable only to a perfect gas. The appropriate form is

$$Fr = \frac{U_R}{(gL\frac{\Delta\rho}{\rho})^{1/2}} \quad ,$$

where ρ represents density. The common method of producing stable density stratification in water is by producing thin layers of various concentrations of salt in water. In view of the very small mass diffusivity of salt in water, an undisturbed stable mass of salt water will remain that way for several days before the density gradient is changed substantially by molecular diffusion. Maximum density differences are limited (about 20% in the dimensionless density difference), so that flow speeds must be reduced as was the case with air as the modeling medium. Recirculating systems using this technique are impractical because of mixing resulting within a pump. An interesting technique is reported by Homma (1969) wherein fresh and saline water are mixed to produce stable density gradients at the entrance of a once-through open water channel. This technique offers the possibility of providing the proper boundary condition of turbulent flow (see next section), which is not possible in the still tank.

BOUNDARY CONDITIONS

A statement was made earlier that it was not necessary to determine a priori whether the flow was laminar or turbulent in order to apply equations (4), (5), and (6) to the determination of the similarity parameters. It is certainly necessary to determine whether or not the flow is turbulent in order to specify the boundary conditions. It is assumed here that the atmospheric flow is always turbulent. Furthermore, it was stated that the model flow would be identical to the prototype flow if, among other things, the nondimensional boundary conditions were identical.

Batchelor (1953) points out

> "Regarding the boundary conditions, we do not know enough about the differential equations concerned to be able to say with certainty what conditions must be specified to make the problem determinate, but it is a plausible inference from physical experience that $\underline{u}'$ and ρ' must be given as functions of t'at all spatial boundaries and $\underline{u}'$, ρ', p' must be given as functions of $\underline{x}'$ at an initial value of t'; it seems certain that such a set of boundary conditions is sufficient, although in some circumstances the conditions may well be over-sufficient."

(The prime here indicates a nondimensional quantity and the underline signifies a vector.) In the problem considered in the present paper, it is clear that $\delta T'$ and χ' also must be specified at an initial value of t' at all vaues of $\underline{x}'$ and at all spatial boundaries as functions of t'. This information is never available; even if it were, it could not be applied to the physical model. In the same sense, such detail in not required nor even desired as the output from the model. What is desired are quantities characteristic of the ensemble of realizations of turbulent flow. Evidently, what is required are properties characteristic of the ensemble of realizations of boundary conditions. This would require the specification of all the statistical properties (all of the moments) of the velocity, temperature, pressure, and density fields both initially everywhere and on the boundaries for all times. Even this much information is not available.

The most complete information which can be supplied at the present time are the first few moments, at least, the mean and the variance. It is not known if the specification of only the first few moments is sufficient; it is plausible, from physical experience, that such a specification is sufficient. Indeed, it is dubious that any moments above the first two could be controlled at will.

Nearly all modelers have considered the specification of boundary conditions from a different viewpoint, that is, through the spectrum of turbulence in the approach flow. Armitt and Counihan (1968) have given qualitative arguments which suggest that, for the study of plume dispersal, not only must the turbulence intensity components be properly modeled, but also the spectrum of each component is required, particularly the low frequency end of the spectrum. This idea is in agreement with the previous discussion on the contributions of the various scales of turbulence to the dispersal of contaminants. Some control of the turbulence spectra in the approach flow is possible (see Armitt and Counihan, 1968).

The specification of the velocity on solid boundaries is simple; it is zero, and all of its moments are zero. Hence, geometrical similarity of model and prototype is required. This raises another question:

how much detail is required? From the standpoint of rigorous similarity, of course, every detail of the prototype must be duplicated in the model. However, in view of the fact that the Reynolds number will not be duplicated, the fine detail is unnecessary. If the roughness length of the prototype, z_o, may be determined (or at least estimated), then it should be scaled according to

$$\frac{z_{om}}{z_{op}} = \frac{L_m}{L_p} .$$

This equation was first deduced by Jensen (1958) and is known as Jensen's criterion. Elements or details smaller than z_o will have very little effect on the overall flow; hence they need not be matched in the model. Details about the same size as z_o need to be matched only approximately (for example, randomly distributed grains of sand). Specifications of the detailed temperature distributions at the solid boundaries is rarely, if ever, discussed from the modeling standpoint. In current practice, the solid boundary is maintained at constant temperature. It is plausible that the amount of detail in the temperature distribution should be determined on the same basis as the amount of detail in the geometrical boundaries. This has never been done, although elementary attempts have been made by Chaudhry and Cermak (1971). Similar considerations apply to the specification of the boundary conditions of the density distributions when the modeling medium is salt water.

Specification of boundary conditions on concentration distributions are, in principle, easy. In practice, the difficulty would depend on the type of problem to be studied. For example, if the problem were to determine the effect of a single source, the boundary conditions could be $\chi' = 0$ initially everywhere and χ' = constant at the location of the source for all time thereafter.

Very little is known about the boundary specification of the pressure, p'. Normally, the mean pressure gradient in a wind tunnel is adjusted to zero. Fluctuating pressures are, in any event, not controllable parameters in a model flow.

In current practice, the upstream boundary conditions on velocity and temperature are specified to be reasonably similar to some theoretical formula such as the logarithmic velocity distribution. Cermak, et. al (1966) argue that boundary layers (kinetic and thermal) grown naturally over long lengths of rough ground must be inherently similar to those in the atmosphere. Others (Ludwig and Sundaram, 1969; Armitt and Counihan, 1968; Mery, 1969) use artificial techniques for generating thick boundary layers over short distances. Only Mery (1969) has attempted to model both the velocity and temperature profiles using artificial techniques. Any of the present techniques for boundary layer generation appears to be suitable; all of them come reasonably close to matching the first two moments of the velocity and temperature distributions. Boundary layer heights must, of course, correspond with the geometrical scale ratio.

SUMMARY AND CONCLUSIONS

Similarity criteria for modeling atmospheric flows in air and water have been derived. Rigorous similarity requires that five nondimensional parameters plus nondimensional boundary conditions must be matched in model and prototype. It has been determined that the Rossby number should be considered when modeling prototype flows with a length scale greater than about 5 kilometers, under neutral or stable atmospheric conditions, in relatively flat terrain. It is concluded that more work needs to be done to determine under what conditions the prototype length scale may be extended while still ignoring the Rossby number criterion. It is recommended that study is begun on methods for simulation of Coriolis forces in a model.

The concept of Reynolds number independence has been found to be extremely useful and powerful. Heuristic arguments have been given through the use of this concept that it was not necessary to match Reynolds number, Peclet number, nor Reynolds-Schmidt product between model and prototype, provided the model Reynolds number is sufficiently large. Current practice indicates that sufficiently large Reynolds numbers are attainable at least for sharp-edged geometrical structures in ordinary meteorological wind tunnels. More work needs to be done to determine if sufficiently high Reynolds numbers may be obtained in the laboratory for the simulation of flow over more streamlined surfaces. The Froude number is the most important single parameter describing the prototype flow which must be duplicated in the model. The specification of boundary conditions was found to be nebulous both in terms of how many variables are necessary and sufficient and also in terms of the type of statistical information required (i.e., is the specification of only a few lower order moments of each variable sufficient). Geometrical similarity was required from the specification of zero velocity at the solid boundaries. It was decided that details of the prototype of size smaller than the roughness length need not be reproduced in the model. Objects about the same size as the roughness length need not be reproduced in geometrical form but an equivalent roughness must be established.

Both air and water appear to be suitable fluids to use as the modeling medium. The choice is a matter of convenience.

REFERENCES

Abe, M., 1941: Mountain Clouds, Their Forms and Connected Air Currents, Part II, Bull. Cent. Meteor. Obs., Tokyo, v. 7, no. 3.

Aris, R., 1956: On the Dispersion of a Solute in a Fluid Flowing through a Tube, Proc. Roy. Soc. (London), Ser. A. v. 235, p. 67-77.

Armitt, J. & Counihan, J., 1968: The Simulation of the Atmospheric Boundary Layer in a Wind Tunnel, Atm. Envir., v. 2, no. 1, p. 49-71.

Batchelor, G. K., 1949: Diffusion in a Field of Homogeneous Turbulence. I. Eulerian Analysis, Austral. J. Sci. Res., Ser. A, v. 2, p. 437-50.

Batchelor, G.K., 1953: The Conditions for Dynamical Similarity of Motions of a Frictionless Perfect-Gas Atmosphere, Quart. J. Roy. Met. Soc., v. 79, p. 224-235.

Birkhoff, G., 1950: Hydrodynamics, Princeton Univ. Press, 186 p.

Cermak, J.E., & Peterka, J., 1966: Simulation of Wind Fields over Point Arguello, Calif. by Wind Tunnel Flow over a Topographic Model, Report to Navy under Contract N123(61756)34361A(PMR), Colo. State. Univ., Nov.

Cermak, J.E., Sandborn, V.A., Plate, E.J., Binder, G.H., Chuang, H., Meroney, R.N., & Ito, S., 1966: Simulation of Atmospheric Motion by Wind Tunnel Flows, Report to Army under Grant DA-AMC-28-043-G20, Colo. State Univ., May.

Chaudhry, F.H. & Cermak, J.E., 1971: Simulation of Flow and Diffusion over an Urban Complex, Paper presented at Conf. on Air Poll. Met., Raleigh, N.C., April 5-9.

Corrsin, S., 1961: Turbulent Flow, Am. Scientist, v. 49, no. 3, p. 300-325, Sept.

Corrsin, S., 1961a: Theories of Turbulent Dispersion, Mechanique de la Turbulence, Marseille, France.

Corrsin, S., 1963: Turbulence: Experimental Methods, Handbuch der Physik, v. VIII/2, Springer Verlag, Berlin.

Csanady, G.T., 1969: Diffusion in an Ekman Layer, J. Atmos. Sci., v. 26, no. 3, May, p. 414-426.

Fuquay, J.J., Simpson, C.L. & Hinds, W.T., 1964: Prediction of Environmental Exposures from Sources near the Ground Based on Hanford Experimental Data, J. Appl. Met., v. 3, p. 761-770.

Golden, J., 1961: Scale Model Techniques, M.S. Thesis, College of Engr., New York Univ., May.

Halitsky, J., Golden, J., Halpern, P., & Wu, P., 1963: Wind Tunnel Tests of Gas Diffusion from a Leak in the Shell of a Nuclear Power Reactor and from a Nearby Stack, Geophys. Sci. Lab. Rept. 63-2, Dept. of Met. & Ocean., New York Univ.

Hidy, G.M., 1967: Adventures in Atmospheric Simulation, Bull. Am. Met. Soc., v. 48, no. 3, p. 143-161, March.

Hinze, J.O., 1959: Turbulence, McGraw Hill, 586 p.

Hogstrom, U., 1964: An Experimental Study on Atmospheric Diffusion, Tellus, v. 16, p. 205-251.

Homma, M., 1969: Main Research Activities on Air Pollution, Cent. Res. Inst. of Elect. Power Industry, (Japan), Sept., Unpublished.

Jensen, M., 1958: The Model-Law for Phenomena in a Natural Wind, Ingeniøren. Int. Ed., v. 2, no. 4.

Kistler, A.L. & Vrebalovich, J., 1966: Grid Turbulence at Large Reynolds Numbers, J. Fluid Mech., v. 26, pt. 1, p. 37-47.

Kolmogoroff, A.N., 1941: The Local Structure of Turbulence in Incompressible Viscous Fluid for Very Large Reynolds Numbers, Compt. Rend. (Doklady) Acad. Sci. U.R.S.S., v. 30, p. 301-305.

Lumley, J.L., 1970: Stochastic Tools in Turbulence, Academic Press, 194p.

Lumley, J.L. & Panofsky, H.A., 1964: The Structure of Atmospheric Turbulence., Interscience, 239 p.

McVehil, G.E., Ludwig, G.R., & Sundaram, T.R., 1967: On the Feasibility of Modeling Small Scale Atmospheric Motions, Cornell Aero. Lab. Rept. ZB-2328-P-1, Buffalo, N.Y.

Mery, P., 1969: Reproduction en Similitude de la Diffusion dans la Couche Limite Atmospherique, La Houille Blanche, No. 4 (translated by Air Poll. Tech. Inf. Cent. No. 1104).

Monin, A.S. & Obukhov, A.M., 1954: Basic Laws of Turbulent Mixing in the Ground Layer of the Atmosphere, Geophys. Inst. Acad. Sci., U.S.S.R., v. 24, no. 151, p. 163-187.

Nemoto, S., 1968: Similarity between Natural Local Wind in the Atmosphere and Model Wind in a Wind Tunnel, Papers in Met. and Geophys. v. 19, no. 2, p. 131-230.

Pao, Y-H., 1965: Structure of Turbulent Velocity and Scalar Fields at Large Wavenumbers, Phys. Fluids, v. 8, no. 6, June.

Pasquill, F., 1962: Some observed Properties of Medium-Scale Diffusion in the Atmosphere, Quart. J. Roy. Met. Soc., v. 88, p. 70.

Pasquill, F., 1969: The Influence of the Turning of Wind with Height on Crosswind Diffusion, Phil. Trans. Roy. Soc. Lond., Ser. A., v. 265, p. 173-181.

Saffman, P.G., 1962: The Effect of Wind Shear on Horizontal Spread from an Instantaneous Ground Source, Quart. J. Roy. Met. Soc., v. 88, no. 378, p. 382-393, Oct.

Smith, E.G., 1951: The Feasibility of Using Models for Predetermining Natural Ventilation, Res. Rep. Tex. Engng. Exp. Stn. 26

Smith, F.B., 1965: The Role of Wind Shear in Horizontal Diffusion of Ambient Particles, Quart. J. Roy. Met. Soc., v. 91, no. 389, p. 318-329, July.

Snyder, W.H. & Lumley, J.L., 1971: Some Measurements of Particle Velocity Autocorrelation Functions in a Turbulent Flow, J. Fluid Mech., v. 48, p. 41-71.

Taylor, G.I., 1921: Diffusion by Continuous Movements, Proc. Lond. Math. Soc, v. 20, p. 196-211.

Townsend, A.A., 1956: The Structure of Turbulent Shear Flow, Cambridge Univ. Press. 315 p.

Tyldesley, J.B. & Wallington, C.E., 1965: The Effect of Wind Shear and Vertical Diffusion on Horizontal Dispersion, Quart. J. Roy. Met. Soc., v. 91, p. 158-174.

Ukeguchi, N., Sakata, H., Okamoto, H. & Ide, Y. 1967: Study on Stack Gas Diffusion, Mitsubishi Tech. Bull., no. 52, p. 1-13, Aug.

Wyngaard, J.C., 1967: An Experimental Investigation of the Small-Scale Structure of Turbulence in a Curved Mixing Layer, Ph.D. Dissertation, Dept. of Mech. Engr., Penn. State Univ.

Chapter XI

ATMOSPHERIC PHYSICAL AND CHEMICAL TRANSFORMATION OF POLLUTANTS AS EFFECTING URBAN POLLUTION MODELING

Dr. Carel Andre Velds

Scientific Officer

Royal Netherlands Meteorological Institute

The Netherlands

ATMOSPHERIC PHYSICAL AND CHEMICAL TRANSFORMATION OF POLLUTANTS AS EFFECTING URBAN POLLUTION MODELING

C.A. Velds

For presentation to the Panel on Modeling,
NATO/CCMS Pilot Project on Air Pollution,
Paris, France, 26-28 July 1971

Mathematical models of urban air pollution should not only reflect the dispersion of the pollutant due to atmospheric motion, but also the physico-chemical behaviour of the pollutant in the atmosphere. This means that all conversion and production reactions of the pollutant in the atmosphere and all removal mechanisms of the pollutant and its reaction products from the atmosphere have to be taken into account.

For example for sulfur dioxide the following mechanisms have to be considered.

Photochemical oxidation to sulfur trioxide by radiation, related to the presence of other pollutants especially strongly oxidizing materials such as nitrogen dioxide, ozone and peroxides.

With available water vapour, droplets of sulfuric acid are formed. The rate of oxidation of sulfur dioxide can be increased by the presence of hygroscopic particles containing dissolved catalysts, such as iron, manganese and copper. This accelerated oxidation may be realized in fogs and stack plumes.

Furthermore the efficiency of the natural removal of sulfur dioxide from the atmosphere by washout, rainout, fall-out, adsorption on surfaces such as soil, vegetation etc. has to be estimated to allow for these scavenging processes in the model.

As most of the processes are dependent on temperature, pressure, relative humidity, radiation, wind speed, precipitation, the presence of fog etc., experiments have to be done in the laboratory as well as during field studies under well-known conditions.

Measurements of vertical profiles of sulfur dioxide and sulfuric acid concentrations may be helpful. Furthermore, it appears necessary to develop measuring methods and techniques for the determination of sulfuric acid and sulfates.

In the Netherlands five institutes are currently engaged on the above mentioned work:

1. Organization for Applied Scientific Research (TNO), Delft
2. Society of Directors of Power Works and Institute for Testing Electrical Equipment Ltd (KEMA), Arnhem
3. National Institute of Public Health (RIV), Bilthoven
4. Royal Netherlands Meteorological Institute (KNMI), De Bilt
5. Technological University (THE), Eindhoven.

The research projects can be arranged into the categories of photochemical smog, sulfur dioxide reactions and interrelating subjects.

Research on the level and origin of photochemical smog started after complaints about oxidant injury to lettuce in 1965. Measurements of the oxidant concentrations are carried out by TNO, KNMI and THE on a routine basis. TNO is also measuring the ozone level. Besides that TNO and THE are developing analytical methods to determine the nitrogen oxide and hydrocarbon level in the atmosphere. Incidental measurements of these pollutants have been made.

In the near future TNO will start experiments in a smog chamber to investigate the kinetics of the chemical process and other fundementel chemical problems related to the formation of oxidants.

In the Netherlands no measurements, so far, have been made of the residence time of sulfur dioxide in the atmosphere. In the study of photochemical smog, as well as in the study of sulfur dioxide reactions, meteorological and chemical aspects are intertwined. Therefore the research in question will be done in close collaboration between chemists and meteorologists. KEMA is interested in the residence time of sulfur dioxide for application to the problem of calculating the dispersion of effluents from power plants and KNMI for applying it in mathematical models of urban air pollution.

KEMA is developing analytical methods for the specifically determination of sulfuric acid aerosols and for sulfate and ammonia in aerosols. After that the apparatuses will be tried out in a field test to measure the concentration of these aerosols in the atmosphere together with routine measurements of sulfur dioxide.

Furthermore the application of SF_6 tracer techniques is studied. Measurements of the SF_6-SO_2 ratio, during transport in the atmosphere, can give information regarding the conversion and removal of sulfur dioxide. The objectives of this study are to define the conversion rate of sulfur dioxide in stack plumes.

Chapter XII

REMOVAL OF SULFUR DIOXIDE FROM THE ATMOSPHERE

Erich Weber
Abteilung Umweltschutz
Bundesministerium des Innern
Bonn
Bundesrepublik Deutschland

Paper Prepared for the Meeting of the NATO/CCMS Panel of Modeling, 26-28 July 1971, Paris, France. Project on Air Pollution.

REMOVAL OF SULFUR DIOXIDE FROM THE ATMOSPHERE

INTRODUCTION

The dispersion of air pollutants depends on meteorological parameters. In addition physical and chemical transformations have a great influence on ground level concentrations. On the basis of long time average concentrations, calculated by a mathematical model, it could be possible to describe the influence of these transformations by diffusion parameters. If we want to calculate time dependent models we need information about the physical and chemical transformation of the air pollutants.

Till now we have only few informations about all types of transformations. With respect to SO_2 there were some investigations about its life time. About physical transformations there exist some publications about the uptake of SO_2 in droplets and about washout and rainout of SO_2, NO_2 and CO_2, found in laboratory experiments. Preliminary results are available from investigations about the absorption of SO_2 by different types of soil, material and plants.

1. THE OXIDATION OF SO_2

Oxidation of sulfur dioxide in the atmosphere may take place by photochemical conversion. COX and PENKETT (1970) monitored the concentration of gaseous SO_2 and of sulfur containing aerosols in the dark and in sunlight, using radioactive ^{35}S. They estimated a photochemical conversion rate of SO_2 up to 0.65% per hour. This is adequate to an average residence time of six to seven days. Former investigations by GERHARD and JOHNSTONE (1955) indicated a photochemical conversion rate of about 0.1 to 0.2 per hour (residence time 20 to 40 days), on the other hand RENZETTI and DOYLE (1960) reported about a photochemical conversion rate of 24% per hour.

The conversion rate of sulfur dioxide by a catalysed solution occurs at a faster rate and depends on the concentration of the reactants and of the type of catalyst. The rate of this process is reduced remarkably when the acidity of the droplet increases by oxidation to sulfuric acid. VAN DEN HEUVEL and MASON (1963) assumed that SO_2 and NH_3 were absorbed by droplets. The reaction between SO_2 and NH_3 leads to $(NH_4)_2SO_4$ and H_2O, the pH of the droplets remains unchanged. SCOTT and HOBBS (1966) calculated the sulfate concentration in droplets for different SO_2 and NH_3 concentration in the surrounding air. Measurements by GEORGII and WEBER (1964) and JUNGE (1963) have been made about the SO_2 and NH_3 concentration of the air, and about the sulfate content of airborne aerosols (GEORGII, JOST and SCHAEFER 1968, Table 1).

Table 1

Site	Period	Concentration ($\mu g/m^3$) SO_2	NH_3	SO_4	Sulfate in Water Droplets calculated after (SCOTT and HOBBS)
Frankfurt/Main	Winter 1956 and 1957	275	20.5	16.0	50
Mt. Zugspitze (3000 m)	Summer 1958	70	6.9	1.7	20
St. Moritz (1800 m)	Summer 1960	10	4.9	3.2	7.5
Florida	Summer 1954	3	5.1	0.6	2.5

The measured sulfate concentrations were always lower than the calculated values from the SO_2-NH_3-liquid water-reaction theory. That means that we mostly can assume the formation of ammoniasulfate by the air chemistry reactions. Till now we have no indications about the conversion rates of SO_2 to sulfates by this process. Though we may assume that under normal conditions ($10\ \mu g/m^3\ SO_2 : 10\ \mu g/m^3\ NH_3$) 50% of the available SO_2 take some hours to convert to sulfates in clouds. This time depends on the liquid water content and on the acidity of the droplets.

HEALY, MCKAY, PILBEAM and SCARGILL (1970) showed that the conversion process of ammonia to ammonia sulfate in a polluted atmosphere is comparably rapid, occuring on a time scale in hours rather than days. MCKAY (1969) indicated that in thick mist ammonia sulfate levels, such as are observed in polluted atmospheres, can build up in less than one hour.

2. THE WASHOUT OF SO_2

The effect of washout of SO_2 by rain has been investigated carefully by BEILKE (1970). Different rain intensities and droplet sizes have been used to find out the degree of the SO_2 concentration in an experimental rain chamber. The half-life-time of sulfur dioxide in the rain chamber (0.5 mm/h, $\bar{r} = 0.46$ mm, distilled water) was determined to 42 minutes. Using normal rain water or 0.001 n NaOH solution it almost takes 20 minutes to get an equal result. The decrease of SO_2 concentration in the chamber was very fast. By investigations from GEORGII and WEBER (1964) we know that there is hardly any decrease of SO_2 concentration in outside air during similar rainfalls at Frankfurt/Main. The loss of SO_2 by washout will be compensated mostly by the emission of SO_2 in the city.

At equal rain intensity and droplet size the washout of SO_2 is more effective than the washout of NO_2, because the solubility of both gases is quite different (BEILKE 1970). In contrary to SO_2 absorption by rain the washout intensity of NO_2 is nearly independent from the pH of the artificial rain water.

3. THE ABSORPTION OF SO_2

We have very few informations about which part of the SO_2 will be oxidized or absorbed by droplets or aerosols, and which part will be absorbed by surfaces on ground levels. During continuous recordings around a power plant in 1966 MARTIN and BARBER (1971) obtained very low values at a site which had its air intake close to a large hawthorn hedge. Significant amounts of SO_2 can be lost near to foliage by absorption on wet surfaces, particularly at night and by gaseous assimilation through the stomata of the plant during daytime. The greatest losses were recorded during rain or dew or when the open air was fairly warm. Zero loss can occur when the hedge is too cold, too dry, wilting or fumigated suddenly.

In a laboratory experiment GEORGII and SCHMID (1970) investigated the loss of SO_2 in an absorption chamber of 1 m^3. They found different absorption coefficients for different types of soils and plants, strongly dependent on the humidity of the surfaces.

It was an interesting result that the absorption rate of soil or plants depends also by the pH. The pH of soil or surfaces of plants changes to lower values during the absorption of SO_2, the absorption will stop after some time. By a rainfall the acidity will wash down and the absorption of SO_2 begins again.

Very little is known about the fate of other air pollutants. The residence time of NO_2 seems to be about one to four days, that of NO some hours to one day. The fate of CO is still unknown, former calculations lead to a residence time of 2.7 years, new measurements using radiocarbon techniques (ratio $^{13}C/^{12}C$) give a lower limit, to one month. The NH_3 can either be oxidized to form NH_4NO_3 or be combined with sulfate to $(NH_4)_2SO_4$, but we have no calculations about its life time.

4. THE RESIDENCE TIME OF SO_2

From an early investigation over the entire United States by JUNGE (1960) the life time of SO_2 has been estimated to last about four to seven days. JUNGE evaluated the emission rate of SO_2 by human activities and natural sources and measured the sulfate content of rain and snow by a sampling network all over the United States. His results are more or less representative for what we call background regions now.

Using data about the sulfate concentration in rain, dry fallout and aerosols MEETHAM (1950) indicated an average life time of about ten hours. In this paper SO_2 emission rates of Central England have been estimated.

GARTRELL, THOMAS and CARPENTER (1964) investigated the degree of the SO_2 concentration in the plume of TVA power station by airborne measurements. The authors' results suggest that the oxidation rate of SO_2 strongly depends on the relative humidity. Very little oxidation occurs for humidities below 70%; the oxidation rate increases rapidly for higher humidities. They found conversion rates of 22% after 12 minutes, increasing to 32% after 96 minutes. This result corresponds to a loss of 50% of the initial concentration after almost two hours. The highest total oxidation rate observed, 55% in 108 minutes, occured in the presence of mist.

At Frankfurt/Main the concentration of CO_2, SO_2 and meteorological parameters have been recorded continuously for several years (WEBER 1970, a). In certain cases short term peaks (5 to 15 minutes) of CO_2 and SO_2 concentration can be defined as an influence of power station effluents (WEBER 1970, b). The CO_2 and SO_2 concentrations leaving the stack are well known. Carbon dioxide is almost inert, whereas the proportion of sulfur dioxide can decrease by oxidation or absorption while being transported through the atmosphere. Using the variations of both the CO_2 and SO_2 concentrations the attempt was made to determine the loss of SO_2 in the plume of power stations at Frankfurt/Main.

By the fact that there is no physical or mechanical separation between the molecules of emitted CO_2 and SO_2, which both are part of the emission from coal or oil fired power plants, it can be assumed that the relation of the CO_2 to SO_2 concentration would remain constant while the plume travels through the atmosphere. According to previous investigations from BREUER and WINKLER (1965) it is possible to calculate the increase of CO_2 and SO_2 (ΔCO_2 and ΔSO_2) by measuring the difference in the concentration between the beginning and the maximum concentrations of parallel increases. Applying this technique the influences of background concentration and of long term variations (GEORGII and WEBER 1970) can be ignored.

FOSTER (1969) has considered a mechanism to explain the oxidation of SO_2 in power station plumes, as observed by GARTRELL, THOMAS and CARPENTER (1963). The catalytic effect was ascribed to iron oxide in the flue gas aerosols. This process requires a relative humidity in excess of about 70%. WEBER (1970, c) calculated the ratio $\Delta CO_2/\Delta SO_2$ for three different categories of relative humidity. There was a distinct increase (that means a decrease in the life time of SO_2) in that ratio between 40 to 60% and 60 to 80% r.h. (Table 2). This result is in good agreement with results from JUNGE and RYAN (1958) and VAN DEN HEUVEL and MASON (1963).

Table 2

Relative Humidity in %	$\Delta CO_2/\Delta SO_2$	Standard Deviation	n
40 - 60	595	493	49
60 - 80	940	710	50
80 - 100	1078	758	68

The high standard deviation may be caused by interferences with wind speed. It is obvious that the rate of oxidation or absorption of SO_2 depends on the transport time, i.e. mostly on wind speed.

Assuming an average wind speed of 3 m/sec between ground level and plume height, we are able to calculate the half life time (time of a 50% decrease of the initial concentration) of the SO_2 content of the plume from the results of our investigations at two monitoring sites in Frankfurt/Main (Fig. 1 and Table 3):

Table 3

Site	Travel Time	Loss of initial SO_2 after Travel Time at:		
		- s	average	+ s
West Station	10 min.	15%	40%	60%
Central Station	20 min.	45%	70%	77%

(assumed average emission ratio CO_2/SO_2 : 150)

Fig. 1

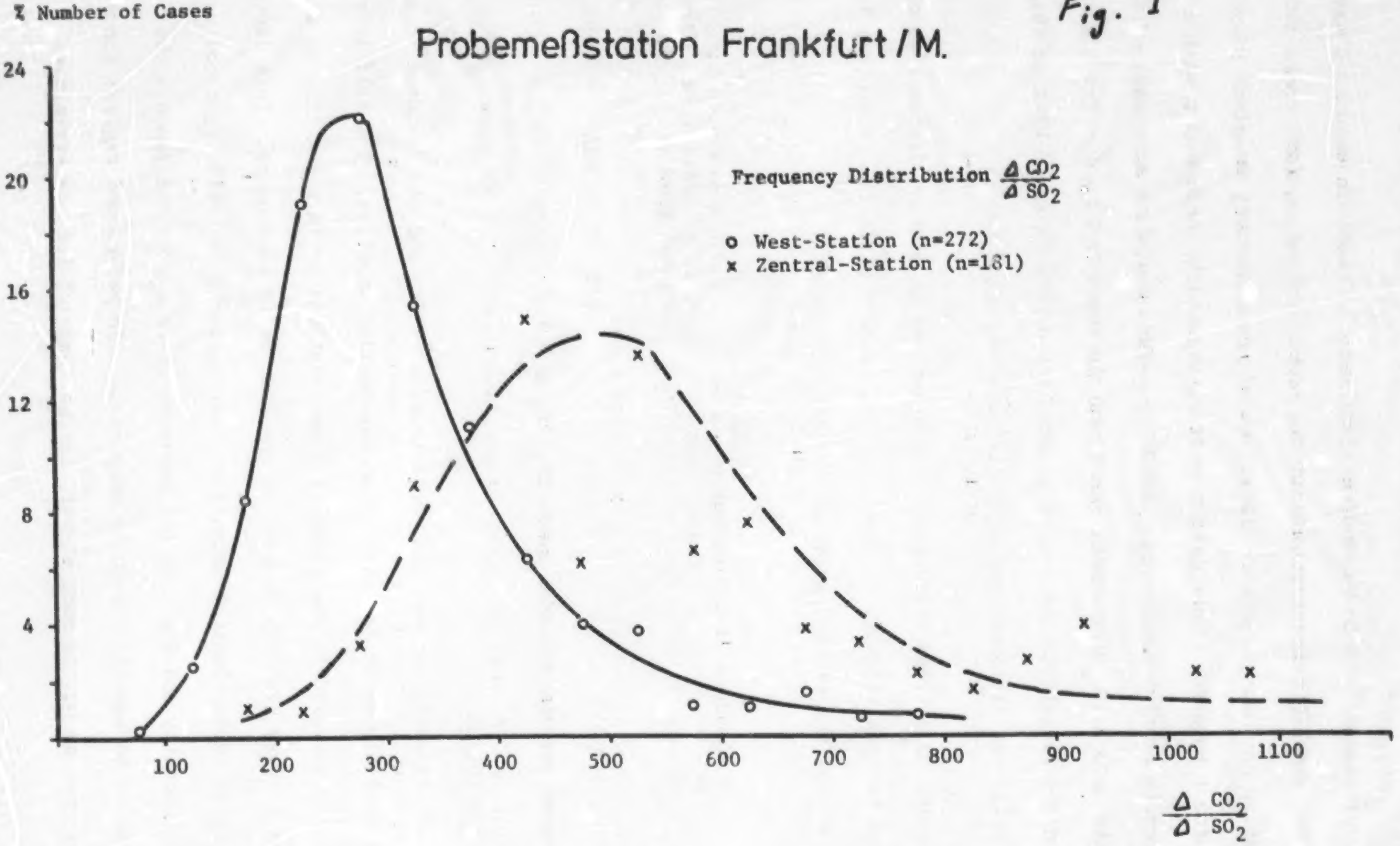
% Number of Cases
Probemeßstation Frankfurt/M.
Frequency Distribution $\frac{\Delta CO_2}{\Delta SO_2}$
o West-Station (n=272)
x Zentral-Station (n=181)
24
20
16
12
8
4
100
200
300
400
500
600
700
800
900
1000
1100
$\frac{\Delta CO_2}{\Delta SO_2}$

From December 1966 to March 1968 there were 72 cases of parallel increases of CO_2 and SO_2 concentrations for the summer period, and 122 cases for the heating period. In winter the effect of space heating emissions plays a dominant role for these sampling sites, especially during days with a moderate or high atmospheric stability. The cumulative frequency of the ratio $\Delta CO_2/\Delta SO_2$ for summer and winter is shown in Fig. 2. The higher standard deviations are caused by the high number of space heating chimneys at different distances and with different emission rates.

Assuming an average wind speed of 2 m/sec and an average distance to the space heating chimneys of about one km, Table 4 gives the percentage loss of SO_2 for the winter period at Frankfurt/Main:

Table 4

Site	Travel Time	Loss of initial SO_2 after Travel Time at: - s	average	+ s
Central Station	8 min.	25%	62%	95%

(assumed average emission ratio CO_2/SO_2 : 300)

5. CONCLUSION

The relationship between the concentration of SO_2 and its residence time will probably be in the form of an exponential function. The half life time, as measured in the plume of power stations or in a big city in winter, seems to vary from ten minutes to one hour or to some hours. This depends mostly on meteorological conditions, particularly on humidity, cloudiness, rain intensity and fog. In the presence of catalysts and ammonia the oxidation to ammoniasulfate is very rapid. In background regions the residence time of SO_2 is much slower, in the range of four to seven days.

Fig. 2

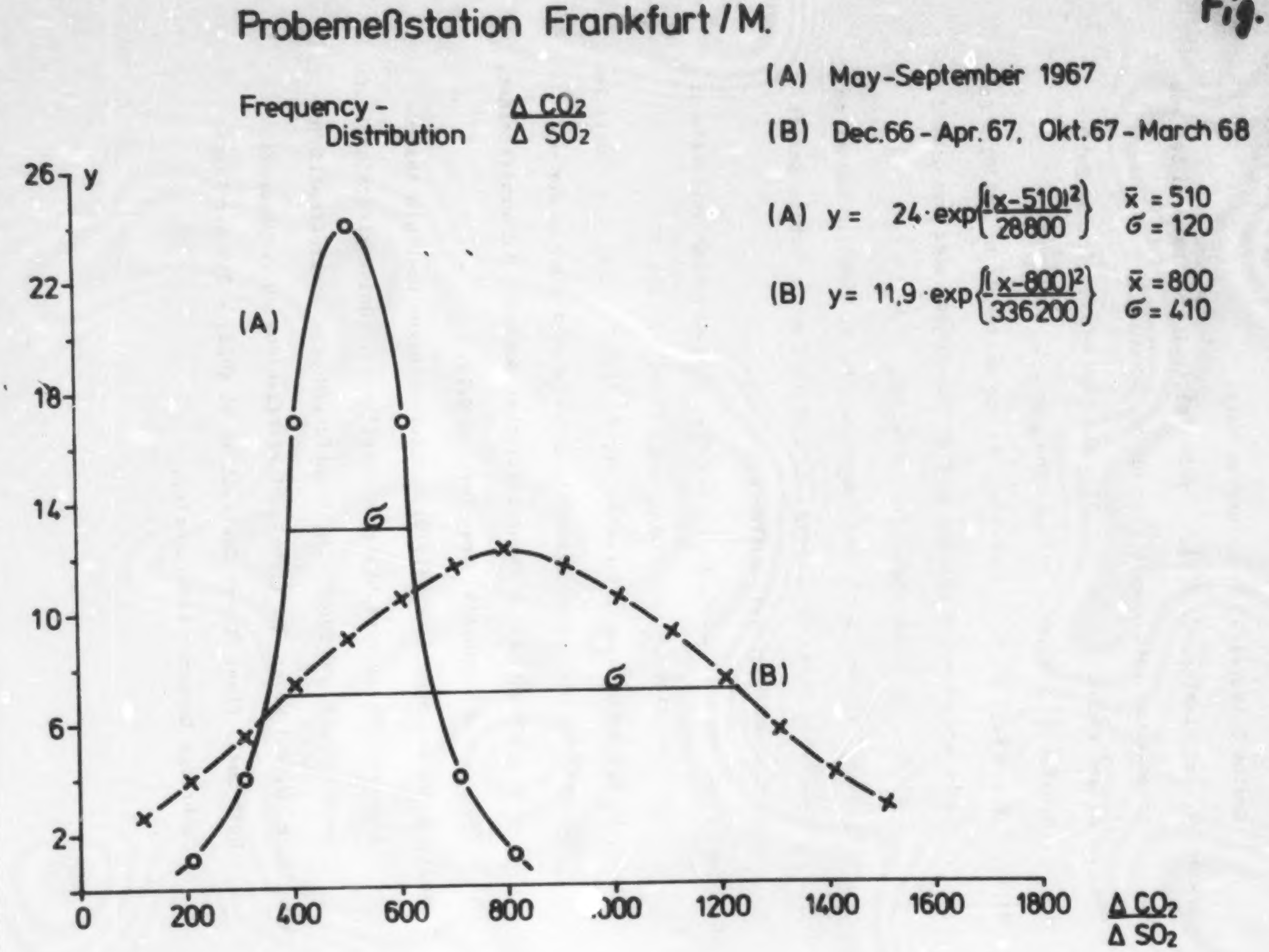
Probemeßstation Frankfurt / M.
Frequency - Distribution $\frac{\Delta CO_2}{\Delta SO_2}$
(A) May-September 1967
(B) Dec.66 - Apr. 67, Okt. 67 - March 68
(A) $y = 24 \cdot \exp\left\{\frac{(x-510)^2}{28800}\right\}$ $\bar{x} = 510$ $\sigma = 120$
(B) $y = 11,9 \cdot \exp\left\{\frac{(x-800)^2}{336200}\right\}$ $\bar{x} = 800$ $\sigma = 410$
y
26
22
18
14
10
6
2
0
200
400
600
800
.000
1200
1400
1600
1800
$\frac{\Delta CO_2}{\Delta SO_2}$
(A)
(B)
σ
σ

REFERENCES

Beilke, S. (1970) Untersuchungen über das Auswaschen atmosphärischer Spurenstoffe durch Niederschläge. Dissertation, Johann Wolfgang Goethe Universität Frankfurt am Main.

Breuer, W. and Winkler, K. (1965). Schwefeldioxid-Immissionen bei austauscharmen Wetterlagen. Staub 25, 98-101.

Cox, R. A. and Penkett, S. A. (1970). The Photo-Oxidation of Sulfur-Dioxide in Sunlight. Atmos. Environm. 4, 425-433.

Healy, T.V., McKay, H. A. C., Pilbeam, A. and Scargill, D. (1970). Ammonia and Ammonium Sulfate in the Troposphere over the United Kingdom. J. Geoph. Res. 75, 2317-2321.

Gartrell, F. E., Thomas, L. F. and Carpenter, S. B. (1964). Report on Full-Scale Study of Dispersion of Stack Gases. Public Health Service and Tennessee Valley Authority.

Gerhard, E. R. and Johnstone, H. F. (1955). Photochemical Oxidation of Sulfur Dioxide in Air. Ind. Engng. Chem. 47, 972-976.

Georgii, H. W., Jost, D. und Schaefer, H. J. (1968). Über die räumliche Verteilung von Schwefeldioxid und Sulfataerosolen in der unteren Troposphäre. Wissenschaftlicher Bericht, Universitätsinst. Meteor. und Geophysik, Frankfurt am Main.

Georgii, H. W. und Schmid, R. (1970). Untersuchungen über die Absorption von SO_2 an verschiedenen Oberflächen. Universitätsinstitut Meteorologie und Geophysik, Frankfurt/Main - unveröffentlicht.

Georgii, H. W. and Weber, E. (1964). Investigations on Tropospheric Wash-Out. Final Report Contract AF 61 (052) - 249 Air Force Cambridge Research Laboratories.

Junge, C. E. (1960). Sulfur in the Atmosphere. J. Geoph. Res. 65, 227-237.

Junge, C. E. (1963). Air Chemistry and Radioactivity. Academic Press, New York.

Junge, C. E. and Ryan, T. G. (1958). Study of the SO_2 Oxidation in Solution and its Role in Atmospheric Chemistry. J. Royal Met. Soc. 84, 46-55.

Martin, A. and Barber, F. R. (1971). Some Measurements of Loss of Atmospheric Sulfur Dioxide near Foliage. Atmosph. Environm. 5, 345-352.

McKay, H. A. C. (1969). Ammonia and Air Pollution. Chem. and Ind. 1162-1165.

Meetham, A. R. (1950). Natural Removal of Pollution from the Atmosphere. Quat. J. Royal Met. Soc. 76, 359-371.

Renzetti, N. A. and Doyle, D. J. (1960). Photochemical Aerosol Formation in Sulfur Dioxide - Hydrocarbon Systems. Int. Journ. Air & Water Poll. 2, 327-345.

Scott, W. D. and Hobbs, P. V. (1967). The Formation of Sulfate in Water Droplets. Journ. Atmos. Sc. 24, 54-57.

Van Den Heuvel, A. P. and Mason, B. J. (1963). The Formation of Ammonium Sulfate in Water Droplets exposed to Gaseous Sulfur Dioxide and Ammonia. Quat. J. Roy. Met. Soc. 89, 271-275.

Weber, E. (1970 a). Contribution to the Residence Time of Sulfur Dioxide in a Polluted Atmosphere. J. Geoph. Res. 75, 2909-2914.

Weber, E. (1970 b). Einrichtung und bisherige Ergebnisse der Probemesstation Frankfurt/Main. SchrReihe Ver. Wass.-Boden-Lufthyg. Berlin-Dahlem Heft 30, 19-45.

Weber, E. (1970 c). Determination of the Life Time of SO_2 by Simultaneous CO_2 and SO_2 Monitoring. 2nd Int. Clean Air Congr., Washington, Dec. 6-11, CP-25F.

Chapter XIII

REPORT ON MATHEMATICAL MODELING OF PHOTOCHEMICAL SMOG

Frank L. Worley, Jr.*
Division of Meteorology
Bureau of Air Pollution Sciences
Office of Research and Monitoring
Environmental Protection Agency

For presentation to the Panel on Modeling, NATO/CCMS Pilot Project on Air Pollution, Paris, France, July 26-27, 1971

*On leave from the Chemical Engineering Department, University of Houston, Houston, Texas

ACKNOWLEDGEMENTS

The analysis presented in this report is based on the detailed technical descriptions of the several photochmeical air pollution models that are listed as references. Grateful acknowledgement is made to the pioneering work of the investigators involved and for the use of figures reproduced from their reports. Thanks are also due A.P. Altshuller, P.L. Hanst, W.M. Cox, W. H. Snyder and K. L. Calder for their invaluable assistance during the preparation of this report.

TABLE OF CONTENTS

1. Introduction... XIII-4
2. Formulation of the Model.............................. XIII-6
3. Presentation and Analysis of Current Models........... XIII-14
4. Summary.. XIII-66
5. References... XIII-72
6. Appendix... XIII-73

INTRODUCTION

Photochemical smog is one more by-product of the major industralized metropolitan area. The large concentration of commercial enterprise, coupled with the use of fossil fuels for energy and internal combustion engines for transportation, has led to an increase of photochemical smog in the U.S.A. The combustion process involving air and hydrocarbons generates the reactive hydrocarbons and oxides of nitrogen needed for photochemical reactions. These compounds plus others will react in the presence of sunlight to form photochemical smog. Although the ingredients for formation of this smog are present in most areas of the world, the incident rate for serious events is low except for major metropolitan areas.

This low rate can be attributed to the need for a unique combination of chemical concentration, meteorological conditions, and residence time. If the concentration of the reactive chemicals is low, the wind high, or cloud cover too great, the level of photochemical pollution will be low. In order to quantitatively predict the conditions which will cause high pollutant concentration, several mathematical models have been proposed. These models combine emission data and meteorological information with reaction kinetics equations in order to predict the temporal and spatial distributions of pollutants in the area of interest.

It is important, at this point, to examine the potential uses of mathematical models for air pollution in general and photochemical smog in particular. Air pollution control, to improve the local air quality, involves both short, or real time, and long term objectives which are not necessarily compatible. Short term problems are usually concerned with answering today's problems: controlling existing sources with available resources such that desired pollution levels are maintained; providing advance warning when it appears that a severe episode will occur; etc. In contrast to these problems, the long term objective is tied to planning or applications. Answers to questions concerning expansion of existing plants or location of new facilities, either commercial or industrial, can be sought by the long term model. Long term, as used here, does not imply that the model is directed to predicting pollution concentration averaged over several days or months.

The long term problem is much more amenable and tractable than the short term or episode version in that real time data are not needed and events (emissions, meteorology, etc) may be adjusted or modified to determine the consequence of such action. This feature will be of significant value in comparing proposed control strategies in order to implement stricter air quality laws with the least difficulty and cost.

Included in this report are sections which:

a) present the general equations required to formulate a mathematical model to describe photochemical smog formation and its distribution;

b) discuss some simplified versions of the general equations;

c) present and analyze current approaches to formulation and solution of mathematical models;

d) summarize current efforts and indicate research needs.

FORMULATION OF THE MODEL

The basic mathematical statement for description of the temporal and spacial distribution of the chemical species is the mass balance or continuity equation. These expressions, one for each species, plus the appropriate boundary and initial conditions complete the description. The photochemical model is concerned with the several species which are undergoing chemical conversion initiated or propagated by sunlight. A separate continuity equation must be written for each compound of interest.

The continuity equation (rectangular coordinate system for the ith species is:

$$\frac{\partial c_i}{\partial t} + V \cdot \nabla c_i = \nabla \frac{(D_i \partial c_i)}{\partial x_j} + R_i \qquad (1)$$

where: c_i = concentration of species i

V = velocity vector (V_x, V_y, V_z)

D_i = diffusivity of species i in the gas mixture

R_i = rate of generation of species i by chemical conversion

For the case of turbulent flow, equation 1 is interpreted as follows:

a. c_i and v are assumed to include a time average (bar over term) and a fluctuating component.

b. Terms including only concentration fluctuation may be neglected.

c. Cross products of velocity and concentration may be represented by Prandtl's mixing length analogy -- eddy diffusion coefficient times the concentration gradient.

d. The chemical conversion rate is proportion to average concentration.

e. Molecular diffusion coefficient is small compared to the turbulent coefficient, K_j.

The resulting equation is:

$$\frac{\partial \overline{C}_i}{\partial t} + \frac{\partial \overline{C}_i}{\partial x} \overline{V}_x + \frac{\partial \overline{C}_i}{\partial y} \overline{V}_y + \frac{\partial \overline{C}_i}{\partial z} \overline{V}_z = \frac{\partial}{\partial x} (K_x \frac{\partial \overline{C}_i}{\partial x}) + \frac{\partial}{\partial y} (K_y \frac{\partial \overline{C}_i}{\partial y}) +$$

$$\frac{\partial}{\partial z} (K_z \frac{\partial \overline{C}_i}{\partial z}) + R_i \qquad (2)$$

for $i = 1, 2, 3, \ldots N$. The bar indicates a time average value, averaging time to be specified.

The eddy diffusion coefficient, K_j, and the mean velocity, V_i, are highly dependent upon position and meteorological parameters and must be estimated by using experimental data and empirical correlations. In addition, the non-linear set of rate equations for R_i includes rate coefficients which are concentration and temperature dependent.

Exact solutions to this set have not been published. However, it is possible to obtain approximate solutions using numerical techniques. To date these solutions have been unsatisfactory except for selected situations, namely simplified versions. The major difficulties arise due to such factors as artificial diffusion due to finite difference approximations, linearization of reaction equations and turbulent diffusion coefficients, and the need for extremely large, fast computers.

Simplified Models

The simplest and most restricted case assumes that wind speed is negligible and that the pollutant sources are uniformly distributed. This case occurs during the early morning hours for a restricted number of days each year. Equation 2 then reduces to

$$\frac{\partial \overline{C}_i}{\partial t} = K_z \frac{\partial^2 C_i}{\partial z^2} + R_i \qquad (3)$$

for each species. Approximate solutions to these equations may be obtained without great difficulty.

A second case of interest (for uniform sources) involves inclusion of the windward advection term ($\frac{\partial \overline{C}_i}{\partial x_i} \overline{V}_x$) to account for transport in at least one direction while assuming that vertical mixing is such that the vertical concentration distribution is uniform ($\frac{\partial \overline{C}_i}{\partial z} = 0$)

$$\frac{\partial \overline{C}_i}{\partial t} = \frac{-\partial C_i}{\partial x} \overline{V}_x + R_i \qquad (4)$$

The solution to these equations are applicable to areas beneath an inversion layer which have a well mixed air mass. They may also be applied to non-constant wind direction situations if the coordinate system is allowed to rotate to account for changing wind direction.

A different and potentially very useful approach, which involves the use of a cell or unit of volume, has recently been proposed. Two variations of the cell model are possible. The first assumes a stationary cell with permeable walls to permit exchange of mass, or a series of such cells stacked one on top of another. The second moves the cell along a trajectory with mass entering only through the bottom and/or top. This latter model may said to be "almost Lagrangian" in that the cell moves with the air. The resulting equation does not contain the usual advection terms. The major restriction of the moving cell model is that the cell does not exchange mass with other cells; that is, there is no lateral diffusion or interaction with any source not on the path of the cell. The continuity equation for the moving cell model is:

$$\frac{\partial \overline{C}_i}{\partial t} = K_z \frac{\partial^2 \overline{C}_i}{\partial z^2} + R_i \qquad (5)$$

The influx of each chemical species is computed by equating the flux to a turbulent diffusion coefficient times a concentration gradient, both evaluated at ground level.

The stationary cell equation is:

$$\frac{d(V_i \overline{C}_i)}{dt} = \Sigma Q_j \overline{C}_i - \Sigma Q_k \overline{C}_i + R_i \qquad (5a)$$

where: V_i = volume of cell

Q_j = inflow rate (volume) from surroundings

Q_k = outflow rate (volume) to surroundings

The summation terms account for the net exchange (of each chemical species) between the cell and the surroundings, including any sources and/or sinks.

Both variations of the cell model may be adapted to account for mean velocity gradient (vertical), changing inversion height and similar effects which cause complications in solving the general continuity equation (1).

The final approach involves transformation of the non-linear partial differential continuity equations into first order non-linear ordinary differential equations by means of the Lagrangian similarity hypothesis. This method can take into consideration atmospheric mixing and its influence on chemical reactions. The model is known as the puff or variable volume batch reactor and has been tested only for simple bimolecular reactions. Although this method appears attractive, many unresolved areas must be tested.

Each of the above transport/diffusion models requires accurate meteorological data for success. Their ability to describe the concentration distribution is directly dependent upon the quality and quantity of these data. At least three types of meteorological data are needed by these models in order to satisfy the differential equations and the boundary conditions: wind speed and direction, atmospheric stability or turbulent mixing, and mixing layer depth or inversion height. In most regions these data are gathered at only one or at most two locations. These sites are usually at or near the local airport which may be many kilometers from the city and may or may not be representative of urban topographical features. Although ground level meteorological data are related to the elevated region (100-1000m) values, calculations based only upon ground level observations at a restricted number of points are of limited value. It is unfortunate that the conditions of low wind velocity, localized instability, and shallow inversion depth are associated with periods of high pollutant concentrations and photochemical smog, because these same conditions are often associated with the largest spatial variations of the meteorological parameters. There is great need for improved prediction techniques and expanded field measurement capability of these variables.

Chemical Reaction Rate

Formulation of the system of rate (time rate of change of concentration) equations which describes the reactions taking place due to photochemical effects has been based upon the Rice-Herzfeld approach. This approach requires an overall reaction composed of a number of elementary irreversible reaction steps. A rate equation is generated for each elementary step.

The steps are grouped into three categories: chain initiating, chain propagating, and chain terminating. The net rate of formation of a given chemical specie is obtained by algebraically summing all rate equations involving that compound. The ultimate purpose of this procedure is to simulate the actual photochemical reaction process which generates the photochemical smog. Unfortunately, this system (urban atmosphere) involves a very large number of reactive species which implies a very large number of elementary steps. The likelihood of determining the true sequence of reaction steps for such systems is extremely remote. However, simplified models, which assume stationarity and/or lumped equations*, and which adequately describe experimentally observed data, have been formulated.

An additional difficulty imposed upon these models is that of obtaining experimental data for validation. These data have been collected in smog chambers of varied design and in many different laboratories. Special care must be taken in such experiments to ensure that wall effects are not significant, that the system is homogeneous, that the concentration levels are the same as those encountered in the atmosphere, that the artificial radiation has the same spectral distribution as in the atmosphere, that the system is sampled properly, and that the chemical analysis is carried out with adequate precision. None of the data sets, particularly those

*See Appendix for discussion of this technique.

obtained prior to the late sixties satisfy all of these requirements. In spite of these difficulties, data must be selected and mechanisms tested if a model is to be implemented.

Emission rates

An additional parameter of prime importance to the model is that of input reactants from ground level or elevated sources. In a large industrialized urban area such as Los Angeles, New York,or Houston, potential pollutants are generated by thousands of stationary sources and millions of automobiles, trucks,and other internal combustion engines. Many hundreds of different chemical compounds, all potential pollutants, enter the atmosphere from these sources. If the model is to have any degree of success, accurate temporal and distributions of these pollutant sources be known.

A number of approaches involving traffic count, gasoline consumption, or direct measurements along primary and secondary roads have been proposed and used for mobile sources. Emission rates for stationary sources are usually obtained by direct survey or by an educated estimate of probable values based upon knowledge of the operation and process.

In each case the data are known to be incomplete, due to the lack of an adequate chemical breakdown (e.g., hydrocarbons), a poor time frame such that changes in rate due to process conditions or production are masked and other difficulties. The major problem associated with emission estimates is the present inability to independently verify data obtained by the various techniques. Although more extensive data collection programs are needed and should be of value in improving the accuracy of existing methods, it is unlikely that significant improvement will soon be achieved for the general problem. The prediction methods or models will still require extensive field data in order to perform satisfactorily in new urban areas.

PRESENTATION AND ANALYSIS OF CURRENT MODELS

In the preceeding section the several approaches to (photochemical smog) modeling and the modules or sub-divisions required to formulate a model which will predict the temporal and spacial distribution of photochemical pollutants were presented. In this section a detailed analysis of the current application of these approaches is made.

General Research Corporation has developed two photochemical smog models for application to the Los Angeles Basin problem. Their earliest model used a simplified version of the general continuity equation; one dimensional transport by advection and vertical turbulent diffusion, a greatly simplified lumped-parameter photochemical reaction mechanism involving seven chemical species and seven rate equations, emission data were estimated from Los Angeles County Air Pollution Control District (LAAPCD) inventory estimates based upon gasoline consumption, with time and space distribution approximated from traffic survey data while non-automotive sources were averaged and employed as constant background emissions.

Transport/diffusion module

The simplified continuity equation of this model is:

$$\frac{\partial \overline{C}_i}{\partial t} = -\frac{\partial \overline{C}_i}{\partial x} \cdot V_x + \frac{\partial}{\partial z}\left(K_z \frac{\partial \vec{C}_i}{\partial z}\right) + R_i \qquad (6)$$

Integration is accomplished by using the Runge-Kutta method.

Mean vertical advection (V_z) is assumed to be unimportant because of the channel like character of the marine layer. Horizontal diffusion is assumed to be relatively unimportant because of the nearly uniform distribution of emission sources. As a result any validation performed is not greatly influenced by individual sources.

The turbulent diffusion coefficient, K_z, is calculated by assuming a trapezodial vertical profile. At low levels, K_z increases linearly with z to some constant value. At intermediate levels K_z is constant. As the inversion layer is approached, it decreases linearly with increasing z. The ground level and inversion layer values are equal. The maximum constant value is computed by

$$K_z = 50\ V_x + 5\ \text{m}^2/\text{min} \tag{7}$$

This occurs at an elevation of 40 to 100 meters depending upon meteorological conditions. Although complete details concerning the actual slope (ground and inversion region) and method for determining the boundary and plateau level are not presented, the method is based upon experimental data and should be adequate for this problem.

The inversion depth or mixing region has been assumed to be constant over the total region and not to vary with time. This assumption is not correct for the Los Angeles Basin (note, the GRC authors did include temporal variation in a later version discussed in the next section) and should result in significant errors. These errors are due chiefly to the fact that the concentration of any compound is closely tied to the total volume for mixing. This volume will be too small and, as a result, concentration and rate of reaction too high if the inversion depth increases during the period of interest and too large if the inversion depth decreases.

Photochemical kinetics module

The photochemical reaction kinetics module proposed for this model includes only seven chemical species and seven rate equations. This simplified version of the kinetics was obtained by successive trials of a much more general set of equations. The basis for selection was the fit of computed concentration profile to smog chamber data. Only those equations which exhibited rate-controlling effects were included in the final version. No claim is made that the scheme is a complete mechanism embodiment of the true chemical kinetics. The reactions are given in List 1, and identified in text as a, b, c, d, e, f, g, and h.

LIST 1

Reactions

$h\nu + NO_2 \rightarrow NO + O$ (a)

$M + O + O_2 \rightarrow O_3 + M$ (b)

$O_3 + NO \rightarrow NO_2 + O_2$ (c)

$O + \text{Hydrocarbon} \rightarrow 2.5RCO_x + \text{Aldehyde}$ (d)

$O_3 + \text{Hydrocarbon} \rightarrow 2.5RCO_x + \text{Aldehyde}$ (e)

$RCO_x + NO \rightarrow NO_2$ (f)

$RCO_x + O_2 \rightarrow 1/2\ O_3$ (g)

$RCO_x + NO_2 \rightarrow 2/3\ PAN$ (h)

The scheme includes three (a, b, c) inorganic reactions which generate oxidants O_3, O and NO_2 from reactions involving sunlight, oxygen, and nitrogen dioxide. These oxidants react (d,e) with the hydrocarbon to form aldehyde products and free radicals (RCO_x). The final equations (f, g, h) are concerned with the reaction of free radicals with nitric oxide, oxygen or nitrogen dioxide to generate organic nitrate (PAN) product or oxidants (O_3 or NO_2).

Reactions involving O or RCO_x are such that quasi-stationarity may be assumed and the differential equation (rate) treated as an algebraic expression, thus reducing the number of variables by two. The oxidation of the hydrocarbon in steps d and e is much more complex than indicated by the two reactions specified. However the steps in the manner indicated appears to yield reasonable agreement with chamber data for the time span validated. Since this is only a curve-fit, extrapolation to longer time periods should not be encouraged.

A typical rate equation, say reaction c, will be

$$R_{NO_2} = \frac{d\overline{C}_{NO_2}}{dt} = k_c\ (\overline{C}_{O_3})(\overline{C}_{NO}) \qquad (8)$$

where: R_{NO_2} = rate of formation of NO_2

k_c = rate coefficient for reaction c

(C_{NO})= concentration of NO

(C_{O_3})= concentration of O_3

The value of k_c is dependent upon the initial concentration of the reactants NO and O_3 and on the state variables temperature and pressure. The reaction is assumed to take place at constant temperature and pressure.

The condition of quasi-stationarity requires that Ri, the rate of appearance of the product i, be set to zero.

In order to develop a complete rate expression for any chemical species, each reaction involving that compound must be included. For example,

$$R_{NO_2} = \frac{d\bar{C}_{NO_2}}{dt} = -r_a + r_c + r_f - r_h \qquad (9)$$

for O (rate set equal to zero)

$$R_O = 0 = r_a - r_b - r_d \qquad (10)$$

$$r_a = r_b + r_d \qquad (11)$$

where

$$r_a = k_a(NO_2) \qquad (12a)$$

$$r_b = k_b(O)(O_2) \qquad (12b)$$

$$r_d = k_d\ (O)(\text{Hydrocarbon}) \qquad (12c)$$

Parentheses around the chemical compound symbol indicates concentration. Substitution of equations 12a, b, and c into 11 yields

$$k_a(NO_2) = k_b\ (O)(O_2) + k_d\ (O)(\text{Hyd}) \qquad (13)$$

Solving for (O)

$$(O) = k_a(NO_2)/(K_b O_2) + k_d\ (\text{Hyd}) \qquad (13a)$$

This expression for the concentration of O can be used to eliminate O from the other rate equations, thus reducing the number of variables.

The interactions between the several compounds can be demonstrated by constructing a block diagram of the reaction set. The diagram for this system is presented in Figure 1.

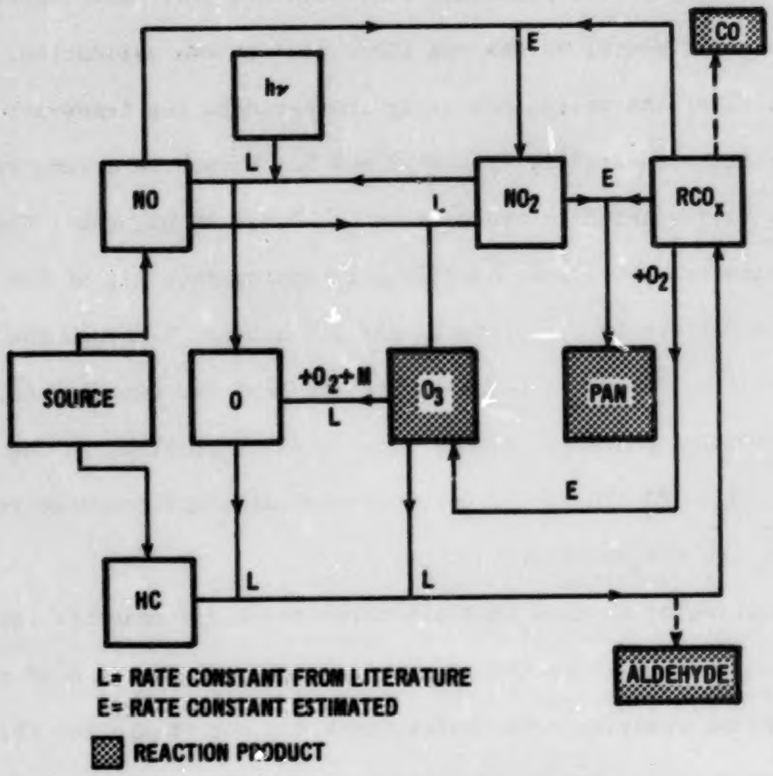
CO
E
hν
L
NO
L
NO$_2$
E
RCO$_x$
+O$_2$
SOURCE
O
+O$_2$+M
L
O$_3$
PAN
E
HC
L
L
ALDEHYDE
L= RATE CONSTANT FROM LITERATURE
E= RATE CONSTANT ESTIMATED
▨ REACTION PRODUCT

Figure 1. Lumped-parameter reaction mechanism.

The rate coefficients for the several reactions were obtained from smog chamber experiments and/or estimated from kinetic rate theories. As previously noted, it was necessary to adjust several of the values to improve the accuracy of the predicted concentration profiles. Table 1 presents both experimental values and those used in the validation.

The results of the validation using chamber data for trans-2-butene and propylene are presented in Figures 2 and 3. Butene is a very reactive species which is converted to products in less than 30 minutes. The calculated concentration curves provide only approximate fit of the experimental data, particularly for products PAN and ozone, although the calculated concentration for NO_2 appears to fit the last two experimental points. The validation using propylene demonstrates similar problems in the intermediate time range (80-120 min.). Concentration data and computed results for NO and NO_2 are not presented.

It is encouraging to note that all three inorganic reaction rate coefficients agreed well with the literature data, and that two of the three free radical reaction rate coefficients did not change for the two hydrocarbon systems tested. According to the GRC authors, it was necessary to increase the lumped oxidation reaction, (e), involving O_3 by a factor of 50 times the experimental value. This adjustment in turn required that additional ozone (O_3) be produced via reaction b or g. They chose to increase the rate for reaction g. (See Table 1).

Less encouraging is the fact that the atmosphere does not contain just one or two reactive species but is in fact a complex mixture. This

TABLE 1

REACTION RATE COEFFICIENTS

Hydrocarbon	Reaction	Experimental	Validation	Units
trans-2-butene (C_4H_8)	a	.072 → .55	.072 → .55	min^{-1}
	b	1.32×10^{-5}	1.32×10^{-2}	$ppm^{-2}\ min^{-1}$
	c	21.8	21.8	$ppm^{-1}\ min^{-1}$
	d	3.34×10^{4}	1.11×10^{5}	$ppm^{-1}\ min^{-1}$
	e	$4.2 \times 10^{-2} \rightarrow 6.4 \times 10^{-1}$	6×10^{-1}	$ppm^{-1}\ min^{-1}$
	f	≤ 50	50	$ppm^{-1}\ min^{-1}$
	g	≤ 50	5×10^{-6}	$ppm^{-1}\ min^{-1}$
	h	≤ 50	6	$ppm^{-1}\ min^{-1}$
Propylene (C_3H_6)	a	0.4	0.4	min^{-1}
	b	1.32×10^{-5}	1.32×10^{-5}	$ppm^{-2}\ min^{-1}$
	c	21.8	21.8	$ppm^{-1}\ min^{-1}$
	d	6.8×10^{3}	4.97	$ppm^{-1}\ min^{-1}$
	e	$9.3 \times 10^{-3} \rightarrow 1.2 \times 10^{-2}$	1.8×10^{-1}	$ppm^{-1}\ min^{-1}$
	f	≤ 50	50	$ppm^{-1}\ min^{-1}$
	g	≤ 50	2.3×10^{-5}	$ppm^{-1}\ min^{-1}$
	h	≤ 50	6	$ppm^{-1}\ min^{-1}$

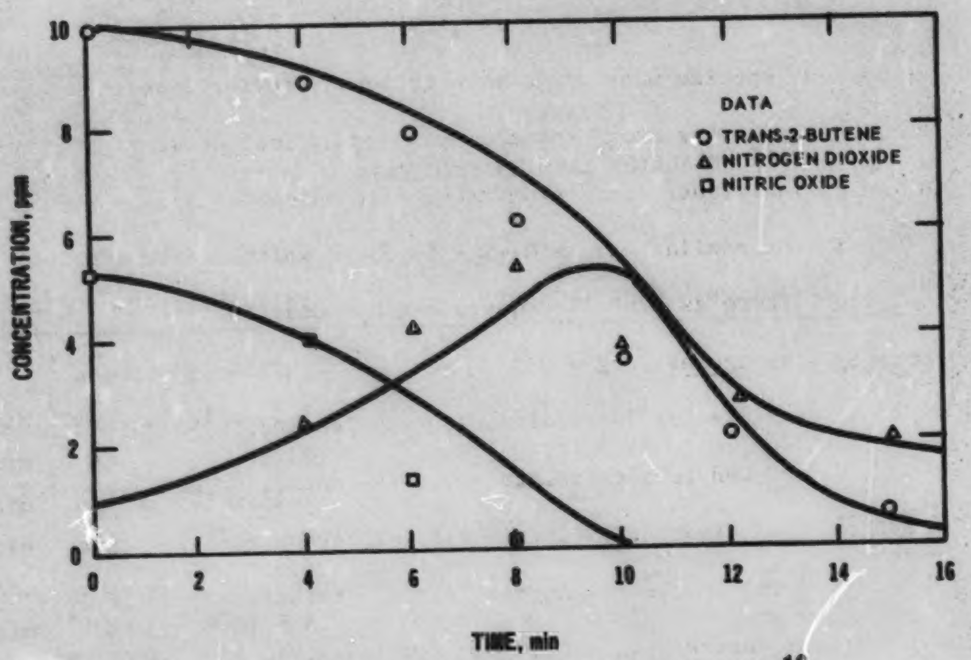

Figure 2. Computed and observed reactant histories[16].

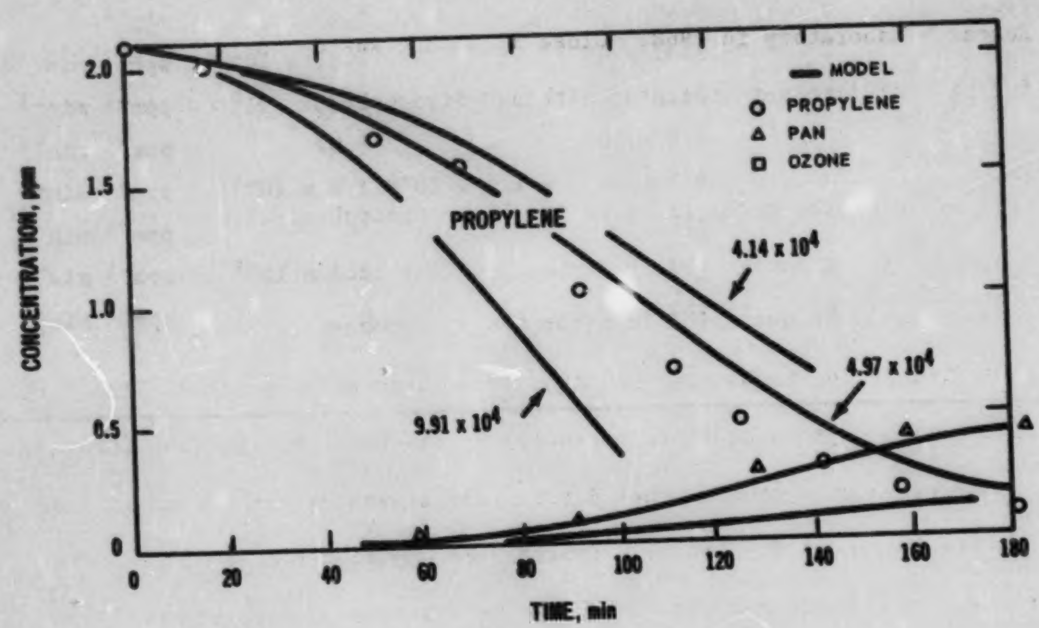

Figure [illegible] ated and observed composition history[22].
Nu[illegible] propylene curves indicate values for model
[illegible] k_4 (ppm^{-1} min^{-1}).

mixture may include species many times more or less reactive than the two reported. Interactions among these compounds may include acceleration or retardation of individual conversion rates. It is doubtful if a simple weighting function or similar approach will be found which can be applied to represent the mixture as a single equivalent hydrocarbon.

Test Results for Los Angeles

In order to test the transport/diffusion modules and to exercise the numerical techniques used to approximate the differential equations, calculations were made to estimate the distribution of carbon monoxide (assumed to be chemically inert) in the Los Angeles Basin. Emission of CO in this region is due almost entirely to automotive sources. The flux distribution for these sources was predicted using gasoline consumption data from LAAPCD. Boundary and initial values were obtained from the field data collected by Scott Research Laboratory in 1968. Close agreement was demonstrated by the model for the one data set presented although divergence appears after six hours lapse time.

Application of the model to cases involving photochemical reactions did not yield this agreement. Many of the problems encountered are of the type which cannot easily be uncoupled from the whole. Concentration is determined by transport, reaction mechanism and rate, as well as emission flux. Transport has been shown to be reasonably well handled as has been the reaction mechanism through comparison with smog chamber data. This leaves emission flux as the most probable source of difficulty. Implicit in the flux problem is that of representing the complex hydrocarbon system by a single hydrocarbon such as propylene. However, it is necessary to use data (per se, modified or adjusted) and information available to validate the model and to make a decision concerning the various modules. Both emission flux and rate constants were adjusted to improve agreement with observed values. The effect of these adjustments on concentration and the range explored is shown in Figures 4, 5, and 6.

The best ratios (flux, 1/4 and rate constant, 1/2), as determined by goodness of fit of calculated values to field data, were used to compute concentration histories at Huntington Park. The results for ozone are presented in Figure 7. The notation, type 2, means that either of the two reference stations had a measured peak oxidant concentration greater than 30 pphm during the day. It is of interest that the very simple homogeneous mixing model predicts ground level concentration very well until about 12:00. After 12:00 this model diverges from the data greatly due to its inability to respond to the changing transport character. In this particular case, concentration gradients which result in different conversion rates ($R_i \alpha \Pi C_i$) must have occurred. This in turn would cause the production rate of ozone to fall as correctly predicted by the Five Station Diffusion Model. Although the model does not predict pollutant ground level concentrations with high accuracy, it has been able to correctly predict the proper trends and approximate time for maximum concentration.

GRC mathematical model (1969 version) for photochemical smog:

1. Transport/diffusion: Transport is in a single direction with

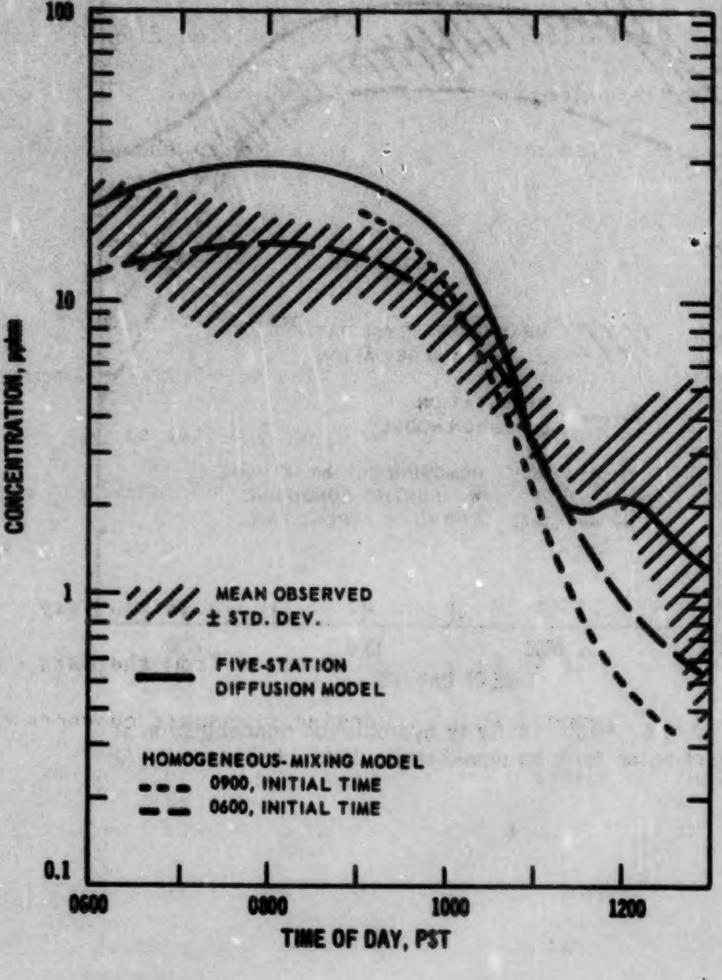

Figure 4. Nitric oxide concentration at Huntington Park on type-2 day, 1968. f = 1/4; r = 1/2.

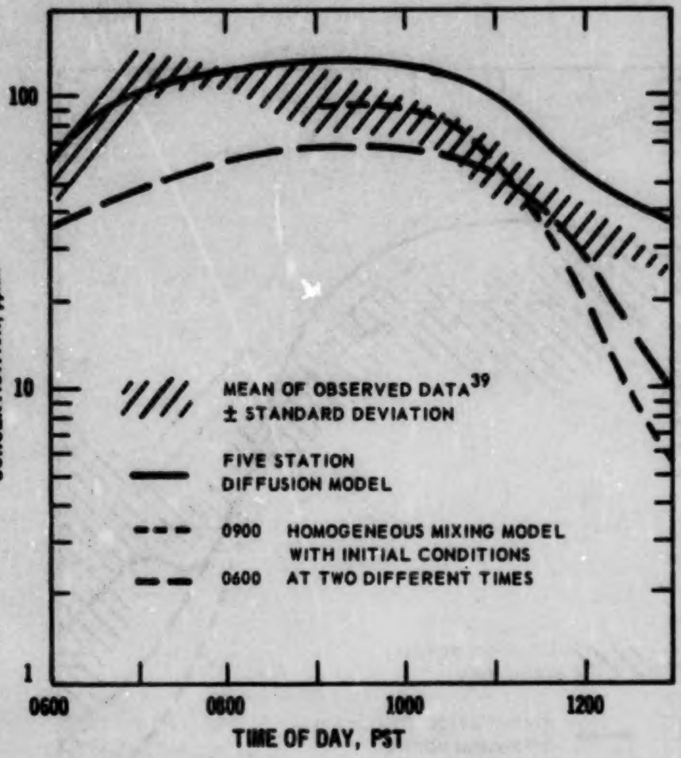

Figure 5. High reactivity hydrocarbon concentration at Huntington Park on type-2 days, 1968. f = 1/4; r = 1/2.

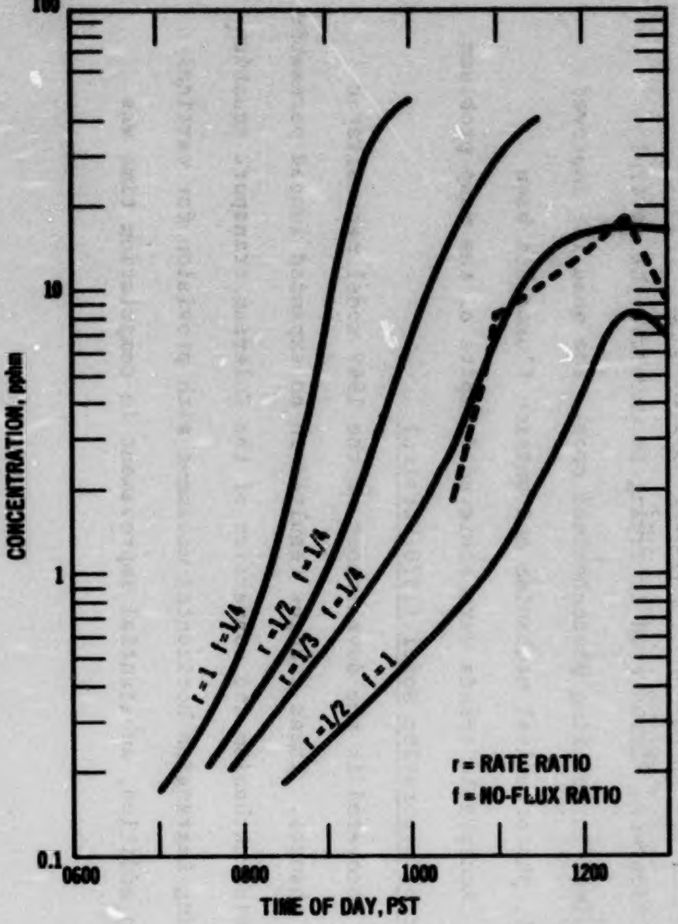

Figure 6. Ozone concentration at Huntington Park. Dashed line represents SRL data[39].

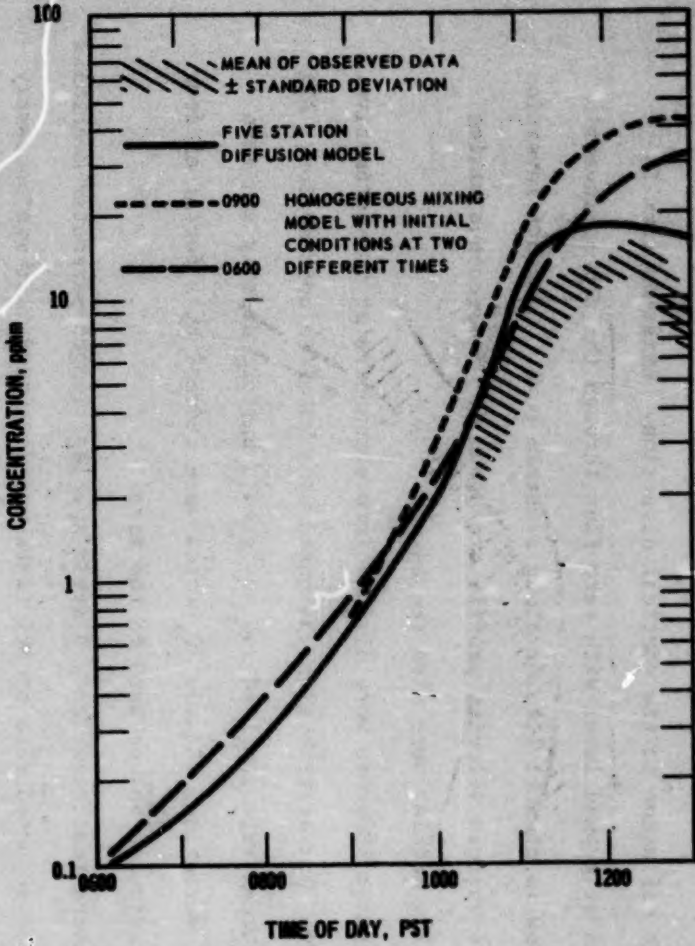

Figure 7. Ozone concentration at Huntington Park on type-2 days, 1968. f 1/4; r 1/2.

turbulent diffusion in the vertical direction. Emission flux is specified at ground level with zero flux through the top or inversion lid. Flow is channel-like or along a stream tube. Constant inversion depth and uniform velocity profile are assumed. Homogeneous mixing and no-flow modules were also tested.

2. Emission: Sources were divided into automotive or non-automotive. Automotive flux distribution was based upon gasoline consumption. All other sources were combined and assigned a uniform density and zero temporal variation. Source NO_x rates were reduced by a factor of four and the adjusted values used in the model.

3. Photochemical kinetics: A seven species, lumped parameter mechanism which uses adjusted rate coefficients was developed. It was necessary to adjust the hydrocarbon (propylene) rate coefficient to one-half of the value found to fit smog chamber data in order to simulate the complex reactions of hydrocarbons in the atmosphere.

Major difficulties were encountered in trying to uncouple the several variables involved in modeling photochemical smog. The need for improved meteorological, photochemical mechanism and emssion fluxes has been demonstrated. Acceptable trends were achieved in spite of the many problems.

General Research Corporation Model (1970 Version)

Problems uncovered in the development of the 1969 model necessitated several major changes. These changes resulted in an expanded lumped parameter chemical kinetics mechanism and conversion of the Eulerian transport equation to one involving Lagrangian horizontal movement with provision for vertical diffusion. In addition, substantial improvement in computation time was accomplished by substitution of Padé approximate technique for the Runge-Kutta method previously used. The net result of these changes is conversion of the model from real time prediction to the strategy or analysis mode of operation.

Modified transport/diffusion module

The Langrangian* form of the continuity equation for a single chemical species is:

$$\frac{\partial \bar{C}_i}{\partial t} = \frac{\partial}{\partial z} \left(K_z \frac{\partial \bar{C}_i}{\partial z} \right) + R_i \qquad (14)$$

This partial differential equation is transformed into an ordinary differential equation by applying what the GRC authors term a "method of lines." This is accomplished by assuming a zero concentration gradient in the lateral direction (actually normal to the trajectory or path) and applying a finite difference approximation to the vertical exchange term. Each line represents a separate elevation, and the resulting ordinary differential equation describes the concentration of an element of fluid or cell moving along the line. The cell can exchange mass (pollutants) only through vertical (z directions) turbulent diffusion. The uppermost cell which corresponds to the inversion lid is constrained by a zero flux plane at the lid. The equation for each species resulting from this transformation is

$$\frac{d\bar{C}_j}{dt} = \frac{K_z}{(\Delta_z)^2} \left(C_{j-1} - 2C_j + C_{j+1} \right) + R_j \qquad (15)$$

*Substantial derivative is denoted by $\partial/\partial t$ as in reference where C_j and R_j are local values of concentration - and reaction rate vectors of length equal to the number of chemical species under consideration. The subscript "j" determines the location in a vertical grid ($1 \leq j \leq m$, where m = number of mesh points from the ground up to the mixing depth or inversion lid).

Movement of the cell along a line or path is described by a trajectory which must be obtained from field measurements of wind speed and direction. The trajectory or advection pattern, as it is called by the GRC authors, is obtained by taking a weighted average of wind station reading surrounding the point in question. This value is then assumed to represent the cell movement during the current time increment. Reciprocal distance weighting is employed, but the algorithm has not been developed adequately to handle situations involving boundary conditions where mountain ridges or coastal areas are involved. These cases must be handled as special problems involving intervention in the computation as these regions are approached.

Mixing depth, which dictates the vertical distance to be handled by the difference equation ($\partial^2\overline{C}/\partial z^2$), must be known as a function of time and position along the trajectory. Although this requirement is noted, an average value for the whole region is assumed for each case tested.

To apply the revised transport/diffusion module the following must be accomplished.

1. Select a receptor location.
2. Specify the time (hour of the day) for which ground level concentration at the receptor is required.

3. Starting at the specified time and site location compute a reverse (upwind) trajectory for a specified time increment using the inverse distance technique.

4. Repeat step 3 until total time and/or distance is covered.

5. Calculate an average inversion base altitude using field data for basin.

6. Estimate initial ground level concentrations.

It would be time consuming and difficult to use this method to determine the effect of a specified source on the basin because of the very large number of trajectories required and the inability of the method to handle cross-wind effects.

Modified chemical kinetics module.

As a result of new information and a better understanding of the photochemical reaction process the seven-step lumped-parameter mechanism has been expanded to account for varying ratios of oxides of nitrogen to reactive hydrocarbon and additional reaction products. These improvements result in an increase in the number of reaction steps to twelve and include additional lumped parameters.

This problem regarding the ozone and elemental oxygen encountered in the previous model has been partially solved by the addition of reaction steps to oxidize hydrocarbons and to generate new free radical species which in turn can generate nitrogen dioxide and additional free radicals. The free radicals are also involved in the formation of organic nitrates and nitric acid end products. It was not possible to construct truly elementary steps involving these new species, and, as a result, non-stoichiometric coefficients must be used to ensure stability of the system.

In addition to the changes in the chemical reaction mechanism, the computer algorithm has been improved to permit a mulitiplicity of reactive hydrocarbons in the reacting mixture. The reaction mechanism, including the coupling and interaction among the several steps, is presented in Figure 8. Free radicals are RO_2 or HO_2 and RO or HO. The twelve reaction steps and rate coefficient values are presented in Table 2. Comparison of these figures with those presented for the earlier version shows that the main differences involve addition of a new radical species, RO, the elimination of ozone (O_3) production from an RO_2 reaction, formation of HNO_3 product and HNO_2 and the provision for a mulitplicity of hydrocarbons.

Rate coefficients were obtained as before; that is, initial estimates are taken from literature values and adjustments made until the best fit of the chamber data is obtained. Three of the rate coefficients for the six reaction steps included from the previous model did not require adjustment. The three adjusted coefficients now agree with experimentally determined values.

Non-stoichiometric coefficients for the free radial steps were determined by a similar hand-fitting process. The accuracy of fit is demonstrated in Figure 9 which presents time-concentration profiles for the photochemical reaction of propylene. Substantial improvement in the fit of the ozone and NO_2 data is demonstrated. However, results for PAN and aldehydes are not presented, and, as a result, a comparison for these products cannot be made. In addition, the multiple hydrocarbon feature was not tested such that chamber data could be compared with calculated values. An interesting exercise of

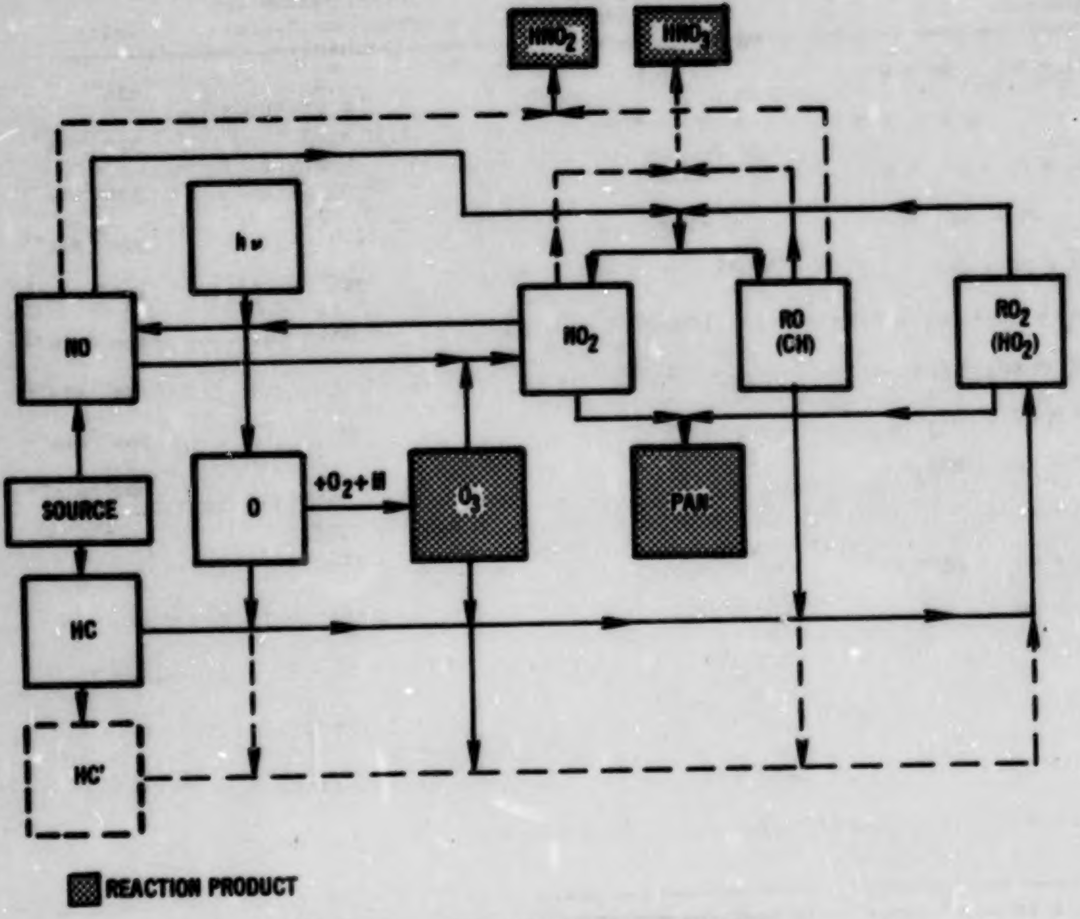
HNO_2
HNO_3
hν
NO
NO_2
RO
(CH)
RO_2
(HO_2)
SOURCE
O
$+O_2+M$
O_3
PAN
HC
HC'
▨ REACTION PRODUCT

Figure 8. Expanded kinetic mechanism.

TABLE 2

RATE COEFFICIENTS FOR MODEL HYDROCARBON/NITRIC OXIDE MECHANISM, GRC

(Stoichiometry imbalances may occur
because of lumped parameter assumptions.)

Reaction	Model Values From Validation	Normal Values for Propylene System	Units
$h\nu + NO_2 \rightarrow NO + O$	0.4	0.4	min^{-1}
$O + O_2 + M \rightarrow O_3 + M$	1.32×10^{-5}	1.32×10^{-5}	$ppm^{-2}min^{-1}$
$O_3 + NO \rightarrow NO_2 + O_2$	40	22-44	$ppm^{-1}min^{-1}$
$O + HC \rightarrow 2RO_2$	6100	6100	$ppm^{-1}min^{-1}$
$OH + HC \rightarrow 2RO_2$	80	244	$ppm^{-1}min^{-1}$
$RO_2 + NO \rightarrow NO_2 + 0.5\ OH$	1500	122	$ppm^{-1}min^{-1}$
$RO_w + NO_2 \rightarrow PAN$	6	122	$ppm^{-1}min^{-1}$
$OH + NO \rightarrow HNO_2$*	10	99	$ppm^{-1}min^{-1}$
$OH + NO_2 \rightarrow HNO_3$*	30	300	$ppm^{-1}min^{-1}$
$O_3 + HC \rightarrow RO_2$	0.0125	0.00927 - 0.0125	$ppm^{-1}min^{-1}$
$NO + NO_2 \rightarrow 2HNO_2$**	0.01		
$h\nu + HNO_2 \rightarrow NO + OH$	0.001		

---

*Rate constant lumps third body concentration

**Water vapor lumped into rate coefficient

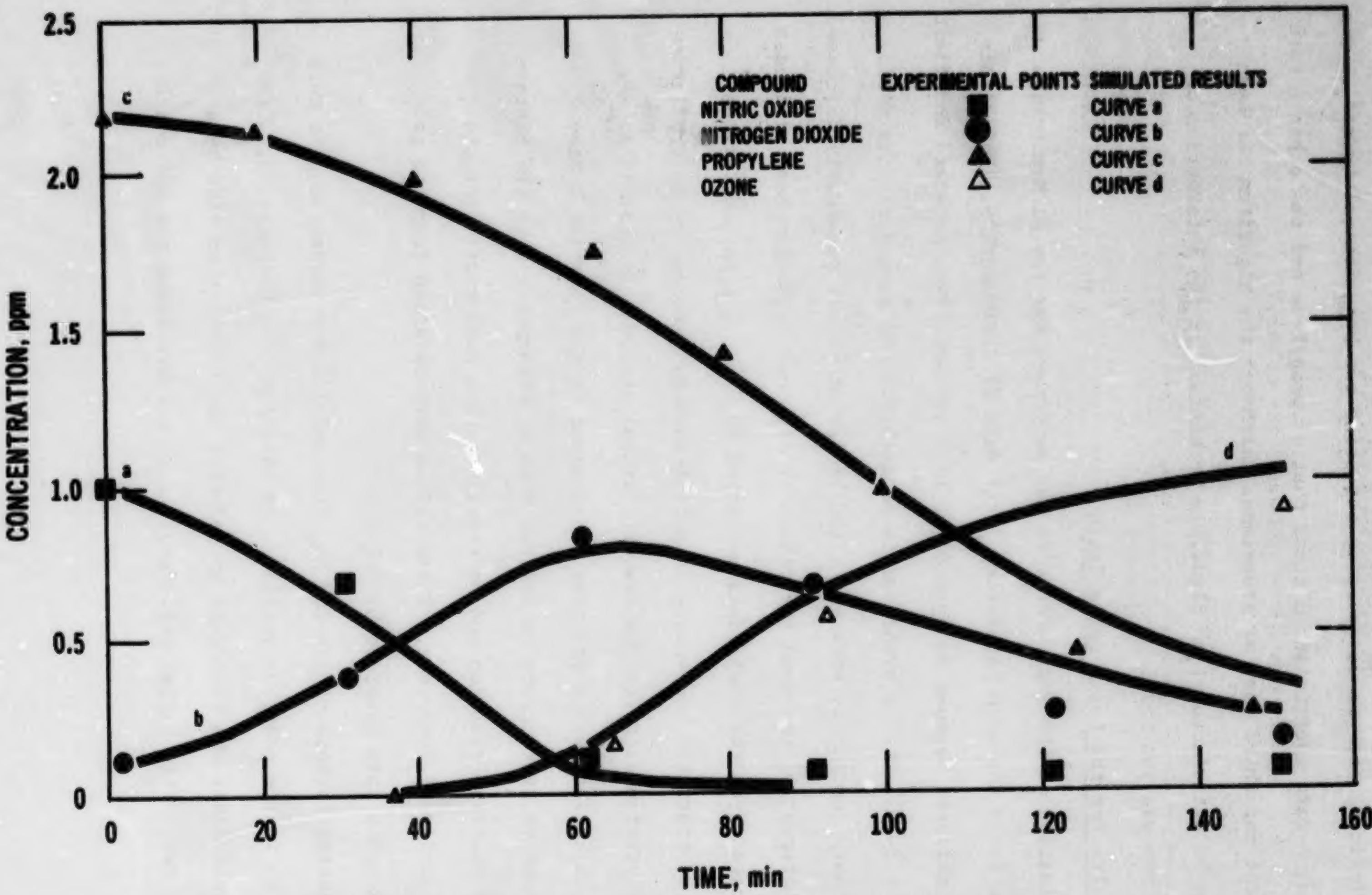

Figure 9. Computed curves compared with experimental points. (Experimental points taken from Altshuller, et al.[15])

the multiplicity feature was carried out using two hypothetical hydrocarbons; one having a rate coefficient 3 times that of propylene and the other a rate coefficient one third that of propylene. Although the algorithm has been proved to be satisfactory, no plausible mechanism for the interaction of hydrocarbons was put forth.

Test Results for the Los Angeles Basin

Validation of the improved model was performed for the El Monte site using the Scott Research Laboratory (SRL) data of September 29, 1969. This date was selected because an episode of high oxidant level occurred and field programs had collected a broad sample of airborne and ground station data.

Boundary conditions were specified by the procedure previously discussed. Updated information was used for vehicular flux and inversion base altitudes were averaged from the field data collected by SRL. Initial conditions required to start the trajectory computations were obtained by interpolation of ground station data for the nearest (Azusa) station. Because it is not possible to include every reactive hydrocarbon in the reaction scheme a pseudo reactive hydrocarbon is derived from an assumption that the mixture has a 34% reactive fraction and an average carbon number of 4 for the reactive family of compounds. These values were obtained from the gas chromatographic data obtained by SRL.

Weighting factors of 1/4 for NO_4 flux and 1/2 for oxidation rate were employed as in the previous version. In addition, the hydrocarbon, HC/NO_x ratio (field data) was preserved by reducing the hydrocarbon flux by a factor of two. This latter adjustment is acceptable since the hydrocarbon flux had previously been adjusted for reactivity in order to use the reaction kinetics module.

Trajectories needed for the validation were generated by the technique perviously noted. Concentrations histories for NO, NO_2 hydrocarbon and ozone were generated by the model for the air parcel or cell arriving at El Monte at 10:30 a.m. In addition, end point-values are presented for trajectories arriving in El Monte at 11:30 and 12:30. The results are presented in Figures 10, 11, 12, and 13.

The trajectory associated with an arrival time of 10:30 begins at 5:30 but computed results apparently start at 7:30. During the three hour period from 7:30 to 10:30, less than ten square miles are traversed and the net distance covered by the trajectory is less than five miles. Only minor spacial variation in emission flux occurs in the region and no significant point sources are encountered. Although the 11:30 and 12:30 trajectories are longer due to increased wind velocity after 9:30, similar flux distributions are encountered. It is unfortunate that trajectories which cross areas having greater variation in pollutant flux were not tested as such tests would aid in determining the validity of using the several weighting factors for emissions and reaction rates. The availability of additional field data for other stations will permit these tests to be made. These data are also needed to establish initial conditions for the trajectory and end point data for validation.

Each figure presents three items of information:

1) the concentration at ground level for the air parcel as it

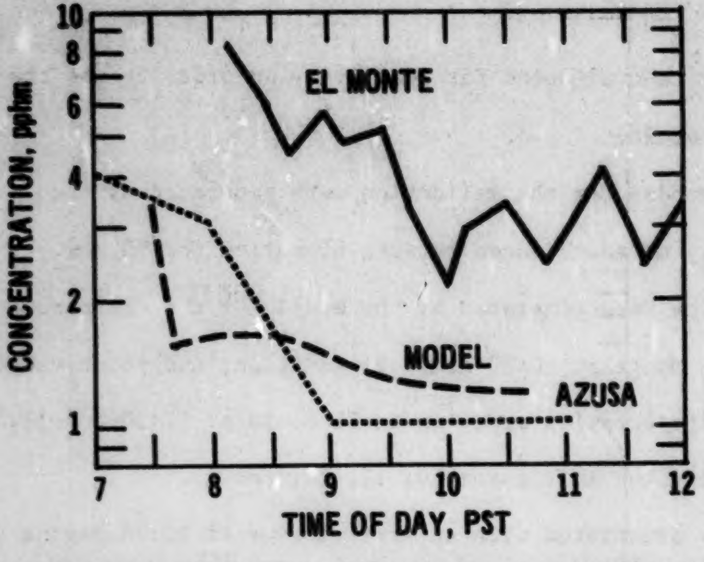

Figure 10. Nitric oxide history along 1030 trajectory; f = 1/4 and r = 1/2 (ground-level concentrations).

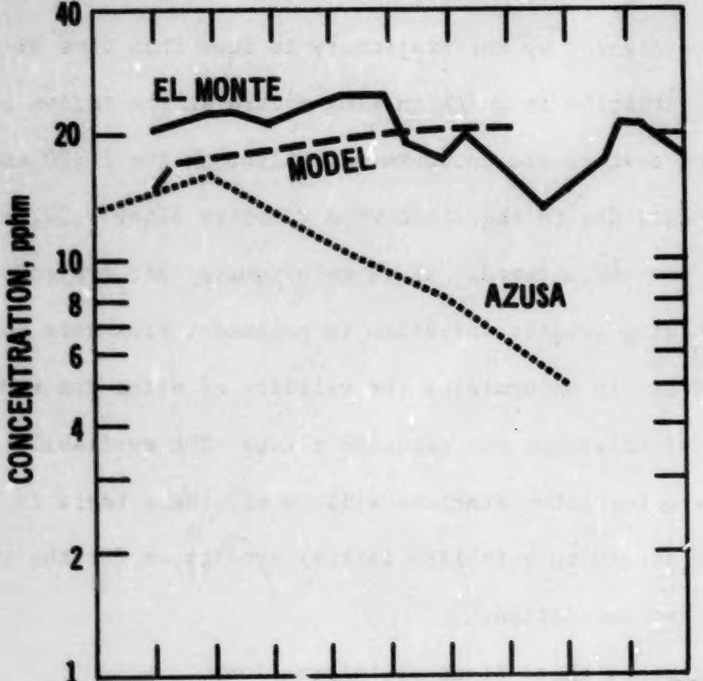

Figure 11. Nitrogen dioxide history along 1030 trajectory; f = 1/4 and r = 1/2 (ground-level concentrations).

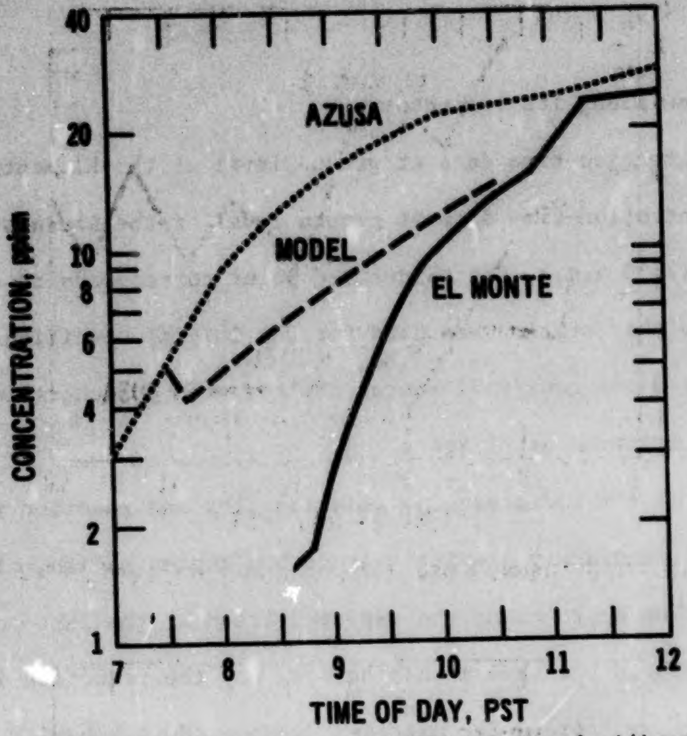

Figure 12. Ozone history along 1030 trajectory; f = 1/4 and r = 1/2 (ground-level concentrations).

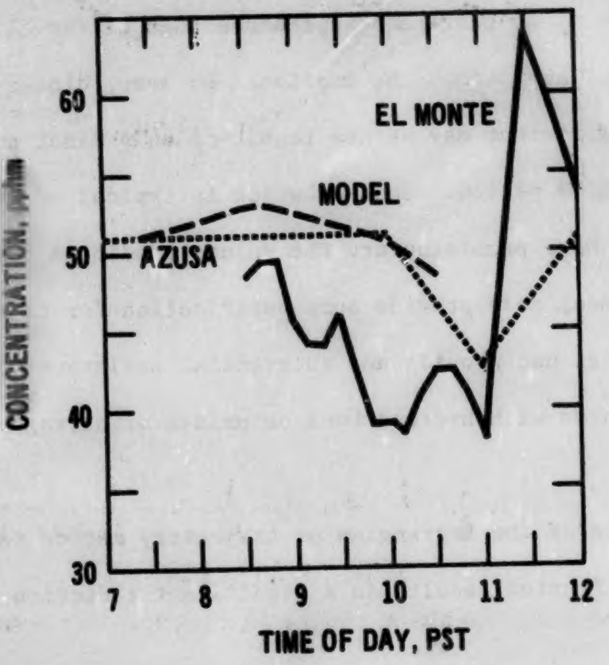

Figure 13. Reactive hydrocarbon history along 1030 trajectory; f = 1/4 and r = 1/2 (ground-level concentrations).

progresses along its trajectory

2) concentration-time data at ground level at the El Monte Station

3) concentration-time data at ground level at the Azusa station.

At time zero (7:30 a.m.), the calculated point corresponds to the data at Azusa since that station was used for the initial conditions. As the air parcel moves toward El Monte, the computed concentration should approach that measured at El Monte.

In spite of the reductions in emission flux and reaction rate the model does not accurately predict hydrocarbon concentration, although it does appear to be approaching the expected trend at the last point. Nitrogen oxide (NO) exhibits the same poor behavior, and the reduction in flux does not seem to be justified. The nitrogen dioxide (NO_2) behavior is much more nearly what one would expect or hope to see; that is, the initial value leaves the Azusa curve and approaches that of the El Monte station as the air parcel approaches the station. However, closer examination reveals that this good agreement may be the result of only minor possible variation in NO_2 for the time period. Such behavior is typical of data obtained in smog chambers. More promising are the values predicted for ozone (O_3). This good agreement does provide some verification for the improved kinetics mechanism but does not provide any substantial assistance in solving the problems associated with hydrocarbons or oxides of nitrogen.

The adoption of the Lagrangian or trajectory method for atmospheric transport and diffusion results in a significant reduction in computation time and computer memory requirement. However, this improvement does change the scope of application from complete area coverage to a single trajectory and (from complete area coverage to a single trajectory) from a predictive or extrapolation mode to one involving only after-the-fact strategy or analysis.

Expansion of the seven species lumped parameter photochemical module to include additional free radicals and nitrogen compounds has resulted in a more accurate prediction of smog products. Good agreement with smog chamber data for single reactive hydrocarbons has been demonstrated. The new model is capable of handling a multiplicity of reactive hydrocarbons. Application of Pade approximate techniques to the matrix obtained from the rate equations has resulted in an increased computation speed of at least five fold as compared to the other methods.

In spite of the improvements in mathematical techniques and photochemical mechanism, serious problems still exist. The model is extremely dependent upon initial conditions obtained from interpolated ground level field measurements. The paucity of these data, coupled with the requirement that the concentration profile at a specific time and location in the total region be known, places a severe constraint on the trajectory method. In addition, the questions concerning the use of multiple weighting factors for emission fluxes and reaction rates must be answered. Cross-wind or lateral diffusion effects must be included if the trajectory approach is to account for individual point sources which are important in many regions.

Systems Development Corporation (SDC) Model

The photochemical smog model developed by SDC is composed of a simplified trajectory type transport module and a complex reaction kinetics module plus several supporting sub-modules used to generate emission rates, inversion depth and reverse trajectories. The system is best described as a homogeneous, variable volume (but constant cross-section) moving cell which is guided by a wind trajectory. Integration of the differential continuity equation is accomplished by use of a Runge-Kutta routine.

The general continuity equation will be reduced to two terms for this model

$$\frac{\partial \bar{C}_i}{\partial t} = R_i \tag{16}$$

Boundary equations to describe the emission flux into the cell must also be developed. The SDC model uses the above equation as the starting point and adds first order perturbation terms to account for stationary and moving sources. The resulting equation is

$$\frac{\partial C}{\partial t} = R + \left.\frac{\partial C}{\partial t}\right|_s + \left.\frac{\partial C}{\partial t}\right|_t + \left.\frac{\partial C}{\partial t}\right|_v \tag{17}$$

where C and R are point values of vectors of length equal to the number of reacting species. Sub-scripts s, t, and v correspond to stationary sources moving sources (traffic) and volume of cell respectively.

Transport

Horizontal movement of the variable volume cell is determined by the local wind trajectory. These trajectories are generated by interpolation of ground level wind data measured at several stations in the region. Absent from the module are the effects of vertical and cross-wind diffusion, and mean velocity gradient. Accuracy of this approach is dependent upon how closely the atmosphere approximates a homogeneous mass and the accuracy of the trajectory and mixing depth predictions.

The major problems associated with predicting the wind trajectory and therefore the motion of the cell are those of determination of the proper distance weighting factors to be used and selection of the stations to be included in the interpolation at each step along the trajectory. An algorithm which can determine if a given station is within the sphere of influence of the point under consideration, or is separated from it by natural barriers such as mountains, is provided. Boundary problems involving missing stations due to ocean fronts or other factors are also resolved by this module.

The mixing depth, which determines the volume of the cell, is generated as a function of location. This sub-module calculates the potential temperature at ground level and then determines the mixing depth which corresponds to the altitude having that potential temperature. Field data are used for these calculations. It is important to recognize that any error in mixing depth will result in errors in concentration and therefore reaction rate. Substantial variation in mixing depth and therefore cell volume is expected for the Los Angeles basin, especially during those days having high concentration of smog.

Many of the accuracy problems of this model can be related to errors in the mixing depth. These errors are in part, due to the limited data available for vertical temperature profiles. In addition, the SDC model is very inaccurate for mixing depth of less than 100 meters or when changes occur between field measurements of the temperature profile.

The reverse trajectory module calculates wind trajectories and interpolates concentration values to generate initial or starting values. The terminus of the trajectory and the time of flight are required input data. The program computes consecutive upwind points (using hourly average wind data) until the indicated time is consumed. It next calculates initial concentrations at the starting point of the trajectory by interpolation of concentration data from the nearest stations. Although some procedure must be used to obtain initial concentration values, it is unfortunate that a more accurate technique is not available since modules using the trajectory approach are quite sensitive to errors in initial conditions.

The moving cell behaves as an accumulator as it moves along the trajectory since pollutants enter through the cell bottom and must remain in the cell unless they are converted via chemical reaction. Although the walls and top of the cell are impermeable to pollutants the total moles in the cell must be adjusted at each point along the trajectory to maintain the proper pressure. This adjustment in total moles always involves non-reacting or inert compounds. An additional error occurs by using ground level barometric pressure to compute the total moles from the ideal gas law (moles = PV/RT).

The overall effect of this moving cell model requires that any errors due to emission rates or initial concentration be propagated from point to point causing errors in concentration and reaction rate at every point along the trajectory.

Chemical kinetics module

SDC has taken the approach that the chemical reaction mechanism largely governs, both quantitatively and qualitatively, ground level concentrations. Accordingly, a detailed mechanism involving thirty-three individual reactions and twenty-two reactive species has been developed. The mechanism is to be an integral part of an air quality model which can predict the concentrations of oxidants and other photochemical pollutants under conditions known to cause high levels of smog pollutants. The Rice-Herzfeld approach to chain reactions, adopted for other models, has also been used in this model.

Substantial effort has been directed to formulation of a chemical reaction mechanism which has sufficient detail to account for free radical reactions and other main reactions, and important secondary steps. In addition to the 33 steps in Table 3, several other possible reaction mechanisms were considered, including the effects of sulfur dioxide and water vapor. To keep the number of steps within bounds for computer solution, the mixture of hydrocarbons in the atmosphere is assumed to consist of reactive hydrocarbons which react like propylene with all remaining hydrocarbons acting like paraffins in their reactivity toward such highly active chemical intermediates as atomic oxygen, ozone, singlet molecular oxygen, and peroxy radicals. To accommodate this division of hydrocarbons, six alternative elementary reactions are included. Although data available for validation are in most cases not sufficient to adequately test these steps, it was felt that these reactions should improve the over-all reaction mechanism.

TABLE 3

CHEMICAL MECHANISM FOR KINETICS MODULE, WITH REACTION CONSTANTS, SDC

	Reaction	Rate Coefficient*
1	$NO_2 + H\nu = NO + O$	0.27
2	$O + O_2 + M = O_3 + M$	0.14×10^7
3	$O_3 + NO = NO_2 + O_2\ S$	0.05
4	$NO_2 + O_3 = NO_3 + O_2$	0.001
5	$O_2\ S = O_2$	100.0
6	$NO_3 + NO = 2NO_2$	245.0
7	$C_2H_4O_2 = CH_3CHU + O_3$	10.0
8	$NO + HO_2 = NO_2 + OH$	10.0
9	$H + O_2 + M = HO_2 + M$	0.1×10^7
10	$DUMHC + O_2\ S = CH_3OOH$	20.0
11	$CH_3OOH + H\nu = CH_3O + OH$	0.015
12	$NO_2 + OH = HNO_3$	0.1×10^4
13	$OH + O_3 = HO_2 + O_2$	100.0
14	$OH + CO = H + CO_2$	3.0
15	$CH_3 + O_2 + M = CH_3O_2 + M$	0.14×10^7
16	$CH_3O_2 + NO = CH_3O + NO_2$	100.0
17	$CH_3O + O_2 + NO = CH_3O_2 + NO_2$	10.0
18	$C_2H_3O + O_2 + NO = C_2H_3O_2 + NO_2$	10.0
19	$C_2H_3O_2 + NO = C_2H_3O + NO_2$	100.0
20	$C_2H_4O_2 + NO = CH_3CHO + NO_2$	100.0

* Units are $ppm^{-1}min^{-1}$ except for first order reaction steps 1, 11, and 32 and reactions steps 2, 7, 15, 21, and 28 which are pseudo first order due to large excess of one reactant; units are min^{-1}.

TABLE 3

CHEMICAL MECHANISM FOR KINETICS MODULE, WITH REACTION CONSTANTS
(continued)

	Reaction	Rate Coefficient*
21	$CH_3O + O_2 = HCHO + HO_2$	100.0
22	$C_3H_6 + O = CH_3 + C_2H_3O$	35.0
23	$C_3H_6 + O_3 = HCHO + C_2H_4O_2$	0.5×10^{-4}
24	$C_3H_6 + O + O_2 = HCHO + C_2H_4O_2$	17.5
25	$C_3H_6 + O_2\ S = CH_3O + C_2H_3O$	1.0
26	$C_3H_6 + HO_2 = CH_3O + CH_3CHO$	2.0
27	$C_3H_6 + MEO_2 = CH_3 + MEO + C_2H_3O$	0.1
28	$C_2H_3O + M = CH_3 + CO + M$	10.0
29	$CH_3O + NO_2 = CH_3ONO_2$	1.0
30	$C_2H_3O + O_2 + NO_2 = C_2H_3O_3NO_2$	2.0
31	$DUMHC + O = CH_3 + C_2H_3O$	7.0
32	$HCHO + H\nu = H + H + CO$	0.005
33	$NO_2 + NO_3 + H_2O = HNO_3 + HNO_3$	0.001

*Units are $ppm^{-1}min^{-1}$ except for first order reaction steps 1, 11, and 32 and reactions steps 2, 7, 15, 21, and 28 which are pseudo first order due to large excess of one reactant; units are min^{-1}.

Finally, simulation tests were carried out to determine the best set of rate coefficients for the prediction of the time-concentration profile for propylene photo-oxidation. In many cases the value of the coefficient thus obtained differed from published data. Although this 33 step mechanism is not unique, it includes almost every reaction step known for this system and has special provisions to account for re-combination of free radicals and for production of singlet oxygen. Validation of this complex kinetics mechanism was obtained by comparing the computed time-concentration profile with smog chamber data for propylene. Initial concentration for both experiment and simulation were 100 pphm for propylene and NO. Nitrogen dioxide initial value was 10 pphm and CO was 100 pphm. Since no paraffinic hydrocarbon was present in the experimental data, the concentration of hydrocarbon for reaction with singlet oxygen was taken to be that of propylene. Inspection of Figure 14 reveals only qualitative agreement between observed and predicted values.

The reason for this poor agreement is not readily apparent because of the complex nature of the mechanism. Only one set of results is presented although an extensive analysis of the contributions to total concentration by intermediate compounds, rates of change of concentrations, and contribution of individual reaction steps to main component concentration was carried out. Further testing of the module against smog chamber data is needed if justification of the level of complexity is to be obtained. These tests should include concentration measurements of some of the secondary products proposed in the SDC mechanism.

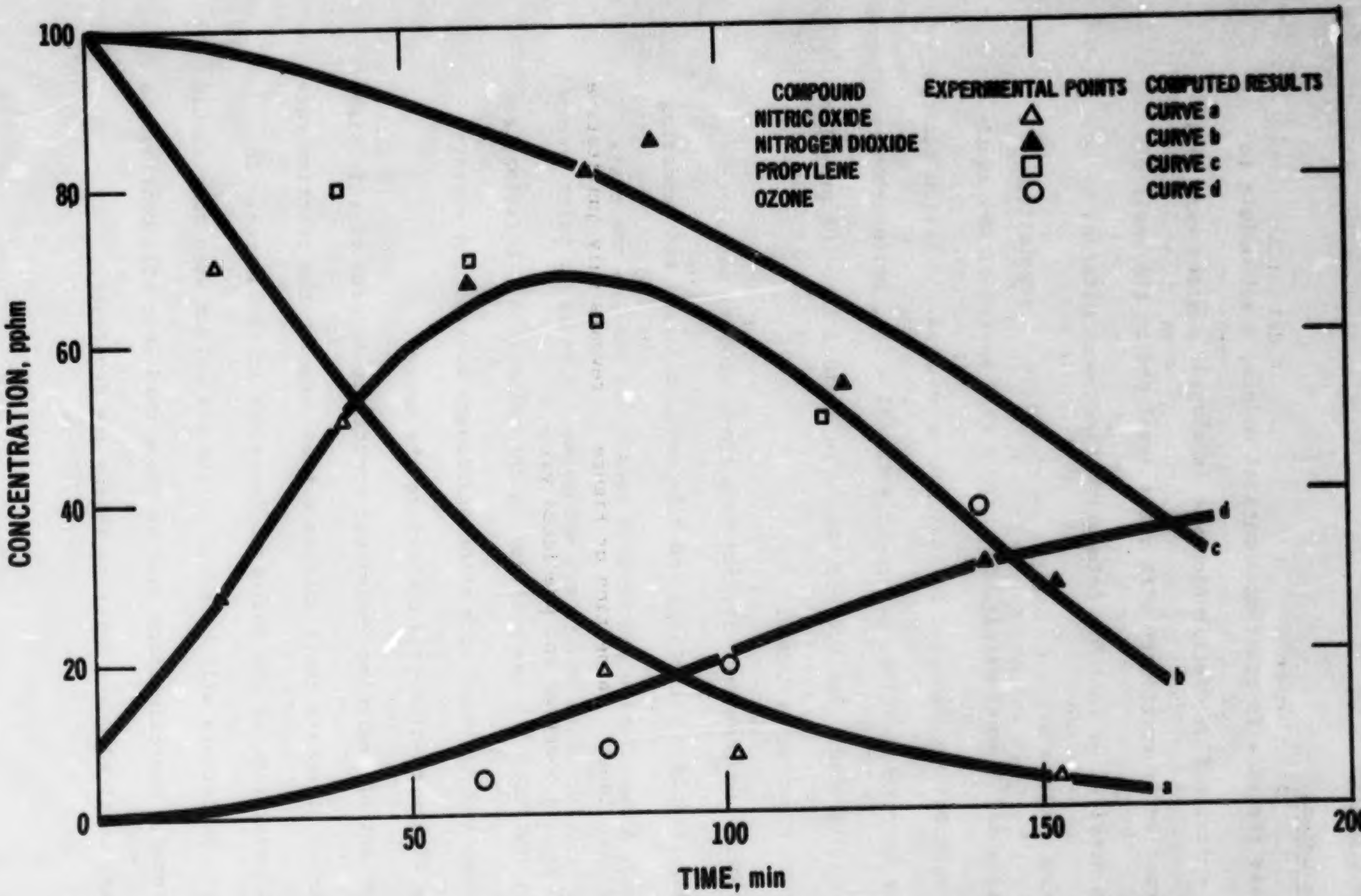

Figure 14. Comparison of simulated and experimental results in photooxidation of propylene.

Source Emissions

As was the case in other mathematical models, a sub-module to generate emission flux distribution was developed. Sources were divided into automotive or stationary with rates developed on the basis of summaries supplied by LAAPCD. Automotive rates were obtained by apportioning vehicle miles to traffic on the basis of population distribution and diurnal mileage factor. A grid system of 784 equal 4 square-mile squares was used for automotive sources. Emission factors taken from literature values were: CO = 68, NO = 4.1, hydrocarbon = 14.5 gm/vehicle mile. The hydrocarbons were divided into 50% propylene and 50% less reactive or DUMHC.

Stationary sources were divided into three groups: petroleum production; petroleum marketing; and bake oven, boilers, and rendering operations. A twenty-five square-mile square was used as the basis averaging unit for these stationary emissions. A stack or point source module was developed but was not used in the validation. Emission from point sources was included with other stationary sources and averaged across the 25 square-mile grid containing the source.

The effect of assigning individual sources to an area of this size is to smear or attenuate their influence thus reducing the reaction rate and the concentration of the pollutant contained in the source. In other cases, pollutants will be added to the air column when none should be encountered. Approximations such as those used here will continue to be necessary until adequate emission models are developed.

Application to the Los Angeles Basin

To test the SDC model, fifteen computer runs were conducted, each representing an air parcel undergoing two to three hours of wind transport. The purpose of the test was to predict ground level concentrations for ozone, nitric oxide, nitrogen dioxide and carbon monoxide at a specified hour and station. The procedure used to meet this objective was to:

1. Select trajectory terminal locations corresponding to air monitoring stations representing conditions of interest to potential users of the model,
2. Select times for arrival of the simulated air parcels at these trajectory terminal locations,
3. Select starting times for the air parcel trajectories, based on potential user interest,
4. Use the reverse trajectory routine to determine appropriate starting locations for the specified air parcels,
5. Use the contaminant interpolation routine to estimate initial contaminant concentrations in the specified air parcel.
6. Run the atmospheric simulation model utilizing input generated by the previous steps.
7. Compare the model output with air monitoring data for the selected stations and times.

Trajectories for the simulation runs are shown in Figures 15 and 16. The results of the computer simulation are presented in Table 4 with the observed field measurements. Examination of these results shows large

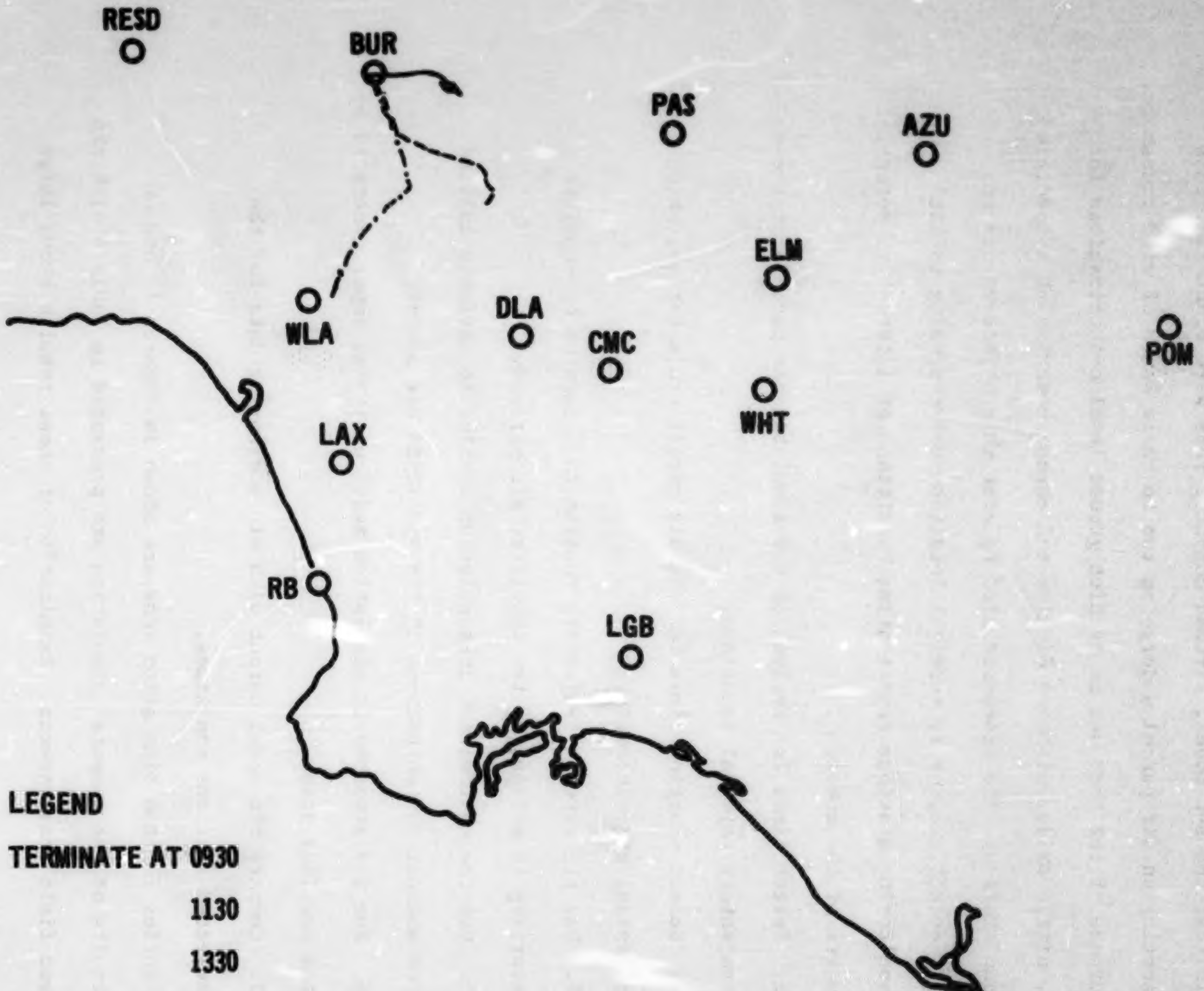
RESD
BUR
PAS
AZU
ELM
WLA
DLA
CMC
POM
WHT
LAX
RB
LGB
LEGEND
TERMINATE AT 0930
1130
1330

Figure 15. Three-hour validation trajectories for September 30, 1969, 22 meteorological stations, runs 1 through 3.

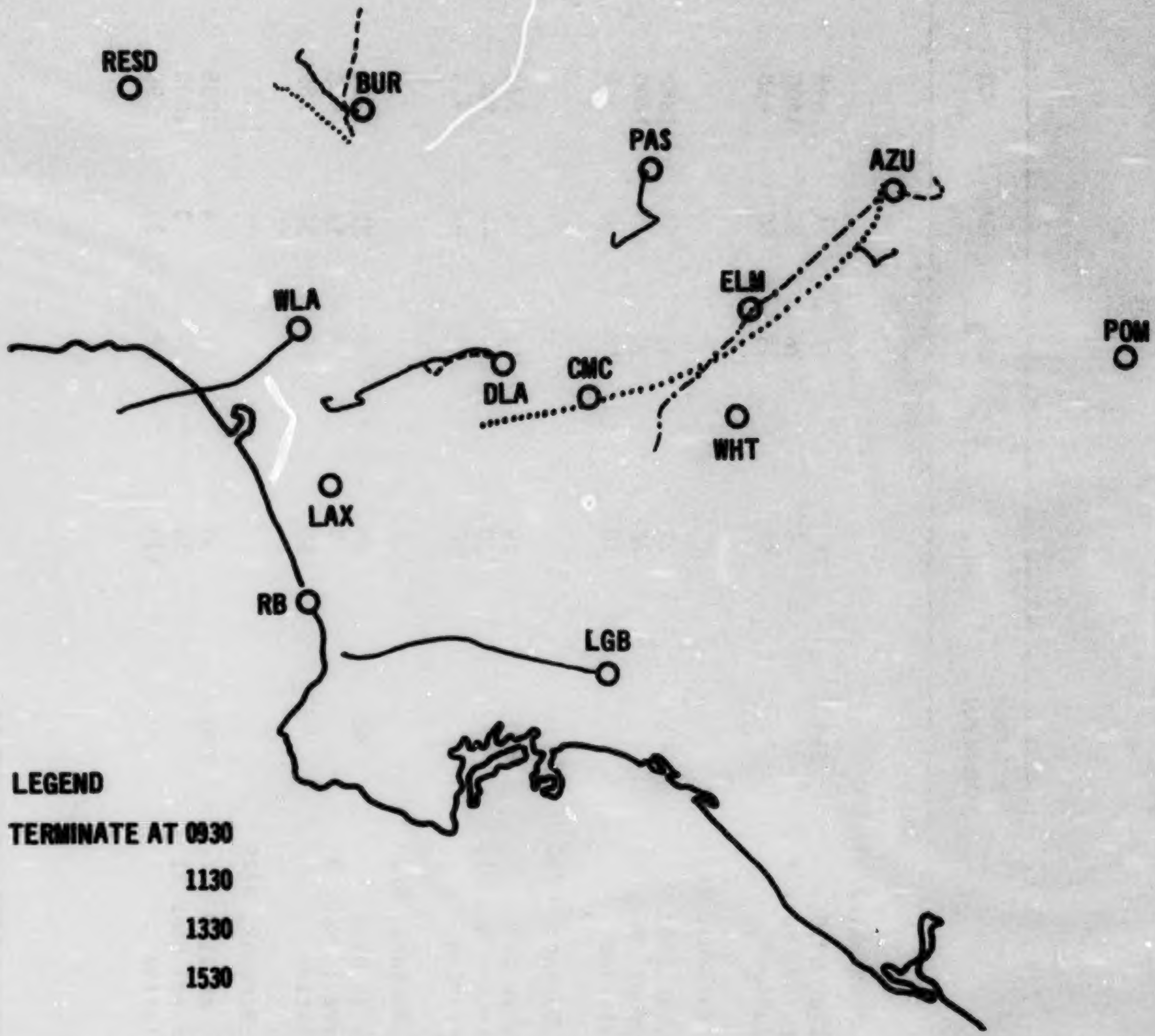
RESD
BUR
PAS
AZU
ELM
POM
WLA
DLA
CMC
WHT
LAX
RB
LGB
LEGEND
TERMINATE AT 0930
1130
1330
1530

Figure 16. Three-hour validation trajectories for September 29, 1969, 29 meteorological stations, runs 4 through 15.

TABLE 4

COMPARISON OF CALCULATED VS. OBSERVED CONCENTRATION

	MIX/DEP (Meters)	O_3	NO_2	NO	CO
Run #1, Burbank, 9/30					
Calc. at 0930	266	10	7	4	698
Observed: Hour 9		6	28	33	1400
%Deviation*		67	-75	-88	-50
Run #2, Burbank, 9/30					
Calc. at 1130	571	22	11	3	1882
Observed: Hour 11		20	50	5	1800
% Deviation		10	-78	-40	4
Run #3, Burbank, 9/30					
Calc. at 1330	840	19	12	4	678
Observed: Hour 13		10	--	--	800
% Deviation		90	--	--	-15
Run #4, Burbank, 9/29					
Calc. at 0930	30	15	53	22	1724
Observed: Hour 9		7	29	14	900
%Deviation		88	83	57	189
Run #5, Burbank, 9/29					
Calc. at 1130	280	33	18	4	1958
Observed: Hour 11		14	19	3	1000
%Deviation		136	-5	33	96

---

* %Deviation = (Calc - observed)/observed * 100

TABLE 4

COMPARISION OF CALCULATED VS. OBSERVED CONCENTRATION
(continued)

	MIX/DEP (Meters)	O_3	NO_2	NO	CO
Run #6, Burbank, 9/29					
Calc. at 1330	2058	22	7	2	942
Observed: Hour 13		14	-	-	700
% Deviation		57	-	-	34
Run #7, Azusa, 9/29					
Calc. at 0930	106	8	13	10	1186
Observed: Hour 9		16	11	1	1000
% Deviation		-50	20	900	19
Run #8, Azusa, 9/29					
Calc. at 1130	418	19	10	4	1172
Observed Hour 11		24	5	1	600
% Deviation		-21	50	300	95
Run #9, Azusa, 9/29					
Calc. at 1330	839	16	4	2	513
Observed: Hour 13		38	-	-	900
% Deviation		-58	-	-	-41
Run #10, Azusa, 9/29					
Calc. at 1230	444	4	1	1	22
Observed: Hour 15		14	5	1	600
% Deviation:		-71	-80	0	-96

---

* % Deviation = (Calc - observed)/Observed * 100

TABLE 4

COMPARISON OF CALCULATED VS. OBSERVED CONCENTRATION
(continued)

	MIX/DEP (Meters)	O_3	NO_2	NO	CO
Run #11, Pasadena, 9/29					
Calc. at 1130	330	39	29	5	2672
Observed: Hour 11		41	12	1	-
% Deviation		-5	142	400	-
Run #12, Long Beach, 9/29					
Calc. at 1130	293	16	12	5	1910
Observed: Hour 11		6	22	8	600
% Deviation		60	-45	-38	218
Run #13, West LA, 9/29					
Calc. at 1130	220	15	29	13	1605
Observed: Hour 11		12	-	-	500
% Deviation			25	-	220
Run #14, Downtown LA, 9/29					
Calc. at 0930	30	38	98	14	5510
Observed: Hour 9		8	19	30	-
% Deviation		375	415	-53	-
Run #15, Downtown LA, 9/29					
Calc. at 1130	235	38	52	9	3183
Observed: Hour 11		9	10	5	600
% Deviation		322	420	80	430

---

* % Deviation = (Calc - observed)/Observed * 100.

differences between computed and measured values.

Carbon monoxide is usually assumed to be inert (not quite true for the SDC model) so that it can be used to validate the transport module. If this standard is applied to the SDC model, validation of the combined effect of the trajectory, mixing depth, and emission sub-modules should be possible. Comparison of these data indicates that one or more of these sub-modules is not adequate. Although it would be very difficult to determine which quantity contributes the greatest error, mixing depth is most suspect. Errors in emission are dampened by the averaging effect and would be important only if large point sources has been near the trajectory. Since carbon monoxide is emitted only by vehicles and to a small degree by petroleum production sources, it should provide a reasonable test of the mixing depth sub-module. The results are not promising. Errors are large and no trend or logical reason(s) for these differences is apparent unless the initial concentration data are grossly in error. These data were not presented, so a judgment is not possible. Therefore, the conclusion must be that the mixing depth sub-module is inadequate.

Errors due to mixing depth are amplified since the reaction rate is proportional to the product of two concentration terms each of which is linearly connected with the mixing depth.

Summary

This model, which includes a complex reaction kinetics mechanism coupled with a very simplified transport module, has not demonstrated that it can provide more than qualitative comparison with either smog chamber or field station data. Although major emphasis was placed upon development of the reaction kinetics mechanisms and studying the interactions and contributions of the several steps to the concentration history, adequate data were not available to validate the mechanism.

Major problems associated with errors in the mixing depth predicted by the meteorology sub-module tend to mask errors from other sources. Initial concentrations predicted by an interpolation scheme are also highly suspect, although these data are not presented. As a result an accurate evaluation of this error source could not be made. Emission source errors due to the use of simple distribution functions most certainly contribute to the overall error as does the use of area averaging of point and large individual sources.

Systems Applications, Inc. Model

This approach is known as the three-dimensional, time dependent model. This model attempts to solve the three-dimensional (eq. 2), time dependent mass balance equations and thus predict the distribution of pollutants at every point and time for the region of interest. An approximate solution is obtained by use of numerical techniques. The speed and accuracy of this approach are dependent upon the type of approximation and the size of the spacial and temporal grid. Recent advances made in this field have greatly increased both speed and accuracy and appear to open the way for use of this modeling approach.

Although this approach will require more computer time than the trajectory model, it is capable of solving both strategy and episode type problems. In addition, until better emission sub-models and more extensive field data systems are available, it should lead to more accurate results.

Transport/Diffusion Module

This module includes subroutines to predict the three-dimensional mean wind field from surface wind data, the inversion depth as a function of position and time and turbulent diffusivities as a function of surface wind and elevation.

The winds aloft are determined by satisfying the continuity equation for each cell. It was assumed that $\partial u/\partial z = \partial v/\partial z = 0$; that the horizontal components of the wind aloft were identical to that at the surface; air was brought down through the inversion, or released upward through it, as needed to satisfy continuity. This flow was constrained so that the wind vector did not vary more than 22 1/2° from the horizontal and did not exceed the horizontal velocity by more than a factor of two. This approach is attractive on physical grounds but extensive evaluation of the constraints is needed.

The inversion routine is the most realistic proposed to date and appears to predict the temporal and spacial variation of the Los Angeles inversion depth quite well. The method is based upon the work of Edinger and has been applied to field data.

Turbulent diffusivity and its variation with wind speed and height was predicted as suggested by Eschenroeder (GRC Model 1970 version).

Chemical Kinetics Mechanism

A 14-step lumped parameter reaction mechanism has been proposed. This mechanism represents a compromise between the need to reduce computer time and the desire to adequately describe the reaction steps. The Rice-Herzfeld approach to chain reactions mechanisms was used by SAI to generate the several steps. The reaction steps making up the mechanism are presented.

in Table 5. Rate coefficients were obtained by adjusting experimental values obtained from smog chamber studies or were estimated. In addition, rate coefficients for hydrocarbon mixtures were computed by using a modification of the "combined rate" approach used by Glasson and Tuesday (1971). This method computed an equivalent coefficient as follows:

$$k'_m = \Sigma f_i k_i$$

where k'_m = rate coefficient for mixture

f_i = fraction of component i in hydrocarbon mixture

k_i = rate coefficient for hydrocarbon i

This method has been applied to one mixture (propylene/N-butane) with good results as shown in Figure 17. Further tests using hydrocarbons with similar reactivity levels is needed to validate this method. Three single hydrocarbon systems, including one test with CO present, were tested against smog chamber data with adequate to good agreement. Typical results are presented in Figures 18 and 19. The basic difficulties associated with using simplified, lumped parameter mechanisms are denibstrated by these two figures. A good fit is obtained with isobutylene, but significant errors occur with the propylene system. Continued experimentation with the rate constants can minimize these difficulties but will not completely eliminate them.

Source Emissions

An extensive, detailed sub-module was developed in order to predict the spacial and temporal distribution of emissions. This module includes algorithms for automotive, aircraft, fixed point, and distributed sources. As was found in other models the fixed point source routine did

TABLE 5

REACTION KINETICS MECHANISM, SAI

1. $NO_x + h\nu \rightarrow NO + O$
2. $O + O_2 + M \rightarrow O_3 + M$
3. $O_3 + NO \rightarrow NO_2 + O_2$
4. $O_3 + 2NO_2 \xrightarrow[H_2O]{} 2HNO_3$*
5. $NO + NO_2 \xrightarrow[H_2O]{} 2HNO_2$
6. $HNO_2 + h\nu \rightarrow OH\cdot + NO$
7. $CO + OH\cdot \xrightarrow[O_2]{} CO_2 + HO_2\cdot$
8. $HO_2\cdot + NO_2 \rightarrow HNO_2 + O_2$
9. $HC + O \rightarrow \alpha RO_2\cdot$
10. $HC + O_3 \rightarrow \beta RO_2\cdot + \gamma RCHO$
11. $HC + OH\cdot \rightarrow \delta RO_2\cdot + \epsilon RCHO$
12. $RO_2\cdot + NO \rightarrow NO_2 + \theta OH\cdot$
13. $RO_2\cdot + NO_2 \rightarrow PAN$
14. $HO_2\cdot + NO \rightarrow NO_2 + OH\cdot$

---

*Reaction 4 is a composite of the three reactions,

$$O_3 + NO_2 \xrightarrow{4a} NO_3 + O_2$$
$$NO_3 + NO_2 \xrightarrow{4b} N_2O_5$$
$$N_2O_5 + H_2O \xrightarrow{4c} 2HNO_3$$

Thus, it is not necessary to retain NO_3 om the mechanism.

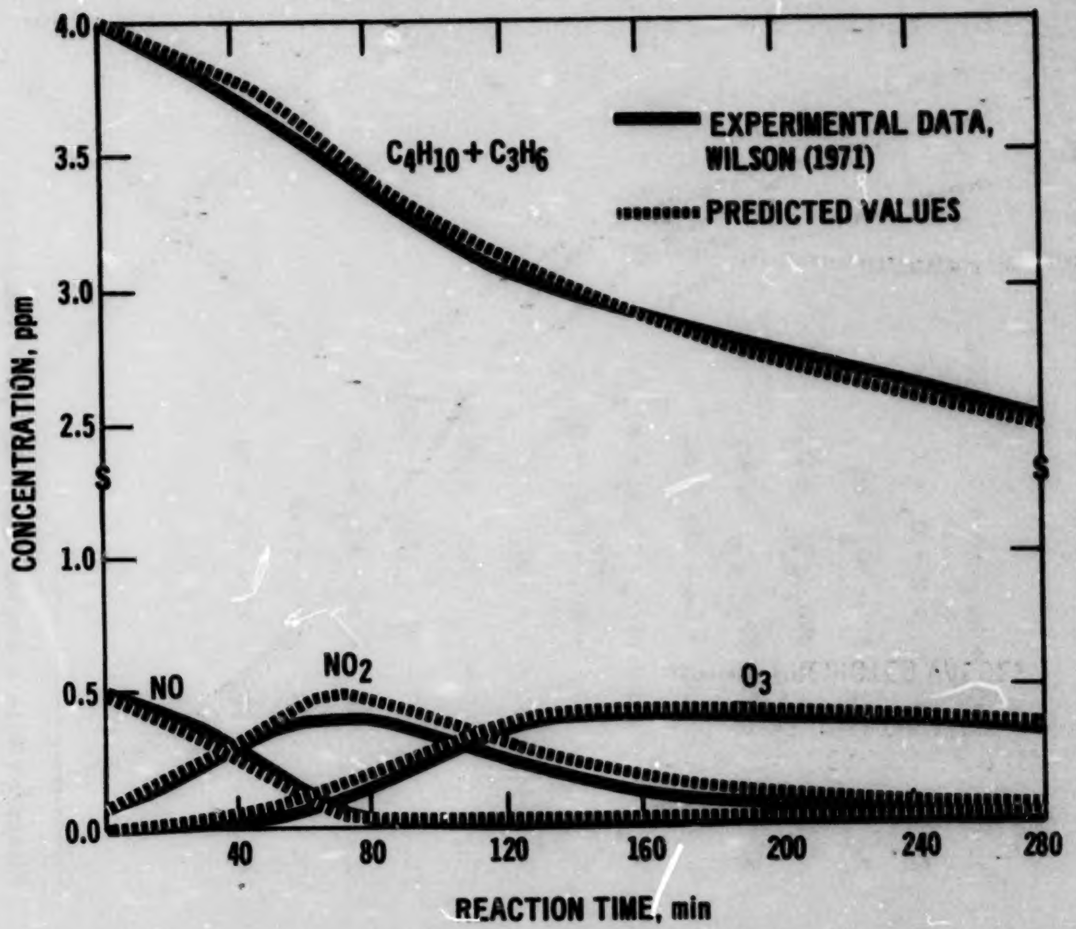

Figure 17. Validation of the new mechanism, propylene/ n-butane.

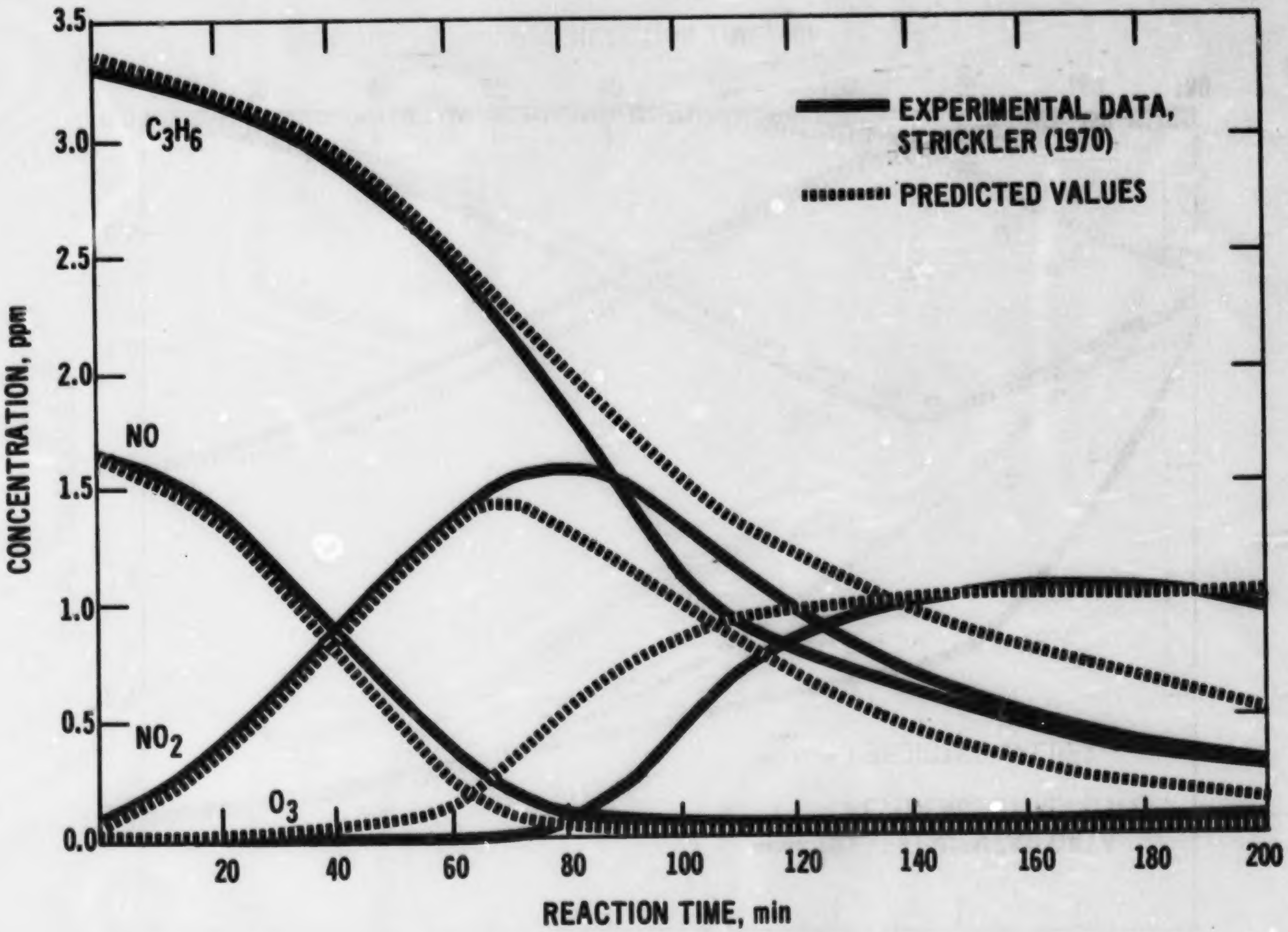

Figure 18. Validation of the new mechanism, propylene.

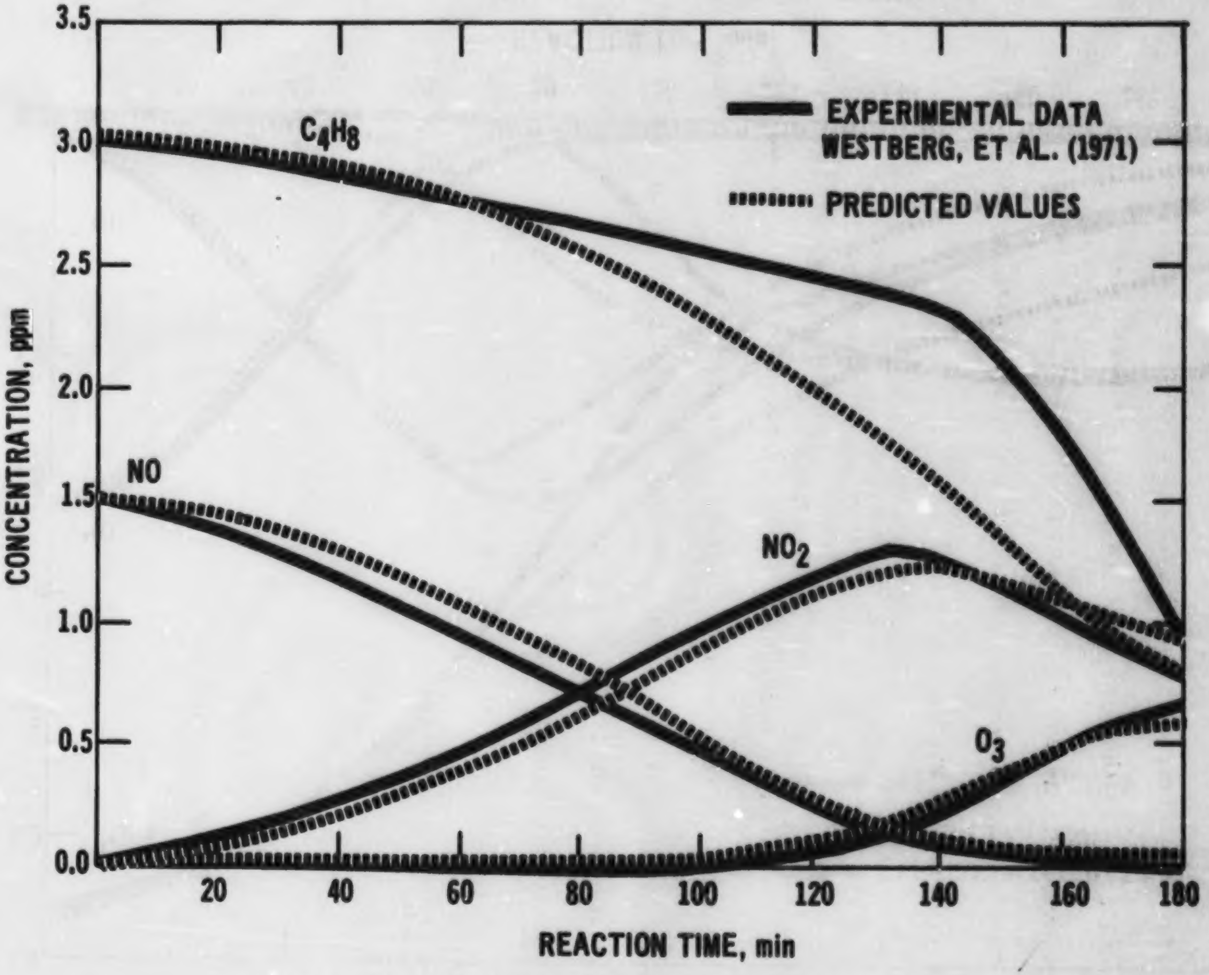

Figure 19. Validation of the new mechanism, isobutylene.

not enter into calculations since none of the air quality measurements used in the validation were likely to be influenced by these sources. The major effort was directed to predicting the distributions for automotive and aircraft, since these two sources represent more than 85% of the total reactive hydrocarbons and 62% of the nitrogen oxides. These submodules, particularly those for automotive and aircraft are quite comprehensive and use the latest data available.

The complete model has not been applied to the Los Angeles basin data. However, preliminary calculations using carbon monoxide indicate that the transport/diffusion model is quite adequate. The reaction mechanism has demonstrated that it can adequately predict smog chamber concentration histories for a variety of systems including one mixture containing two hydrocarbons. However, the complete model must be tested to determine the utility of the system and to validate the numerical techniques used to solve the general equations.

The S.A.I. approach is the most difficult of any proposed, but it is also potentially the most rewarding. Each of the sub-modules has been tested, but the combined system, including the numerical techniques used, has not been adequately validated.

SUMMARY

Photochemical smog is one more by-product of the major industrialized metropolitan area. The large concentration of commercial enterprise, coupled with the use of fossil fuels for energy and internal combustion engines for transportation, has lead to the increase of photochemical smog in the U. S. A. The combustion process involving air and hydrocarbons generates the reactive hydrocarbons and oxides of nitrogen needed for the photochemical reactions. These compounds plus others will react in the presence of sunlight to form photochemical smog. Although the ingredients for formulation of this smog are present in most areas of the world, the incident rate for serious events is low outside of the major metropolitan areas.

This low rate can be attributed to the need for a unique combination of chemical concentration, meteorological factors, and residence time. If the concentration of the reactive chemicals is too low, the wind too high, or the residence time too short, the level of photochemical pollution will be low. In order to quantitatively predict the conditions which will cause high pollutant concentration, mathematical models have been proposed.

Mathematical modeling, as applied to photochemical smog, is interpreted to mean the formulation of equations which describe the accumulation of photochemical pollutants during a specified time and at a given place. These equations attempt to describe the interactions among and the effects of emission rates, chemical reactions, and meteorological variables on this accumulation. Each of these main variables is of prime importance, and the results obtained by any mathematical model are no more accurate than the least accurate main variable.

Formulation of the Model

The mathematical statement for description of the temporal and spacial distribution of the chemical species in the planetary boundary layer is the mass balance or continuity equation. These expressions, one for each species, plus appropriate boundary and initial conditions, complete the description. The photochemical model is concerned with the several species which are undergoing chemical conversion, initiated or propagated by sunlight.

To date, exact solutions for the general problem have not been published, and it is improbable that any will be. Several approximate solutions of very simplified versions have been obtained, but these are of minor importance because of the many constraints imposed by the simplification. The model must incorporate equations or sub-models which describe emission fluxes, chemical reactions, and meteorological variables.

In a large industrialized urban area such as New York, Los Angeles, or Houston, pollutants are generated by thousands of stationary sources and by millions of automobiles, trucks, and other vehicles. The emission flux sub-model must generate accurate values of the spacial and temporal distribution of these stationary and moving sources since they are generating pollutants and reactive compounds which enter the photochemical reaction mechanism. At present much of the data needed for this sub-model are not available or are in an unuseable form. As a result estimates and incorrect distribution must be used.

Formulation of the system of equations required to describe the photochemical reactions taking place is based upon the Rice-Herzfield mechanism. This approach requires that a number of elementary reaction steps involving the pollutants and intermediate compounds called free radicals be proposed such that the observed rate of formation of smog can be predicted. Although it is possible to generate these steps for simple reactions involving a single reactive hydrocarbon, the multiplicity of hydrocarbons in polluted air makes the likelihood of proposing the true mechanism extremely remote. However, it is possible to formulate simplified mechanisms which assume stationarity, and group together certain steps such that the reaction sub-model can adequately describe the photochemical process.

Of equal importance to the reaction sub-model validation is the availability of accurate experimental smog chamber data. These date are needed to test and verify the reaction mechanism. Only during the past few years have good quality data of the type needed for this purpose been obtained. Much more data, especially for systems involving two or more reactive hydrocarbons, are needed.

The weakest link in the chain of variables making up the photochemical model is the meteorology sub-model needed to predict transport and diffusion in the atmosphere. The ability of the model to successfully predict smog distribution and intensity is directly dependent upon the quality and quantity of meteorological data. At least four types of data are needed in order to make these predictions: wind speed and direction, atmospheric stability, solar energy distribution, and mixing depth or inversion height. Ideally these data would be generated without using a large number of field measurements; however, that is not possible at this time. In fact, few measurements are made in most regions and those available are of limited value due to the location of the station or time of data collection. Interpolation and extrapolation schemes using these few field data generate additonal data which, although needed by the model, are usually of questionable quality. There is a great need for expanded field measurements and for improved prediction techniques for the meteorological variables.

Current Modeling Effort

Two approaches to the solution of the general equations are presently being considered. Each approach includes sub-modules which predict the temporal and spacial distribution of emissions, compute the rate of generation of smog components by photochemical reactions, and predict transport and diffusion of the pollutants. The main difference in the two approaches concerns the method for prediction of transport and diffusion effects. Although there are some difference in the techniques for handling emissions and reaction kinetics, the basic approach is common for all models

The trajectory approach which can be applied only to planning or strategy problems is the simpler of the two. It uses wind trajectories in predicting the movement of an air parcel or cell through the region and is totally dependent upon extensive field measurements which are needed to develop the trajectory and initial pollutant concentration to date. The cell or air parcel may be divided (vertical direction) into several sub-cells to account for vertical diffusion or may be considered a single well mixed or homogeneous air mass.

Although this approach is attractive because of its mathematical simplicity, major difficulties are associated with its use. The air parcel acts as an accumulator for pollutants which are being emitted by sources along its path or are formed by chemical reactions. That is, any pollutant entering the parcel or cell remains unless it is converted by chemical reaction into another compound. In addition, errors which influence local concentration, such as initial concentration where the trajectory begins, local mixing depth and emission flux are propagated. The net result is that trajectory models are extra sensitive to any error along the path because it cannot be averaged to reduce its effect on the final concentration.

A trajectory model may be applied to a specified receptor location by selecting the hour(s) for which local ground level pollutant concentration is required. A reverse trajectory is generated by interpolation of wind speed and direction data for a specified time or distance. The reverse trajectory describes the path along which the air parcel traveled in order to arrive at the specified receptor. The user must then obtain the initial values of pollutant concentration at the terminus of the reverse trajectory in order to start the calculations. These calculations are performed in a step-wise manner until the receptor is reached. This procedure must be repeated for each result (receptor and time) required.

Two versions of the trajectory model have been applied to the Los Angeles Basin. The (SDC) version which uses a single well mixed cell has been tested with fifteen runs. It has not demonstrated a good agreement with field data, although some computed values to agree reasonably well, and others follow the expected trends. Use of multiple cells (GRC) to account for vertical diffusion appears to improve the quality of the prediction. Although improvement was noted for the four cases tested, additional verification is needed if more than qualitative agreement is to be obtained.

The second approach to modeling attempts to solve the three-dimensional, time dependent mass balance equations and thus predict the distribution of pollutants for the region of interest. An approximate solution is obtained by use of numerical techniques. The speed and accuracy of this approach are dependent upon the type of approximation, and the size of the spacial and temporal grid. Recent advances made in this field have greatly increased both speed and accuracy and appear to open the way for use of this modeling approach. One version (SAI) of the transport/diffusion sub-model which incorporated the new advances has been partially tested using carbon monoxide. The preliminary results are quite encouraging and represent a definite improvement over previous efforts.

Although this approach will require more computer time than the trajectory model, it is capable of solving both strategy and episode type problems. In addition, until better emission sub-models and more extensive field data systems are available, it should lead to more accurate results.

In conclusion, mathematical models have achieved a modest level of success in predicting the distribution of photochemical smog in the Los Angeles Basin. During the past two years, significant advances in developing realistic mathematical models have been achieved. Many facets of the total problem have been explored, critical areas have been isolated, and new approaches and mathematical algorithms tested. One result of this effort has been the development of limited scope mathematical models which may be used for qualitative purposes. Several problems remain and significant progress in the development of a general photochemical smog model is not to be expected until they are at least partially solved. The critical areas involve prediction of the meteorological variables, distribution functions for emissions, and formulation of chemical reaction mechanisms for multiple hydrocarbon systems.

REFERENCES

1. A.Q. Eschenroeder and J.R. Martinez, "A Modeling Study to Characterize Photochemical Atmospheric Reactions to the Los Angeles Basin Area," General Research Corporation, CR-1-152, November 1969.

2. S.K. Friedlander and J.H. Seinfeld, "A Dynamic Model of Photochemical Smog," Environmental Science and Technology, Vol 3, No. 11, 1969.

3. A.Q. Eschenroeder and J.R. Martinez, "Further Developments of the Photochemical Smog Model for the Los Angeles Basin," General Research Corporation, CR-1-191, March 1971.

4. M. Weisburd, L.G. Wayne, et. al., "Development of a Simulation Model for Estimating Ground Level Concentrations of Photochemical Pollutants," System Development Corporation, TM-(L)-4673/000/00, January 1971.

5. L. G. Wayne, et. al., "Comprehensive Technical Report on All Atmospheric Contaminants Associated with Photochemical Air Pollution," Systems Development Corporation, July 1970.

6. P. Roth, Preliminary Draft of final report, Appendices A and B, contract CPA-70-148, "Development of a Simulation Model for Estimating Ground Level Concentrations of Photochemical Pollutants," Systems Applications, Inc., May 1971.

7. P. Roth, personal communication, June 1971.

APPENDIX

APPENDIX

Lumped-Parameter Techniques

Formulation of a reaction kinetics mechanism for complex hydrocarbon systems frequently involves the use of lumped parameters. This approach represents a compromise between the actual chemistry of the reactions and the desire to minimize computation difficulties.

The complex hydrocarbon mixture which exists in the atmosphere may result in hundreds of reaction steps which may produce several dozen compounds not in the original mixture. Although it is theoretically possible to construct reaction steps to describe the overall reaction, there is no guarantee that the set is unique. In most cases several sets may be generated. The difficulty in generating a unique set coupled with the need for large computers to solve the resulting equations has lead to the development of approximation techniques. The use of lumped parameters is one such approach.

The lumped-parameter approach is illustrated by the following example.

The reaction of atomic oxygen with an olefin will result in the production of two free radicals, generally an alkyl and an acyl. For example,

$$\begin{array}{lcclcl}
\text{olefin} & + & \text{oxygen} & \rightarrow \text{free radicals} & & \\
\text{ethylene} & + & 0 & \rightarrow CH_3^{\circ} & + & H\dot{C}O \\
\text{propylene} & + & 0 & \rightarrow CH_3^{\circ} & + & CH_3\dot{C}O \\
\text{isobutylene} & + & 0 & \rightarrow (CH_3)_2CH^{\circ} & + & H\dot{C}O
\end{array}$$

The free radical products then react rapidly with molecular oxygen to form other radicals such as peroxyacyl. The steps proposed above are not unique, and others which result in similar products are also known. All of these steps may be lumped or grouped together and represented by a single parameter. The reacting hydrocarbon(s) is denoted HC and the free radicals, RO°_2. If a wide range of reactivity exists the hydrocarbon may be divided into two or three groups in order to better simulate the actual steps.

$$HC + O \rightarrow \alpha RO^{\circ}_2$$

Where RO°_2 is the lumped parameter, radical species and α is a stoichiometric coefficient which relate the number of RO°_2 radicals produced by the hydrocarbon lumped parameter, HC. Each of these lumped species represents the total population of its group (i.e., RO°_2 the oxygen-containing free radicals) some of which may not contain two oxygen atoms.

In a similar manner, reactions between hydrocarbons and ozone which result in aldehydes (RCHO) and oxygen containing free radicals (RCO°_2) may be represented by a single lumped-parameter reaction step.

$$HC + O_3 \rightarrow \beta RO^{\circ}_2 + \partial RCHO$$

Where β and ∂ are stoichiometric coefficients whose value depends upon the specific hydrocarbon mixture.

The use of lumped parameters will result in greatly reduced computation time for the photochemical smog system. However, this reduction is accomplished by reducing the rigor of the actual chemistry. If an acceptable mechanism is to be obtained, it must provide a balance between accuracy of prediction and ease of computation.

Chapter XIV

SULFUR DIOXIDE REACTIONS IN THE ATMOSPHERE

Frank L. Worley, Jr.*
Division of Meteorology
Bureau of Air Pollution Sciences
Office of Research and Monitoring
Environmental Protection Agency

For Presentation to the Panel on Modeling, NATO/CCMS Pilot Project on Air Pollution, Paris, France, July 26-27, 1971

*On leave from the Chemical Engineering Department, University of Houston, Houston, Texas

This paper presents a brief discussion of sulfur dioxide conversion mechanisms in the atmosphere and removal processes from the atmosphere. The rate of removal or conversion of sulfur dioxide in a polluted atmosphere is difficult to predict due to the number of possible mechanisms. It may: react with other gases, with or without photochemical effects; be absorbed by water droplets; be chemisorbed on to dry metal oxides; or be absorbed by aerosols containing solutions of metal salts which convert it to a sulfate. Sulfur dioxide is both very soluble in water and very reactive in the dilute concentrations found in the atmosphere. The end product of reactions is sulfuric acid or a sulfate salt. Some studies conducted during the past 15 years appear to contradict each other and thus contribute to the general uncertainty.

Sulfur dioxide oxidation by molecular oxygen has been found to be insignificant, but photochemical oxidation in the presence of NO_2 and hydrocarbons can be important in the atmosphere at the low concentrations found in urban areas. The rate and extent of this reaction depend on the concentration of water vapor in the air and the SO_2 concentration. At least two reaction paths are involved: one results in aerosol formation; the other apparently interferes with ozone formation and is favored at higher levels of water vapor. In relatively dry systems, SO_2 results in a general slowing down of the secondary reactions in the photochemical mechanism. At humidity levels encountered in many coastal or maritime climates, the inhibiting influence is less pronounced,but the peak concentration of ozone is significantly reduced. In addition, recent studies of Urone and Miller (1970) indicate that SO_2 and NO_2 react to form a solid product which has been identified as nitrosylbisulfate, $NOHSO_4$. This photochemically induced reaction occurs in addition to the usual SO_3 and NO products. Experimental studies in smog chambers have consistently shown that the presence of SO_2 increases aerosol production when hydrocarbons in the air are irradiated with sunlight. However, if the SO_2 concentration is below 2 ppm, the inverse is true.

Reactions of sulfur dioxide with hydrocarbons are puzzling. Laboratory studies show that the SO_2 increases the amount of hydrocarbon aerosols under some conditions, but it is not known whether this aerosol is formed using sulfuric acid as a nucleating agent or is a sulfur containing organic compound. Detailed knowledge is limited in part because of the difficulty of analyzing directly for SO_3 or sulfuric acid aerosols.

Sulfur dioxide can be adsorbed by particulates containing a metal oxide, hydroxide, or carbonate. Rates of adsorption on lead, iron and vanadium oxides have been measured experimentally and found to be very high. Since these compounds are generated by combustion of leaded gasoline, coal, or fuel oil, this mechanism may be significant in urban, industrialized areas. Any SO_2 removed by adsorption on sub-micron oxide particles may be later converted to sulfate salts if water vapor such as found in clouds or rain is encountered. If the particulate material containing adsorbed SO_2 remains dry, it is possible for some of it to be desorbed and re-enter the atmosphere at a point far removed from its capture location.

The absorption of SO_2 by water particles containing catalysts or alkaline material such as ammonia or soluble hydroxides results in the formation of sulfate salts or sulfuric acid. Iron and manganese sulfate salts formed by the reaction of sulfuric acid on the metal oxides are very effective in converting SO_2 to SO_3. (These reactions have effective rates of about 1% per minute). Other metal sulfate salts are also catalytic for the oxidation reaction but not to the same degree. Although these reactions are rapid, conversion can be reduced by absorption rates and solubility limitations if alkaline materials are not present to maintain the pH above 4. Ammonia, generated by the combustion of coal at the same time that SO_2 is formed, is very soluble in water and should readily react rapidly to form ammonium sulfate. The presence of low clouds or fog should ensure this reaction. In addition, water vapor present in the effluent stream or plume will condense and form droplets in which these reactions may proceed.

Sulfate salts formed by adsorption or absorption may be transported many kilometers if the particles are not removed by washout, rainout, or gravity. Agglomeration or growth of particles due to absorption of moisture can aid in the removal of particles by gravity. In addition, field studies indicate that SO_2 may be absorbed and removed without oxidation. This removal process is complicated by the fact that the dissolved SO_2 is readily desorbed by changing temperature, pressure, or gas concentration.

An adequate, validated mechanism to explain the reaction and removal of SO_2 from the atmosphere is not available at this time. However, the several processes discussed above indicate that several possible mechanisms exist which may compete with each other and result in moderate to very rapid conversion and removal. Important variables include humidity, presence of metal oxides, particulate material, sunlight, and rain. During the daylight hours in dry clean atmospheres, photochemical conversion by reactions with nitrogen oxides and hydrocarbon should be most important. However, at night or during overcast days and under high humidity, fog or rain physical absorption and reaction with alkaline water apparently determine the conversion and removal rate.

References

1. Urone, Paul and Miller, S.R., "Reactions of Sulfur Dioxide in Air" presented before the Second International Air Pollution Conference, Washington, D.C., December, 1970.

2. Jost, D., "Remarks on the Effects of CLouds on Transformation and Long Range Transport of Sulfur Compounds in the Atmosphere," OECD Meeting on Long Range Transport of Pollutants, Paris, June, 1971.

3. Wilson, W. E. and Levy, A., "A Study of Sulfur Dioxide in Photochemical Smog," J.A.P.C.A., Vol. 20, #6, 1970.

4. Bufalini, J.J. and Altshuller, A.P., "Photochemical Aspects of Air Pollution, A Review," N.A.P.C.A., 1970.

5. Bufalini, Marijon, "Oxidation of Sulfur Dioxide in Polluted Atmospheres," Environmental Science and Tech., late 1971.

6. Robinson, E. and Robbins, R.C., "Final Report: Sources, Abundance and Fate of Gaseous Atmospheric Pollutants," Stanford Research Institute, 1968.

7. Weber, Erich, "Determination of the Lifetime of SO_2 by Simultaneous CO_2 and SO_2 Monitoring," J.G.R. 75, 1970.

8. Foster, P.M., "The Oxidation of Sulfur Dioxide in Power Station Plumes," Atmos. Envir. Vol. 3, 1969.

9. Smith, B.M., Wagman, J., and Fish, B.R., Atmos. Science & Tech. Vol. 3, 1969.

Chapter XV

SOME PRELIMINARY RESULTS OF MODELING
FROM THE
AIR POLLUTION STUDY
OF
ANKARA, TURKEY

June 1971

John R. Zimmerman *
Environmental Protection Agency
Division of Meteorology
Raleigh, North Carolina

Paper Prepared for 2nd Meeting of the NATO/CCMS
Panel on Modeling, 26-27 July 1971, Paris, France

*On assignment from the National Oceanic and Atmospheric Administration, U.S. Department of Commerce.

Acknowledgements

This project could not have been accomplished without the contributions of Mrs. Aysen Muezzinoglu, who supervised the collection and analysis of the Ankara quality data, and Mr. Taskin Tuna of the Turkish Meteorological Office, who expeditiously provided meteorological data required for the climatological dispersion model.

I. Introduction

Ankara, capital of Turkey, has grown from 20,000 in 1920 to a modern metropolis of over a million. This expansion has brought a serious air pollution problem created by the combustion of smoke producing fuels with high sulfur contents.

Windflow over Ankara is normally weak, being further retarded by rugged valley terrain. The combination of a sluggish atmosphere and intense pollution emissions produces poor air quality during the heating season. Urban dispersion models were contrived to treat the dispersion of pollutants over terrain that is relatively level and for circulations that are not becalmed.

A long-term pollution dispersion model described by Calder (1970) has been applied to the analysis and projection of seasonal air quality. Data collected during the winter of 1970 were compared to air quality concentrations produced by the climatological dispersion model. Linear correlations of observed and computed air quality were used to calibrate the model and produce mean seasonal distributions of urban air pollution. Projections of air quality for 1990 were made using projected pollution emission rates determined from expected population and fuel use trends.

II. Comparison of Observed and Computed Air Quality for Winter 1970 in Ankara

Sulfur Dioxide

As a large number of physical parameters influence the dispersal of atmospheric pollutants, it is evident that there are a number of input variables which must be specified in the operation of the climatological dispersion model*.

In Ankara most of the emission, a direct result of burning fuel, occurs during the daytime and early evening, the period of greatest activity. Rather than use a mean emission rate and ignore, in an unrealistic manner, the actual emission variations during the day, emission rates were varied in a step fashion by increasing daytime values above the mean value and reducing nighttime emission rates. To achieve realism, the nighttime emission rates were reduced and the daytime emission rates were increased in such a manner that the total emission rate continued unchanged.

Pollutant removal can be arbitrarily introduced into the program by specifying an exponential decay rate. The half life of sulfur dioxide, however, is not known precisely and has been given values from days to tens of minutes (Weber, 1970)**. Therefore, for the subsequent computer calculations, no decay rate was used. If a decay rate were specified, the calculated value of air quality would be reduced, tending to create better agreement between observed and calculated air quality values.

---

* Calder, K. L., 1970. A climatological model for multiple source urban air pollution. Paper presented at the first meeting of NATO/CCMS. Panel on Modeling, 9 October 1970, Frankfort, Germany.

** Weber, E., 1970. Contributions to the residence time of sulfur dioxide in a polluted atmosphere, JGR, Oceans and Atmospheres, Vol. 75, No. 15, May 20, 1970, pp 2909-14.

Information on the air quality monitoring network is given in Table I, and the location of the sampling sites is provided in Fig. 1.

The mixing height, mean air temperature and the relative frequency of wind speed, wind direction and stability were taken from the Turkish Meteorological Office records. These records contained climatological information for the five-year period of 1964 through 1968. Also, during the winter of 1970, hourly data were collected for verifying the model.

With these parameters specified, calculations were first made using the full climatological model. Fig. 2 shows calculated versus observed sulfur dioxide concentrations. Readings from Station 2 appear to be consistently higher than the remaining stations; therefore, this station was omitted in obtaining the regression line and from the figures. Station 2 may differ from the others because of sampling location or some aspect of the topography which channels pollution to this receptor. Investigation of air trajectories making use of constant level balloons would help to answer this question.

Table 1. Ankara Air Quality Sampling Network

		Hundreds of Meters			
No.	Location	x	y	z(m)	Instruments
1.	Maden Teknik Arama Enstitusu Balgat	4825.0	44192.5	845	A,B
2.	Cumhuriyet Lisese, Bahcelievler	4846.3	44194.2	900	A,B
3.	Karayollari, Varlik Mahallesi	4852.5	44231.2	840	A,B
4.	Fen Fakultesi, Anittepe Mah.	4854.7	44206.3	855	A,B
5.	Harpokulu, Yorganci Mah.	4862.5	44173.8	920	A,B
6.	Meteoroloji Genel Mudurlugu, Mebusevleri	4882.5	44245.0	880	A,B,C
7.	Vilayet Binasi, Ulus	4876.7	44216.2	865	A,B
8.	Hifzisihha, Sehhiye	4880.7	44200.0	870	A,B,C,D
9.	Cumhurbaskanligi Koshu, Cankaya	4866.3	44157.5	1020	A,B,C
10.	Tip Fakultesi, Dikimevi	4901.3	44203.8	920	A,B
11.	Ilkokulu Samamlik Baglori	4907.5	44178.0	900	A,B
12.	Polis Karakolu, Siteler	4911.0	44235.0	885	A,B
13.	Ciftlici, Esenboga (background) 15 km north of Ankara				A,B

A = Part (Hi Vol) 24-hour measurements

B = SO_2 (West-Gaeke) 24-hour measurements

C = SO_2 (Coulometric Tritration) continuous measurements

D = SO_2 (Flame Photometric) continuous measurements

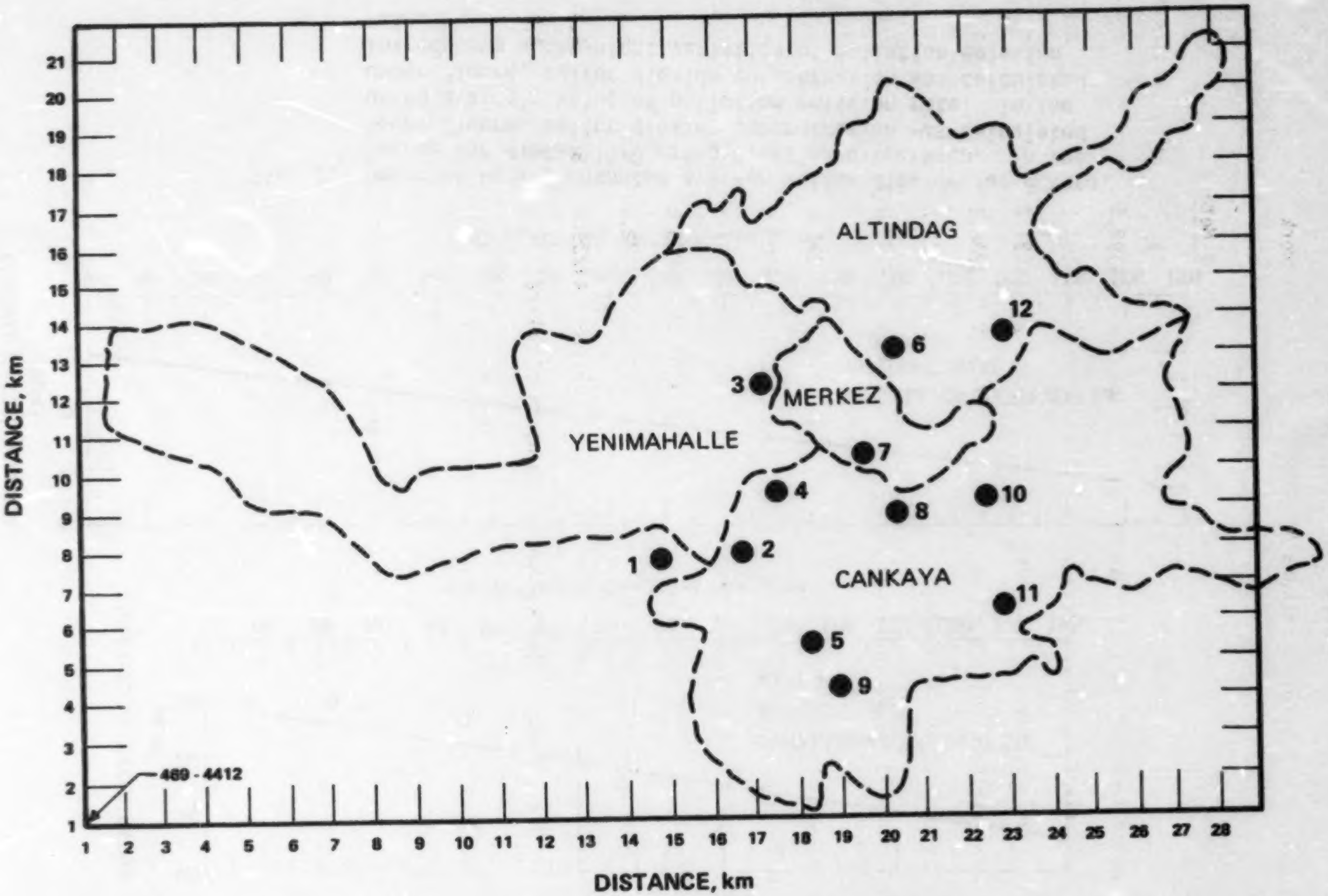
ALTINDAG
MERKEZ
YENIMAHALLE
CANKAYA
1
2
3
4
5
6
7
8
9
10
11
12
469 - 4412
DISTANCE, km
DISTANCE, km
1 2 3 4 5 6 7 8 9 10 11 12 13 14 15 16 17 18 19 20 21 22 23 24 25 26 27 28
1 2 3 4 5 6 7 8 9 10 11 12 13 14 15 16 17 18 19 20 21

Fig. 1. Ankara Air Quality Sampling Network.

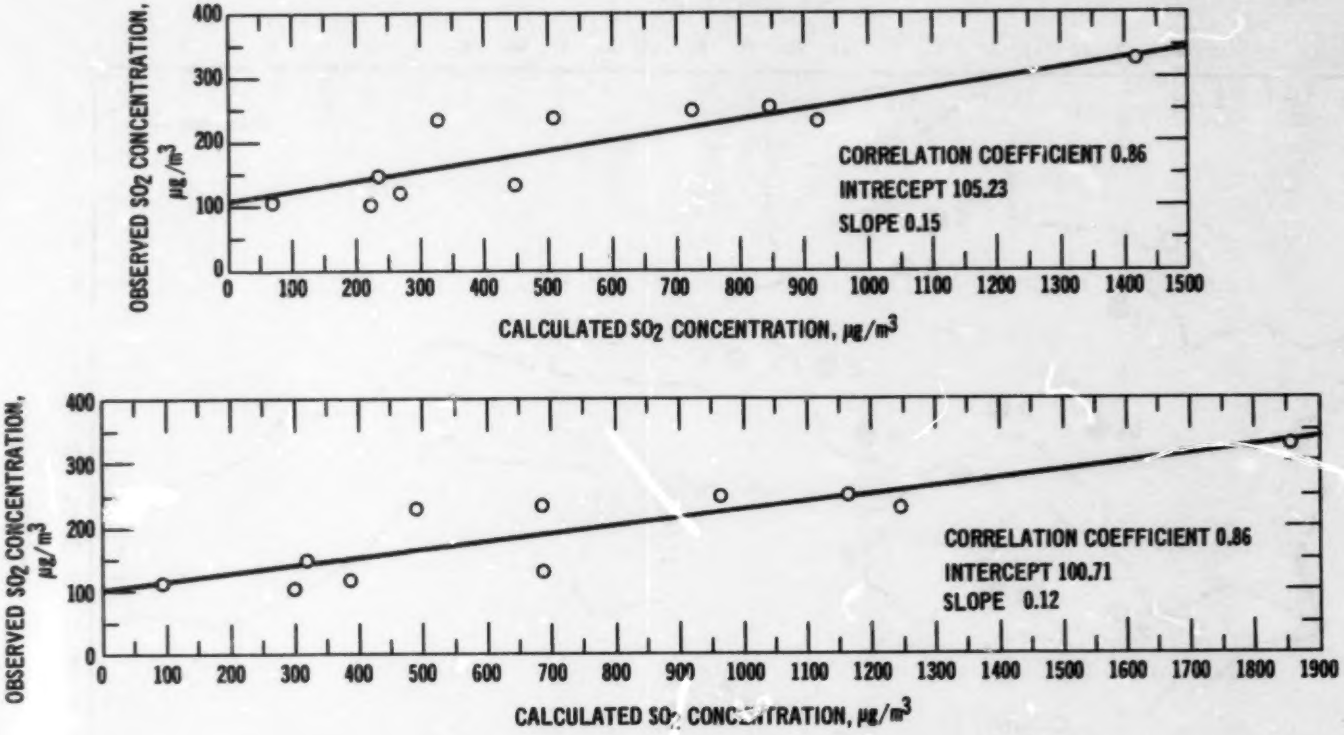

Fig. 2. Observed versus computed average sulfur dioxide for Ankara, Turkey for winter 1970 using Gaussian dispersion. In the lower figure, sulfur dioxide concentration was calculated using a single value of pollution emission rate. In the upper figure, sulfur dioxide concentration was calculated introducing a day-night variation of pollution emission rate.

Operating the computer model in this manner results in considerable overcalculation of air quality. There can be no doubt that some of the emission sources of Ankara are deflected or blocked by the irregular terrain from contributing their pollution to downwind receptors. It is also true that elevated sources such as the emission sources in the region of Altindag, the strongest area source, release their emissions at a much higher effective stack height than do the valley sources. This results in lower air quality values being observed at valley levels downwind of these sources.

In Ankara, more than 50 percent of the wind speeds observed were below 1.5 m/s. This model was not designed for application in situations where the wind circulation is weak and variable.

With complex terrain, especially urban valley areas, calculations of air quality are frequently made using "box" model dilution instead of Gaussian plume dispersion. The climatological dispersion model may be modified to compute concentration with a box model type of dilution by considering pollutants spread uniformly in the vertical but allowing for lateral spread. This is accomplished by giving σ_z the constant value of (0.8) x (mixing height). Fig. 3 shows the linear correlation of observed data and the results of the box model version of the climatological dispersion model.

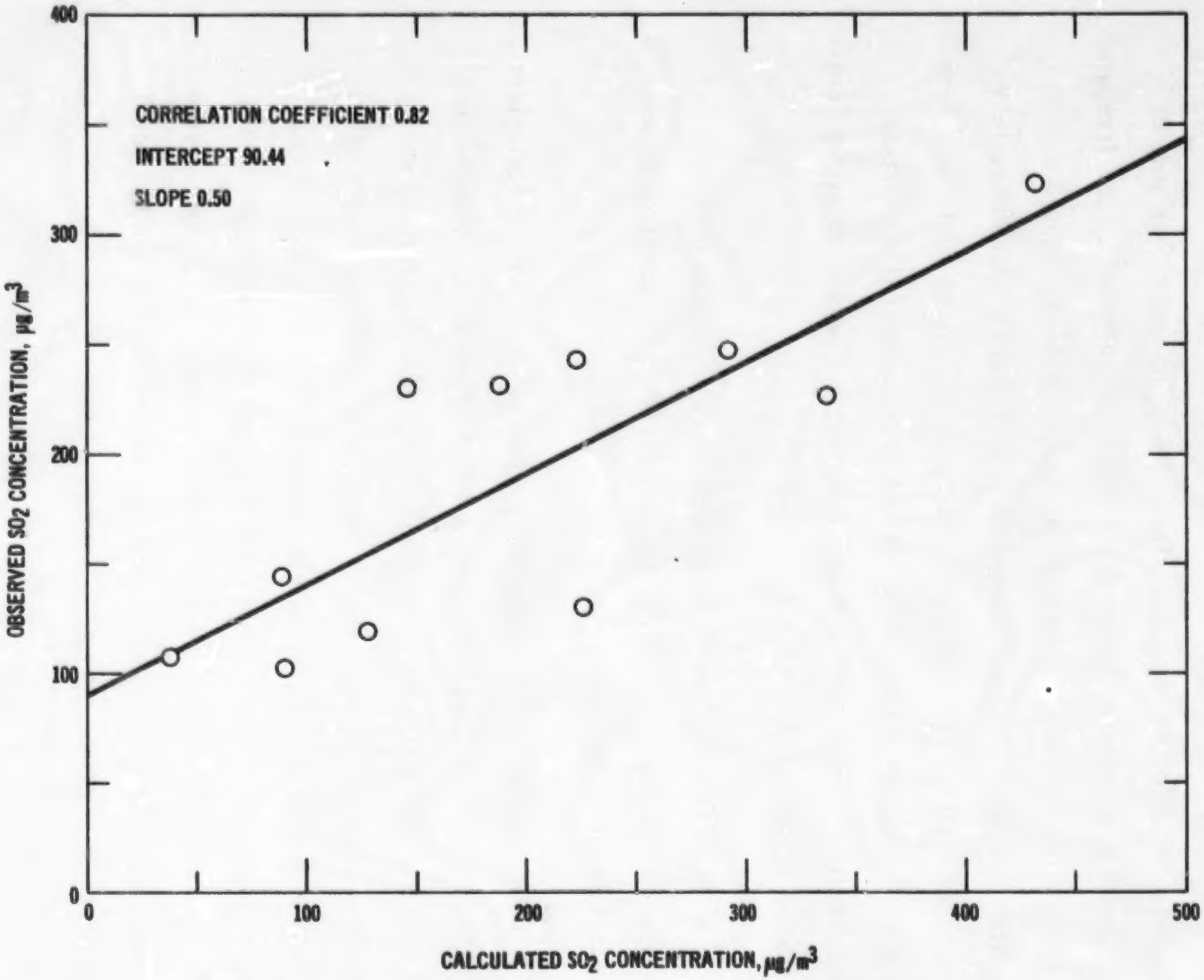

Fig. 3. Observed versus computed average sulfur dioxide for Ankara, Turkey for winter 1970 using box model dispersion.

Using the box model version of the climatological dispersion model increases the slope of the regression line so that the calculated values now lie within a factor of two of the observed values.

As previously mentioned, emissions from sources located on elevated terrain will produce lower concentration values at the valley bottom. This effect is probably most pronounced at night, when much of the pollution will pass high over the city and not be sensed at ground level.

Although computer technology enables an accounting of each individual pollution source, it is nevertheless worthwhile to make simplified estimates of air quality by hand in order to illustrate underlying principles.

A valid criteria for judging the usefulness of computer computation is the question, whether improvement over simple hand computations can be produced with computer analysis.

For a simple box model dispersion estimate which can be made by hand, overall mean values for each of the parameters as listed below were used, Q (total winter SO_2 emission rate) = 3,878 g/s

U (average wind speed) = 2 m/s

H_1 (estimated nocturnal mixing height) = 150 m

H_2 (average afternoon mixing height) = 1,000 m

W (width of city) 10,000 m

When put into the simple box model formula, the average concentration is,

$$C = \frac{Q}{UHW} \times 10^6 = \begin{array}{l} 194, \; H_1 = 1000 \text{ m} \\ 1293, \; H_2 = 150 \text{ m} \\ \text{where C is in } \mu g/m^3 \end{array}$$

The average observed concentration of 206 $\mu g/m^3$ (12 stations) is close to the value calculated using the afternoon average mixing height. As the mixing height undergoes a diurnal variation between nocturnal and afternoon values, the average concentration will lie between the two extremes of concentration calculated using these limiting values of mixing height. The low value of average concentration observed is evidence that the effective dispersion rate, in this region where emission sources have widely different elevations, is much greater than the level terrain Gaussian dispersion rate.

Particulate Matter

The analysis for particulate matter made in the same manner as for sulfur dioxide also used no decay rate. The correlation of observed to calculated air quality, ignoring Stations 12 and 9, is below the 95 percent significance level, so that there is more than a 5 percent probability that this result occurred due to chance (Fig. 4, 5).

It is possible that the scatter of data caused by the many natural local sources of particulate matter in this dry, dusty region obscures predictions by the climatological dispersion model. Many of the samples were unavoidably placed in locations where, as a result of traffic, wind, and building activity, particulate matter was constantly being stirred back into the atmosphere.

The Ankara background station is situated about 15 km north of the city, and is separated from Ankara by hilly terrain. Average background for Ankara (Station 13) is 40.5 $\mu g/m^3$. This high natural background with the re-entering dust makes it difficult to isolate background and local sources of particulate matter from urban produced particulate matter.

Calculations of the box model version of the climatological dispersion model for particulate matter predicts mean concentrations which are lower than observed particulate matter values and the correlation coefficient remains below the 95 percent significance

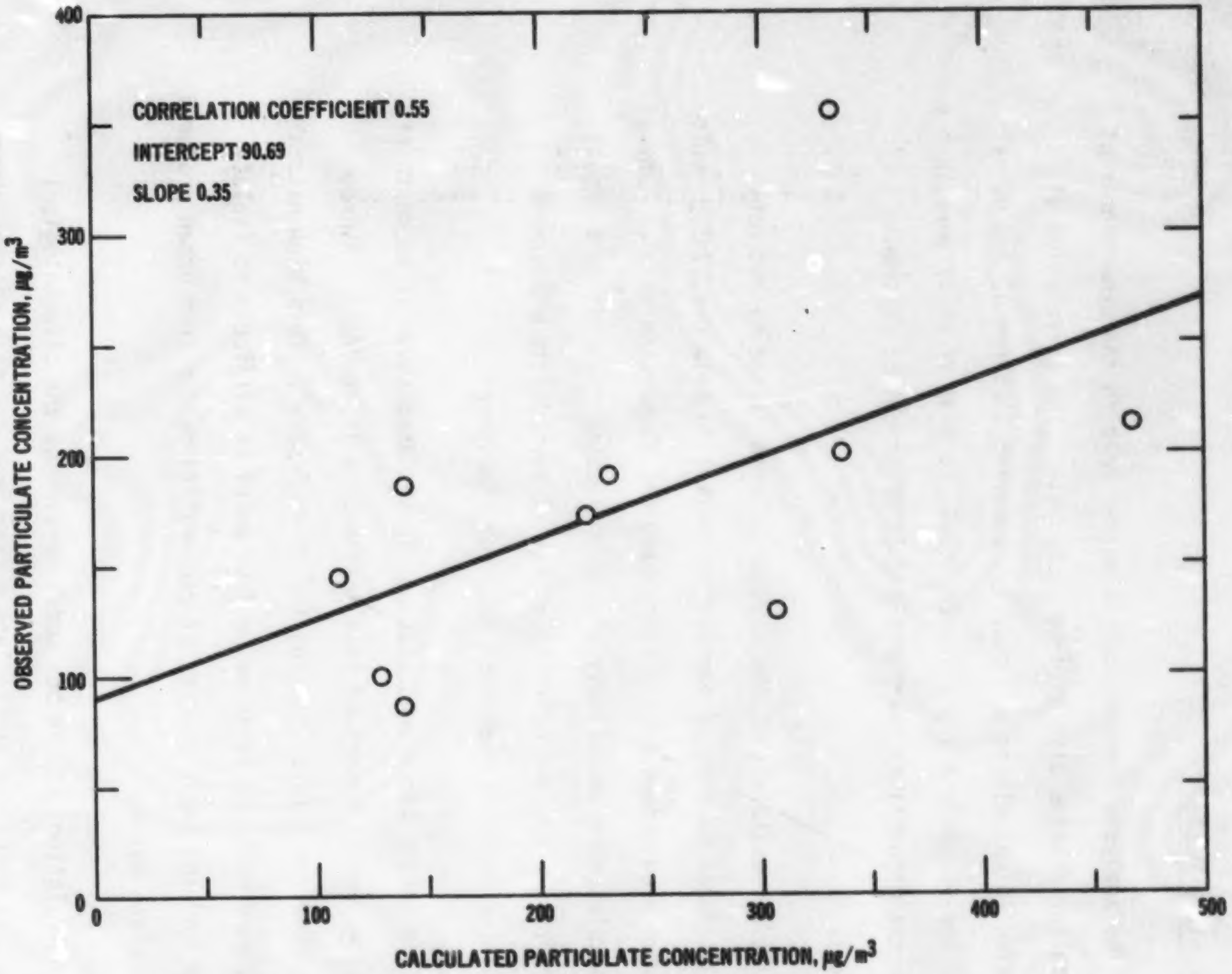

Fig. 4. Observed versus computed average particulate matter for Ankara, Turkey for winter 1970 using Gaussian dispersion. For this calculation of particulate matter concentration, a single value of pollution emission rate was used.

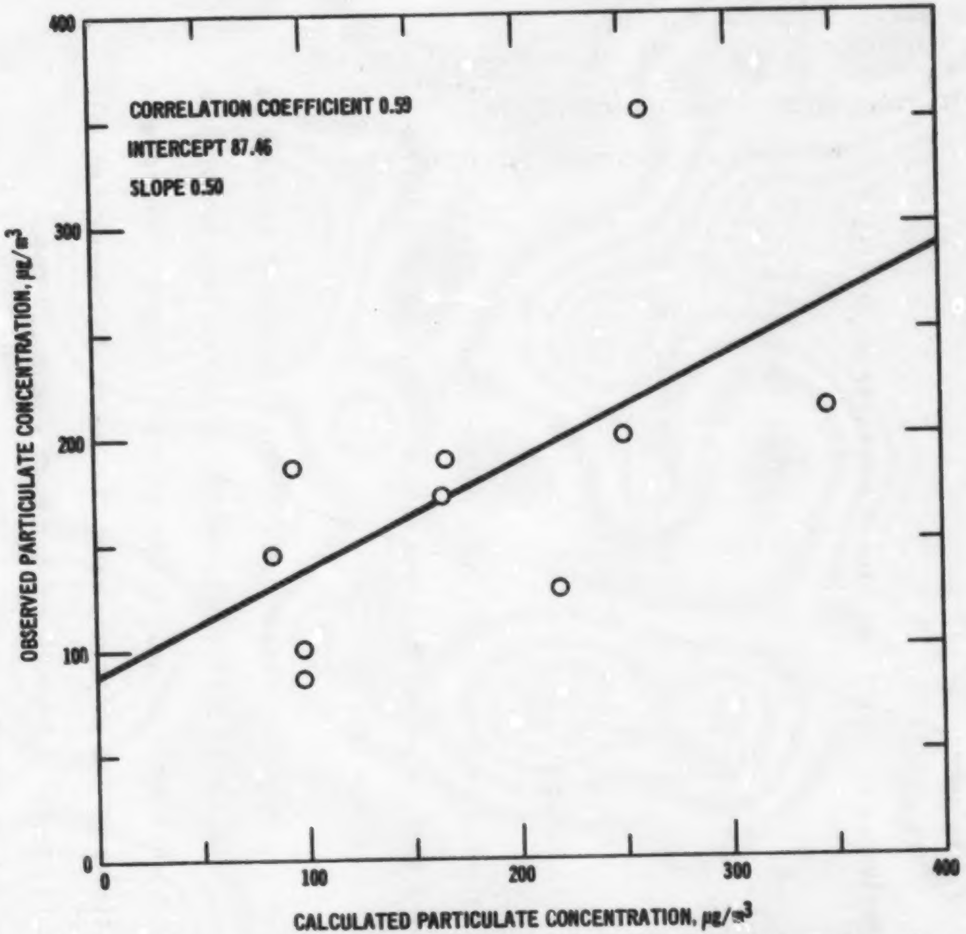

Fig. 5. Observed versus computed average particulate matter for Ankara, Turkey for winter 1970 using Gaussian dispersion. For this calculation of particulate matter concentration, a day-night variation of pollution rate was introduced.

level (Fig. 6). The same general remarks which apply to sulfur dioxide may be also made for particulate matter calculations. For the same meteorological conditions, the effective dispersion rate is above that used by the full climatological dispersion model. There can be no doubt that this greater dispersion rate is a result of irregular terrain as previously discussed.

The simple box model estimate for particulate matter is,

$$C = \frac{Q}{UHW} \times 10^6 = \begin{cases} 66, & H_1 = 1000 \text{ m} \\ 440, & H_2 = 150 \text{ m} \end{cases}$$

Where C is in $\mu g/m^3$

The winter emission rate for particulate matter of Q = 1,317 g/s, along with the same values of U, H and W as were applied with sulfur dioxide, were used for this calculation.

The observed mean particulate concentration for the 12 stations is 174 $\mu g/m^3$. This value also lies between the concentrations computed using the nocturnal and afternoon values of mixing height. Considering that the estimate of the emission rates for sulfur dioxide is probably high, there is general agreement between both simple box model computations made for sulfur dioxide and those for particulate matter.

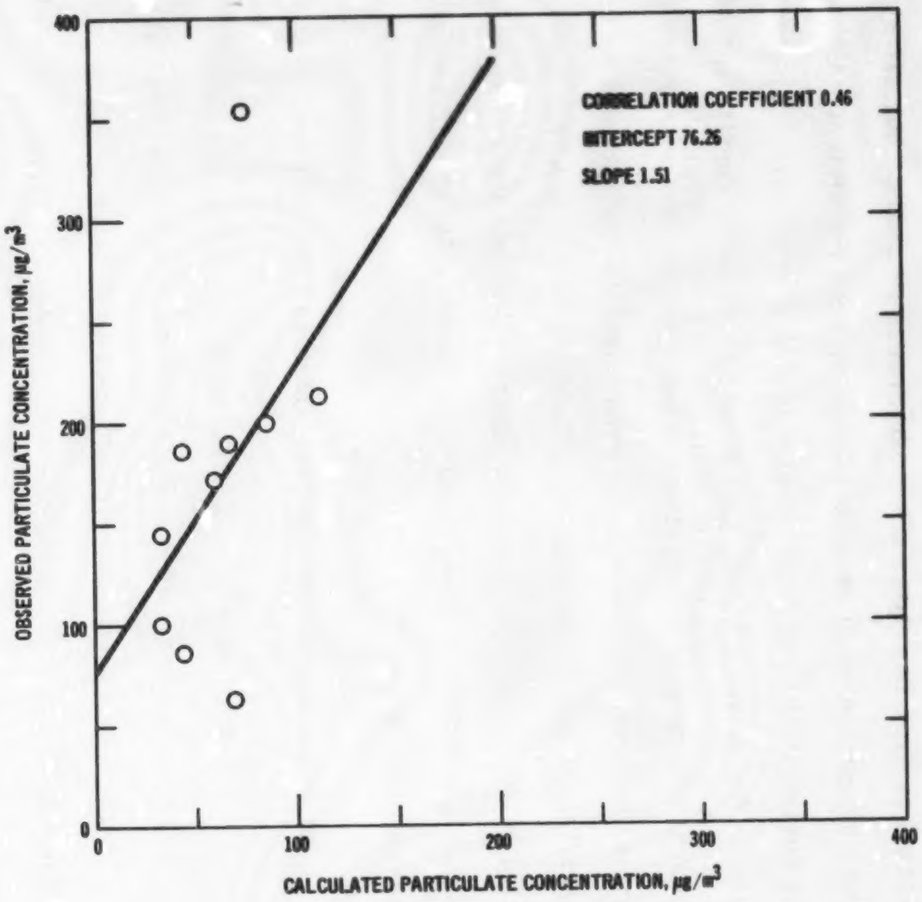

Fig. 6. Observed versus computed particulate matter for Ankara, Turkey for winter 1970 using box model dispersion.

III. Analysis and Projection of Air Quality for Ankara.

Linear relationships of observed and computed pollution concentration derived from the modified box model version of the climatological dispersion model were found. These were employed to calibrate the output of the box model version of the climatological dispersion model. For sulfur dioxide, this linear correlation coefficient is above the 95 percent significance value. In the case of particulate matter, however, the correlation coefficient is under the 95 percent significance level. Nevertheless, an analysis was made for both pollutants. As agreement between observed and calculated values of particulate matter is poor, results for particulate matter should be used cautiously.

The linear expressions applied for concentration were,

Observed = 90 + 0.50 Calculated, (sulfur dioxide)

and Observed = 76 + 1.51 Calculated, (particulate matter)

Sulfur Dioxide

Winter and annual mean sulfur dioxide analysis for Ankara are shown in Figs. 7, 8. The emission inventory indicates that during winter the use of heating fuel creates the highest average sulfur dioxide values, With summer, air pollution emissions reduce sharply and atmospheric dispersion improves so that the average sulfur dioxide concentration becomes insignificant.

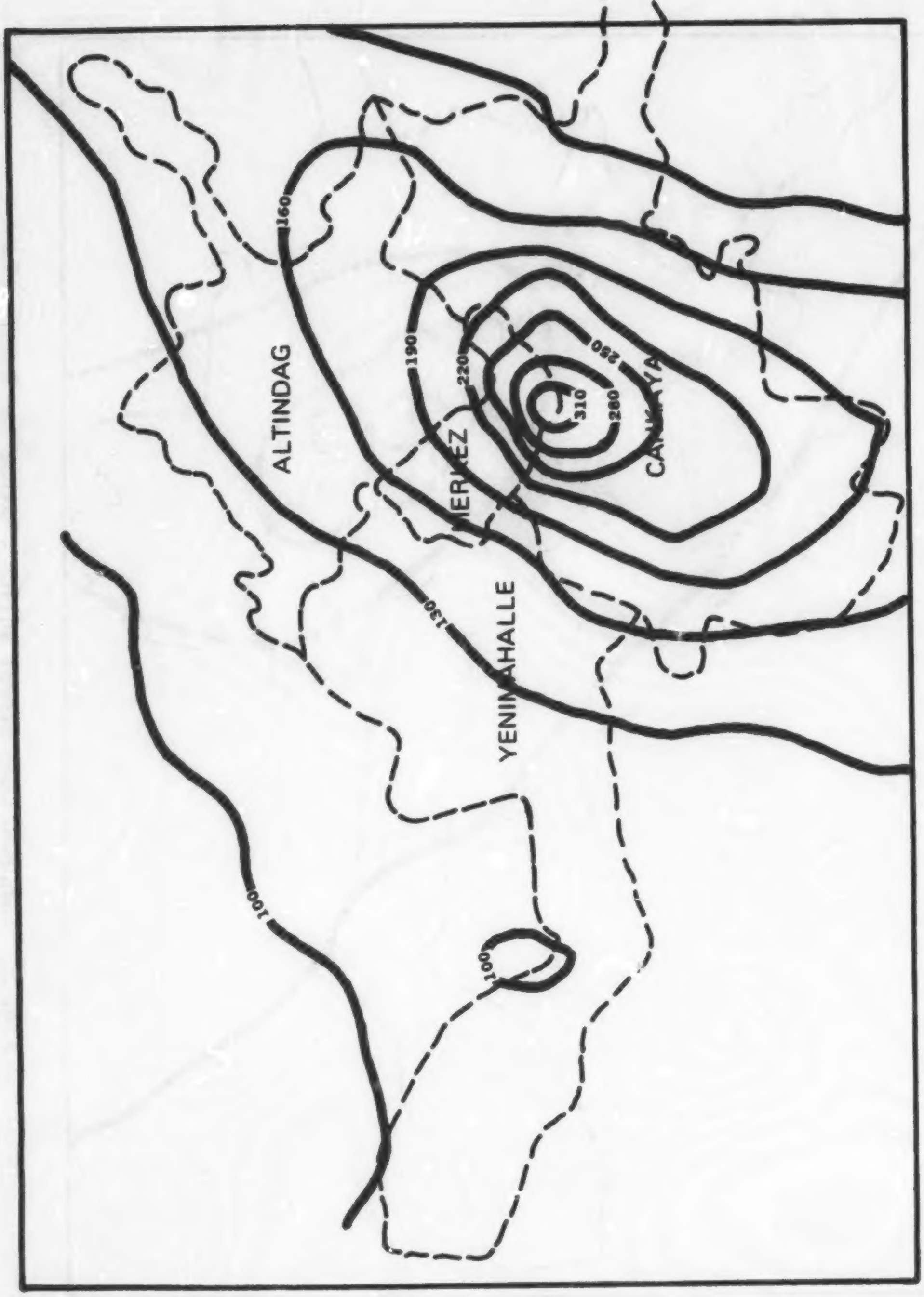
ALTINDAG
MERKEZ
CANKAYA
YENIMAHALLE
160
190
220
250
280
310
130
100
100

Fig. 7. Computed mean winter sulfur dioxide for Ankara, Turkey.

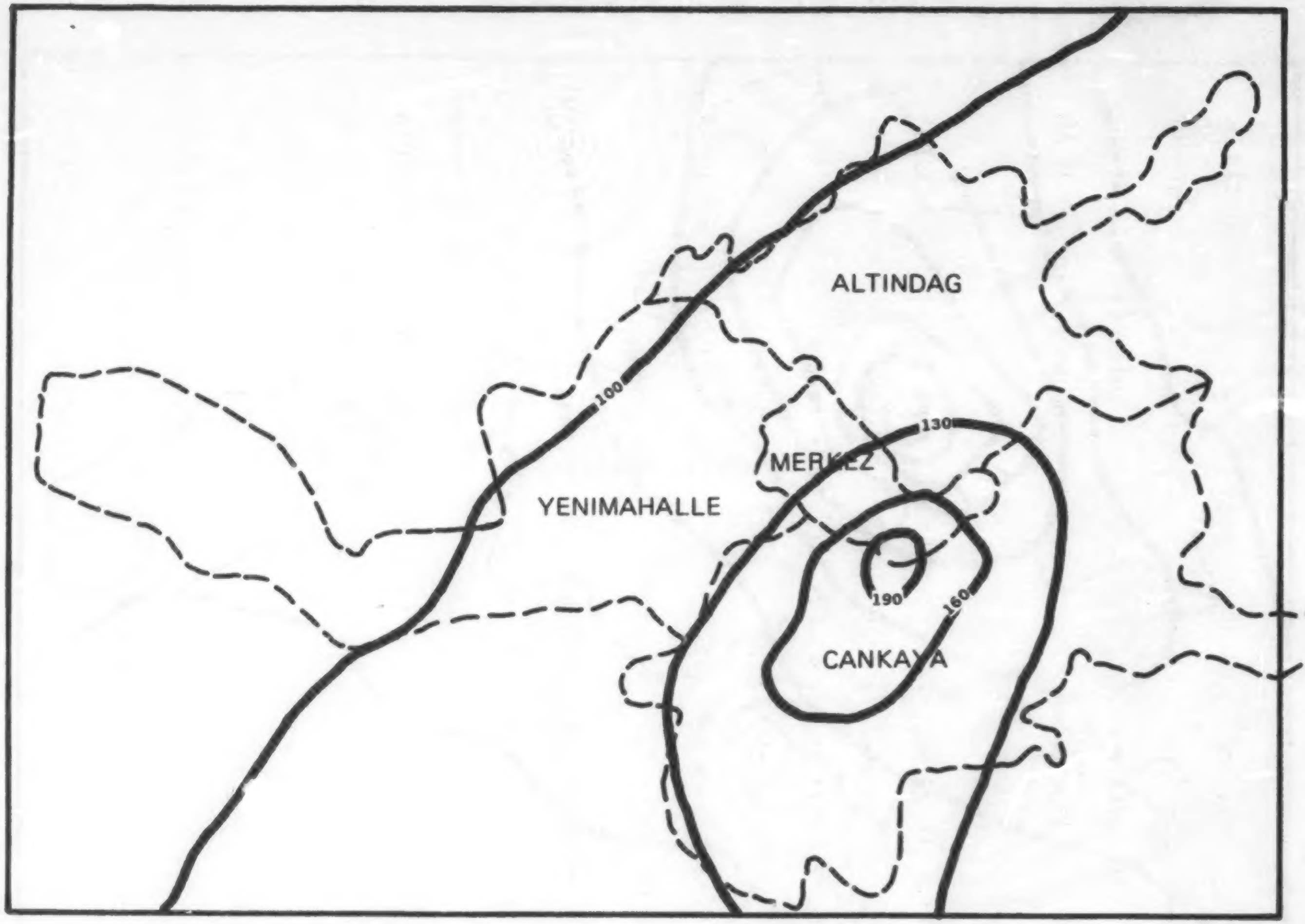
ALTINDAG
MERKEZ
YENIMAHALLE
CANKAYA
100
130
160
190

Fig. 8. Computed mean annual sulfur dioxide for Ankara, Turkey.

The pattern of calculated mean sulfur dioxide is almost congruent to the pattern of sulfur dioxide emissions, displaced slightly southward due to the prevalence of northerly winds. The highest computed concentration is centered over the core of the city, the region of highest population density. The contours of sulfur dioxide diminish from this location outward and approach background between 5-10 km from the center of the city.

Within the city, hills and ridges distort the wind flow producing departures of air quality from the simple patterns presented here. To the south, east, and north of Ankara, terrain elevations rise steeply deflecting the trajectory of air pollutants so that some of these locations are shielded from a full exposure to the air pollutants from the central city.

Projected data (Fig. 9) indicate that the center of maximum sulfur dioxide concentration shifts southward from Station 8 (Hifzissihha) to Station 5 (Harpokola) following a projected maximum emission rate centered about 1 km north of Station 5. Although total emissions for Ankara are projected to quadruple, maximum annual mean sulfur dioxide increases from about 190 $\mu g/m^3$ to about 280 $\mu g/m^3$. As the population spreads east of present day Ankara, substantial increases of pollution levels appear in areas which are now relatively pollution free. The projected air quality distribution will be modified by terrain features. The rise of terrain south of Ankara may

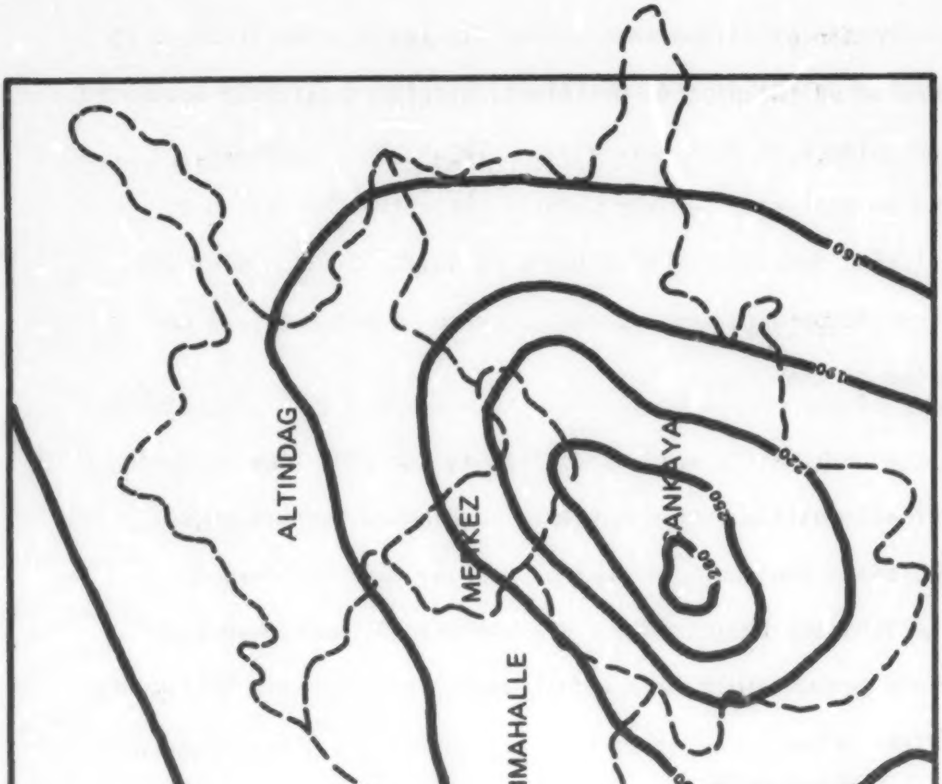
ALTINDAG
MERKEZ
CANKAYA
YENIMAHALLE
130
160
160
190
190
220
250
280

Fig. 9. Projected (1990) mean annual sulfur dioxide for Ankara, Turkey.

cause deflection of pollution trajectories eastward which would increase concentration of sulfur dioxide above the values indicated by the projected analysis, and reduce the expected concentrations due south of the city.

Particulate Matter

Plots of winter and annual particulate matter are presented in Figs. 10, 11. This analysis is derived from calculations which have little correlation with observed data. Nevertheless, some general observations can be made. As with sulfur dioxide, the highest pollution is found during winter with no significant urban produced particulate matter indicated during summer. High particulate matter values found in the summer can be attributed to natural sources of blown dust.

Maximum particulate matter is located over the heart of Ankara in a general pattern not unlike that of sulfur dioxide.

The projected 1990 contours of particulate matter, Fig. 12, show essentially the same features as the projections of sulfur dioxide except that maxima of particulate matter concentration remains about in the same position on its present location. Maximum concentration increases from a mean annual value of 160 $\mu g/m^3$ to 250 $\mu g/m^3$, and a substantial increase of pollution is found to the east of present day Ankara

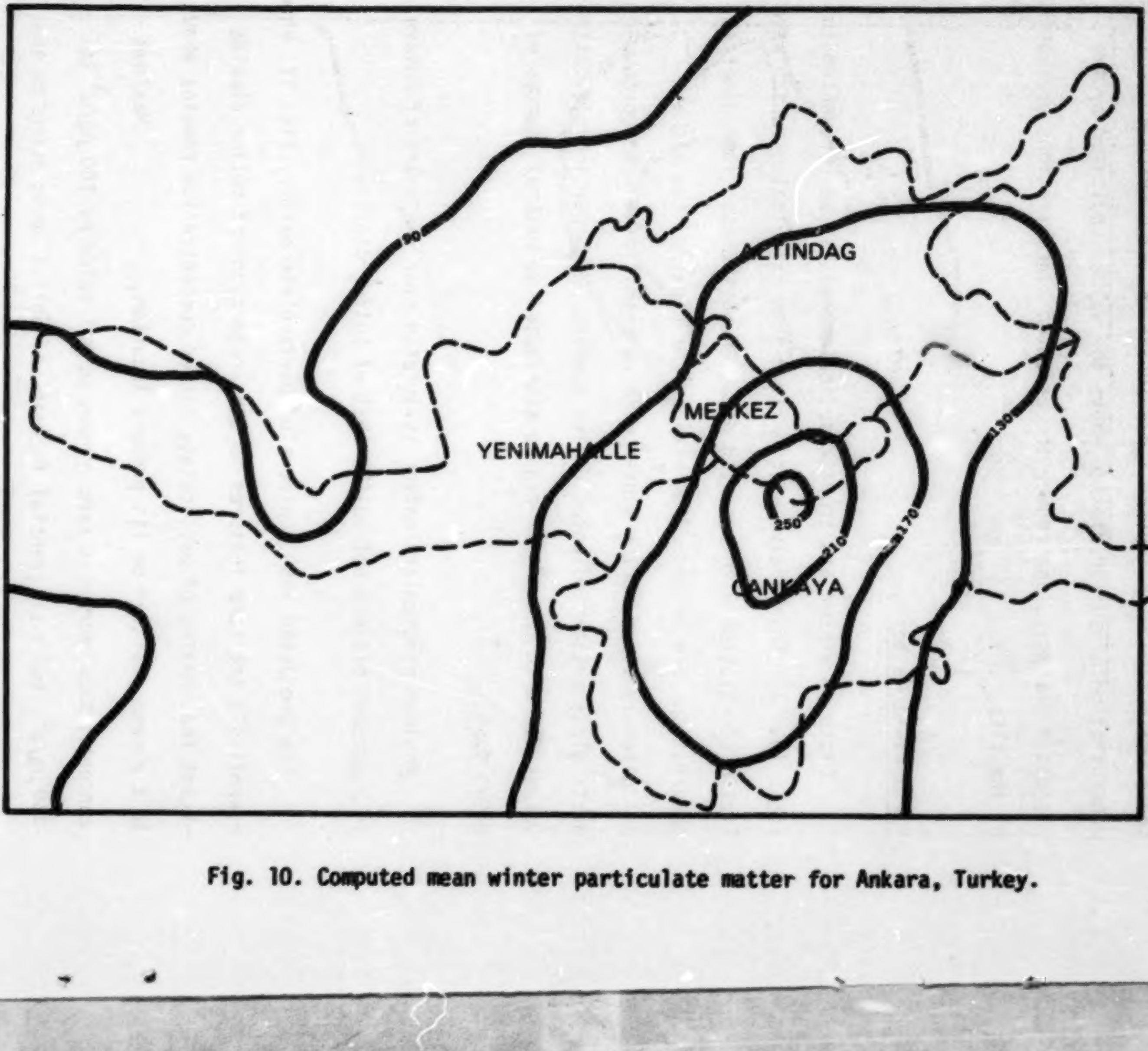
ALTINDAG
MERKEZ
YENIMAHALLE
CANKAYA
90
130
170
210
250

Fig. 10. Computed mean winter particulate matter for Ankara, Turkey.

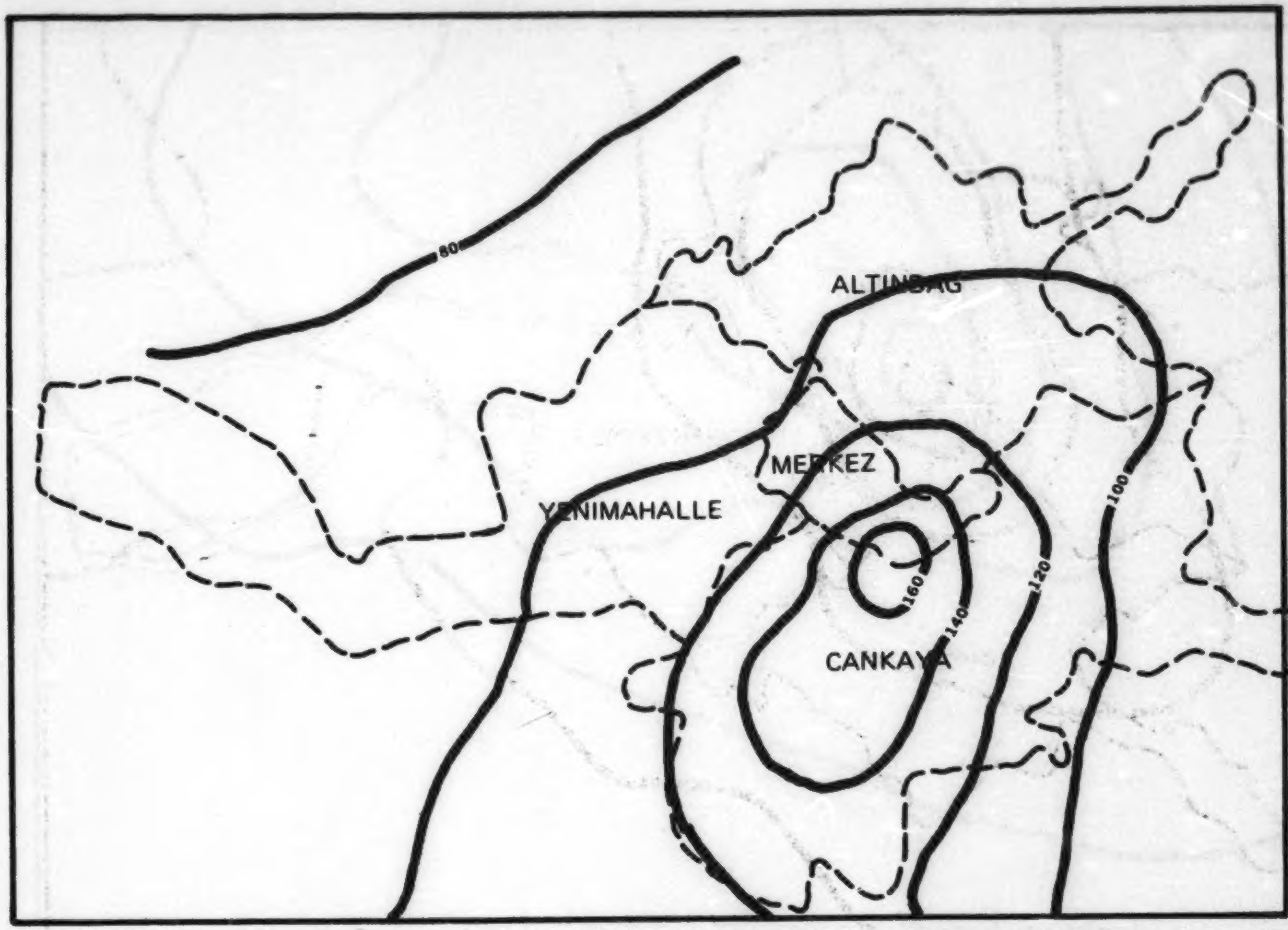
80
ALTINDAG
MERKEZ
YENIMAHALLE
CANKAYA
100
120
140
160

Fig. 11. Computed mean annual particulate matter for Ankara, Turkey.

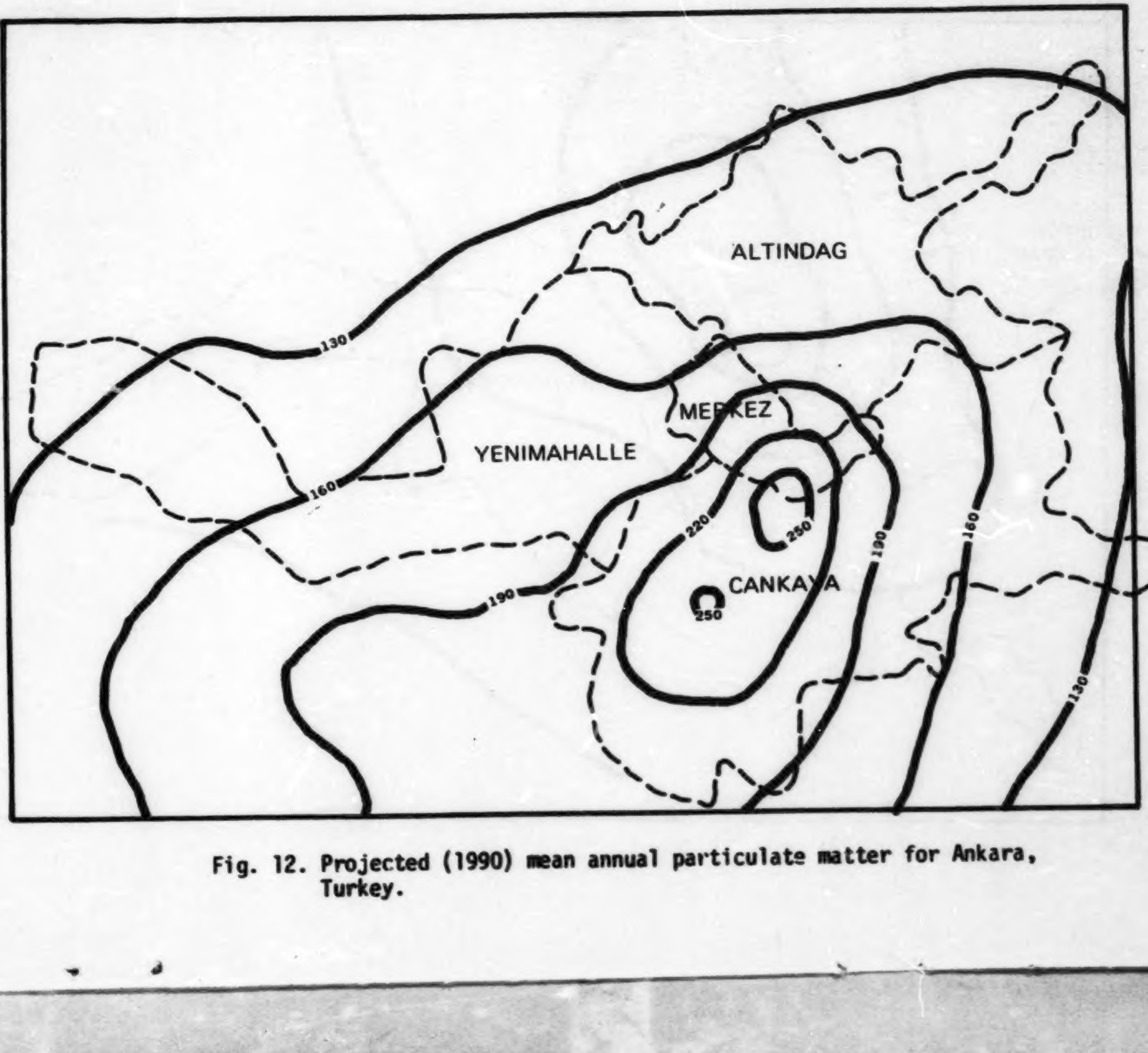
ALTINDAG
MERKEZ
YENIMAHALLE
CANKAYA
130
160
190
220
250
250
190
160
130

Fig. 12. Projected (1990) mean annual particulate matter for Ankara, Turkey.

IV. Summary

This report describes some preliminary results in the application of a dispersion model to compute the distribution of air pollution over the city of Ankara. In this initial evaluation of air quality, it is found that the application of Gaussian plume dispersion, with no allowance for variation of terrain elevation in this valley city, is unrealistic.

The climatological model used was originally developed for an idealized city situated on level terrain where calms do not predominate. To date, little computer air pollution modeling has been created for terrain as undulating as that of Ankara. At present, when modeling is applied in valley terrain, a simple variation of the box model concept can be employed that gives as good or better results than Gaussian plume dispersion.

Unfortunately, the development of a model which adequately treats uneven terrain, as well as the calculation of air quality under calm air conditions, and which allows for the computation of pollution air trajectories, is for the future. Such models will be considerably more complex than the computer model presented here.

Clearly, although a small step has been taken to analyze air pollution over Ankara, much valuable information can still be derived from the collected data by further study. Many interesting projects suggest themselves among which a partial listing includes:

a) Development of air quality forecasting techniques by relating observed air quality to synoptic weather conditions.

b) Investigations of pollution trajectories by constant level balloons.

c) Revision of the computer model to allow for irregular terrain and for calm weather.

Most of these projects will require air pollution scientists intimately acquainted with the Ankara locale who will be able to observe firsthand the daily interaction of atmosphere and urban pollution.

*U.S. GOVERNMENT PRINTING OFFICE: 1972 484-487/322 1-3